University of Nottingham

Investigation of male reproductive traits of agronomic importance in cereals

Johanna Astrand

Thesis submitted to University of Nottingham
for the degree of Doctor of Philosophy

University of Nottingham
School of Biosciences

Sutton Bonington Campus
Leicestershire, LE12 5RD

March 2022

Acknowledgments

First and foremost, I would like to thank all my wonderful colleagues and friends in Plant Sciences for all the support, advice, laughs and adventures throughout the years. I especially want to thank Ute, Morena, Elina, Martina, Michele, Cindy, Jordan, Jason, Dylan, and Jack who have made my time in Nottingham so memorable and how have given me advice and insights into so many aspects of science.

I would like to send a special thanks to my supervisors Zoe Wilson and José Fernández Gómez. Zoe you have really helped me with everything throughout the project and I am very grateful for your support. I would also like to thank every member of the Wilson group (past and present) for all the chats and help over the years.

I am deeply grateful to my family: Rune, Birgitta, Niklas and of course Caroline and Alex, who have always been there for me. Mom and dad, you have always believed in me and encouraged me to go for every opportunity and I am forever grateful for that. Calling you and Niklas always helps to keep me sane and motivated.

Caroline, it is fair to say I would not be where I am today without you. I can always count on you being there for whatever I need, and your support has meant everything to me. All our talks, rants and laughs has gotten me through it all. Thank you for everything!

Ane and Lovisa, you are two of my favourite people and I can't wait to live closer to you so we can finally hang out again. Talking to you always makes me happy and I hope you will always be in my life.

This work was funded by the Biotechnology and Biological Sciences Research Council's Industrial Collaborative Awards in Science and Engineering studentship scheme with support from an industrial scholarship from KWS UK Ltd, Limagrain UK Ltd, RAGT Seeds Ltd, SECOBRA Recherches SA, and Agriculture and Horticulture Development Board as well as the BBSRC. I especially wish to thank everyone at KWS, RAGT and Limagrain who hosted me throughout the placements and who were always happy to help with the project.

Table of contents

List of figures

List of tables

Abbreviations

ABA	abscisic acid
AE	anther extrusion
AL	anther length (mm)
AR cell	archesporial cell
bHLH	basic Helix Loop Helix
BLAST	Basic Local Alignment Search Tool
BLINK	Bayesian-information and linkage-disequilibrium iteratively nested keyway
BLUE	Best Linear Unbiased Estimate
BOP	Breeders Observation Panel
bp	base pair
BW	Bowman
cDNA	complementary Deoxyribonucleic acid
CDS	coding sequence
CI	callus induction
cm	centimetre
cM	centiMorgan
CRISPR	Clustered Regulatory Interspaced Short Palindromic Repeats
Ct	cycle threshold
DAPI	4',6-diamidino-2-phenylindole
dATP	Deoxyadenosine triphosphate
DNA	Deoxyribonucleic acid
dNTP	Deoxynucleotide Triphosphate
dPCD	developmentally programmed cell death
EDTA	Ethylenediaminetetraacetic acid
ESEM	environmental scanning electron microscopy
ETR	electron transport rate
FDR	False Discover Rate
FPKM	fragments per kilo base of transcript per million mapped fragments
gDNA	genomic deoxyribonucleic acid
GOI	gene of interest
GP	Golden Promise
GWAS	Genome-Wide Association Study
h	hour(s)
ID	identity
IPTG	Isopropyl β- d-1-thiogalactopyranoside
KASP	Kompetitive Allele Specific PCR
kb	kilobase pair
L	litre
JA	jasmonic acid
LB	Lysogeny Broth
LD	linkage disequilibirum
M	molar
Ma	million years ago
Mbp	mega base pairs
Mg	milligram
$MgCl_2$	magnesium chloride
min	minute(s)
ml	millilitre
MLM	mixed linear model
mM	millimolar

mm	millimeter
MoClo	Modular Cloning
MRCA	most recent common ancestor
msg	male sterile genic
NaCl	sodium chloride
ng	nanogram
NILs	near isogenic lines
nm	nanometer
NPQ	non-photochemical quenching
OD_{600}	optical density at wavelength 600 nm
OE	overexpression
PAM	Protospacer Adjacent Motif
PBS	Phosphate Buffered Saline
PCA	Principal Component Analysis
PCD	Programmed Cell Death
PCR	Polymerase Chain Reaction
PHD	Plant Homeo Domain
pM	picomol
PMC	pollen mother cell
PP cell	primary parietal cell
PS cell	sporogenous cell
PSII	photosystem II
PxJ	Piko x Julius
qP	photochemical quenching
QQplot	Quantile-quantile plot
qRT-PCR	Quantitative Reverse-Transcriptase Polymerase Chain Reaction
QTL	Quantitative trait locus
QY_{max}	Maximum quantum yield
REF	reference
REML	restricted maximum likelihood
RNA	ribonucleic acid
rpm	revolutions per minute
s	second(s)
SDS	Sodium Dodecyl Sulfate
sgRNA	single guide RNA
SNP	single nucleotide polymorphism
SP cell	secondary parietal cell
SRDX	plant-specific EAR-motif repression domain
TE	Tris-EDTA
TrisHCL	trisaminomethane hydrochloride
U	units
µg	microgram
µl	microliter
µm	micrometer
µM	micromolar
v	volume
w	weight
YFP	Yellow Fluorescent Protein

Abstract

Male fertility in flower development is important for breeding and yield stability in cereals. An intricate gene regulatory network in close association with environmental cues are required for formation of viable pollen and timely release of pollen from the anther. Hybrid breeding, the crossing of two elite cultivars, have the potential of generating varieties with increased yield and resistance to abiotic stresses but for crossing of elite parents for large scale seed production, certain qualities are required. The male parent should have high pollen production and effective dispersal whereas the female parent needs to exhibit male sterility to prevent self-pollination and be receptive of non-self pollen. In this project the impact of male traits on fertility and pollen dispersal have been studied in cereals to enhance understanding of processes useful for hybrid breeding. Three separate studies were carried out using forward and reverse genetic approaches to study traits related to male fertility and its effect on yield and traits of agronomic importance. In addition, anther development in angiosperm flowers was reviewed in an evolutionary perspective.

Abiotic stresses such as cold stress can severely affect floral development and lead to yield losses due to inhibited plant growth or flowering. However, there is limited knowledge of how genes involved with pollen development in cereals are connected to abiotic stress management processes under cold and drought stress. Here, a putative orthologue of the *Arabidopsis INDUCER OF CBF EXPRESSION1* (*ICE1*) was identified and investigated in barley in relation to yield and stomatal formation under cold and drought stress. Vectors carrying CRISPR/Cas9 single guide RNA (sgRNA) targets, *HvICE1-1* overexpression or *HvICE1-1* silencing constructs were transformed into barley to study the gene *in planta*. The overexpression of *HvICE1-1* was found to reduce the induction of the downstream *HvCBF3* after freezing stress, a process which is critical for cold response, as well as reduce yield due to inhibited plant growth, whereas silencing of *HvICE1-1* interfered with the formation of stomata on the leaf surface. *HvICE1-1* was further shown to influence the photosynthetic capacity of the plant suggesting that the putative *HvICE1* orthologue is involved with a diverse set of processes in plant development and physiology.

Anther traits were investigated in hexaploid wheat to study the genetic component of these traits. To identify quantitative trait loci (QTLs) controlling anther length and anther extrusion in wheat, three populations with varying degree of genetic diversity were phenotyped and used for genome wide association studies (GWA studies). In total 427 elite wheat cultivars, 95 wild wheat introgression lines, and a bi-parental mapping population with 475 plants were used to identify 11 and 6 loci potentially involved with the regulation of anther length and extrusion. Heritability was found to be high for anther extrusion and anther length in all populations with a medium correlation between anther extrusion and plant height. Finally, underlying loci involved with genic male sterility were studied in barley using a collection of male sterile barley mutants. The lines were genotyped with a high density 35k SNP array to identify regions of interest and to enable future fine-mapping of loci of interest.

Together these studies of male fertility in cereal flowers and the effect of abiotic stresses on yield have increased the understanding of cereal floral biology to enable future hybrid breeding.

Chapter 1. Introduction and literature review

1.1.1 The need for improved hybrid breeding

The population of the world is predicted to reach 9.8 billion people by the year 2050 which generates an increased demand for food production (United Nations, Department of Economic and Social Affairs, Population Division, 2017). The required increase in crop productivity is expected to be 200% over the coming three decades, generating pressure on the agricultural sector to meet this growing demand (Bradshaw, 2016). Along with a growing population, extreme weather is predicted to increase in the coming decades, causing a significant challenge with changes in precipitation and extreme temperatures resulting in abiotic stresses which can severely reduce grain yield (Lobell et al., 2011; Ray et al., 2019; Zhao et al., 2017). To ensure future food safety the breeding of climate resilient varieties with an increased yield is essential and poses a great challenge for the breeding community.

Hybrid breeding has been recognised as an approach to increase yield for some of our most important crops. Hybrid plants, the direct progeny of a cross between two inbred parental lines, have the potential to exhibit heterosis, by outperforming both parents with an increased stress tolerance, a more uniform growth pattern, increased yield, improved decease resistance, or better grain quality (Kim & Zhang, 2018; Longin et al., 2012; Mühleisen et al., 2014). In an effort to improve the grain yield of these cereals, hybrid varieties emerged commercially during the 20th century (Mühleisen et al., 2013), but hybrid wheat and barley is still not widely used (Mühleisen et al., 2014; Whitford et al., 2013).

In barley the generation of hybrid varieties has seen an increase in yield of up to 11% with the hybrids outperforming inbred lines (Mühleisen et al., 2013; Philipp et al., 2016), compared to the increases in rice with 55%, and in wheat with 15% (Kim & Zhang, 2018). For outcrossing cereals such as rye and maize the increase in yield of hybrid varieties has been greater however efforts with self-pollinating crops such as wheat and barley have been less successful (Longin et al., 2012). Hybrid barley has been commercially available for years and in 2021 hybrid barley varieties made up 35% of the area of winter barley grown in the UK but wheat still trails behind with 0.2% of the total global wheat production (Jones, 2021, Gupta et al., 2019). Development of fertility control systems to enable forced outcrossing of self-pollinating species is needed for efficient and stable hybrid breeding systems.

The production of hybrid seed in autogamous species requires the prevention of self-pollination of one parent to allow crossing with a pollen donor. Maintaining a male sterile line is laborious and has been accomplished with the use of maternally inherited cytoplasmic male sterility (CMS) traits or with chemical hybridising agents (CHA), which is more common commercially, however this leads to problems with toxicity and selectivity (Eavis et al., 1996). The hybrid barley on the market today is mostly generated through the use of CMS whereas hybrid wheat has been accomplished with CHA to generate the female parents (Gupta et al., 2019, Mühleisen et al., 2013). Another approach is to generate female parents with recessive male sterile traits which has for a long time been of interest to plant breeders

for the simplified generation of hybrid varieties (Longin et al., 2012). To develop systems for the large-scale production and maintenance of male sterile lines and subsequently hybrid varieties a better understanding of the development of pollen and anther formation is needed.

1.1.2 Male sterility in wheat and barley

Despite the interest in genic male sterility only a limited number of mutants have been characterised to cause male sterility in barley and wheat. The size and the structure of the wheat genome complicates identification of genes related to anther and pollen development due to potential redundancies of the homeologs where knock-outs of all three homeologs can be required to generate complete male sterility (Singh et al., 2018). In spite of these difficulties several genes have been identified as required for male fertility in wheat including the wheat specific *MALE STERILE1* (*MS1*) (Tucker et al., 2017), and *MS5* (Pallotta et al., 2019), and wheat orthologues of known genes including *NO POLLEN1* (*TaNP1*) (Li et al., 2020), *TaMs26* (Cigan et al., 2017), *MALE STERILE 45* (*TaMS45*) (Singh et al., 2018), *CALLOSE SYNTHASE 5* (*TaCalS5*) and *RUPTURED POLLEN GRAIN1* (*TaRPG1*) (Milner et al., 2020) where knock-outs of the homeologs are required to generate a male sterile phenotypes. The identified orthologues highlight the conservation between species and the genes have been suggested to be valuable for use in hybrid breeding systems (Singh et al., 2021).

The introduction of the wheat *Ms2* region, responsible for wheat male sterility, in barley generated a male sterile phenotype however no identification of a potential barley orthologue has been carried out (Ni et al., 2017). Studies of male sterile alleles have been carried out and another potential gene, *CYP704B*, expressed in the anther has been implicated in male fertility in barley but has not been characterised (Qi et al., 2019). The barley orthologue of *MS1* (*HvMS1*) remains the only characterised male sterile mutant in barley, showing defects in tapetum degeneration and microspore development (Fernández Gómez & Wilson, 2014). Understanding of processes required for anther and pollen development is needed for the identification of other genes involved with male fertility in barley.

1.1.3 Conditional sterility for hybrid breeding

Conditional male sterility is a process where the pollen production or spreading ability is inhibited under specific conditions, causing a sterile phenotype in an otherwise fertile plant. Lines exhibiting conditional sterility can be maintained by self-propagation under favourable conditions and be used as the female parent for hybrid breeding by exhibiting male sterility under stress conditions.

Hybrid rice breeding using photoperiod sensitive and thermo-sensitive lines has generated some of the most high yielding varieties with the majority of the rice cultivated in China

being hybrid rice (Cheng et al., 2007). There is great potential for the identification of conditional sterile traits in rice with numerous reports of mutations of genes exhibiting genic male sterility with thermo-sensitive or photoperiod properties (Chen et al., 2007; Ku et al., 2001; Qi et al., 2014; Zhang et al., 2013).

In wheat and barley few genes have been reported to exhibit abiotic stress induced conditional male sterility but there are some reports of fertility changes linked to environmental changes. Among them is the temperature sensitive wheat line BS366 which exhibits low pollen production at 10˚C (Tang et al., 2011; Xu et al., 2013) and the transgenic line overexpressing the barley *MALE STERILE1* (*HvMS1*) gene which exhibits sterility at normal growth temperatures (15˚C) but shows reversible fertility when grown at increased temperatures (Fernández-Gómez, Talle, & Wilson, 2020). These lines suggests that conditional sterility could be a viable option for hybrid breeding in cereals with complex genomes such as wheat and barley. The development of stable conditional sterile lines without adverse effects poses a challenge and more knowledge of the pollen development and release is necessary for the incorporation of these traits into the breeding population.

Floral development is remarkably conserved in land plants and the understanding of the pollen development pathway in an evolutionary context can provide a useful perspective for future research. Investigating of how male fertility traits have evolved and identification of processes that can be used for the generation of male sterile traits is useful for the breeding of our most important commercial crops.

1.3 Review article: Evolution and diversity of the angiosperm anther: trends in function and development

Plant Reproduction (2021) 34:307–319
https://doi.org/10.1007/s00497-021-00416-1

REVIEW

Evolution and diversity of the angiosperm anther: trends in function and development

Johanna Åstrand[1] · Christopher Knight[1] · Jordan Robson[1] · Behzad Talle[1] · Zoe A. Wilson[1]

Received: 11 February 2021 / Accepted: 28 May 2021 / Published online: 26 June 2021

Abstract
Key message Anther development and dehiscence is considered from an evolutionary perspective to identify drivers for differentiation, functional conservation and to identify key questions for future male reproduction research.
Abstract Development of viable pollen and its timely release from the anther are essential for fertilisation of angiosperm flowers. The formation and subsequent dehiscence of the anther are under tight regulatory control, and these processes are remarkably conserved throughout the diverse families of the angiosperm clade. Anther development is a complex process, which requires timely formation and communication between the multiple somatic anther cell layers (the epidermis, endothecium, middle layer and tapetum) and the developing pollen. These layers go through regulated development and selective degeneration to facilitate the formation and ultimate release of the pollen grains. Insight into the evolution and divergence of anther development and dehiscence, especially between monocots and dicots, is driving greater understanding of the male reproductive process and increased, resilient crop yields. This review focuses on anther structure from an evolutionary perspective by highlighting their diversity across plant species. We summarise new findings that illustrate the complexities of anther development and evaluate how they challenge established models of anther form and function, and how they may help to deliver future sustainable crop yields.

Keywords Anther evolution · Pollen development · Anther dehiscence · Microsporogenesis · Anther wall formation

Introduction

The anther is the pollen producing part of the stamen, which is supported by a stalk-like filament, and together, they make up the male reproductive structure of the angiosperm flower. Throughout the evolution of the angiosperms, the stamen has undergone a variety of adaptations to enhance reproductive success (Doyle 2012; Endress and Doyle 2009; Sauquet et al. 2017). The range of complexity in anther wall formation, filament attachment and anther dehiscence emphasise the scale of anther adaptability (Endress 1996). The differentiation and formation of the anther walls enclosing the developing microsporangia are still poorly understood across a wide range of angiosperm families. Generally, the anther wall comprises the tapetum, the middle layer and the endothecium which are enclosed by the epidermis (Gómez et al. 2015). The innermost tapetum layer is perhaps the most studied due to its crucial role in microspore development (Cigan et al. 2001; Feng and Dickinson 2010; Furness and Rudall 1998, 2001; Parish 2012; Wilson and Zhang 2009). It is adjacent to the developing pollen, providing materials for pollen wall formation and

Communicated by Frederic Berger.

A contribution to the special issue 'Evolution of Plant Reproduction'.

✉ Zoe A. Wilson
zoe.wilson@nottingham.ac.uk

Johanna Åstrand
stxjea@exmail.nottingham.ac.uk

Christopher Knight
stxck6@exmail.nottingham.ac.uk

Jordan Robson
jordan.robson1@nottingham.ac.uk

Behzad Talle
behzad.talle@nottingham.ac.uk

[1] School of Biosciences, University of Nottingham, Sutton Bonington Campus, Loughborough, Leicestershire LE12 5RD, UK

coordinating the progression of pollen development. There is growing understanding of the gene networks involved in tapetum differentiation and pollen wall synthesis, and evidence of conservation of these networks across monocot and dicots species (Callens et al. 2018; Drábková and Honys 2017; Gómez et al. 2015; Silva et al. 2016; Theissen and Melzer 2007). This highly regulated process is essential for viable pollen production and male fertility, but despite its importance there are still many unresolved questions regarding the origin, function and communication between the different tissues within the anther. In this review, we explore the conservation and divergence of the anther cell layers to provide an overview of their role in reproductive success. We focus on the complexities of the male reproductive system and evaluate the functions of anther structure and the conservation of the mechanisms behind pollen production and release, and the associated drivers of reproductive success.

Anther development in angiosperms

Since the first appearance of flowering plants, the angiosperms have become the dominant group of land plants (Bell et al. 2010). The occurrence of the most recent common ancestor (MRCA) of the angiosperms has long been of interest, but has proved difficult to accurately place in an evolutionary timeline. Rapid angiosperm expansion occurred during the Cretaceous period about 65–145 million years ago (Ma) (Doyle 2012; Coiro et al. 2019), possibly with multiple radiation events occurring during this period (Bell et al. 2010). Variability in predictions of the molecular clock and lack of fossil evidence of transitory species add to the difficulty of determining the timing of the MRCA (Barba-Montoya et al. 2018; Bell et al. 2010; Coiro et al. 2019; Murat et al. 2017). The discrepancy between fossil evidence and current molecular models is further complicated by differences in molecular evolution between angiosperms and gymnosperms (De La Torre et al. 2017). Overall angiosperms have a molecular evolution rate that is seven times higher compared to gymnosperms making phylogenetic comparisons more complex (De La Torre, et al 2017). The speed and diversification during the early radiation events of the angiosperms further complicate the dating of the MRCA (Li et al. 2019).

A reconstruction of the anatomy of the ancestral flower suggests the MRCA had ten stamens with introrse (inward-facing) anthers, arranged in a whorl and separated from other floral organs (Sauquet et al. 2017). This model, based on floral traits across species, has sparked debate regarding the configuration of the angiosperm MRCA flower (De-Paula et al. 2018; Rümpler and Theißen 2019; Sokoloff et al. 2018). Despite the controversy regarding the exact anatomy of the first flower structure, anther ontogeny has remained largely unchanged within the angiosperm family (Endress and Doyle 2009).

To address trends in evolution of the angiosperm flower and to put developmental events in perspective, comparisons are often made to living basal angiosperms. The earliest diverging angiosperm is *Amborella trichopoda*, the only member of the Amborellales order, that various reports have concluded is the sister group of all living angiosperms (Fig. 1) (Amborella Genome Project 2013; Burleigh et al. 2011; Jansen et al. 2007). Phylogenetic studies where eudicots and monocots are compared to the *Amborella* genome suggest that most of the evolutionary changes in gene networks are shared between closely related taxa (e.g. Solanaceae family), or in terminal branches of the tree (Amborella Genome Project 2013).

Despite complications in determining the MRCA, there is agreement over the initial molecular steps in male reproduction due to the high level of conservation of fundamental stamen development genes within the angiosperm clade (Callens, et al. 2018; Doyle 2012, Theissen and Melzer 2007). Floral development within the angiosperm clade varies extensively, with differences in organisation, number and type of floral organs. Flowers in *Arabidopsis* develop as four whorls of the floral meristem with the outermost, whorl 1, forming sepals, whorl 2 forming petals, whorl 3 stamens and the innermost whorl 4 forming the carpel (Coen and Meyerowitz 1991). The development and distinctions of these whorls are regulated by classes of genes summarised in the ABCDE model of organ formation. In this model, each class encompasses MADS-box transcription factors that are required for a specific organ differentiation, where the B and C genes together with the E genes, generate stamens (Rijpkema et al. 2010; Theißen and Saedler 2001).

Despite differences in flower development, the MADS-box transcription factors described in the ABCDE model are highly conserved among flowering plants (Callens et al. 2018 and references therein). Molecular models suggest the BC genes responsible for reproductive organ formation predate angiosperms and gymnosperm separation and probably existed 300 Ma (Theissen and Melzer 2007). Despite this timescale, orthologues of the B class genes isolated from the gymnosperm *Gnetum gnemon* can partially rescue B class mutants in *Arabidopsis*, supporting a high degree of functional conservation of the MADS-box genes across the plant kingdom (Winter et al. 2002).

Diversity of stamen function and organisation

The fundamental role of the stamen is to produce and release viable pollen; however, stamen diversification has led to additional functions within the angiosperm clade. Stamen reduction, or repurposing, has occurred many times within angiosperm evolution and has been used to prevent self-pollination, trigger pollinator–stamen contact, protect the ovary from damage and attract pollinators, via intense coloration

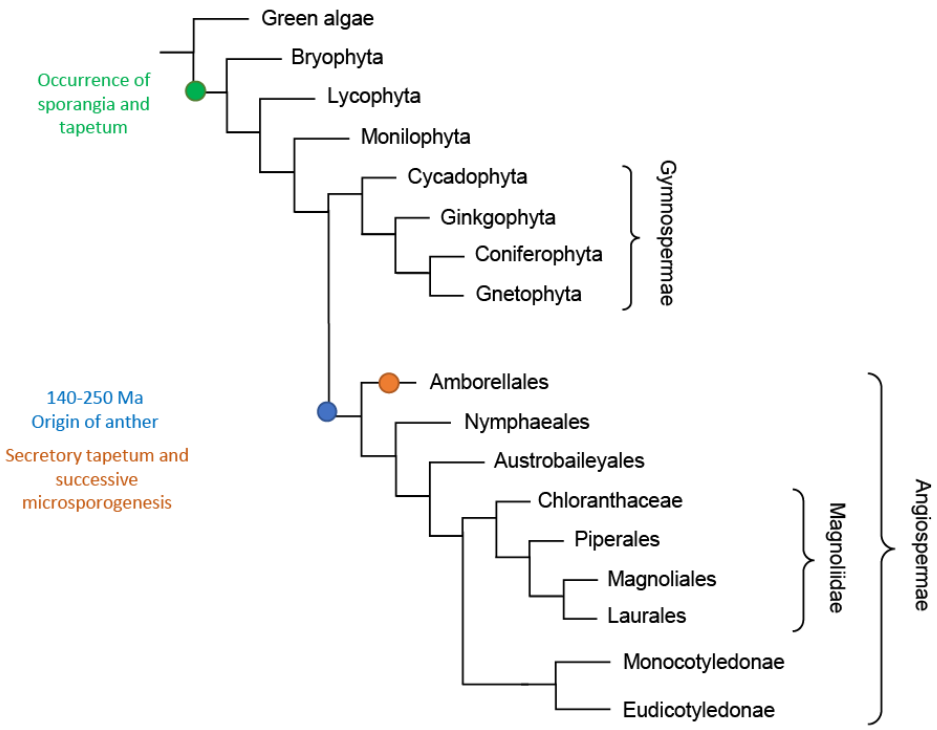

Fig. 1 Phylogenetic tree of land plant evolution. The first angiosperm anther is believed to have occurred 140–250 Ma with the advent of the angiosperm flower (Sauquet et al. 2017). Adapted from (Bhattacharya and Medlin 1998; Endress and Doyle 2009)

and the production of nectar (Walker-Larsen and Harder 2000 and references therein). The diversification of stamens within the same flower, heteranthery, is thought to serve to attract pollinators and enable specific pollinator targeting by sacrificing so-called feeding anthers without impacting overall pollen production (Vallejo-MarÍn et al. 2009). However, recently this view has been challenged by the fact that feeder anthers appear to produce viable pollen and can serve to enhance pollination success by prolonging the timing of pollen release (Kay et al. 2020). This questions this "division of labour" hypothesis and highlights the adaptability and redundancy of the anthers to maximise pollination success (Kay et al. 2020).

In addition to the diversity of stamen function in the angiosperm flower, there is also significant variation in the organisation of stamens. The number of stamens per flower and the type of stamen attachments differ greatly, and these traits are often used as a taxonomic tool for identification of plant families. Stamen filaments also vary, in some basal taxa (e.g. Amborella and some Austrobaileyales) these are flattened sporophyll-like organs with abaxial–adaxial polarity, and this contrasts with the radially symmetrical filaments that are typical of more recently emerged angiosperm lineages (Buzgo et al. 2004; Endress 2001a, b; Endress 1996). Nevertheless, the development and the overall structure of the anther has remained remarkably conserved across the angiosperm clade (Doyle2012; Endress 2001a, b; Hufford and Endress 1989), with divergence in structure and function focusing towards traits that enhance reproductive success (Endress 1996).

Formation of anther structures from the floral meristem

The development of the stamen is initiated with the differentiation of the floral primordia in the third whorl. The stamen primordia differentiate early into the filament and the anther, with loss of any of the B and C homeotic genes preventing stamen formation (Coen and Meyerowitz1991). The meristematic cells divide and differentiate to form the reproductive microsporocytes [pollen mother cells (PMCs)] that give rise to the male gametophyte (pollen) and the somatic cell layers that form the surrounding maternal anther walls (Fig. 2).

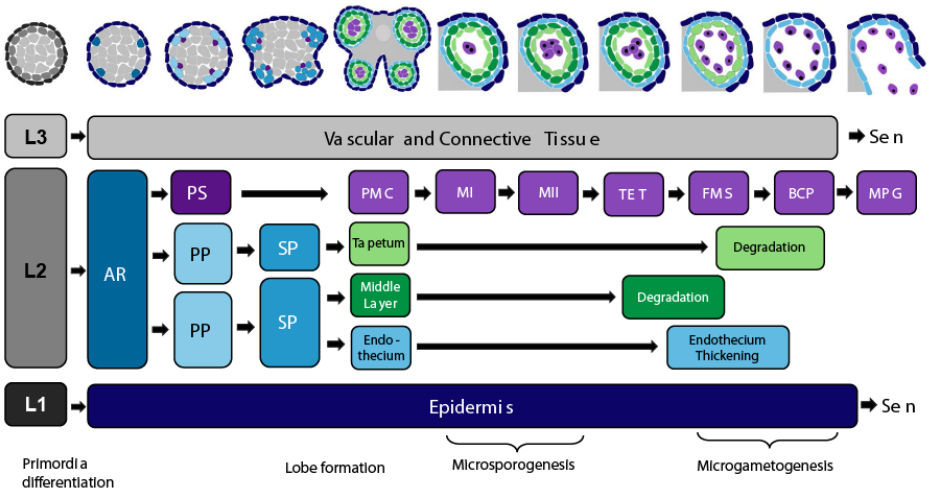

Fig. 2 Schematic view of development of anther layers and microsporogenesis in Arabidopsis. Stamen primordia differentiate into three cell types, L1, L2 and L3, which further differentiate into the epidermis, the archesporial cells and vascular and connective tissues, respectively. Development of the tapetum, middle layer and endothecium follow the dicot model. AR: archesporial cells, BCP: bicellular pollen, FMS: free microspore, MI: meiosis I, MII: meiosis II, MPG: mature pollen grain, PMC: pollen mother cell, PP: primary parietal, PS: primary sporogenous, Sen: senescence, SP: secondary parietal, TET: tetrad

The meristematic cells consist of three germ layers designated L1, L2 and L3 which differentiate to form the anther (Gómez et al. 2015). L1 gives rise to the outermost epidermis and the stomium cell cluster; L2 gives rise to archesporial cells; and L3 gives rise to the connective tissue, vascular bundle and the circular cell cluster (Schnittger et al. 1996). Specification of the anther is initiated by periclinal division of the L2 layer to form archesporial (AR) cells. The AR cells divide to form two cell layers: the reproductive primary sporogenous (PS) cells that later become the microspores and the somatic primary parietal (PP) cells that differentiate into secondary parietal (SP) cells (Canales et al. 2002). These SP cells divide to form the non-reproductive anther wall layers: endothecium, middle layer and tapetum (Scott et al. 2004; Zhang and Yang, 2014). All anther wall layers except the epidermis are derived from L2 cells (Kelliher and Walbot 2011). Timely formation and degeneration of the various anther layers are essential for viable pollen production. Each layer provides vital functions for microspore development or subsequent pollen release, with failure to form or degenerate at the correct developmental stage leading to male sterility. This is particularly evident for defects associated with the tapetum, which is seen in both cytoplasmic male sterile and genic male sterile mutants used in hybrid plant breeding (Kaul 1988).

Differential formation of anther layers

The anther wall layers develop through division of the SP layers in one of four types: basic, dicotyledonous, monocotyledonous and reduced (Fig. 3) (Kelliher et al. 2014). It appears that all types follow the same pattern of stamen primordia differentiation until the development of the SP layers, after which the division of these two cell layers determines the formation type. According to Davis (1966) in the most primitive type (basic type), the two SP cell layers divide once each to form four layers: one endothecium, two middle layers and one tapetum. The dicot and the monocot types both result in three layers: one endothecium, one middle layer and one tapetum. The difference is in the origin of these layers, in the dicot model only the outer SP layer divides to form the endothecium and the middle layer, whereas in the monocot model only the inner SP layer divides to form the middle layer and tapetum. In the reduced form, no division occurs, but the two SP layers differentiate to form the endothecium and the tapetum without the middle layer (Davis 1966).

After the differentiation of the cell layers, additional divisions can occur in the endothecium or middle layer to produce extra layers (Carrizo García 2002b). The number of additional layers produced depends on the species and can vary greatly within plant families (Carrizo García 2002b). In members of the Solanaceae family, species forming via the basic type appear to have more variation in the number of middle layers formed, whereas species developing via the dicot formation type rarely formed more than one additional layer (Carrizo García 2002a). In the vast majority of plant species, only one type of anther wall formation is deployed and the same number of wall layers are produced, but there

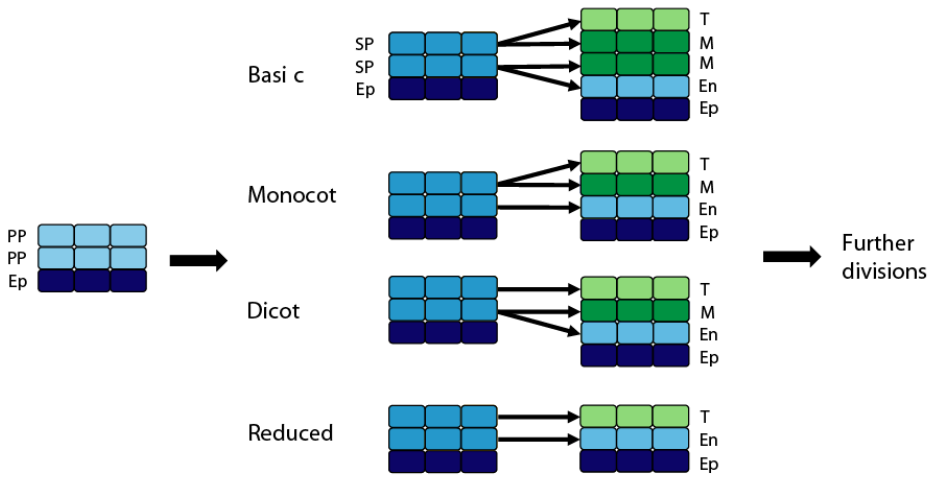

Fig. 3 Anther wall formation types (adapted from Davis1966). In all formation types, the epidermis (dark blue) surrounds the primary parietal cells that differentiate to form secondary parietal cells. The SP cells then differentiate into the endothecium (light blue), middle layer (dark green) and tapetum (light green), according to the formation type associated with each species. Ep: epidermis, En: endothecium, M: middle layer, PP: primary sporogenous cells, SP: secondary sporogenous cells, T: tapetum

are also examples of two formation types being used within the same anther (Bhandari and Sharma1987; Hermann and Palser 2000); however, the significance of these differences for pollen development remains unclear.

It has been suggested that the number of cells in the individual anther layers is important to microspore development. Kelliher and Walbot (2011) hypothesise that the middle layer and tapetum form clusters of cells dedicated to the development of specific pollen grains in maize. Derivates of a single SP cell are then earmarked for individual microspores; mutants where the cell layers are abnormal often fail to produce viable pollen (Feng and Dickinson2010). There is also evidence that the somatic cell layers provide developmental cues to the forming microsporocytes (Wilson and Zhang 2009), including hormone signals regulating anther development (Cecchetti et al. 2017). These observations further support the importance of the correct division, timing and differentiation of SP cells for viable pollen development.

Anther wall development and function

To a certain extent, the anther cell wall division type is conserved within a phylogenetic group; however, some families display multiple division types suggesting they have evolved several times in angiosperms (Carrizo García 2002b). Anthers in the earliest divergent angiosperm *Amborella*, develop via the "basic type" system (Tobe et al. 2000), whilst the "dicot type" appears to have evolved early in the angiosperm clade in Schisandraceae, in the Austrobaileyales order (Vijayaraghavan and Dhar1975). In monocots, most members of the Poales order have the monocot type of anther wall development, but some early divergent members have the reduced or the basic type (Sajo et al. 2009). In the Asteraceae, the largest family of the dicots, anthers tend to develop through the dicot type (Ao et al. 2009), whereas in the Solanaceae species, 64% have a basic-type anther and 36% dicot (Carrizo García 2002b). In other families, such as the Ericaceae, several anther types exist (Hermann and Palser 2000), suggesting that the formation type is labile and highly variable throughout the angiosperm clade.

Since the introduction of this system of anther wall classification by Davis (1966), the pattern of cell division of the lineages is generally represented as occurring sequentially in all cells. This view is further supported by studies of anther development where a transverse anther section shows synchronised cells in one plane as representative for the entire anther. There is, however, very little information on the timing of the specification throughout the length of the anther, and the division pattern might not be as rigid as previously thought. When the anther is imaged longitudinally, there seems to be more flexibility in the origin of the cell layers rather than the strict somatic or germinal cell fates depicted in the traditional models (Kelliher, et al. 2014). The cells do not differentiate immediately after divisions, but go through mitosis at different rates making it difficult to determine a single anther wall formation type (Kelliher et al. 2014). Additionally, the classifications offered by Davis (1966) might not encompass all forms of anther wall development.

For example, in many species in the Ericaceae the anther wall layers divide in a pattern that cannot be applied to any of the current types (Hermann and Palser 2000), suggesting that the manner of division of the SP cell layers is complex and diverse.

Evolution of sporogenous cells

Alongside the formation of the anther wall layers from secondary sporogenous cells, the reproductive primary sporogenous cells divide to form the pollen mother cells (PMCs), which go through meiosis to form microspores and subsequently develop into pollen grains. It is in the microsporangia that the microspores divide and develop into mature pollen grains, through the support of the surrounding anther wall layers and the deposition of the intricate pollen wall (Furness et al. 2002). In general, an anther contains four microsporangia divided into two thecae (Endress 1996). The development of sporangia was one of the key innovations which enabled plants to colonise the land, since within these structures hardy spores could be formed which enabled dispersal of genetic material in dry environments (Tanurdzic and Banks 2004).

As a crucial part of the lifecycle of all plants, sporangia exist even in the most basal of land plants: the non-vascular bryophytes (liverworts, hornworts and mosses) and vascular lycophytes (club mosses, spike mosses and whisk ferns) and monilophytes (true ferns). Sporangia have evolved to efficiently disperse spores. In the case of ferns the developing spore mother cells undergo meiosis surrounded by a layer of annulus cells, which dehydrate to cause the sporangia to open at the stomium in a catapult-like manner to rapidly discharge the spores (Noblin et al. 2012). In turn, these spores develop into the gametophytes, which contain antheridia where the sperm cells are produced.

In seed-setting plants, the gametophyte stage is simply condensed into the developing microspore and the mature pollen is essentially the antheridium. Stamens evolved from leaf-like structures bearing microsporangia. Most extant spermatophytes possess stamen-like structures, containing microsporocytes which undergo meiosis to form haploid microspores and subsequently develop into mature pollen grains. The development of pollen from microsporangia is a conserved process for all heterosporous plants including angiosperms and gymnosperms. In terms of thecal organisation, the "stamens" of gymnosperms such as *Ginkgo biloba*, Gnetumand conifers are more simplistic than their angiosperm counterparts. Whereas angiosperm stamens typically have four microsporangia arranged into two theca on each side of the stamen, gymnosperm stamens are disporangiate with a singular microsporangium situated on each side of the filament and thus have no theca (Endress 2001a, b). Whilst there are some angiosperm groups that lack theca (Endress and Stumpf 1990) arguably, organisation of microsporangia into theca was a key innovation in angiosperm anther evolution that has enabled more efficient pollen release.

Microsporogenesis types

During microsporogenesis, the microsporocytes go through two rounds of meiosis inside the microsporangia to form microspores. Generally, there are two types of microsporogenesis observed, simultaneous and successive, although intermediate types are increasingly being discovered. The types differ in the timing of meiosis in relation to the separation of microspores by the formation of the callose wall. In simultaneous microsporogenesis, meiosis I and II occur without interruption simultaneously alongside callose wall deposition, generally resulting in tetrahedral tetrads. In the successive type there is a pause between meiosis I and II where the callose wall is deposited to form distinct dyads, typically producing tetragonal tetrads (Sajo et al. 2009). However, Furness et al. (2002) argue that the types of microsporogenesis are more complicated than just the simultaneous and the successive, and that the intermediate type is more common than previously thought. Fossil records from the Ordovician period (444–489 Ma) have identified the simultaneous type, prior to the appearance of angiosperms (Furness et al. 2002). In the earliest divergent species from the angiosperms, the Amborellales (Tobe et al. 2000) and members of the Nymphaeales (Taylor and Osborn 2006), the microsporogenesis is successive, suggesting the first angiosperm anther developed via the successive type of microsporogenesis. Most eudicots have simultaneous microsporogenesis with few exceptions (Furness et al. 2002), whereas in the monocots the successive type is predominant, but there are several families where the simultaneous is seen. Taken together, this suggests there have been multiple events of either secondary loss or divergent evolution of the simultaneous and successive types, and a high degree of specificity is preferred in the microsporogenesis type (Furness et al. 2002). However, the significance of this in relation to pollen function and resilience is currently unclear.

Evolution of tapetum formation and function

The tapetum is the innermost layer of the anther walls (Fig. 2), which is critical for the regulation of pollen development and the synthesis of the pollen wall. Tapetal cells go through a regulated Programmed Cell Death (PCD) that is required for viable pollen formation, where wall materials, such as carbohydrates, lipidic molecules, sporopollenin precursors and nutrients, are secreted into the locules and the developing microspores (Zhang et al. 2011). This specialised cell layer is essential for microspore nutrition and is present in all land plants from the more basal bryophytes to

spermatophytes under various descriptors, such as "nutritive cells" or "spore sac layer cells" (Pacini et al. 1985).

The tapetum is almost exclusively single layered; multilayered tapeta are very rare in angiosperms, and in monocotyledons, it has been reported only in Abolboda and Orectanthe in the Xyridaceae family (Oriani and Scatena 2015). The number of layers of the anther wall seems to be critical for pollen production, with changes in the tapetum being particularly detrimental, with additional tapetum layers resulting in male sterility (Cecchetti et al. 2015; Chaubal et al. 2000, Feng and Dickinson 2010).

There are generally two types of tapeta. The first is the secretory, or glandular, where the tapetum remains in situ in the anther locule whilst synthesising and secreting pollen wall materials, and subsequently breaks down. The other is the plasmodial, or amoeboid type, where the tapetum cell walls break down to release protoplasts that fuse to form a multinucleate plasmodium. A third, less common, type is the invasive tapetum, which is mostly found in the Asteraceae, where the cell walls of the tapetum dissolve and disperse among the developing microspores (Tiwari and Gunning 1986). Individuals usually have only one type of tapetum, but there are occasions, e.g. in safflower Carthamus tinctorius, where two types of tapetal cells coexist (Yeung et al. 2011). Additionally, Sajo et al (2005) hypothesise there might be an intermediate tapetum type, where an early-stage secretory tapetum subsequently becomes invasive. The significance of two types coexisting, working independently or transitioning from one to another is still unclear, but it suggests there are intricate adaptations and specific regulation of tapetum development.

Both secretory and plasmodial types are common in dicots and monocots. The secretory tapetum probably had several independent origins (Oriani and Scatena 2015) and is regarded as the most primitive form (Furness and Rudall 1998; Pacini et al. 1985). The early divergent angiosperm Amborella has a secretory tapetum (Tobe et al. 2000), which also appears to be the most common type in primitive dicotyledons (Furness and Rudall 1998). Both types of tapeta are found throughout the monocot clade, suggesting secretory and plasmodial forms have evolved several times in monocotyledons (Furness and Rudall 1998). The variability in tapetum type within the angiosperm clade, where reversals or re-evolving of the types occurs throughout the taxa, again further supports the significance of the tapetum and the importance of precise control of its development and function.

Variability and function of the anther middle layer in pollen development

The function of the middle layer is not fully established since mutants displaying middle layer defects also tend to show tapetum abnormalities, making it difficult to determine its independent function. The middle layer was long thought to have no function and be a leftover relic from pre-angiosperm anther structures (Davis 1966). More recently, however, it has been shown to have a secretory function similar to the tapetum, with failure in degeneration leading to male sterility through delayed exine deposition (Falasca et al. 2013). Once the middle layer has formed it becomes thinner throughout pollen formation and is completely degenerated by anther dehiscence. Kelliher and Walbot (2011) hypothesise that the tapetum and middle layer derive from a single secondary parietal cell, providing the nutrients required for the development of a single microspore.

The middle layer is important for pollen formation in many species yet there is high variability in the number of middle layers. No middle layer is formed in reduced-type anthers (Fig. 3), whereas some species undergo additional divisions to form multiple layers, with as many as nine middle layers in Hawkesiophyton panamense in the Solanaceae family (Carrizo García 2002a). The reason for this diversity in the number of layers, along with the specific function of the middle layer is currently not known, although may be due to environmental responses. In cereal crops, drought stress during the meiotic and mitotic stages can lead to an expanded middle layer, possibly due to increase sugar transport to the microspores in response to water deficiency (Yu et al. 2019). In late stamen development, the middle layer is involved in pollen maturation and anther dehiscence by controlling auxin signalling (Cecchetti et al. 2017), suggesting that the middle layer may be important in signalling during multiple stages of anther and pollen development.

The importance of anther wall PCD for sex determination

Developmentally programmed cell death (dPCD) is an integral process for pollen development and release, as well as floral organ differentiation (reviewed in Wang et al. 2021). Degeneration of the tapetum and the middle layer provides nutrients to the developing microspore, and degradation of the septum and stomium facilitates anther opening. A common cause of male sterility is the mistimed degeneration of anther wall layers, primarily the tapetum. Mistimed PCD prevents viable pollen formation and is one of the strategies developed by angiosperms to produce unisexual flowers (Flores-Rentería et al. 2013; Hernández-Cruz et al. 2019; Ren et al. 2019). Normal degeneration of the tapetum and middle layer tissues is vital for the provision of nutrients and wall materials for pollen maturation. Infertility in a variety of species such as Tapiscia sinensis, an androdioecious tree, or in dioecious cacti, in the Opuntia family is ensured by preventing the deposition of essentials materials for mature pollen formation, without the need to restructure the anther

(Flores-Rentería et al. 2013; Hernández-Cruz et al. 2019; Ren et al. 2019).

Anther dehiscence

Types of anther dehiscence

Across the angiosperm clade, many different types of dehiscence have evolved. The way in which the anther opens is one of many factors that determines the pollination syndrome of a flower (Bernhardt1996). The dehiscence process is determined by the shape, position and anatomical features of the stomium, endothecium as well as the anther attachment point.

There are four known types of anther splitting: longitudinal, transverse, poricidal and valvate that can occur as introrse (pollen release towards the centre of the flower) or extrorse (pollen release outwards, away from the centre of the flower). In longitudinal dehiscence, the anther splits along the long axis of the theca and is the most common method of anther opening. It is typical of many angiosperms and is found in both monocotyledonous and dicotyledonous species in a wide taxonomic range. Transverse dehiscence is similar to longitudinal dehiscence; however, the split is at right angles to the long axis of the theca. Poricidal dehiscence can be seen in anthers that shed their pollen via terminal apertures, for example in members of the Melastomataceae (Renner1989), Solanaceae (Bohs 2005) and Leguminosae (Marazzi et al. 2007). Poricidal dehiscence has adaptive value to pollinators capable of collecting pollen by the high frequency vibration of stamens (De Luca and Vallejo-Marín 2013; Larson and Barrett 1999). Finally, valvate dehiscence is where pollen is released through a pore that is covered by a flap of tissue. This type of dehiscence is rare, but is occasionally seen in members of the Hamamelidaceae (Hufford and Endress1989), Magnoliids (Endress and Hufford1989) and Berberidaceae (Batygina2002).

Endothecium development and secondary thickening

Multiple anther wall layers appear to work collectively not only in the development of the microspores, but in the release of mature pollen grains. The endothecium plays an important role in anther dehiscence and pollen release by interacting with the middle layer and the tapetum. After microspore meiosis, alongside degeneration of the tapetum and middle layers, the endothecium undergoes specific secondary thickening (Wilson et al. 2011). Thickening of the endothecial layer occurs prior to anther dehiscence and serves to build tension in the remaining anther layers to generate sufficient force to break the stomium, retract the anther walls as they dehydrate and disperse the pollen (Keijzer 1987; Nelson et al. 2012). In addition to aiding anther dehiscence, the endothecium appears to serve as a last storage site for lipids during the final stages of pollen development, and fatty acids derived from the endothecium are thought to help facilitate pollen hydration (Zhan et al. 2018; Zhu et al. 2020). Formation of secondary wall thickening in the Arabidopsis endothecium layer appears to be regulated principally by three transcription factors MYB26, NAC Secondary Wall Promoting Factor 1 (NST1) and NST2 (Mitsuda et al. 2005; Yang et al. 2007 2017). This secondary thickening process appears conserved across different species and is at least in part orchestrated via auxin signalling (Cecchetti et al. 2013); however, few genes have been isolated that are specific to the endothecium.

Endothecial secondary thickening is highly variable between taxa with distinct deposition patterns impacting anther opening. Attempts have been made to draw phylogenetic information from these patterns, but this has been unsuccessful due to the complex interspecies variation observed (Carrizo García 2002a). Endothecial thickening patterns seem insensitive to ecological influences and there is no direct correlation between them and the dehiscence type (Manning 1996). For example, Manning (1996) highlights that "U-shaped" thickenings occur in different species with each of the different dehiscence types, in anthers that are versatile (filament attached at the centre) or basifixed (filament attached at the base).

Some angiosperm clades do not develop endothecium thickening, but utilise alternative mechanisms to generate the force required to open the stomium. These include some species within the Ericaceae (Hermann and Palser2000), Leguminosae (Marazzi et al. 2007) and Melastomataceae (Cortez et al. 2014). Most species within the Ericaceae form an alternative specific fibrous tissue called the resorption tissue that has been reported to be involved in anther dehiscence (Hermann and Palser2000). The Senna group of the Leguminosae rely on thick walled hypodermal and subhypodermal cells as an alternative to the classical thickening of the endothecium (Marazzi et al. 2007). Uniquely, the Melastomataceae represents one of few families with poricidal dehiscence that does not have a specialised mechanical tissue (Cortez et al. 2014). Successful dehiscence in this family relies on specific dehydration of cells in the pore region of the anther, whilst the cuticle prevents dehydration of the surrounding cells (Cortez et al. 2014).

Anther stomium and septum degeneration

For pollen to be released from the anther, the septum and stomium must undergo controlled degeneration. During anther dehiscence the septum, a region of cells located between the lobes of the theca, degrades to create a single

lobe. The stomium is formed by differentiation of epidermal cells along the anther which produces a single cell region through which pollen will be released (Wilson et al. 2011). This differentiation of cells in the epidermis occurs early in development, at a similar time to when the tapetum forms (Bonner and Dickinson 1989).

Solanaceous species have a unique adaptation that is not found in either *Arabidopsis* or Lilium. They possess specialised cells in the "notch" region under the stomium called the circular cell cluster (also referred to as: intersporangial septum, hypodermal septum or oxalate package). These highly specialised subepidermal cells, derived from the L2 primordium that accumulate and release calcium oxalate, which is thought to be important for dehiscence and to provide calcium for pollen germination (Iwano et al. 2004). Cells within the circular cell cluster degenerate prior to those in the stomium, facilitating the formation of a bilocular anther. In other non-solanaceous species that lack a circular cell cluster, this role is facilitated by different non-specific cells found in the "notch" region.

Anther dehydration

Anther dehydration is one of the final processes that facilitate anther dehiscence and pollen release. Firstly, once the pollen grains have fully developed, the locular fluid is removed to facilitate pollen dispersal. Next, the anther wall is dehydrated, which is hypothesised to be crucial to generate the required force to bend and open the anther (Nelson et al. 2012). This process is orchestrated by dehydration of the anther walls causing the anthers to retract (Keijzer 1987). In cereal crops, temperature has been shown to influence anther dehiscence (Fernández-Gómez et al. 2020; Matsui and Hasegawa 2019). In barley, the fertility of HvMS1 overexpression lines display temperature dependent reversible sterility. Anthers of the HvMS1 overexpression line produce viable pollen, but fail to dehisce at lower temperature and lead to a reduction in seed set in barley (Fernández-Gómez et al. 2020). Additionally, the duration of anther dehiscence influences seed set in rice, specifically at higher temperatures longer anther dehiscence is seen which favourably improves pollination (Matsui and Hasegawa 2019).

Impact of hormones on stamen development and pollen release

Most hormones have been shown to be involved in all stages of stamen development, as reviewed by Chandler (2011). Gibberellins have generally been associated with early filament elongation and tapetum development, whereas jasmonic acid (JA) has been linked to later stages of pollen maturation, filament extension and anther dehiscence in higher land plants (Marciniak and Przedniczek 2019; Susheng Song et al. 2011). The effects of hormonal signalling on fertility are not always conserved among land plants. In *Arabidopsis*, MYC proteins promote stamen development by activating JA signalling (Chen et al. 2016), whereas the orthologous MYC proteins in the liverwort Marchantia polymorphado not affect fertility despite being involved with JA signalling (Peñuelas et al. 2019).

Defects in auxin signalling through the disruption of ARF6 and ARF8 function prevents stomium degeneration and pollen release (Nagpal et al. 2005; Zheng et al. 2019). In addition, the function and production of auxin in regard to floral organ initiation have been shown to be conserved in highly diverged plant families, suggesting the hormonal network evolved in an common ancestor (Chandler 2011 and references therein).

Lack of information in basal lineages has made it difficult to confirm the evolution of the auxin pathway in vascular plants. The auxin response is proposed to have emerged as a response to multicellular growth in land plants, although this can be questioned by the presence of auxin pathways in green, red and brown algae (De Smet et al. 2011; Lau et al. 2009; Le Bail et al. 2010; Rensing et al. 2007; Sztein et al. 2000). Identification of a putative functional YUCCA gene, involved in auxin biosynthesis, in green algae suggests some conservation in basal lineages of land plants (De Smet et al. 2011). Furthermore, bryophytes have been shown to have a basic nuclear auxin pathway that contains three classes of ARFs and TIR1/AFB-AUX/IAA co-receptor, indicating the presence of an auxin response pathway in a common ancestor of land plants (Kato et al. 2018; Lavy et al. 2016; Plavskin et al. 2016; Tsuzuki et al. 2016). It is thought that ARF-like transcription factors and auxin co-receptors were established in charophytes, but their involvement in auxin signalling is unknown (Kato et al. 2018; Wang et al. 2015). The role of auxin in the regulation of anther dehiscence has been established in land plants such as *Arabidopsis* (Cecchetti et al. 2013) and rice (Shiyong Song et al. 2018; Zhao et al. 2013). However, better understanding of the evolutionary development of this response in land plants, compared to basal lineages, requires the identification of hormonal response in more diverse species.

Conclusions

The evolution of the anther was a key event associated with the reproductive success of the angiosperms. The complexity and diversity in the formation, anatomy and dehiscence of the male reproductive organ highlight the importance of the stringent control required for successful pollination. Model species allow detailed study of these phenomena; however, significant diversity exists throughout the angiosperm clade which is important to acknowledge to prevent

generalisations about pollination. Studying pollen development and the anther function in an evolutionary context helps facilitate understanding of essential genetic pathways and developmental events, and can be used to further sustainable plant breeding and agricultural practices.

Authors' contribution All authors contributed to the article conception. JA wrote the manuscript with support from CK and BT. JA and CK designed the artwork. JA, JR, CK and ZW edited the manuscript.

Funding ZAW receives funding from the Biotechnology and Biological Sciences Research Council (BBSRC) [grant no. BB/P002080/1]; JA is supported by a University of Nottingham (UoN) BBSRC Doctoral Training Partnership (DTP) NPIF CASE award with support from Agriculture and Horticulture Development Board (AHDB), KWS UK Ltd, Limagrain UK Ltd, RAGT Seeds Ltd, and SECOBRA Recherches. CK is supported by a UoN BBSRC DTP CASE with KWS UK Ltd, and Syngenta Seeds. JKR is supported through UoN BBSRC DTP; BT is supported by the Royal Society Challenge-led (Grant No. CHL\R1\180496).

Declarations

Conflict of interests The authors have no conflicts of interest to declare that are relevant to the content of this article.

References

Amborella Genome Project (2013) The Amborella genome and the evolution of flowering plants. Science.https://doi.org/10.1126/science.1241089

Ao C, Wang L, Liang L, Wang X (2009) Anther wall formation, microsporogenesis and male gametogenesis of four closely related species in Astereae (Asteraceae): description, comparison and systematic implications. Nord J Bot 27(4):292–297. https://doi.org/10.1111/j.1756-1051.2009.00331.x

Barba-Montoya J, dos Reis M, Schneider H, Donoghue PCJ, Yang Z (2018) Constraining uncertainty in the timescale of angiosperm evolution and the veracity of a Cretaceous Terrestrial Revolution. New Phytol 218(2):819–834. https://doi.org/10.1111/nph.15011

Batygina TB (2002) Embryology of flowering plants: Terminology and concepts. Generative organs of flowers, 1st edn. Science Pub Inc., Enfield

Bell CD, Soltis DE, Soltis PS (2010) The age and diversification of the angiosperms re-revisited. Am J Bot 97(8):1296–1303.https://doi.org/10.3732/ajb.0900346

Bernhardt P (1996) Anther adaptation in animal pollination. In: D'Arcy WG, Keating RC (eds) The anther form, function and phylogeny. Cambridge University Press, Cambridge, pp 192–220

Bhandari N, Sharma M (1987) Histochemical and ultrastructural studies during anther development in Solanum nigrumL I. Early ontogeny. Phytomorphology 37:249–260

Bhattacharya D, Medlin L (1998) Algal phylogeny and the origin of land plants. Plant Physiol 116(1):9–15. https://doi.org/10.1104/pp.116.1.9

Bohs L (2005) Major clades in solanum based on ndhF sequence data. In: Keating R, Hollowell VC, Croat T (eds) A festschrift for William G. D'Arcy: The legacy of a taxonomist. Missouri Botanical Garden Press, St. Louis, pp 27–49

Bonner LJ, Dickinson HG (1989) Anther dehiscence in Lycopersicon esculentum Mill. New Phytol 113:97–115. https://doi.org/10.1111/j.1469-8137.1989.tb02399.x

Burleigh JG, Bansal MS, Eulenstein O, Hartmann S, Wehe A, Vision TJ (2011) Genome-scale phylogenetics: Inferring the plant tree of life from 18,896 gene trees. Syst Biol 60(2):117–125. https://doi.org/10.1093/sysbio/syq072

Buzgo M, Soltis PS, Soltis DE (2004) Floral Developmental Morphology of Amborella trichopoda(Amborellaceae). Int J Plant Sci 165(6):925–947

Callens C, Tucker MR, Zhang D, Wilson ZA (2018) Dissecting the role of MADS-box genes in monocot floral development and diversity. J Exp Bot 69(10):2435–2459. https://doi.org/10.1093/jxb/ery086

Canales C, Bhatt AM, Scott R, Dickinson H (2002) EXS, a putative LRR receptor kinase, regulates male germline cell number and tapetal identity and promotes seed development in Arabidopsis. Curr Biol 12(20):1718–1727. https://doi.org/10.1016/S0960-9822(02)01151-X

Carrizo García C (2002a) An approach to the diversity of endothecial thickenings in Solanaceae. Flora 197(3):214–223.https://doi.org/10.1078/0367-2530-00032

Carrizo García C (2002b) Anther wall formation in Solanaceae species. Ann Bot 90(6):701–706. https://doi.org/10.1093/aob/mcf248

Cecchetti V, Altamura MM, Brunetti P, Petrocelli V, Falasca G, Ljung K, Costantino P, Cardarelli M (2013) Auxin controls Arabidopsis anther dehiscence by regulating endothecium lignification and jasmonic acid biosynthesis. Plant J 74(3):411–422. https://doi.org/10.1111/tpj.12130

Cecchetti V, Brunetti P, Napoli N, Fattorini L, Altamura MM, Costantino P, Cardarelli M (2015) ABCB1 and ABCB19 auxin transporters have synergistic effects on early and late Arabidopsis anther development. J Integr Plant Biol 57(12):1089–1098. https://doi.org/10.1111/jipb.12332

Cecchetti V, Celebrin D, Napoli N, Ghelli R, Brunetti P, Costantino P, Cardarelli M (2017) An auxin maximum in the middle layer controls stamen development and pollen maturation in Arabidopsis. New Phytol 213(3):1194–1207. https://doi.org/10.1111/nph.14207

Chandler JW (2011) The hormonal regulation of flower development. J Plant Growth Regul 30(2):242–254. https://doi.org/10.1007/s00344-010-9180-x

Chaubal R, Zanella C, Trimnell MR, Fox TW, Albertsen MC, Bedinger P (2000) Two male-sterile mutants of Zea mays (Poaceae) with an extra cell division in the anther wall. Am J Bot 87(8):1193–1201. https://doi.org/10.2307/2656657

Chen X, Huang H, Qi T, Liu B, Song S (2016) New perspective of the bHLH-MYB complex in jasmonate-regulated plant fertility in arabidopsis. Plant Signal Behav 11(2):1–4. https://doi.org/10.1080/15592324.2015.1135280

Cigan AM, Unger E, Xu R, Kendall T, Fox TW (2001) Phenotypic complementation of ms45 requires tapetal expression of MS45.

Sex Plant Reprod 14:135–142. https://doi.org/10.1007/s00497-001-00099

Coen ES, Meyerowitz EM (1991) The war of the whorls: genetic interactions controlling flower development. Nature 353(6339):31. https://doi.org/10.1038/353031a0

Coiro M, Doyle JA, Hilton J (2019) How deep is the conflict between molecular and fossil evidence on the age of angiosperms? New Phytol 223(1):83–99. https://doi.org/10.1111/nph.15708

Cortez PA, Caetano AP et al (2014) Elucidating the mechanism of poricidal anther dehiscence in Miconia species (Melastomataceae). Flora 209(10):571–579. https://doi.org/10.1016/j.flora.2014.07.002

Davis GL (1966) Systematic embryology of the angiosperms. Wiley, New York

De-Paula OC, Assis LCS, Ronse de Craene LP (2018) Unbutton - ing the ancestral flower of angiosperms. Trends Plant Sci 23(7):551–554. https://doi.org/10.1016/j.tplants.2018.05.006

De La Torre AR, Li Z, Van De Peer Y, Ingvarsson PK (2017) Con - trasting rates of molecular evolution and patterns of selection among gymnosperms and flowering plants. Mol Biol Evol 34(6):1363–1377. https://doi.org/10.1093/molbev/msx069

De Luca PA, Vallejo-Marín M (2013) What's the "buzz" about? The ecology and evolutionary significance of buzz-pollination. Curr Opin Plant Biol 16(4):429–435. https://doi.org/10.1016/j.pbi.2013.05.002

De Smet I, Voß U, Lau S, Wilson M, Shao N, Timme RE, Swarup R, Kerr I, Hodgman C, Bock R, Bennett M, Jürgens G, Beeck - man T (2011) Unraveling the evolution of auxin signaling. Plant Physiol 155(1):209–221. https://doi.org/10.1104/pp.110.168161

Doyle JA (2012) Molecular and fossil evidence on the origin of angiosperms. Annu Rev Earth Planet Sci 40(May):301–326. https://doi.org/10.1146/annurev-earth-042711-105313

Drábková LZ, Honys D (2017) Evolutionary history of callose synthases in terrestrial plants with emphasis on proteins involved in male gametophyte development. PLoS ONE 12(11):1–24.https://doi.org/10.1371/journal.pone0187331

Endress PK, Stumpf S (1990) Non-tetrasporangiate stamens in the angiosperms: structure, systemic distribution and evolutionary aspects. Schweizerbart'sche Verlagsbuchhandlung, Stuttgart

Endress PK (1996) Diversity and evolutionary trends in angiosperm anthers. In: D'Arcy WG, Keating RC (eds) The anther form, function and phylogeny. Cambridge University Press, Cambridge, pp 92–110

Endress P (2001a) The flowers in extant basal angiosperms and inferences on ancestral flowers. Int J Plant Sci 162(5):1111–1140

Endress PK (2001b) Origins of flower morphology. J Exp Zool 291(2):105–115. https://doi.org/10.1002/jez.1063

Endress PK, Doyle JA (2009) Reconstructing the ancestral angiosperm flower and its initial specializations. Am J Bot 96(1):22–66. https://doi.org/10.3732/ajb.0800047

Endress PK, Hufford LD (1989) The diversity of anther structures and dehiscence patterns among Magnoliidae. Bot J Linn Soc 99(4):301–346. https://doi.org/10.1111/j.1095-8339.1989.tb00406.x

Falasca G, D'Angeli S, Biasi R, Fattorini L, Matteucci M, Canini A, Altamura MM (2013) Tapetum and middle layer control male fertility in Actinidia deliciosa. Ann Bot 112(6):1045–1055. https://doi.org/10.1093/aob/mct173

Feng X, Dickinson HG (2010) Tapetal cell fate, lineage and proliferation in the Arabidopsis anther. Development 137(14):2409–2416. https://doi.org/10.1242/dev.049320

Fernández-Gómez J, Talle B, Wilson ZA (2020) Increased expression of the MALE STERILITY1 transcription factor gene results in temperature-sensitive male sterility in barley. J Exp Bot 71(20):6328–6339. https://doi.org/10.1093/jxb/eraa382

Flores-Rentería L, Orozco-Arroyo G, Cruz-García F, García-Campu - sano F, Alfaro I, Vázquez-Santana S (2013) Programmed cell death promotes male sterility in the functional dioecious Opuntia stenopetala(Cactaceae). Ann Bot 112(5):789–800. https://doi.org/10.1093/aob/mct141

Furness CA, Rudall PJ (1998) The tapetum and systematics in monocotyledons. In: Bot rev 64(3) https://doi.org/10.1007/bf02856565

Furness CA, Rudall PJ (2001) The tapetum in basal angiosperms: early diversity. Int J Plant Sci 162(2):375–392. https://doi.org/10.1086/319580

Furness CA, Rudall PJ, Sampson FB (2002) Evolution of microsporogenesis in angiosperms. Int J Plant Sci 163(2):235–260. https://doi.org/10.1086/338322

Gómez JF, Talle B, Wilson ZA (2015) Anther and pollen development: a conserved developmental pathway. J Integr Plant Biol 57(11):876–891. https://doi.org/10.1111/jipb.12425

Hermann PM, Palser BF (2000) Stamen development in the Ericaceae. I. Anther wall, microsporogenesis, inversion, and appendages. Am J Bot 87(7):934–957. https://doi.org/10.2307/2656993

Hernández-Cruz R, Silva-Martínez J, García-Campusano F, Cruz-García F, Orozco-Arroyo G, Alfaro I, Vázquez-Santana S (2019) Comparative development of staminate and pistillate flowers in the dioecious cactusOpuntia robusta Plant Reproduction 32(3):257–273. https://doi.org/10.1007/s00497-019-00365-w

Hufford LD, Endress PK (1989) The diversity of anther structures and dehiscence patterns among Hamamelididae. Bot J Linn Soc 90:301–346

Iwano M, Entani T, Shiba H, Takayama S, Isogai A (2004) Calcium crystals in the anther of petunia: the existence and biological significance in the pollination process. Plant Cell Physiol 45(1):40–47. https://doi.org/10.1093/pcp/pch004

Jansen RK, Cai Z, Raubeson LA et al (2007) Analysis of 81 genes from 64 plastid genomes resolves relationships in angiosperms and identifies genome-scale evolutionary patterns. Proc Natl Acad Sci USA 104(49):19369–19374. https://doi.org/10.1073/pnas.0709121104

Kato H, Nishihama R, Weijers D, Kohchi T (2018) Evolution of nuclear auxin signaling: Lessons from genetic studies with basal land plants. J Exp Bot 69(2):291–301. https://doi.org/10.1093/jxb/erx267

Kaul MLH (1988) Male Sterility in Higher Plants. Springer, Berlin. https://doi.org/10.1007/978-3-642-83139-3

Kay KM, Jogesh T, Tataru D, Akiba S (2020) Darwin's vexing contrivance: a new hypothesis for why some flowers have two kinds of anther: heteranthery in Clarkia. Proc R Soc B Biol Sci. https://doi.org/10.1098/rspb.2020.2593rspb20202593

Keijzer CJ (1987) The processes of anther dehiscence and pollen dispersal. New Phytol 105:499–507. https://doi.org/10.1111/j.1469-8137.1987.tb00886.x

Kelliher T, Egger RL, Zhang H, Walbot V (2014) Unresolved issues in pre-meiotic anther development. Front Plant Sci 5:1–9.https://doi.org/10.3389/fpls.2014.00347

Kelliher T, Walbot V (2011) Emergence and patterning of the five cell types of theZea mays anther locule. Dev Biol 350(1):32–49. https://doi.org/10.1038/jid.2014.371

Larson BMH, Barrett SCH (1999) The pollination ecology of buzz-pollinated Rhexia virginica (Melastomataceae). Am J Bot 86(4):502–511. https://doi.org/10.2307/2656811

Lau S, Shao N, Bock R, Jürgens G, De Smet I (2009) Auxin signaling in algal lineages: fact or myth? Trends Plant Sci 14(4):182–188. https://doi.org/10.1016/j.tplants.2009.01.004

Lavy M, Prigge MJ, Tao S, Shain S, Kuo A, Kirchsteiger K, Estelle M (2016) Constitutive auxin response in Physcomitrella reveals complex interactions between Aux/IAA and ARF proteins. Elife 5:1–22. https://doi.org/10.7554/eLife.13325

Le Bail A, Billoud B, Kowalczyk N, Kowalczyk M, Gicquel M, Le Panse S, Stewart S, Scornet D, Cock JM, Ljung K, Charrier B (2010) Auxin metabolism and function in the multicellular brown alga ectocarpus siliculosus. Plant Physiol 153(1):128–144. https://doi.org/10.1104/pp.109.149708

Li HT, Yi TS, Gao LM et al (2019) Origin of angiosperms and the puzzle of the Jurassic gap. Nature Plants 5(5):461–470.https://doi.org/10.1038/s41477-019-0421-0

Manning JC (1996) Diversity of endothecial patterns in the angiosperms. In: D'Arcy WG, Keating RC (eds) The anther form, function and phylogeny. Cambridge University Press, Cambridge, pp 136–158

Marazzi B, Conti E, Endress PK (2007) Diversity in anthers and stigmas in the buzz-pollinated genus Senna (Leguminosae, Cassiinae). Int J Plant Sci 168(4):371–391. https://doi.org/10.1086/512105

Marciniak K, Przedniczek K (2019) Comprehensive insight into gibberellin- and jasmonate-mediated stamen development. Genes. https://doi.org/10.3390/genes10100811

Matsui T, Hasegawa T (2019) Effect of long anther dehiscence on seed set at high temperatures during flowering in rice (Oryza sativa L.). Sci Rep 9(1):3–10. https://doi.org/10.1038/s41598-019-56792-2

Mitsuda WN, Seki M, Shinozaki K, Ohme-Takagi M, Mitsuda N, Seki M, Shinozaki K, Ohme-Takagi M (2005) The NAC transcription factors NST1 and NST2 of Arabidopsis regulate secondary wall thickenings and are required for anther dehiscence. Plant Cell 17(11):2993–3006. https://doi.org/10.1105/tpc.105.036004

Murat F, Armero A, Pont C, Klopp C, Salse J (2017) Reconstructing the genome of the most recent common ancestor of flowering plants. Nat Genet 49(4):490–496. https://doi.org/10.1038/ng.3813

Nagpal P, Ellis CM, Weber H, Ploense SE, Barkawi LS, Guilfoyle TJ, Hagen G, Alonso JM, Cohen JD, Farmer EE, Ecker JR, Reed JW (2005) Auxin response factors ARF6 and ARF8 promote jasmonic acid production and flower maturation. Development 132(18):4107–4118. https://doi.org/10.1242/dev.01955

Nelson MR, Band LR, Dyson RJ, Lessinnes T, Wells DM, Yang C, Everitt NM, Jensen OE, Wilson ZA (2012) A biomechanical model of anther opening reveals the roles of dehydration and secondary thickening. New Phytol 196(4):1030–1037.https://doi.org/10.1111/j.1469-8137.2012.04329.x

Noblin X, Rojas NO, Westbrook J, Llorens C, Argentina M, Dumais J (2012) The fern sporangium: a unique catapult. Science 335(6074):1322. https://doi.org/10.1126/science.1215985

Oriani A, Scatena VL (2015) Anther wall development, microsporogenesis, and microgametogenesis in Abolboda and Orectanthe: contributions to the embryology of xyridaceae (Poales). Int J Plant Sci 176(4):324–332. https://doi.org/10.1086/680401

Pacini E, Franchi GG, Hesse M (1985) The tapetum: Its form, function, and possible phylogeny in Embryophyta. Plant Syst Evol 149(3–4):155–185. https://doi.org/10.1007/BF00983304

Parish A et al (2012) Tapetal development and abiotic stress: a centre of vulnerability. Funct Plant Biol 39:553–559. https://doi.org/10.1071/FP12090

Peñuelas M, Monte I, Schweizer F, Vallat A, Reymond P, García-Casado G, Franco-Zorrilla JM, Solano R (2019) Jasmonate-related MYC transcription factors are functionally conserved in marchantia polymorpha. Plant Cell 31(10):2491–2509.https://doi.org/10.1105/tpc.18.00974

Plavskin Y, Nagashima A, Perroud PF, Hasebe M, Quatrano RS, Atwal GS, Timmermans MCP (2016) Ancient trans-acting siRNAs confer robustness and sensitivity onto the auxin response. Dev Cell 36(3):276–289. https://doi.org/10.1016/j.devcel.2016.01.010

Ren X, Xin G, Du X, Ni X, Jia G, Liu H, Hao N, Liu W (2019) Abnormal tapetum development in hermaphrodites of an androdioecious tree, Tapiscia Sinensis. Tree Physiol 40(1):108–118. https://doi.org/10.1093/treephys/tpz080

Renner SS (1989) A survey of reproductive biology in neotropical Melastomataceae and Memecylaceae. Ann Mo Bot Gard 76:496–518. https://doi.org/10.2307/2399497

Rensing SA, Lang D, Zimmer A et al (2007) The Physcomitrella genome reveals evolutionary insights into the conquest of land by plants. Science 319(5859):1. https://doi.org/10.1126/science.1150646

Rijpkema AS, Vandenbussche M, Koes R, Heijmans K, Gerats T (2010) Variations on a theme: changes in the floral ABCs in angiosperms. Semin Cell Dev Biol 21(1):100–107. https://doi.org/10.1016/j.semcdb2009.11.002

Rümpler F, Theißen G (2019) Reconstructing the ancestral flower of extant angiosperms: the "war of the whorls" is heating up. J Exp Bot 70(10):2615–2622. https://doi.org/10.1093/jxb/erz106

Sajo MG, Furness CA, Prychid CJ, Rudall PJ (2005) Microsporogenesis and anther development in Bromeliaceae. Grana 44(2):65–74. https://doi.org/10.1080/00173130510010503

Sajo MG, Furness CA, Rudall PJ (2009) Microsporogenesis is simultaneous in the early-divergent grass Streptochaeta, but successive in the closest grass relative Ecdeiocolea. Grana 48(1):27–37. https://doi.org/10.1080/00173130902746466

Sauquet H, Von Balthazar M, Magallón S et al (2017) The ancestral flower of angiosperms and its early diversification. Nat Commun. https://doi.org/10.1038/ncomms16047

Schnittger A, Grini PE, Folkers U, Hülskamp M (1996) Epidermal fate map of the Arabidopsis shoot meristem. Dev Biol 175(2):248–255. https://doi.org/10.1006/dbio.1996.0112

Scott RJ, Spielman M, Dickinson HG (2004) Stamen structure and function. In The plant cell 16:S46–S60. https://doi.org/10.1105/tpc.017012

Silva CS, Puranik S, Round A, Brennich M, Jourdain A, Parcy F, Hugouvieux V, Zubieta C (2016) Evolution of the plant reproduction master regulators LFY and the MADS transcription factors: the role of protein structure in the evolutionary development of the flower. Front Plant Sci 6:1–18. https://doi.org/10.3389/fpls.2015.01193

Sokoloff DD, Remizowa MV, Bateman RM, Rudall PJ (2018) Was the ancestral angiosperm flower whorled throughout? Am J Bot 105(1):5–15. https://doi.org/10.1002/ajb2.1003

Song S, Chen Y, Liu L, See YHB, Mao C, Gan Y, Yu H (2018) OsFTIP7 determines auxin-mediated anther dehiscence in rice. Nat Plants 4(7):495–504. https://doi.org/10.1038/s41477-018-0175-0

Song S, Qi T, Huang H, Ren Q, Wu D, Chang C, Peng W, Liu Y, Peng J, Xie D (2011) The jasmonate-ZIM domain proteins interact with the R2R3-MYB transcription factors MYB21 and MYB24 to affect jasmonate-regulated stamen development in Arabidopsis. Plant Cell 23(3):1000–1013. https://doi.org/10.1105/tpc.111.083089

Sztein AE, Cohen JD, Cooke TJ (2000) Evolutionary patterns in the auxin metabolism of green plants. Int J Plant Sci 161(6):849–859. https://doi.org/10.1086/317566

Tanurdzic M, Banks JA (2004) Sex-determining mechanisms in land plants. Plant Cell 16:S61–S71. https://doi.org/10.1105/tpc.016667

Taylor ML, Osborn JM (2006) Pollen ontogeny in Brasenia (Cabombaceae, Nymphaeales). Am J Bot 93(3):344–356. https://doi.org/10.3732/ajb.93.3.344

Theissen G, Melzer R (2007) Molecular mechanisms underlying origin and diversification of the angiosperm flower. Ann Bot 100(3):603–619. https://doi.org/10.1093/aob/mcm143

Theißen G, Saedler H, Theissen G, Saedler H (2001) Floral quartets. Nature 409:469–471. https://doi.org/10.1111/dom.13526
Tiwari SC, Gunning BES (1986) Development and cell surface of a non-syncytial invasive tapetum inCanna: ultrastructural, freeze-substitution, cytochemical and immunofluorescence study. Protoplasma 134(1):1–16. https://doi.org/10.1007/BF012 76371
Tobe H, Jaffré T, Raven PH (2000) Embryology of Amborella (Amborellaceae): descriptions and polarity of character states. J Plant Res 113(3):271–280. https://doi.org/10.1007/pl00013935
Tsuzuki M, Nishihama R, Ishizaki K, Kurihara Y, Matsui M, Bowman JL, Kohchi T, Hamada T, Watanabe Y (2016) Profiling and characterization of small RNAs in the liverwort, Marchantia polymorpha, belonging to the first diverged land plants. Plant Cell Physiol 57(2):359–372. https://doi.org/10.1093/pcp/pcv182
Vallejo-Marín M, Manson JS, Thomson JD, Barrett SCH (2009) Division of labour within flowers: heteranthery, a floral strategy to reconcile contrasting pollen fates. J Evol Biol 22(4):828–839. https://doi.org/10.1111/j.1420-9101.2009.01693.x
Vljayaraghavan MR, Dhar U (1975) Kadsura heteroclita—microsporangium and pollen. J Arnold Arbor 56(1):176–182
Walker-Larsen J, Harder LD (2000) The evolution of staminodes in angiosperms: patterns of stamen reduction, loss, and functional re-invention. Am J Bot 87(10):1367–1384. https://doi.org/10.2307/2656866
Wang C, Liu Y, Li SS, Han GZ (2015) Insights into the origin and evolution of the plant hormone signaling machinery. Plant Physiol 167(3):872–886. https://doi.org/10.1104/pp.114.247403
Wang Y, Ye H, Bai J, Ren F (2021) The regulatory framework of developmentally programmed cell death in floral organs: a review. Plant Physiol Biochem 158:103–112. https://doi.org/10.1016/j.plaphy2020.11.052
Wilson ZA, Song J, Taylor B, Yang C (2011) The final split: the regulation of anther dehiscence. J Exp Bot 62(5):1633–1649. https://doi.org/10.1093/jxb/err014
Wilson ZA, Zhang DB (2009) From arabidopsis to rice: Pathways in pollen development. J Exp Bot 60(5):1479–1492.https://doi.org/10.1093/jxb/erp095
Winter KU, Saedler H, Theißen G (2002) On the origin of class B floral homeotic genes: functional substitution and dominant inhibition in Arabidopsis by expression of an orthologue from the gymnosperm Gnetum. Plant J 31(4):457–475.https://doi.org/10.1046/j.1365-313X. 2002.01375.x
Yang C, Song J, Ferguson AC, Klisch D, Simpson K, Mo R, Taylor B, Mitsuda N, Wilson ZA (2017) Transcription factor MYB26 is key to spatial specificity in anther secondary thickening formation. Plant Physiol 175(1):333–350. https://doi.org/10.1104/pp.17.00719
Yang C, Xu Z, Song J, Conner K, Vizcay Barrena G, Wilson ZA, Barrena GV, Wilson ZA (2007) Arabidopsis MYB26/MALE STERILE35 regulates secondary thickening in the endothecium and is essential for anther dehiscence. Plant Cell 19(2):534–548. https://doi.org/10.1105/tpc.106.046391
Yeung EC, Oinam GS, Yeung SS, Harry I (2011) Anther, pollen and tapetum development in safflower, Carthamus Tinctorius L. Sex Plant Reprod 24(4):307–317. https://doi.org/10.1007/s00497-011-0168-x
Yu J, Jiang M, Guo C (2019) Crop pollen development under drought: from the phenotype to the mechanism. Int J Mol Sci 20(7):1. https://doi.org/10.3390/ijms20071550
Zhan H, Xiong H, Wang S, Yang ZN (2018) Anther Endothecium-derived very-long-chain fatty acids facilitate pollen hydration in arabidopsis. Mol Plant 11(8):1101–1104. https://doi.org/10.1016/j.molp.2018.05.002
Zhang D, Luo X, Zhu L (2011) Cytological analysis and genetic control of rice anther development. J Genet Genomics 38(9):379–390. https://doi.org/10.1016/j.jgg.2011.08.001
Zhang D, Yang L (2014) Specification of tapetum and microsporocyte cells within the anther. Curr Opin Plant Biol. https://doi.org/10.1016/j.pbi.2013.11.001
Zhao Z, Zhang Y, Liu X et al (2013) A role for a dioxygenase in auxin metabolism and reproductive development in rice. Dev Cell 27(1):113–122. https://doi.org/10.1016/j.devcel.2013.09.005
Zheng L, Nagpal P, Villarino G, Trinidad B, Bird L, Huang Y, Reed JW (2019) MiR167 limits anther growth to potentiate anther dehiscence. Development (cambridge).https://doi.org/10.1242/dev.174375
Zhu T, Li Z, An X, Long Y, Xue X, Xie K, Ma B et al (2020) Normal structure and function of endothecium chloroplasts maintained by ZmMs33-mediated lipid biosynthesis in tapetal cells are critical for anther development in maize. Mol Plant 13(11):1624–1643. https://doi.org/10.1016/j.molp.2020.09.013

1.4 Aims and objectives

The aims of the project were to enhance the understanding male fertility traits in barley under abiotic stress conditions and to analyse the genetic factors that underlie anther traits valuable for hybrid breeding in wheat. The findings were anticipated to provide useful avenues for continued research in barley male fertility and abiotic stress responses as well as identify the genetic components that make up a good male for hybrid wheat breeding. A more detailed list of the objectives of each chapter is specified below:

Chapter 3

- Identification of genes putatively involved with male reproduction in barley through the identification of orthologues of known pollen development genes from *Arabidopsis thaliana* and *Oryza sativa*
- Generation of transgenic lines for the study of the putative genes *in planta* using CRISPR/Cas9 genome editing as well as overexpression and silencing of the genes of interest
- Phenotyping of the generated transgenic lines for effects on reproductive fertility

Chapter 4

- Analysis of stomatal formation and stomatal conductance in the HvICE1-1 transgenic lines to determine the effect of *HvICE1-1* on the stomatal formation gene regulatory network
- Measurement of photosynthetic parameters in the HvICE1-1 transgenic lines
- Expression analysis of putatively HvICE1-1 interacting genes to understand the effect of differentially expressed *HvICE1-1* in control conditions and under cold stress

Chapter 5

- Analysis of selected barley lines from a population of near-isogenic lines containing uncharacterized male sterile genic mutations through phenotyping and genotyping
- Genotyping of the mutant lines with a high-density genotyping platform to identify introgressed regions

Chapter 6

- Genome-wide association study of anther traits in three diverse wheat populations for the identification of genetic loci associated with anther length and anther extrusion
- Evaluation of candidate markers and genes identified through the GWAS
- Analysis of germplasm origin and the genetic diversity in the populations as well as the correlation between anther length, anther extrusion, and plant height

Chapter 2. General materials and methods

2.1 Seed sterilisation, germination and growth conditions

In chapters 2 and 3 the two-rowed spring barley *Hordeum vulgare* cultivar Golden Promise was used as the wild type for comparisons to the transgenic lines. Seeds of Golden Promise was supplied by the Wilson Lab.

Seeds were sterilised by incubation in 70% (v/v) ethanol for 30 seconds, rinsed with sterile water twice, and incubated in 5% (v/v) bleach in water for 15 min with occasional stirring. The seeds were then rinsed with sterile water three times before placed on moist filter paper for germination at 20 ˚C.

To improve germination of seeds with low germination of the BW-lines used in chapter 5, the seeds were sterilised as above, placed in dH_2O at 4˚C for 48h, and then transferred onto moist sterile filter paper at 20˚C for 4 days until roots emerged.

Germinated seedlings with root and shoots of 3-5 cm were transferred to Levington M3 compost (The Scotts Company (UK) Ltd, Surrey UK). Unless specified three plants were grown in each 5 L pot. Barley plants were grown in a growth room under a 16 h photoperiod in controlled conditions of day/night temperatures of 15/12˚C (±2˚C) with light levels of 500 µmol/m^2/s at canopy level of mature plants provided by halide lamps supplemented with tungsten bulbs. The plants were kept well-watered. Deviating growth conditions are specified in the respective chapters.

Staging of barley plants until spike development was carried out with the Zadoks staging guide (Zadoks et al., 1974) and spike stages were determined using the additional staging described in Fernández-Gómez et al. (2020).

2.2 Pollen viability and anther length measurements

Pollen viability was assessed using the iodine pollen starch test (Chang et al., 2014). Yellow pre-anthesis anthers were prefixed in 70% (v/v) ethanol, placed in water on a glass slide and dissected to break the anther wall. Released pollen grains were incubated for 5 min in a 1% (w/v) iodine and 0.2% (w/v) potassium iodide solution before imaging with Leica DMRB microscope in Leica Application Suite 4.12.0, Leica microsystems Limited. Mature anthers were imaged for anther length measurements with Zeiss Stemi SV 6 microscope. Images were processed in ImageJ 1.52a (National Institutes of Health, USA) (Schneider et al., 2012).

2.3 Genomic DNA (gDNA) extraction from leaf tissue

Genomic DNA (gDNA) was extracted using different protocols depending on downstream applications. For high throughput genotyping of barley lines crude gDNA was extracted using the REDExtract-N-Amp Plant PCR kit (Sigma-Aldrich). A 5-10 mm piece of leaf tissue was placed in 20 µl of Extraction Solution (E7526) and heated to 95˚C for 10 min, 20 µl of Dilution Solution (D5688) was then added and mixed briefly. The DNA was stored at 4˚C and used within 2 weeks.

gDNA used for downstream applications i. e. for cloning or sequencing was extracted with Speed DNA Extraction protocol (Ute Voss, personal communication). A 10 mm leaf sampled was ground in liquid nitrogen and 600µl extraction buffer was added consisting of 1 M TrisHCL (pH 7.5), 4 M NaCl, 0.5 M EDTA, and 10% SDS. The sample was vortexed and centrifuged for 5 min at 12000 g before the supernatant was transferred into a new tube where an equal volume of 500 µl isopropanol was added. After 2-3 min incubation at room temperature the sample was centrifuged at 12000 g for 5 min, the pellet was retained, washed with 70% ethanol and air dried for 1-12h before resuspension in 50µl H_2O. DNA samples were stored at -20°C.

For use in downstream applications such as cloning, gDNA was extracted using the Isolate Plant II Plant DNA kit (Bioline), following the manufacturer's instructions. DNA was eluted in 30 µl molecular grade water (Sigma Aldrich) and stored at -20˚C.

2.4 Genotyping using Polymerase Chain Reaction (PCR)

Genotyping was carried out with Polymerase Chain Reactions (PCRs). The sequence of interest was amplified in 10 µl reactions using the REDExtract-N-Amp PCR ReadyMix, Sigma Aldrich, (Table 2.1) with primers specific to the DNA sequence of interest specified in the relevant chapters.

Primer optimisation was carried out with gradient PCR for each primer pair. A reaction using 5 µl 2x REDExtract PCR Ready Mix, 50 ng/µl gDNA from the wild type, 0.3 µl of 10 pM of each primer and molecular grade water to a final volume of 10 µl, was used. The respective primer pairs was tested at five temperatures (56, 58, 60, 62, 64°C) to determine the optimal annealing temperature. The amplicons of each reaction were analysed with gel electrophoresis (section 2.5) and the reaction temperature with the highest amplification efficiencies were used for further PCRs. Temperatures specified in Table 2.4 and Appendix 1, Table S3.2, Table S5.1

Table 2.1. General REDExtract PCR conditions. Annealing temperatures were optimised for each primer pair and elongation time was adjusted for the length of the amplicon.

Stage	Temperature (˚C)	Time	Repeats
Initial denaturation	94	3 min	1
Denaturation	94	30 sec	24-35
Annealing	56-64	30 sec	
Elongation	72	1 kb/min	
Final elongation	72	5 min	1

2.5 Agarose gel electrophoresis and purification of PCR product from gel and in solution

The amplicons from the PCR were validated using agarose (Bioline, USA) gel electrophoresis ranging from 1-2% w/v depending on DNA size, in 0.5x TBE buffer (45 mM Tris-borate, 1 mM EDTA) by applying 60-130 V for 40 min-1.5 h. For each sample 10 µl of the genotyping PCR sample was loaded onto a gel with 2 µl 5x loading buffer for PCR samples using Phusion High Fidelity DNA polymerase, Q5 DNA polymerase (New England Biolabs) and PrimeSTAR GXL polymerase (TaKaRa). An appropriate reference molecular weight marker HyperLadder 1 kb or 50 bp (Meridian Bioscience, Bioline) was used as reference. The gel was stained with 500 µg/ml ethidium bromide (Sigma-Aldrich) and imaged with Molecular Imager Gel Doc XR+ System with Image Lab (BioRad).

Purification of the PCR product for downstream applications was carried out with the Wizard SV Gel and PCR Clean-Up System (Promega). Where only one amplicon was visible on the gel, the PCR mixture was purified from solution, however where multiple amplicons were present the amplicon of the predicted size was cut from the gel and used for purification. The DNA was eluted in 20-30 µl molecular grade water. The concentration of the purified amplicon was measured using NanoDrop Spectrophotometer 2000 (Thermo Scientific).

2.6 Sequencing validation

To verify sequences amplified by PCR and cloned sequences, samples were sequenced using the Sanger sequencing TubeSeq service (Eurofins Genomics). In a total 15 µl reaction volume plasmid DNA was prepared to a sample concentration of 50-100 ng/µl, and purified PCR products to 1-10 ng/µl, with 2 µl of 10 pM/µl primer, according to the instructions of the Eurofins sequencing service.

2.7 Bioinformatic analysis

Gene identifiers of genes of interest from *Arabidopsis thaliana* and *Oryza sativa Japonica* were obtained from literature and from EnsemblPlants (Howe et al., 2021). The sequences were used to search for orthologues in the barley genome through the Basic Local Alignment

Search Tool (BLAST) service provided by EnsemblPlants (Howe et al., 2021). The protein sequences of confirmed genes in *A. thaliana* and *O. sativa* were used to identify potential orthologues in barley and the barley gene identifier was used to obtain the sequences of interest from BARLEX (Colmsee et al., 2015) available at https://apex.ipk-gatersleben.de/apex/f?p=284:10:::::: from the Morex v2 Gene models 2016 and 2019, TRITEX genome assembly (Monat et al., 2019). The protein sequences of the barley genes were compared back to the genomes of *A. thaliana* and *O. sativa* to confirm that the identified barley orthologue was the best candidate for the gene of interest. Sequence alignments were carried out by ClustalW Multiple Sequence Alignment tool (https://www.genome.jp/tools-bin/clustalw).

2.8 RNA extraction and cDNA synthesis for gene expression analysis

For gene expression analysis, barley tissues were collected and immediately transferred to liquid nitrogen. A maximum of 100 mg of tissue was ground to a fine powder using a mortar and pestle, avoiding thawing of the sample. RNA was extracted using the QIAshredder (Qiagen) and RNeasy Mini Kit (Qiagen) according to the manufactures' protocol. RNA was eluted in 87.5 µl molecular grade water and DNase treatment was carried out in solution with 2.5 µl RNase-free DNase (Qiagen), and 10 µl RDD buffer (Qiagen), incubated at room temperature for 20 min. The RNA was purified using the RNeasy Mini Kit (Qiagen) and eluted in 30 µl molecular grade water. RNA samples were stored at -80˚C.

The quality and quantity of RNA samples were measured using NanoDrop Spectrophotometer 2000 (Thermo Scientific). cDNA was synthesised using 1-1.5 µg of total RNA, 1µl (0.5 µg/µl) oligo (dT) (Invitrogen), 1µl (10 mM) dNTP (Bioline) and the volume of molecular grade water to make up a final volume of 13 µl. The reaction was heated for 65˚C for 5 min and immediately incubated on ice for 1 min. To each reaction 4 µl 5x First strand buffer (Invitrogen), 1 µl (0.1 M DTT), 1 µl (40 units/µl) RNase OUT (Invitrogen) and 1 µl (200 units/µl) SuperScript IV Reverse Transcriptase (Invitrogen) was added. The reaction was incubated for 10 min at 50˚C and 10 min at 80˚C. The cDNA was stored in -20˚C.

The cDNA was tested for gDNA contamination with primers for a reference gene α-Tubulin (*HvTub)* (primer sequence in Table 2.4) which amplifies a 400 bp product in gDNA and a 250 bp product cDNA. PCR was conducted with REDExtract (section 2.4) and analysed by gel electrophoresis. No gDNA contamination was found for samples treated with DNase in solution during RNA extraction.

2.9 Identification of gene sequences for RT-qPCR analysis

In chapter 3 barley orthologues of genes of interest were identified. These genes were used to study the gene expression in the transgenic lines. Confirmed orthologues of *HvMS1* (Fernández Gómez & Wilson, 2014), *HvCBF3* (Choi et al., 2002) and *GAMYB* (Gubler et al.,

1995) as well as the genes identified as *HvDEX1*, *HvICE1-1*, *HvICE1-2* and *HvMMD1-1* were used. To identify potential orthologous sequences of genes of interest in barley the protein sequences of the orthologues from rice and *Arabidopsis* were analysed using the BLAST tool of EnsemblPlants. In each BLAST analysis the five candidates with the highest gene identify between barley and *Arabidopsis,* or barley and rice were compared. The best candidate genes with the respective orthologue and sequence identity were used to design primers for RT-qPCR analysis using the NCBI Primer-BLAST tool (https://www.ncbi.nlm.nih.gov/tools/primer-blast/index.cgi).

Genes predicted to interact with *HvICE1,* based on previously studied gene interactions of *ICE1,* were identified to investigate if the gene regulatory network is conserved in barley and if the *HvICE1-1* candidate could affect their expression. *HvCBF3* was identified in (Choi et al., 2002), whereas *HvFAMA*, *HvHOS1*, *HvSIZ1* were identified using Ensembl and BLAST analysis with sequences from *Arabidopsis*. No potential orthologue of the *ICE1* regulator *OST1* was identified. It was not possible to design qRT-PCR primers that were specific to *HvICE1-3* due to the high sequence similarity between *HvICE1-1* and *HvICE1-3*.

In the silencing transgenic lines with the SRDX-tagged transgenes of *HvICE1-1* and *HvMMD1-1* the expression of the *HvICE1-1* and *HvMMD1-1* was measured with the same primers as for the native transcript, i.e. it is picking up on the expression of the native *HvICE1-1* or *HvMMD1-1* as well as the plant-specific EAR-motif repression domain (SRDX)-tagged transcript. Interpretation of this expression profile is therefore difficult however it is worth noting the presence of the expressed gene and the difference in transcript levels.

Barely orthologues were identified from *Arabidopsis* and rice orthologues. The *HvDEX1* orthologue was identified from sequences of *DEX1* (Paxson-Sowders et al., 2001) and *OsDEX1* (Yu et al., 2016). Genes related to *ICE1* (Chinnusamy et al., 2003, Kanaoka et al., 2008) i.e. *CBF3* (Gilmour et al., 1998), *FAMA* (Ohashi-Ito & Bergmann, 2006), *HOS1* (Ishitani et al., 1998), *SIZ1* (Miura et al., 2005), *OsCBF3* (Dubouzet et al., 2003), *OsFAMA* (Liu et al., 2009), *OsHOS1* (Lourenço et al., 2013), and *OsSIZ1* (Park et al., 2010) were used to identify *HvFAMA*, *HvHOS1*, *HvSIZ1* and *HvCBF3* (Choi et al., 2002) (Table 1.2). Sequences of *MMD1*/*DUET* (Reddy et al., 2003, Yang et al., 2003), *EAT1* (Niu et al., 2013), *DYT1* (Zhang et al., 2006), *UDT1* (Jung et al., 2005), were used to identify *HvEAT1* and *HvDYT1* along with *GAMYB* (Gubler et al., 1995) and *HvMS1* (Fernández Gómez & Wilson, 2014).

Table 2.2. Gene sequences used for RT-qPCR primer design. The barley orthologue IDs were identified as genes of interest using the orthologous gene IDs of Arabidopsis *and rice. Barley gene sequences were obtained from BARLEX.* HvCBF3, GAMYB, HvICE1-1 *and* HvMS1 *had previously been confirmed or hypothesised as barley orthologues.*

Gene	Barley orthologue ID	*Arabidopsis* gene ID	Rice gene ID	Barley orthologue reference
HvCBF3	*HORVU.MOREX.r2.5HG0412820.1*	*At4G25480*	*Os03g0737200*	Choi et al., 2002
HvDEX1	*HORVU.MOREX.r2.5HG0438930.1*	*At3G09090*	*Os03g0825700*	NA
HvDYT1	*HORVU2Hr1G042710*	*At4g21330*	*Os07g36460*	NA
HvEAT1	*HORVU.MOREX.r2.2HG0161050.1*	NA	*Os04g0599300*	NA
HvFAMA	*HORVU.MOREX.r2.1HG0058670.1*	*At3G24140*	*Os05g0586300*	NA
GAMYB	*HORVU.MOREX.r2.3HG0246570.1*	NA	NA	Gubler et al., 1995
HvHOS1	*HORVU.MOREX.r2.4HG0284290.1*	*At2G39810*	*Os03g0737200*	NA
HvHSP70	*HORVU5Hr1G113180.1*	NA	NA	NA
HvICE1-1	*HORVU.MOREX.r2.7HG0583410.1*	*At3G26744*	*Os11g0523700*	Tondelli et al., 2006
HvICE1-2	*HORVU.MOREX.r2.3HG0260940.1*	*At1G12860*	*Os06t0724800*	NA
HvMMD1-1	*HORVU.MOREX.r2. 4HG0281670.1*	*At1G66170*	*Os03g0716200*	NA
HvMS1	*HORVU5Hr1G067420*	*At5g22260*	*Os09g0449000*	Fernández Gómez et al., 2014
HvSIZ1	*HORVU.MOREX.r2.1HG0010970.1*	*At5G60410*	*Os05g0125000*	NA
HvTub	*HORVU5Hr1G098960.2*	NA	NA	NA

Primers used for the RT-qPCR were based on the sequences of the confirmed or putative barley orthologues (Table 2.2). The primers were designed to amplify a region of 70-350 base pairs and to preferentially span an exon-intron border to avoid amplification of the gDNA (Rodríguez et al., 2015). Primer design was carried out in Primer-BLAST (National Center for Biotechnology Information) and were routinely between 18-23 nucleotides with melting temperatures of 56-62˚C.

The expression of the genes of interest were normalised to two reference genes, *Hvα-Tubulin* and *HvHSP70* (*HEAT SHOCK PROTEIN70*), sequence ID in Table 2.2, selected based on the principle described in (Hellemans et al., 2007).

2.10 Expression analysis

Gene expression data of the transcripts of *HvDEX1*, *HvICE1* homologs and *HvMMD1* homologs throughout plant tissues was obtained from BARLEX (https://apex.ipk-gatersleben.de/apex/f?p=284:10::::::) based on the barley genome assembled by International Barley Genome Sequencing Consortium (2012).

Expression analysis was carried out by RT-qPCR in a 386 well plate in qTower3 84G (analytik jena) using Maxima SYBR Green Master Mix or PowerUp SYBR Green Master Mix (Applied Biosystems). In each reaction 0.1 µl (50 ng/µl) cDNA, 20 pM of each primer, 5 µl 2x SYBR Green Master Mix, and 4.7 µl molecular grade water was added to a final volume of 10 µl. The reaction conditions are specified in Table 2.3 and each reaction was performed with four technical replicates.

Table 2.3. Reaction conditions for RT-qPCR using Maxima or PowerUp SYBR Green Master mix. Fluorescence was scanned once per cycle to generate the C_t values and every 2˚C in the melting curve.

Stage	**Temperature (˚C)**	**Extension time**	**Cycles**
Initial denaturation	95	30 sec	1
Denaturation	95	15 sec	40
Annealing	60	15 sec	
Elongation	72	30 sec	
Melting curve	ΔT 2	15 sec per temperature	1

Primers for each gene of interest were designed and tested for efficiency (Rodríguez et al., 2015). The efficiency of the primers used for each gene were tested in a serial dilution of cDNA (50 ng/µl) with 1, 0.2, 0.04, 0.008 and 0.0016 µl cDNA used per 10 µl reaction to determine the amplification efficiency (E-value) in RT-qPCR (Table 2.4). Each amplicon was analysed through a melting curve analysis to confirm that only a single sequence had been amplified. The melting curve was set to measure absorbance at 2˚C increments from annealing temperature of 60˚C to 95˚C.

The RT-qPCR analysis was carried out according to Equation 2.1 (Vandesompele et al., 2002):

$$Relative\ gene\ expression = \frac{(E_{GOI})^{\Delta Ct\ GOI}}{GeoMean[(E_{REF})^{\Delta Ct\ REF}]}$$

where E_{GOI} is the amplification efficiency of the gene of interest, and E_{REF} is the amplification efficiency of the reference gene. RT-qPCR data was analysed with two reference genes for each tested gene and cDNA stage. For each gene and cDNA stage the C_t values of four technical replicates were averaged. The gene of interest was normalised to two reference genes, *HvTubulin-α* and *HvHSP70* (*HEAT SHOCK PROTEIN70*) (Hellemans et al., 2007; Vandesompele et al., 2002).

Table 2.4. Primers used for RT-qPCR of genes of interest with the amplicon size and amplification efficiencies (E-value) with PowerUP SYBR green. Annealing temperature 60°C for all primer pairs.

Gene	Primer number	Primer sequence 5' – 3'	Amplicon size	E-value
HvCBF3	8576	TTGACTTGTTCCCGGAAATGGAC	104	2.10
	8577	TTCGTACGCGTGGATGATGGTC		
HvDEX1	7947	CTGCTGATGTGCATGGTAATG	96	1.83
	7948	CAGTAGGTCTCTGTGGAACAAG		
HvDYT1	7620	CAGCAGCTTCCACGGCTTTC	139	1.95
	7621	GATCACCGTGGCCCTATCCTC		
HvEAT1	8512	CCCAGTGAGGATGAAAGAGATGTC	103	2.03
	8513	CTTCTGCCCTCCAGTACAGTATCA		
HvFAMA	8872	ATCCTACGTCCAGAGGGGAG	92	3.63
	8873	ACTCGAGGCACTGGATTAGC		
GAMYB	4928	GGCTCATCATCCAGCTCCAC	354	2.00
	4933	AGTACGCCCTGGCAAATGAG		
HvHOS1	8574	AGTGCAGGATTTCGTCGTGA	98	1.75
	8575	CCTTCACCAACTGGGGGTTT		
HvHSP70	8462	GCTCAACATGGACCTCTTCAGG	101	1.97
	8463	CCGACAAGGACAACATCATGG		
HvICE1-1	8196	CCAACCGTTGAGGTTAGGCT	258	2.04
	8193	CATCGTGGGATGGAACCC		
HvICE1-2	8578	TGCTGCCGGAGGAAATTAAGGC	69	2.13
	8579	GATTCGCCTACATCGCGTTCTG		
HvMMD1-1	8772	GTGCTGGACTGCAAACACTG	87	2.48
	8773	CGGTCGCCATTCAACAAGGA		
HvMS1	8510	TGCGATTCCATCTCACCAGG	209	2.04
	8511	GTACACATGCCCGACTACGC		
HvSIZ1	9021	CTTCTCTGTTGCGCGATTGT	139	2.66
	9022	TTCGAGATACAGAGCGTGCC		
HvTub	7618	GCCCGTGGTCACTACACAATC	115	2.02
	7619	CGACGGCGTTGAAGACAAGG		

2.11 Statistical analysis

Unless otherwise stated, the statistical analysis was carried out in Excel using the Student's t-Test, using a two-tailed distribution assuming equal variance in the samples (homoscedastic).

Chapter 3. Identification and characterisation of putative orthologues of pollen development genes, *HvDEX1*, *HvMMD1,* and *HvICE1*

3.1 Introduction

3.1.1 Identification of orthologues

3.1.1.1 Conservation of genes between *Arabidopsis* and cereal crops

Arabidopsis thaliana is one of the best studied plant species with large mutant collections and robust genomic resources which provide a source for knowledge of plant systems for other species. Direct transfer of knowledge of the dicot *Arabidopsis* gene regulatory pathways to grass crops of agronomic importance however can be problematic. From the point of separation between dicots and monocots numerous alterations to the genome, such as shuffling, deletions, inversions etc., has taken place making the isolation of orthologues challenging when solely looking at conserved gene sequences. The likelihood of finding an orthologue based on sequence conservation alone has been estimated to be very low between *Arabidopsis thaliana*, *Brachypodium distachyon*, *Sorghum bicolor*, and *Oryza sativa*, suggesting that additional approaches such as the conservation of gene order (synteny) and gene expression patterns can be necessary for the identification of orthologues (Duran et al., 2009; Spannagl et al., 2010).

3.1.1.2 Bioinformatic tools for the identification of barley orthologues from *Arabidopsis thaliana* and *Oryza sativa*

Sequence similarity alone is not sufficient to enable identification of functional orthologues, instead, a combination of bioinformatic approaches are needed (Duran et al., 2009). Synteny is the preserved order of genes in related species originating from a common ancestor and has been used as a complementation to sequence similarity (Duran et al., 2009). Synteny has been shown to provide a useful tool for the analysis of orthologous genes across species assisting the transfer of knowledge from model plants to crops (Rensink & Buell, 2004; Salse et al., 2002; Spannagl et al., 2010).

Comparative mapping strategies have suggested a high degree of macro-synteny, the collinearity of gene order on the chromosome level, in cereals dating back as far as 60 million years (Gale & Devos, 1998). Since the divergence of dicots and monocots around 120-200 million years ago, little of that macro-synteny has been conserved suggesting that a different approach to synteny is useful (Salse et al., 2002). Studies of microsynteny, the conservation of local gene clusters, have shown that the photoperiodic flowering pathway (Hayama et al., 2003) and circadian-clock-regulation (Izawa et al., 2003, Mouradov et al., 2002) are functionally conserved between *Arabidopsis* and rice. The regulatory network might differ, however these results open up the possibility of more flowering related pathways being similarly conserved.

Comparisons of flower development genes between *Arabidopsis* and grasses suggests that several key regulatory genes are conserved across the dicot-monocot divide (Gómez et al., 2015; Izawa et al., 2003). Highly conserved genes such as *MS1* has been identified in *Arabidopsis* (*MS1*), rice (*PTC1*), and barley (*HvMS1*) where knock-out mutations of the individual genes led to male sterility with defective tapetum and microspores in the respective species (Fernández Gómez & Wilson, 2014; Li et al., 2011; Wilson et al., 2001). Interestingly, comparisons of specific genes between rice and *Arabidopsis* have revealed differences in the number of homologs within the species where the *FLOWERING LOCUS T* is represented by one gene in *Arabidopsis* but eleven homologous sequences in rice (Isawa et al., 2003). The genes controlling anther and pollen development are highly conserved however detailed study of identified putative orthologues are needed to confirm functional conservation in addition to the sequence conservation (Gómez et al., 2015).

Combining sequence similarity with a synteny analysis, and expression data for individual genes offers in a higher chance of identifying conserved gene functions but cannot assure direct homology on its own. To aid the translation of knowledge between *Arabidopsis* and grass crops identified putative orthologues should be investigated with functional analysis of the genes *in planta* through knock-out mutants generated by targeted mutagenesis or through overexpression or silencing of the putative genes (Lloyd, 2003; Mitsuda et al., 2011; Rensink & Buell, 2004).

3.1.2 Selected genes for study in barley

With the increase in sequenced genomes there is a growing interest in developing tools for the prediction and identification of orthologues between species (Brendel et al., 2002; Conte et al., 2008; Spannagl et al., 2010; Walker et al., 2007). The gene network involved with pollen development in monocots has mostly been studied in rice where several genes have been identified as orthologues to *Arabidopsis* genes however only one gene, *HvMS1*, has been characterised and identified to affect male fertility in barley (Gómez et al., 2015, Fernández-Gómez et al., 2014, Izawa et al., 2003). Genes where critical domains and expression patterns are conserved potentially have preserved gene functions however differences between the species optimal growth conditions, tolerance to abiotic stresses, and flower morphology variances generates a need for the specific study of the male reproduction in barley as gene functions and interactions might differ (Spannagl et al., 2010). Genes of interest in *Arabidopsis* were therefore used to identify potential orthologous gene sequences in barley.

Selection of genes for further study were based on three criteria: i) number of confirmed interactions in the *Arabidopsis* pollen development gene network, ranging from key regulators to highly specific genes to examine potential redundancy in the pathway, ii) orthologue conservation between barley and rice, where conserved synteny and high gene identity between *Arabidopsis*, rice and barley was favoured, and iii) the expression profile of the putative gene where genes expressed in tissues of developing inflorescences were favoured (Duran et al., 2009; Spannagl et al., 2010). By combining the data from these

criteria putative orthologues were selected based on their likelihood of being involved in pollen development in barley.

Based on the approaches described above two genes, *DEFECTIVE EXINE FORMATION1* (*DEX1*) and *MALE MEIOCYTE DEATH1* (*MMD1*), which are known to be involved with pollen development in *Arabidopsis* were selected for study in barley. In addition, an orthologue of *INDUCER OF CBF3 EXPRESSION1* (*ICE1*) was identified as a gene of interest from a transcriptome analysis of the conditional sterile barley *HvMS1* overexpression lines. These genes were selected for targeting with the CRISPR/Cas9 gene editing system to disrupt gene expression and characterise gene function.

3.1.2.1 *DEFECTIVE* EXINE *FORMATION1* (*DEX1*) plays a critical role in pollen exine formation

DEX1 encodes a plasma membrane protein involved in calcium binding which is expressed in the tapetum where it is essential during the early stages of exine formation and sporopollenin secretion (Ma et al., 2013; Paxson-Sowders et al., 2001). The *DEX1* gene was identified as a suitable target for study in barley because of its implication in formation of the outermost layer of the pollen grain, the exine layer, and due to the high degree of conservation of function between *Arabidopsis* and rice (Yu et al., 2016; Paxson-Sowders et al., 2001). Additionally, it has a highly specific function which is restricted to the anther (Ma et al., 2013). *DEX1* is thought to act downstream of the early anther specification pathway where a *dex1* knockout leads to defective pollen wall formation from microspore release, ultimately leading to the abortion of the microspore (Paxson-Sowders et al., 2001).

Formation of pollen exine is critical for the viability of the pollen grain. In *Arabidopsis* a mutant of the *FACELESS POLLEN-1* gene has been found to exhibit conditional male sterility under varying degrees of humidity through defects in production of sporopollenin a compound required for the development of the exine layer (Ariizumi et al., 2003). Similar conditional sterility induced by *Eceriferum* (*cer*) mutants involved with the formation of the exine layer epicuticular wax has been found in other genes (Fiebig et al., 2000; Hannoufa et al., 1996; Koornneef et al., 1989; Millar et al., 1999). This suggests that the exine development process, which is dependent on *DEX1* function, could be an interesting target for mutagenesis in cereals for the use in hybrid breeding systems in terms of conditional sterility.

In rice, the *OsDEX1* orthologue displays a conserved tapetum expression pattern and Ca^{2+} binding function, suggesting that the conserved function of *DEX1* orthologues in pollen development is critical in both monocot and dicot species (Yu et al., 2016). The *osdex1* knock out mutant displays smaller pale-yellow anthers lacking mature pollen grains and the flower is completely male sterile in addition to delayed tapetal degradation and aborted exine formation (Yu et al., 2016). Despite its essential role in microspore development, little is known about the function of *DEX1* in pollen development and the interactions of DEX1 with other pollen development genes.

3.1.2.2 *MALE* MEIOCYTE *DEATH1 (MMD1)/DUET* acts as a regulator of male meiosis progression

MMD1 was independently identified as *MMD1* (Yang et al., 2003) and *DUET* (Reddy et al., 2003), and characterised as essential for male meiosis in *Arabidopsis* where it acts as a transcriptional regulator (Reddy et al., 2003; Yang et al., 2003). It has a sex-specific function and is expressed only during male meiosis, specifically in the diplotene stage of prophase I where it regulates genes involved in meiosis progression and facilitates microtubule organisation (Andreuzza et al., 2015). The *Arabidopsis mmd1* mutant caused abnormal cell death of male meiocytes with reduced condensation of chromosomes during meiosis suggesting that MMD1 is involved with chromatin organisation (Jun Wang et al., 2016). The *MALE STERILE1* (*MS1*) involved with regulation of the male gametogenesis was identified as the closest homolog to *MMD1* with both proteins containing a plant homeodomain (PHD) in the C-terminal end (Reddy et al., 2003; Wilson et al., 2001). The PHD finger interacts with chromatin by binding to the histone H3K4me2, a process which is critical for the function of MMD1 (Andreuzza et al., 2015; Yang et al., 2003).

MMD1 was selected as a gene of interest due to its highly specialised expression pattern and function in male meiosis. *MS1* and *MMD1* are required for the development of viable pollen in *Arabidopsis* however disruption of these genes have limited effects on general plant morphology (Andreuzza et al., 2015; Reddy et al., 2003; Wilson et al., 2001) making them interesting possible candidates for the generation of male sterile plants for hybrid breeding.

During the course of this project the sequence used as the *MMD1* orthologue in rice at the Os03g50780 locus, *OsMMD1*, was confirmed as the *MMD1* orthologue and was named *TDR INTERACTING PROTEIN3* (*TIP3*) (Yang et al., 2019). In contrast to *Arabidopsis MMD1*, *TIP3* is expressed later in the microspore development, and is required for tapetum development and degradation, and pollen wall formation (Yang et al., 2019). *TIP3* contains the conserved PHD finger similar to the *Arabidopsis MMD1,* and the gene was identified as a potential candidate for use in rice hybrid breeding due to its specific and pollen development restricted function (Yang et al., 2019). The barley sequence identified from the *MMD1* and *TIP3* (*OsMMD1*) orthologues, named *HvMMD1-1*, was used to study the effect of a highly specific male fertility transcription factor in barley.

3.1.2.3 Involvement of *ICE1* in temperature and humidity-controlled sterility

In barley, *HvMS1* was identified as an orthologue of *MS1*, where overexpression or silencing of *HvMS1* lead to male sterility caused by tapetum degeneration defects and sticky pollen (Fernández Gómez & Wilson, 2014). Interestingly, overexpression of *HvMS1* resulted in temperature dependent male sterility where the plants were fully fertile at 18˚C or above, but display sterility at 15˚C (Fernández-Gómez et al., 2020). This sterility was reversible during early stages of pollen development where anthers grown at 15˚C produced viable pollen however pollen was not released, possibly indicating a defect in the anther dehiscence process (Fernández-Gómez, Talle, & Wilson, 2020). To determine the cause of the temperature dependent conditional male sterility, the transcriptome of anthers from

the *HvMS1* overexpression lines grown at 15˚C and 18˚C were compared to identify differentially expressed genes as possible candidates for further analysis. Among the genes expressed in the sterile anthers at 15˚C but not in the fertile anthers at 18˚C was *HORVU7Hr1G074490/HORVU.MOREX.r2.7HG0583410*, annotated as a barley orthologue of *INDUCER OF CBF3 EXPRESSION1*/*SCREAM* (*ICE1*/*SCRM*), where *HvICE1* was downregulated 1.5 times in the overexpression lines compared to the wild type at 15°C (José Fernandez-Gómez, unpublished data).

ICE1/*SCRM* was first identified as a key regulator of cold response and later as a regulator of stomatal patterning in *Arabidopsis* indicating a link between abiotic stress response and processes critical for plant growth and development (Chinnusamy et al., 2003; Kanaoka et al., 2008). *ICE1* can also affect flowering by repressing floral transition through the activation of the repressor *Flowering Locus C*, with knock-out mutants of *ice1* reducing fertility and shorten inflorescences (Kanaoka et al., 2008; Wei et al., 2018). Interestingly, an *ice1* mutant displayed humidity dependent sterility caused by disruptions in anther dehydration (Wei et al., 2018). Anthers of plants grown in high humidity did not dehisce but the pollen was shown to viable after dehydration treatment (Wei et al., 2018).

The candidate *HvICE1* orthologue isolated from the transcriptome of the temperature dependent *HvMS1* overexpression lines was selected as a gene of interest for analysis in barley due to its potential effects on temperature sensing and anther development.

For the study of the candidate barley orthologues *HvDEX1*, *HvMMD1-1*, and *HvICE1-1*, in barley, transgenic lines were generated that had differential expression of the genes of interest, achieved through overexpression, and inactivation using SRDX repressor technology. Transgenic lines with overexpression or SRDX-mediated silencing of the gene sequences were produced and the generation of knock-out mutations was attempted through CRISPR mediated mutagenesis.

3.1.3 Using CRISPR/Cas9 to investigate putative gene function

Since its discovery the Clustered Regulatory Interspaced Short Palindromic Repeats (CRISPR)-Cas9 system has been widely used as a genome editing technology for targeted mutagenesis (Sander & Joung, 2014). The Cas9 nuclease is directed to the specific region by a single guide RNA (sgRNA) where Cas9 introduces a double stranded break in the DNA. The system has been used successfully in barley where the mutations have been shown to be carried over across generations making it a valuable system for targeted mutagenesis for the creation of mutant lines (Kapusi et al., 2017; Lawrenson et al., 2015).

The sgRNA needed to direct the Cas9 to the target sequence must contain a Protospacer Adjacent Motif (PAM) for correct recognition (Sander & Joung, 2014). Cas9 recognizes the “NGG” PAM sequence and introduces a double strand break 3-4 bp upstream of the PAM

(Figure 3.1) (Lawrenson et al., 2015). The sgRNA should contain a 20-24 bp sequence ending in the PAM sequence to direct the Cas9 to the target of interest (Zhang et al., 2014). Off-targets in coding regions should be avoided and can be minimized through BLAST analysis of a sequence of interest to look for highly similar sequences containing the PAM sequence (Lawrenson et al., 2015).

Targeted gene editing using CRISPR has successfully been applied in barley. The transformation efficiency of immature embryos using *Agrobacterium tumefaciens* is generally low, however, the mutation efficiency in the transformed plants has been shown to be as high as 78% (Harwood, 2019; Kapusi et al., 2017). The majority of the mutations are small insertions or deletions that are inherited to the T1 generation with up to 100% success (Holme et al., 2017; Kapusi et al., 2017; Kumar et al., 2018; Lawrenson et al., 2015).

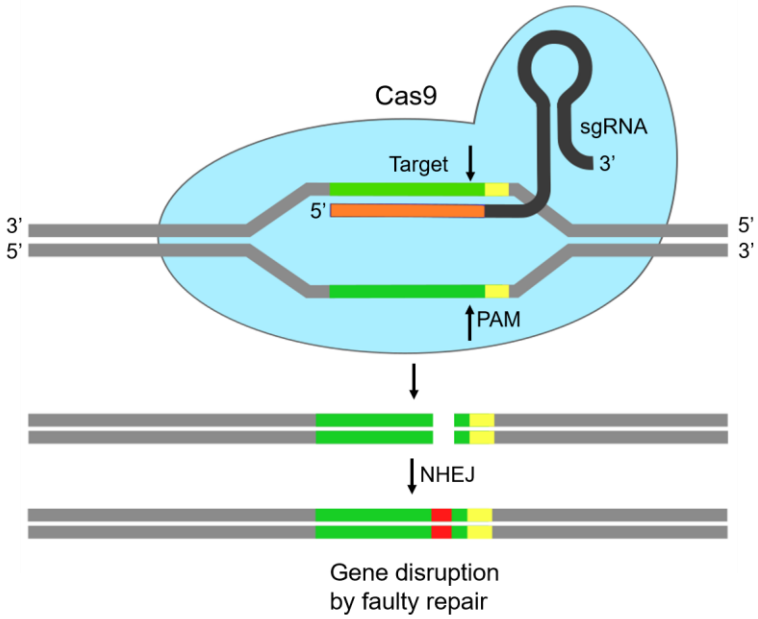

Figure 3.1. The interaction between the nuclease Cas9 and double stranded DNA. Cas9 recognizes and introduces a double strand break 3-4 bp upstream of the PAM site. The break is then repaired by the cell's native DNA repair system. Repairs, via for example via non-homologous end joining, (NHEJ) could potentially introduce mutations causing gene disruption when faulty.

3.1.4 Silencing and overexpression of genes of interest

In addition to knock-out mutants it is of interest to study differential expression of the gene of interest *in planta*. This can be accomplished by the generation of lines overexpressing (OE) or constitutively repressing the target gene through the chimeric repressor silencing technology (CRES-T) (Hiratsu et al., 2003; Lloyd, 2003; Mitsuda et al., 2011). To generate overexpression lines the full length coding sequence of the gene is placed under the control

of a constitutively activated promoter leading to an enhanced non-specific expression (Lloyd, 2003; Mitsuda et al., 2011).

Silencing of a gene can be accomplished by the addition of a plant-specific EAR-motif repression domain (SRDX) sequence, which when fused to the transcription factor dominantly represses the targets of the transcription factor (Hiratsu et al., 2003). For both SRDX and OE lines the construct is placed under the control of the constitutively activated promoter. Plant transcription factor families can in many cases contain multiple homologous members with conserved domains, with structural or functional redundancies, making the study of individual genes difficult (Riechmann et al., 2000). Overexpressing and silencing lines can be used to study functionally redundant genes where a knockout mutation can be fully or partially compensated by homologs (Lloyd, 2003; Mitsuda et al., 2011).

In this study putative barley orthologues in the pollen development gene network from *Arabidopsis* have been identified. The genes were investigated via targeted gene disruption by the CRISPR/Cas9 gene editing system and the generation of overexpression and silencing lines.

3.2 Methods

3.2.1 Selection of genes using bioinformatics approaches

To find putative genes involved with pollen development in barley, genes of interest (GOI) from *Arabidopsis thaliana* and *Oryza sativa* were compared to the barley genome using the BLAST service available through EnsemblPlants (http://plants.ensembl.org/) (Howe et al., 2021) as described in section 2.7. Barley gene sequences with a high sequence similarity to the genes from *Arabidopsis* and rice were treated as potential candidates. The predicted protein sequences of the barley candidates were obtained from BARLEX (IBGSC, 2012). These protein sequences were compared back to the protein databases of *Arabidopsis* and rice to determine if the barley candidate shared a high sequence similarity to other proteins in these species. The barley candidates were also compared to the barley genome to identify possible homologous genes. Sequences from the unique gene identifiers for *HvDEX1* (HORVU.MOREX.r2.5HG0438930, *HvICE1-1* (HORVU.MOREX.r2.7HG0583410) and *HvMMD1-1* (HORVU.MOREX.r2.4HG0281670) were used as the putative barley orthologues.

The barley candidates were further investigated in terms of micro-synteny conservation using EnsemblPlants (Howe et al., 2021). The micro-synteny was investigated by BLAST analysis of seven annotated gene sequences, from EnsemblPlants, on either flanking side of the putative orthologue in barley to the rice genome to look for conserved gene order between the species.

The expression profiles of the barley candidate genes were retrieved from BARLEX (IBGSC, 2012) showing the expression of the genes in various tissues.

3.2.2 Phylogenetic tree and bioinformatics

Protein sequences from *Arabidopsis* and rice were obtained from EnsemblPlants (Howe et al., 2021) and barley sequences from BARLEX (IBGSC, 2012). Sequence alignments were carried out with ClustalW (https://www.genome.jp/tools-bin/clustalw) and protein domain prediction with Motif (https://www.genome.jp/tools/motif/), ScanProsite, ExPASy (https://prosite.expasy.org/), with transmembrane domains predicted by TMHMM 2.0 (https://services.healthtech.dtu.dk/service.php?TMHMM-2.0).

For the building of the phylogenetic tree the sequences were aligned using the built in ClustalW alignment function in MEGA-X 10.1.6 (Kumar et al., 2018). The alignment was used to generate a phylogenetic tree in MEGA-X with the Neighbor-joining tree function with 1000 bootstrap replications.

3.2.3 Cloning and bacterial transformation

3.2.3.1 Transformation of *E. coli* chemically competent cells

Chemical transformation of the *Escherichia coli* (*E. coli*) strain DH5α was conducted by addition of 2-3 µl (100-200 ng) plasmid DNA to 40 µl DH5α chemically competent cells (prepared in house) (Sambrook and Russell, 2001). The cells with the DNA were incubated on ice for 30 min, heat shocked for 45 sec at 42°C, and returned to ice for 1 min before addition of 300 µl LB media (Table 3.1) and incubation at 37˚C for 1.5 h. 50-250 µl of the cells were plated on LB+agar with the relevant antibiotics, concentrations specified in Table 3.2. The plates were incubated at 37°C overnight. Colonies were screened with colony PCR (section 3.2.3.3.1).

Table 3.1. Components of Lysogeny broth (LB) media

Reagent	**Quantity (g/l)**
Tryptone	10
Yeast extract	5
NaCl	5
Agar (for plates only)	7.5

Table 3.2. Components added to bacterial growth media and the final concentration. Ampicillin, hygromycin, kanamycin, rifampicin, spectinomycin and timentin were used as selection agents in bacterial and callus growth media. IPTG and x-gal were used for screening of blue-white bacterial colonies.

Reagent	**Stock concentration**	**Final concentration**
Ampicillin	100 mg/ml	100 µg/ml
IPTG (Isopropyl β-D-1-thiogalactopyranoside)	25 ml/ml	25 µl/ml
Hygromycin	50 mg/ml	50 µg/ml
Kanamycin	50 mg/ml	50 µg/ml
Rifampicin	50 mg/ml	50 µg/ml
Spectinomycin	50 mg/ml	50 µg/ml
Timentin	160 mg/ml	160 µg/ml
x-gal (5-bromo-4-chloro-3-indolyl-β-D-galacto-pyranoside)	40 mg/ml	40 µg/ml

3.2.3.2 Transformation of *Agrobacterium* electro-competent cells

Constructs to be used in tobacco were transformed into *Agrobacterium tumefaciens* strain GV3101 whereas constructs for barley transformation were introduced into strain AGL1. *Agrobacterium* cells were transformed via electroporation (Dulk-Ras & Hooykaas, 1995). Electro-competent *Agrobacterium* cells were co-transformed with 1.5 µl (100-200 ng/µl) of the pBract214 with the relevant transgene and 1 µl (15 ng/µl) of the helper plasmid pSOUP

to 40 µl cells (Smedley & Harwood, 2015). The DNA and cells were kept on ice and transferred to pre-chilled electroporation cuvettes with 0.2 cm electrode gap. The cuvettes were placed under a short electric pulse at 2.5 kV, 25 µF, and 200 Ω, and the cells were immediately suspended in 250 µl LB media (Dulk-Ras & Hooykaas, 1995). The cells were placed on ice for 1 min and then incubated at 28˚C for 3 h. 50-250 µl of the culture was plated on LB+agar with the relevant antibiotic and rifampicin to select against non-*Agrobacterium* microorganisms. The plates were incubated at 28°C for 1-3 days. Colonies were screened by colony PCR (section 3.2.3.3.1).

Glycerol stocks of *E. coli* and *Agrobacterium* were prepared from 5ml overnight cultures in LB with the appropriate antibiotic, using 750 µl cell culture and 250 µl 80% glycerol solution. The samples were mixed and immediately frozen in liquid nitrogen and stored at -80°C. The stocks of *E. coli* were used for plasmid extractions and downstream cloning and the *Agrobacterium* stocks were used for bacterial cultures for transformation of barley and tobacco.

3.2.3.3 Cloning procedures

The cloning procedures used for the generation of constructs used for plant transformation depended on the destination vectors and will be described in the relevant construct description. Cloning procedures used are described in detail here. Vectors used for the cloning of the CRISPR constructs, overexpression and SRDX-silencing lines were supplied by the Wilson Lab.

3.2.3.3.1 Colony PCR and verification of plasmid insertions

To verify the cloning of inserts into vectors, transformants generated through bacterial transformation with the cloning products were screened through colony PCR. Individual bacterial colonies were added to REDExtract PCR mixture, in place of purified DNA, and with the relevant primers for the insert of interest as described in section 2.4. Single colonies from the transformants with the predicted amplicon size were grown in liquid culture over night for plasmid extraction (section 3.2.3.3.4) and further analysis. Plasmids generated through cloning had the inserts confirmed with sequencing of plasmid by Sanger sequencing (Eurofins Genomics) (section 2.6).

3.2.3.3.2 TOPO cloning procedure

Gene sequences were introduced into the entry vectors pCR8/GW via TOPO TA blunt end cloning and pENTR/D (Invitrogen) through TOPO blunt end cloning. Through TOPO cloning the gene of interest was inserted between attL cloning sites used in the Gateway Technology recombinant reactions to facilitate downstream cloning into destination vectors (Hartley et al., 2000).

Gene sequences were amplified as specified in section 3.2.4. Before the insertion of the gene of interest into the vector a poly-A tail was added to the gene sequence through incubation at 72˚C for 15 min with Taq polymerase (New England Biolabs, NEB) and dATP (Table 3.3). The TOPO TA cloning reaction was then carried out with the gene with the poly-A tail overhang and the pre-digested entry vector (Table 3.4). 2-4 µl of the TOPO reaction mixture with the ligated vector was transformed into 40 µl *E.coli* DH5α (section 3.2.3.1) and 50-200 µl was plated on LB+agar with the relevant antibiotic for the vector.

Table 3.3. Reaction for the introduction of poly-A tail to gene product. The linear gene of interest was incubated with Taq polymerase to add poly-A tail before TOPO cloning into the pCR8/GW vector. NEB = New England Biolabs

Reagent	**Quantity (µl)**
10x Taq buffer (NEB)	2
Taq polymerase (5 U/µl) (NEB)	1
dATP (10 mM)	2
Amplicon (50-100 ng/µl)	4
water	6

Table 3.4. Components for the TOPO reaction for cloning into pCR8/GW. The linearized vector pCR8/GW and salt solution was provided in the pCR8/GW/TOPO TA Cloning Kit (Invitrogen).

Reagent	**Quantity (µl)**
Amplicon+Poly-A tail	4
pCR8/GW/TOPO vector TOPO adapted (5-10 ng/µl linearised plasmid)	1
Salt solution (1.2 M NaCl, 0.06 M $MgCl_2$)	1

3.2.3.3.3 Gateway LR cloning into destination vectors

Entry vectors, pCR8/GW and pENTR, with the verified insert were used in further cloning into the relevant destination vector through Gateway Technology LR-cloning. In LR-cloning a gene sequence is transferred from one vector to another by recombinational cloning of compatible sites, attL and attR sites (Hartley et al., 2000).

The entry vector, destination vector, TE buffer (AppliChem GmbH) and the Gateway LR clonase reaction buffer (Invitrogen) were mixed together before incubation at 25˚C overnight (Table 3.5). To terminate the reaction 1 µl (20 mg/ml) of Proteinase K (Thermo Scientific) was added and the mixture was incubated as 37˚C for 10 min before transformation into DH5α and plating onto LB+agar with relevant antibiotic selection. Transformants were verified with colony PCR and sequencing of extracted plasmid.

Table 3.5. Reagents used in TOPO cloning. The entry vectors with the gene of interest were used in the LR reaction to transfer the genes to the destination vector. Destination vectors are summarised in Appendix 1 Table S3.1.

Reagent	Quantity
pCR8GW/pENTR D with gene of interest	50 ng
Destination vector	100 ng
5x LR Clonase reaction buffer (Invitrogen)	4 µl
TE buffer pH 8 (AppliChem GmbH)	to 8 µl

3.2.3.3.4 Plasmid extraction

Overnight cultures of 5 ml LB with the appropriate antibiotic selection agent inoculated with *E. coli* were used to extract plasmid DNA with GenElute Plasmid Miniprep Kit (Sigma Aldrich) according to the manufacturers protocol. The plasmid DNA was eluted in 50 µl molecular grade water and stored at -20°C.

3.2.4 Amplification of genes of interest from cDNA

The coding sequences (CDS) of the putative sequences for *HvDEX1*, *HvMMD1-1*, and *HvICE1-1* were amplified from cDNA extracted from barley spikes from the spring barley cultivar Golden Promise grown at control conditions of 15/12˚C day/night temperatures with a 16 h photoperiod (specified in section 2.1). A mixture of cDNA from different spike stages were used to ensure the sequence of interest was present as a template for amplification. The full length gene sequences of the CDS of *HvDEX1*, *HvICE1-1* and *HvMMD1-1* were sequenced and compared with the annotated sequences obtained from BARLEX (IBGSC, 2012), to confirm that the amplified genes corresponded to the predicted sequence. Further details about the amplification of the sequences for downstream cloning are stated in the sections related to the generation of the overexpression and SRDX-silencing constructs (section 3.2.5) and to the transient expression analysis (section 3.2.9).

Primers for the amplification of the CDS were based on the annotated barley genes from BARLEX designed using the NCBI Primer-BLAST tool (https://www.ncbi.nlm.nih.gov/tools/primer-blast/index.cgi) (sequences specified in Appendix 1, Table S3.2).

3.2.5 Generation of CRISPR, overexpression and silencing constructs

Overexpression constructs of *HvDEX1*, *HvMMD1-1*, and *HvICE1-1* were generated by the cloning of the CDS amplified from cDNA using primers containing the starting ATG and stop codons into the pBract214 vector, specified in Appendix 1, Table S3.2. The pBract214 vector is a Gateway-compatible vector used for *Agrobacterium*-mediated plant transformation of barley (Smedley and Harwood, 2015). For the generation of constructs used for

overexpression and silencing the CDS of genes were amplified with PrimeSTAR GXL polymerase (TaKaRa) according to manufacturer's protocol. 10 µl 5x PrimeSTAR GXL Buffer, 4 µl dNTP micture (10 mM), 10 pmol of each primer, 3 µl of 50 ng/µl cDNA from a mixture of barley spike stages of Golden Promise, 1 µl PrimeSTAR GXL DNA polymerase and molecular grade water to a volume of 50 µl was combined (all components supplied by TaKaRa except primers and cDNA). The reaction was cycled through 98°C for 10 sec, 60°C for 15 sec and 68°C for 1min/kb for 30 cycles. Prior to cloning the amplicons of each gene were analysed through gel electrophoresis.

For the silencing constructs of the transcription factors *HvMMD1-1* and *HvICE1-1*, the CDS were amplified with primers containing the start ATG and an SRDX-sequence in the C-terminal end before the stop codon (primers in Appendix 1, Table S3.2). The reverse complement of the reverse primer containing the SRDX tag would be: gene specific (green), SRDX (blue), stop codon (red):

5' TCA AGCGAAACCCAAACGGAGTTCTAGATCCAGATCCAG GCCGTTGATGTGGCTC 3'

The CDS of the genes were amplified from cDNA using primers containing the starting ATG and stop codons (primers in Appendix 1, Table S3.2). These unmodified sequences were cloned into entry vector pCR8/GW via TOPO TA blunt end cloning (Invitrogen) before transformation into *E. coli* DH5α (as described in section 3.2.3.3.2 and 3.2.3.1). The entry vectors with the CDS insert was used for LR-cloning into pBract214 (section 3.2.3.3.3) where the gene is under control of the ubiquitous promoter *ZmUbi* (Smedley & Harwood, 2015). The sequence insertion into the destination vector was verified before transformation into *Agrobacterium* AGL1 for further barley transformation.

To potentially maximise the severity of the mutations, CRISPR targets were design close to the N-terminal domain in the coding sequence. The target sequences were analysed through BLAST searches through EnsemblPlants (Howe et al., 2021) against the barley genome to look for off-targets. Sequences with off-targets in coding regions were avoided to prevent unwanted gene disruptions. Off-targets without the PAM-sequence, or without high identity around the PAM region were considered negligible.

3.2.6 Assembly of the CRISPR-Cas9 constructs

The vectors used for targeted mutagenesis through CRISPR were assembled using the Golden Gate Modular Cloning system (MoClo) described in Engler et al., (2014) using plasmids from Lawrenson et al., (2015). In the MoClo system sgRNA target sequences are cloned into level 1 acceptor vectors which are then used for the assembly of the destination level 2 vectors containing the sgRNAs with TaU6 promoters, Cas9 protein sequence, and hygromycin resistance in a backbone vector suitable for *Agrobacterium* mediated plant transformation (Lawrenson et al., 2015).

sgRNA targets were amplified from a sgRNA vector template with primers specific for each target sequence and were designed according to Lawrenson et al., (2015). Target sgRNA were chosen as 20 bp sequence starting with a "G" and ending with the PAM "NGG" sequence. The sequence was analysed through BLAST against the barley genome to look for off-targets.

The primers contained flanking regions with BsaI restriction sites enabling the assembly of the final vector using the MoClo system. The forward primers consisted of the BsaI restriction site in the 5' end, the target sgRNA without the G and PAM sequence (Table 3.6), and a sgRNA template sequence for the amplification from the pICH86966 vector.For a target with the sequence GAGGACTGGTACTTCGGCGCAGG (PAM and initial G marked in green) the primer will be:

5' TGTGGTCTCACTTG AGGACTGGTACTTCGGCGC GTTTTAGAGCTAGAAATAGCAAG 3'

Where the sequence in blue contains the BsaI restriction site, the black is the sgRNA specific sequence and the pICH86966 recognition sequence is in red. The reverse primer is standardized for all sgRNAs, containing BsaI restriction site and a pICH86966 recognition sequence for the amplification from the template. The sgRNAs were amplified with the Phusion High-Fidelity DNA polymerase (Thermo Scientific) according to manufacturer's protocol (Table 3.7, Table 3.8). The resulting amplicons were analysed by gel electrophoresis and extracted and gel purified using the Wizard SV Gel and PCR-clean-up system (Promega).

Table 3.6. CRISPR-constructs for each gene with the targets selected in the exons of the putative barley genes.

Gene	Construct	sgRNA number	Exon target	sgRNA sequence 5' – 3'
HvDEX1	1	1	2	GTACCAAGTGTCCAAAACACGTGG
		2	4	GCACACGGGAAATAGTGTTGG
		3	5	GCGAAACAAGCTGCTTCTGAGG
	2	4	3	GAAGTGCTTGAAGGTTCCGATGG
		5	5	GACAAGCTAGAGGTACCTCGTAGG
		6	6	GAAACTCATGGTAGTGATGCAGG
HvICE1-1	1	1	1	AGGACTGGTACTTCGGCGC
	2	2	1	AAGCATCGGGGTCCAGCTC
	3	3	1	ACCTCGGCAGCTCCGGCGC
	4	4	1	GGCGACGGCCATGAACAACA
	5	5	1	GCACAGATGACAGAGTTTGG
	6	6	1	GTTTCGACTTGTTCGACACC
HvMMD1-1	1	1	1	GTCGGCCTCGAAGCCCGCCGG
		2	2	GCCACCACTGGGTGTCAAAACGG
		3	3	GCCGACATGTCCGTCGCGTGG
	2	4	2	GCGGACGCAGACTGGGACCGG
		5	3	GCTGGGGATACTGCCTTGCCAGG
		6	3	GAAGCCGTGTACGATGAAGAGG

Table 3.7. Reagents for Phusion DNA polymerase PCR.

Reagent	**Volume (µl)**
Water	7
5x Phusion HF-buffer	2
dNTP (10 mM)	0.3
DMSO	0.3
Reverse primer (10 µM)	0.3
Forward primer (10 µM)	0.3
pICH86966 (200ng)	0.3
Phusion polymerase	0.2

Table 3.8. PCR program for Phusion DNA polymerase.

Temperature (˚C)	**Time**	**Cycles**
98	1 min	1
98	30 sec	35
57-65	30 sec	
72	30 sec	
72	6 min	1
10	->	->

The sgRNAs were introduced into the level 1 vectors through MoClo cloning system (Table 3.9, Table 3.10) where the level 1 backbone was dependent on the number of targets used per final level 2 to facilitate proper assembly of the level 2 plasmid (Figure 3.2). *HvICE1* CRISPR level 2 plasmids contained one target per construct (all introduced into p47751) whereas *HvDEX1* and *HvMMD1-1* contained 3 targets (introduced into p47751, p47761 and p47772) per level 2 vector. To ligate different numbers of level 1 sgRNAs into the level 2 vectors the required 3'-linker vector was used (Figure 3.2, Appendix 1, Table S3.1).

Table 3.9. Reagents for the MoClo assembly of level 1 vectors.

Reagent (final amount)	**Quantity**
Acceptor	5 ng
Target insert	1-3 µl
p90003, promoter sequence	3 ng
10x Bovine serum albumin	2 µl
10x T4 ligase buffer (NEB)	2 µl
BsaI (10 U/µl) (NEB)	1 µl
T4 DNA Ligase (5 U/µl) (NEB)	1 µl
water	To 20 µl

Table 3.10. Protocol for the MoClo assembly of level 1 and level 2 vectors for the ligation of the sgRNA sequences into the acceptor vector.

Temperature (˚C)	Time	Cycles
37	3 min	26
16	4 min	
50	5 min	1
80	5 min	1

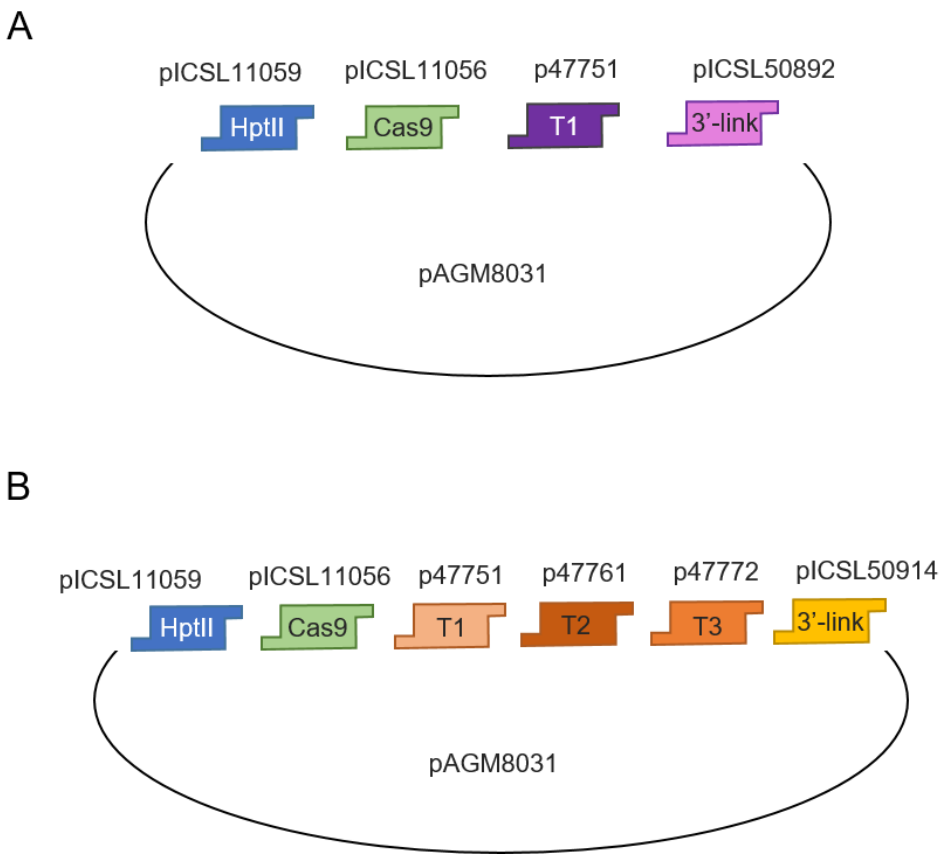

Figure 3.2. Illustration of the MoClo level 2 reaction combining level 1 vectors with one sgRNA (A) or three sgRNA (B) for the final level 2 vector. The vectors carrying hygromycin resistance (pICSL11059) and Cas9 (pICSL11056) were introduced into the backbone (pAGM8031) along with one sgRNA T1 (p47751) and the required 3'-linker (pICSL50892) or with three sgRNAs T1-3 (p47751, p47761, p47772) and the 3'-linker (pICSL50914). Further information about the plasmids is available in Appendix 1 Table S3.1.

Level 1 vectors were transformed into DH5α and plated on LB+agar with relevant antibiotic and IPTG and x-gal for blue white colony screening. After validation by colony PCR the plasmids were extracted and used for level 2 cloning where the sgRNAs for each construct were incorporated together with the Cas9 gene, and a hygromycin resistance gene, into the acceptor backbone (Figure 3.2, Figure 3.3) (Engler et al., 2014) using the restriction enzyme BsaI and subsequent ligation into a final backbone (Table 3.11). The final vector was transformed into DH5α for amplification and plasmid extraction before transformation into *Agrobacterium* AGL1. The transformants were verified by Sanger sequencing (Eurofins, MWG-Biotech) at each step.

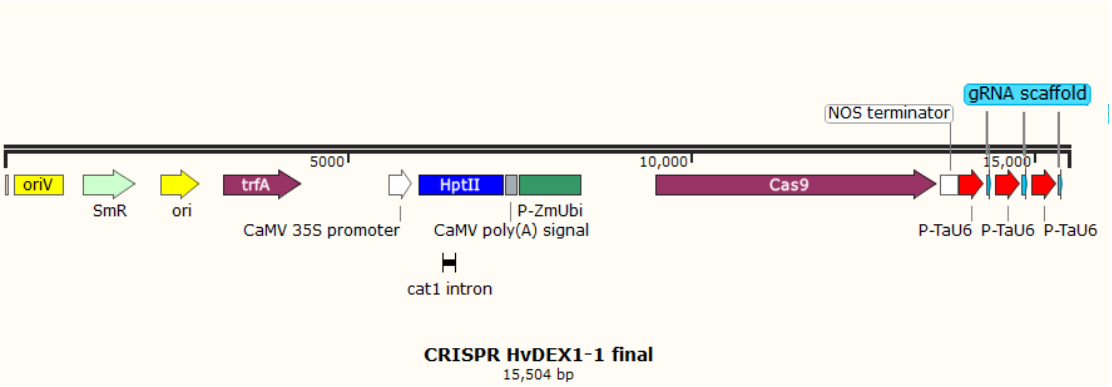

Figure 3.3. Map of HvDEX1 *CRISPR construct with the hygomycin resistance gene, Cas9, and three target sgRNA. SmR, resistance to spectinomycin and streptomycin; P-CaMV35s and T-CaMV35s, Cauliflower mosaic virus promoter and terminator; HptII, hygromycin phosphotransferase II; P-ZmUbi, Ubiquitin promoter from Zea mays; Cas9, Cas9 from Streptococcus pyogenies; SV40 NLS, nuclear localisation signal from Simian vacuolating virus 40; T-AtNos, nopaline synthase terminator from Agrobacterium; P-TaU6, U6 promoter from Triticum aestivum, T1-T3, sgRNA targets.*

Table 3.11. Reagents for the assembly of CRISPR vectors level 2. The vectors used for the assembly of the level 2 vector was depending on the number of sgRNAs incorporated in the final level 2 vectors as illustrated in Figure 3.2.

Reagent	**Quantity**
p47751	5 ng
p47761 (for 3 sgRNAs/level 2 vector)	5 ng
p47772 (for 3 sgRNAs/level 2 vector)	5 ng
pICSL11059	5 ng
pICSL11056	5 ng
pAGM8031	5 ng
pICSL50914/pICH50892 (1 or 3 sgRNAs)	5 ng
BpiI (10 U/µl) (NEB)	2 µl
10x Bovine serum albumin	2 µl
T4 ligase (5 U/µl)	1 µl
10x T4 buffer	2 µl
Water	To 20µl

3.2.7 Transformation of immature barley embryos

The CRISPR constructs, overexpression and silencing constructs were transformed into the two-rowed spring barley variety Golden Promise according to Harwood (2014). All media components for *Agrobacterium* growth media MG/L, callus induction (CI) media, transition media, and regeneration media are specified in Harwood, (2014) and in Appendix 1, Table S3.3 - Table S3.10. In all stages the plates were sealed with micropore surgical tape.

For successful extraction of immature embryos the general plant health was critical. Plants were grown as specified in section 2.1 until anthesis had occurred and grains were filling. The embryos at this stage were 1.5-2 mm in diameter and the endosperm was still milky and soft. Spikes were collected and immature seeds were removed from the spike and sterilised as specified in section 2.1. Immature barley embryos were extracted by opening the seed with forceps without damaging the embryo. The axis was removed and the embryo was placed on callus induction (CI) medium with growth regulators, with the removed axis side against the media. The embryos were incubated for 24 h in the dark at 22°C.

The embryos were transformed by inoculation of an overnight culture of *Agrobacterium* containing the construct of interest grown in 10 ml MG/L media with 10 µl 150mM acetosyringom without antibiotics in a shaker at 28°C. 200-300 µl of *Agrobacterium* culture was used to transform 25 embryos by inoculation for 2 min before the plate was tilted for 10 min to allow excess culture to drain from the embryos. The embryos were transferred to fresh CI plates without antibiotics. The calluses in the following steps were grown at 22°C in the dark. The embryos were transferred to CI medium for three days of co-cultivation with the *Agrobacterium* before being transferred to CI medium with hygromycin (50 mg/L) and timentin (160 mg/L) to select against the *Agrobacterium*.

One of the major issues faced while applying these techniques was the survival of calluses, especially after *Agrobacterium* co-cultivation. Failed transformation of the constructs carrying antibiotic resistance or transmission of *Agrobacterium* on the calluses led to embryo death. To mitigate this and improve transformation and embryo survival a range of parameters were optimised. The optical density at wavelength 600 nm (OD_{600}) of the *Agrobacterium* culture was reduced to increase viability of the cells and the length of *Agrobacterium* application directly to the embryos was reduced from 2 min to 45 sec with excess culture removed to avoid redundant exposure to the embryos.

After six weeks of selection on CI media, where the calluses were transferred to fresh plates every two weeks, the calluses were transferred to transition medium and placed at 24°C in low light conditions, under a sheet of paper to simulate low light, for 2 weeks. Calluses with generated roots and green shoots were then transferred to regeneration medium and placed under light conditions without the paper (140 µmol/m^2s), at 24°C. After 2 weeks plantlets with shoots and roots longer than 2 cm were transferred to tubes containing 12 ml CI medium without growth regulators. Once the plantlets reached the top of the 15-20 cm long tubes the plantlet was transferred to soil (Levington C2) in 10 cm pots and were grown

in growth rooms as specified in section 2.1. Until the plantlets were established the pots were covered with plastic bags to maintain high humidity, normally 1-2 weeks. The plants were transferred to 5 L pots (three plants per pot) once the plants were established and growing upright, normally after 3-4 weeks. Generated transgenic plants were allowed to self-pollinate in every generation.

3.2.8 Genotyping of barley transgenic lines

All generations of the barley CRISPR transformants were genotyped for the presence of Cas9 through genotyping PCR for the Cas9 gene, to determine if the transformation was successful and if Cas9 was retained in the plants. Plants positive for the Cas9 transgene were genotyped for mutations in the targets through sequence analysis. The full length genes were amplified for each gene and the target sequences were sequenced using primers 80-400 bp from the PAM site summarised in Table 3.12. The sequence data was analysed with the Cas9 editing detection software Tracking of Indels by Decomposition (TIDE) (https://tide.nki.nl/) which detects polymorphisms in the sequencing sample to estimate the mutation frequency.

Table 3.12. Primers used for sequencing of the sgRNA target sequences for the identification of CRISPR/Cas9 induced mutations in the genes of interest, HvDEX1, HvICE1-1 *and* HMMD1-1*. The targets are named T1-T6 and were sequenced using the amplified full length gene sequenced with the stated primer located upstream of the PAM sequence (except for primer 8218). Primer sequences are stated in Appendix Table S3.2.*

Gene	Target	Primer	Distance from PAM (bp)
HvDEX1	T1	8534	181
	T2	7658	86
	T3	7736	135
	T4	8401	144
	T5	7735	173
	T6	7869	84
HvICE1-1	T1+T2+T3	8192	218 + 296 +392
	T4	8221	110
	T5+T6	8218	79 + 109
HvMMD1-1	T1	2379	113
	T2+T4	8397	88 + 130
	T3+T5+T6	8399	129 + 229 + 393

3.2.9 Subcellular localisation assay with transient expression

For the study of subcellular localisation of the genes of interest the coding sequences of *HvMMD1-1*, *HvDEX1* and *HvICE1-1* were cloned into a vector containing the Yellow Fluorescent Protein (YFP), pUBC-YFP, for transient expression in epidermal tobacco cells.

The CDS of *HvDEX1*, *HvMMD1-1* and *HvICE1-1* were amplified from cDNA without stop codon using the Q5 polymerase reaction according to manufacturer's protocol (Table 3.13, Table 3.14) (New England Biolabs). The amplicons were analysed with gel electrophoresis as in section 2.5 to ensure only one amplicon of right size had been amplified. The sequences were cloned into entry vector pENTR/D using TOPO cloning and were transformed into DH5α (as in section 3.2.3.3.2 and 3.2.3.1). After verification by colony PCR (section 3.2.3.3.1) and sequencing (section 2.6) the vectors were extracted and purified (section 3.2.3.3.4). The CDS was introduced into the destination vector pUBC-YFP under the control of the pUBQ10 promoter through LR-cloning (section 3.2.3.3.3). The LR cloning mixture was transformed into DH5α where the construct was verified to contain the CDS and the YFP through genotyping with primers specific to the CDS and YFP (Appendix 1, Table S3.2). The plasmids were then extracted (section 3.2.3.3.4) and sequenced for the CDS and YFP. The final vector was then transformed into *Agrobacterium* strain GV3101 for further plant transformation.

Table 3.13. Reagents used for PCR with Q5 polymerase for the amplification of coding sequence of barley orthologues. The cDNA template was a mixture of spike stages from Golden Promise grown in control conditions. NEB: New England Biolabs

Reagent	**Quantity (µl)**
5x Q5 buffer (NEB)	10
dNTP (10 mM)	1
Forward primer (10 µM)	2.5
Reverse primer (10 µM)	2.5
cDNA (50-150 ng/µl)	1
Q5 polymerase (NEB)	1
water	To 50 µl

Table 3.14. Temperature and duration for Q5 polymerase (New England Biolabs) PCR for the amplification of coding sequences of barley orthologues.

Temperature (°C)	**Time**	**Cycles**
98	30 sec	1
98	10 sec	35
X	20 sec	
72	1 min	
72	2 min	1

Tobacco (*Nicotiana benthamiana*) was grown for 4-6 weeks in growth rooms with 20/18°C day/night cycles with 16 h photoperiod. The vectors were transformed into tobacco leaves by infiltration of *Agrobacterium* culture according to Sparkes et al. (2006). The *Agrobacterium* cultures were grown in 10 ml cultures to an OD_{600} of 0.9-1.1, after which it was centrifuged for 10 min at 4000 g and resuspended to OD_{600} of 0.4 in Infiltration buffer (Table 3.15). The solution was incubated at room temperature for 1h under slight agitation before infiltration into tobacco leaves (Sparkes et al., 2006). 100-200 µl of the bacterial solution was infiltrated into the abaxial side of the leaves and the outlines of the absorbed liquid was traced on the leaves. The tobacco plants were returned to the growth room. After 2-3 days the transformed leaves were imaged with Confocal Leica TCS SP5 (Leica Microsystems). To confirm nuclear localisation of *HvMMD1-1* and *HvICE1-1* the leaves were co-stained with DAPI through vacuum infiltration for 3 minutes with DAPI (100 µg/ml) in 1x PBS pH 8 and 0.2% Triton x100 before rinsing with water to remove excess DAPI solution.

Table 3.15. Infiltration solution for Agrobacterium mediated transformation for transient expression in tobacco leaves (Sparkes et al., 2006).

Reagent	**Final concentration**
$MgCl_2$	10 mM
MES (pH 5.6)	10 mM
Acetosyringone	150 µM

3.2.10 Environmental scanning electron microscopy (SEM)

Pollen grains and anther wall tissue of HvMMD1-1 and HvDEX1 overexpression lines were imaged with Environmental Scanning Electron Microscope (ESEM) conducted by Nicola Weston and Elisabeth Steer at the Nanoscale and Microscale Research Centre at University Of Nottingham. Anthers at growth stage LFE3-4 with yellowing anthers about to release pollen (Gomez & Wilson, 2012) were collected and imaged within 3-4 h to prevent drying. Anthers were placed directly onto SEM stubs and dissected to release pollen grains. The chamber pressure was kept at 100% humidity with imaging using the Peltier cooling stage at 2°C with the FEI Quanta 650 ESEM.

3.2.11 Gene expression analysis

Relative gene expression was carried out as described in general methods (section 2.10). Total RNA was extracted from barley spike tissue from Golden Promise, HvDEX1:OE, HvMMD1:OE, and HvMMD1:SRDX lines and from leaf tissue of Golden Promise, HvICE1:OE and HvICE1:SRDX lines grown at control conditions of 15/12˚C day/night temperatures with a 16 h photoperiod (described in section 2.1). The expression of each gene of interest was normalised to two reference genes, *α-TUBULIN* (*HvTub*) and to *HvHSP70* (*HEAT SHOCK PROTEIN70*) and to the expression of the wild type (Golden Promise) for each tissue (described in section 2.10).

3.3 Results

3.3.1 Selection of genes putatively related to pollen development

Three genes that had previously been linked to male fertility in *Arabidopsis* were selected, *DEFECTIVE IN EXINE FORMATION1* (*DEX1*), *MALE MEIOCYTE DEATH1* (*MMD1*) and *INDUCER OF CBF3 EXPRESSION1* (*ICE1*), to determine if they were conserved in barley and had equivalent roles in pollen development and plant physiology in barley. Barley orthologous gene sequences for *DEX1, ICE1* and *MMD1* were identified through the BLAST analysis of the orthologues of *Arabidopsis thaliana* and *Oryza sativa* sequences to barley (Table *3.16*). The gene IDs for the putative barley orthologues were obtained from two different datasets, the Morex v1 Gene Models (2016) and Morex v1 Gene Models (2019) from BARLEX, however the gene sequences from both annotations were identical. The gene identity of the protein sequences between the three species was compared to identify conserved protein domains to ensure a reasonable likelihood of a conserved function. Orthologous gene sequences of *DEX1*, *ICE1* and *MMD1* were analysed based on the sequence conservation and micro-synteny between *Arabidopsis thaliana*, *Oryza sativa* and *Hordeum vulgare* as well as analysis of expression pattern of the selected genes to determine if they were expressed in floral tissues.

Table 3.16. Gene sequence identifiers of confirmed and predicted orthologues of the selected genes in Arabidopsis thaliana*,* Oryza sativa*, and* Hordeum vulgare*. The gene IDs for the putative barley orthologues were obtained from the Morex v1 Gene Models (2016) and Morex v1 Gene Models (2019).*

Gene	*A. thaliana* gene	*O. sativa* orthologue	Putative barley orthologue
DEX1	*AT3G09090*	*OsDEX1 Os03g0825700*	*HORVU.MOREX.r2.5HG0438930/ HORVU5Hr1G114910*
ICE1	*AT3G26744*	*OsICE1 Os11g0523700*	*HORVU.MOREX.r2.7HG0583410/ HORVU7Hr1G074490*
MMD1	*AT1G66170*	*TIP3 Os03g0716200*	*HORVU.MOREX.r2. 4HG0281670/ HORVU4Hr1G008160*

Expression data from BARLEX was collected for the candidate genes in Table 3.16 to analyse the expression profile in different tissues throughout the plant (Figure 3.4). Genes with increased expression in tissues related to the inflorescence were considered as having increased likelihood to be the putative orthologue. The putative *HvDEX1* transcript was present and showed high expression in all stages and organs present in the dataset, including floral tissues, compared to the expression of the *HvICE1-1* and *HvMMD1-1*. The *HvMMD1-1* transcript displayed a very low to no expression in most tissues with the highest expression in the rachis tissue. *HvICE1-1* was mostly present in the developing inflorescence and the developing grain (Figure 3.4).

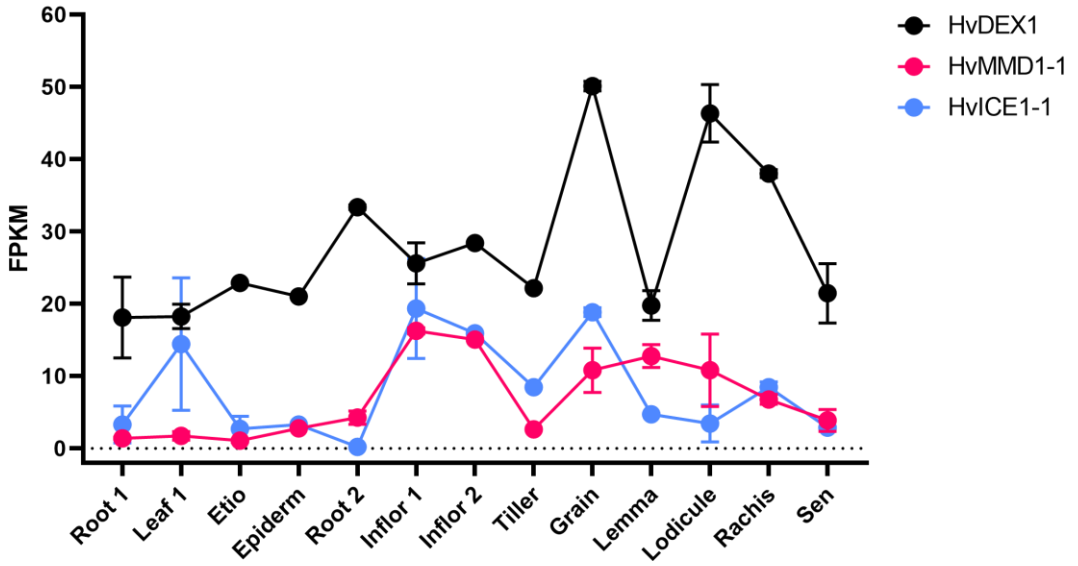

Figure 3.4. Expression data of the putative genes of interest in barley, HvMMD1-1, HvDEX1, *and* HvICE1-1 *from BARLEX. Out of the genes* HvDEX1 *displayed the highest expression in all tissues with the highest transcript level detected in the developing grain and in the lodicule and rachis. The* HvMMD1-1 *transcript showed a very low level of expression with the highest in the rachis tissue.* HvICE1-1 *was detected in most tissues with seedling leaf, flowering tissue and developing grain showing the highest. FPKM = Fragments per kilo base of transcript per million mapped fragments. Root 1: Roots from seedlings (10 cm shoot stage), Leaf 1: Shoots from seedlings (10 cm shoot stage), Etio: Etiolated seedling, Epiderm: Epidermal strips, Root 2: Roots, Inflor 1: young developing inflorescence (5mm), Inflor 2: Developing inflorescences (1-1.5 cm), Tiller: Developing tillers, 3rd internode, Grain: Developing grain, Lemma: Inflorescences, lemma, Lodicule: Inflorescences, lodicule, Rachis: Inflorescences, rachis, Sen: Senescing leaves.*

3.3.1.1 *DEX1* orthologous sequence

To identify a *HvDEX1* candidate the protein sequences of *DEX1* and the confirmed rice orthologue *OsDEX1* (Yu et al., 2016) were compared to the barley genome. The *HORVU.MOREX.r2.5HG0438930* was identified through BLAST analysis as the only candidate *HvDEX1* from both *DEX1* and *OsDEX1*. The putative *HvDEX1* protein sequence was compared back to the proteome of *Arabidopsis* and rice where the *DEX1* and *OsDEX1* sequences were the only identified sequences in the respective genome, suggesting that the *HvDEX1* orthologue is the sequence with the highest similarity to both orthologues. The *DEX1* orthologues showed a high degree of sequence identity between rice and barley (82.2%) which was slightly lower when comparing the rice and barley genes to *Arabidopsis* (Table 3.17). In addition, the gene sequences for *AtDEX1* , *OsDEX1* and the putative *HvDEX1* all contain a FG-GAP domain (Figure 3.5), a region that has been shown to be important for ligand binding and a putative Ca^{2+} binding motif has been found in some of the repeats (Rigden et al., 2011). To further confirm that *HvDEX1* was a potential orthologue of *OsDEX1* the protein coding sequences in the region surrounding *HvDEX1* was compared to the rice proteome through BLAST analysis to detect micro-synteny. Four out of six genes upstream of *HvDEX1*, and two out of six genes downstream had orthologues which were located in the region surrounding *OsDEX1* (Table 3.18). This suggests there is a level of conserved micro-synteny in this region between barley and rice.

Table 3.17. Gene sequence comparison of DEX1 *orthologues for the identification of a putative* HvDEX1 *sequence. Each protein sequence of* A. thaliana *(At),* O. sativa *(Os) and* H. vulgare *(Hv) were compared to each other to detect the level of gene identity (%ID) and only one sequence was detected in either genome. The* HvDEX1 *candidate was annotated through EnsemblPlants to be an orthologue of* DEX1*.*

Comparison	Gene with highest gene identity	Subject description	Genomic location (Mbp)	Length (bp)	%ID
At-Os	Os03t0825700-01	OsDEX1	Chr3: 34.68	457	77.5
At-Hv	HORVU.MOREX.r2.5HG0438930.1	Protein DEFECTIVE IN EXINE FORMATION 1	Chr5: 521.30	456	76.3
Os-At	AT3G09090.1	DEX1	Chr3: 2.78	498	77.7
Os-Hv	HORVU.MOREX.r2.5HG0438930.1	Protein DEFECTIVE IN EXINE FORMATION 1	Chr5: 521.30	497	89.9
Hv-At	AT3G09090.1	DEX1	Chr3: 2.78	613	67.7
Hv-Os	Os03t0825700-01	OsDEX1	Chr3: 34.68	576	85.2

Table 3.18. Investigation of micro-synteny between rice and barley in the region surrounding OsDEX1*. The protein coding sequences upstream and downstream of* HvDEX1 *were compared to the rice proteome using BLAST analysis. The rice sequence with the highest similarity to the barley protein sequence is given as the best rice orthologue with the corresponding sequence similarity (gene ID). Marked in green are the rice sequences located on chromosome Os3 around* OsDEX1 *which suggests a conserved micro-synteny.*

	Barley gene	Best rice orthologue	Gene ID
-6	HORVU.MOREX.r2.5HG0438870	Os03t0825300	91.7
-5	HORVU.MOREX.r2.5HG0438880	Os03t0825400	79.7
-4	HORVU.MOREX.r2.5HG0438890	Os03t0825500	89.3
-3	HORVU.MOREX.r2.5HG0438900	Os03t0825600	84.1
-2	HORVU.MOREX.r2.5HG0438910	Os11t0302500	87.8
-1	HORVU.MOREX.r2.5HG0438920	Os07t0635500	74.8
0	HORVU.MOREX.r2.5HG0438930 HvDEX1	Os03t0825700 OsDEX1	85.2
1	HORVU.MOREX.r2.5HG0438940	Os09t0549450	68.9
2	HORVU.MOREX.r2.5HG0438980	Os03t0825800	69.2
3	HORVU.MOREX.r2.5HG0439020	Os08t0468400	66.1
4	HORVU.MOREX.r2.5HG0439040	Os03t0826300	87.3
5	HORVU.MOREX.r2.5HG0439050	Os07t0243150	34.8
6	HORVU.MOREX.r2.5HG0439060	Os01t0852500	31.2

The sequences of *DEX1*, *OsDEX1* and *HvDEX1* were aligned using ClustalW and protein domains were predicted with ScanProsite, ExPASy. All three sequences were predicted to contain FG-GAP domains, a representation of integrin, which is required for Ca^{2+} binding (Figure 3.5) (Rigden et al., 2011). Conservation of this domain in *HvDEX1* indicates that the Ca^{2+} binding function could be retained in HvDEX1.

Through the conservation of predicted protein domains, micro-synteny, and the expression profile matching predicted inflorescence related genes, the *HORVU.MOREX.r2.5HG0438930* gene sequence appeared as the best match for the *HvDEX1* orthologue and was therefore selected for further analysis of gene function in barley.

3.3.1.2 Identification of potential *HvMMD1* orthologues

To identify a potential orthologue of *MMD1* in barley the protein sequences of *MMD1* and its confirmed orthologue in rice, *TIP3*, were compared to the barley proteome through BLAST analysis and the three resulting sequences with the highest gene identity are summarised in Table 3.19. Interestingly, *TIP3*, the confirmed *MMD1* orthologue, had only the second highest gene identity to *MMD1* with two other predicted PHD finger sequences also identified. However, all of the rice sequences shared a low gene identity with *MMD1*.

In barley the three sequences with the highest gene identity to *MMD1* were annotated as PHD fingers. One of the sequences was identified as *HvMS1* and the other sequences were investigated through further bioinformatics analysis to determine the best *HvMMD1* candidate. When comparing *TIP3* to barley, the best hits were all the same sequence, *HORVU.MOREX.r2.4HG0281670.1*, marked in yellow in Table 3.19. The candidate sequences in Table 3.17 *HORVU.MOREX.r2.3HG0248440.1* (marked in orange) and *HORVU.MOREX.r2.4HG0281670.1* (marked in yellow) were compared back to the *Arabidopsis* and rice genomes to investigate if the putative barley orthologues shared high gene identity with other proteins (Table 3.19). The first sequence (marked in yellow) shared the highest similarity with predicted PHD fingers with no studied function in the rice and the *Arabidopsis* genome. The second sequence (marked in orange), which was the best hit from rice, displayed high sequence similarity with the *TIP3* and *MMD1* protein sequences among other predicted PHD proteins. The second sequence *HORVU.MOREX.r2.4HG0281670.1* was therefore used as the best putative orthologue for further bioinformatics studies.

From the BLAST analysis it was also evident that there is a high level of similarity between different PHD proteins, i.e. *MS1* and *MMD1*. This suggests that there are sequences in the different genomes with highly similar PHD fingers and additional approaches are needed to identify candidate orthologues.

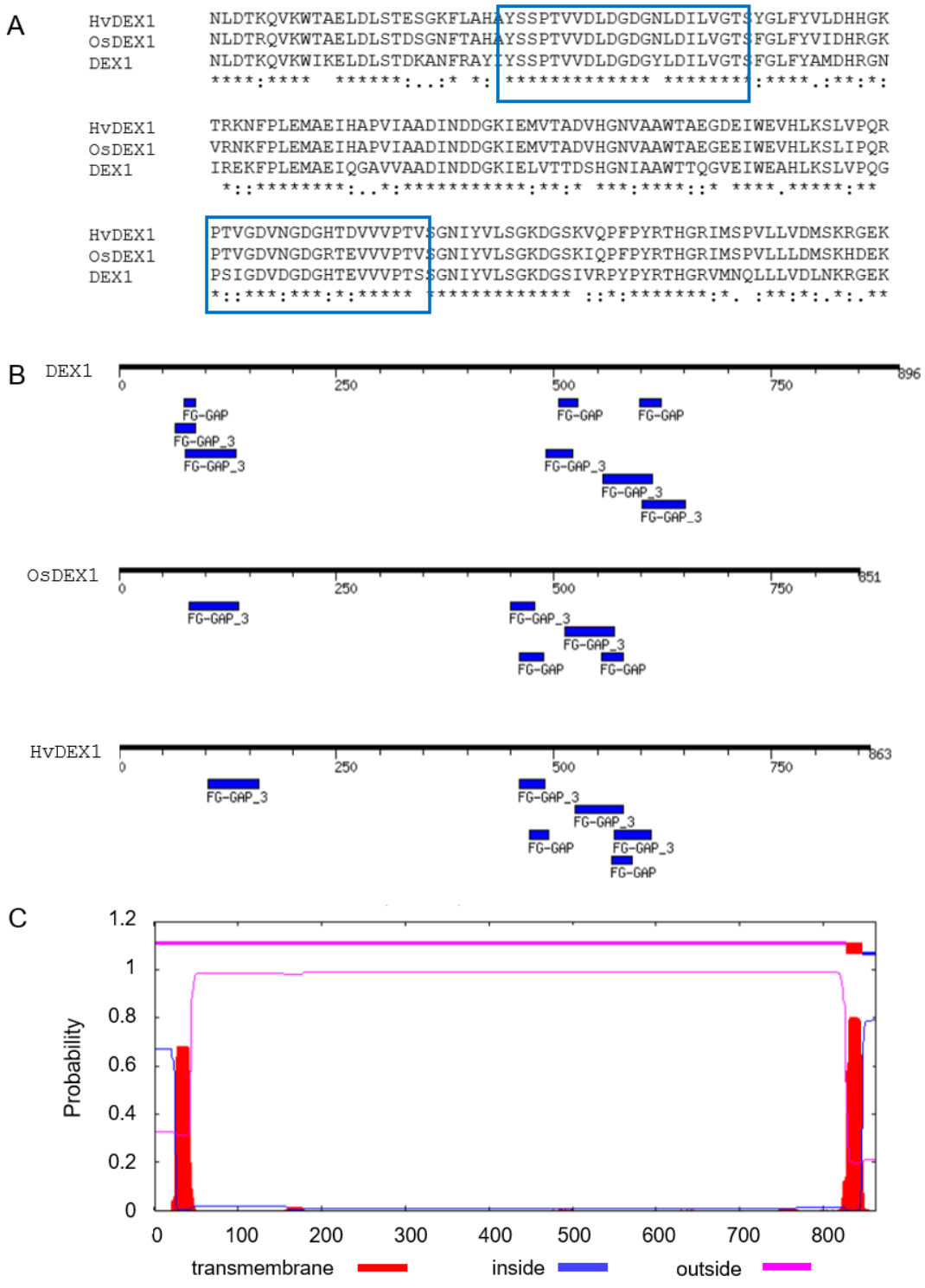

Figure 3.5. Alignment of protein sequences of orthologues of DEX1, OsDEX1 *and* HvDEX1. *In a protein sequence alignment of* DEX1 *orthologues the FG-GAP domain is marked in purple (A). This domain which is predicted in all three species (B) has been shown to be important for ligand binding and a putative Ca2+ binding (Rigden et al., 2011).* HvDEX1 *protein sequence is also predicted to have transmembrane domains (C). DEX1 domains predicted by ScanProsite, ExPASy. Transmembrane domains predicted by TMHMM 2.0.*

3.3.1.2.1 Barley HvMMD1 *homologs*

Through BLAST analysis of the *HvMMD1-1* candidate to the barley genome, using the BLAST tool of BARLEX (https://apex.ipk-gatersleben.de/apex/f?p=284:10::::::) two highly similar sequences were identified, *HORVU.MOREX.r2.4HG0281670* and *HORVU.MOREX.r2.7HG0574180* named *HvMMD1-1*, and *HvMMD1-2*. Both of these barley orthologues were found to share high gene identity with *TIP3* however *HvMMD1-2* was not identified through BLAST analysis of the *TIP3* protein sequence to barley (Table 3.19). In many cases several potential orthologues in barley corresponded to only a single locus in rice, due to duplications of certain genomic blocks multiple times (Thiel et al., 2009), which might explain why there are two barley orthologues with a high gene identity to the *TIP3* locus.

The *HvMMD1* potential orthologues were aligned and the sequences shared an almost identical Plant Homeo Domain (PHD) finger sequence, however the *HvMMD1-1* sequence was significantly longer with a predicted protein sequence of 676 amino acids, compared to 358 amino acids for *HvMMD1-2* (Figure 3.6). *TIP3* is located on chromosome Os3 at position 28.99 Mbp reverse strand which corresponds to a syntenic region in barley on chromosome 4H, matching the position of *HvMMD1-1* (Mayer et al., 2011). To further investigate the potential *HvMMD1* orthologues, the region surrounding the respective *HvMMD1* loci were analysed through BLAST analysis. Seven annotated genes flanking either side of the *HvMMD1* orthologues, in total 15 genes per homolog, were analysed in the rice genome to potentially identify regions of conservation between the genomes. Genes with a gene identity higher than 70% were considered as good candidates. Nine of the fifteen barley genes in the *HvMMD1-1* region had a potential rice candidate orthologue with a high gene identity, most of which were located on rice chromosome Os3 suggesting that this small region share micro-synteny (Table 3.20). The annotated genes in the flanking regions surrounding *HvMMD1-2* had few orthologues with a high gene identity in the rice genome and they were spread over several rice chromosomes.

Gene expression data of the putative *HvMMD1* orthologues was collected from BARLEX to analyse the expression patterns. *HvMMD1-1* was preferentially expressed in floral tissues, notably in the developing inflorescence (spikes of 1-1.5 cm) and in the lemma, loducule and palea (Figure 3.7). Interestingly, *HvMMD1-2* was not expressed throughout the plant or was only marginally expressed in floral tissues. This lack of expression could indicate that the gene has very low expression or is not expressed in the tissues available in the BALREX database.

HvMMD1-1 was selected as the best potential orthologue of *MMD1* and *TIP3* due the high gene identity with *MMD1* and *TIP3*, the conserved micro-synteny with the rice orthologue *TIP3*, and the expression pattern which suggests a role of *HvMMD1-1* in floral development.

Table 3.19. Gene sequence comparison of MMD1, TIP3 *and* HvMMD1 *orthologues for the identification of a putative* HvMMD1-1 *sequence showing the three best hits from the BLAST analysis. Each protein sequence of* A. thaliana *(At),* O. sativa *(Os) and* H. vulgare *(Hv) were compared to each other to detect the level of gene identity (%ID). Marked in blue is* MMD1, *in green* TIP3, *in orange is a PHD finger identified from* Arabidopsis, *and the putative* HvMMD1-1 *is marked in yellow.*

Comparison	Gene	Subject description	Genomic location	Length (bp)	%ID
At-Os	Os01t0877500-01	Zinc finger, PHD-type domain	Chr1: 38.08	110	48.2
	Os03t0716200-01	*TIP3*	Chr3: 28.99	109	51.4
	Os11t0234200-01	Zinc finger, PHD-type domain	Chr11: 7.13	110	47.3
At-Hv	HORVU.MOREX.r2.3HG0248440.1	PHD finger protein	Chr3: 501.23	110	49.1
	HORVU.MOREX.r2.4HG0281670.1	PHD finger protein, Putative HvMMD1-1	Chr4: 14.64	117	47.0
	HORVU.MOREX.r2.5HG0402180.1	*HvMS1*	Chr5: 426.21	109	46.8
Os-At	AT2G01810.1	PHD finger protein	Chr2: 0.35	140	46.4
	AT1G66170.1	*MMD1*	Chr1: 24.64	109	51.4
	AT1G33420.2	PHD finger protein	Chr1: 12.12	106	48.1
Os-Hv	HORVU.MOREX.r2.4HG0281670.1	Putative HvMMD1-1	Chr4: 14.64	226	79.2
	HORVU.MOREX.r2.4HG0281670.1	Putative HvMMD1-1	Chr4: 14.64	244	76.6
	HORVU.MOREX.r2.4HG0281670.1	Putative HvMMD1-1	Chr4: 14.64	116	65.5
HORVU.MOREX.r2.3HG0248440.1					
Hv-At	AT1G33420.2	PHD finger protein	Chr1: 12.12	173	52.6
	AT1G33420.1	PHD finger protein	Chr1: 12.12	173	52.6
	AT5G22260.1	MS1	Chr5: 7.37	132	41.7
Hv-Os	Os01t0877500-01	Zinc finger, PHD-type domain	Chr1: 38.08	352	88.1
	Os01t0877500-02		Chr1: 38.08	233	82.8
	Os01t0877500-01		Chr1: 38.08	233	82.8
HORVU.MOREX.r2.4HG0281670.1 (HvMMD1-1)					
Hv-At	AT5G22260.1	MS1	Chr5: 7.37	140	47.1
	AT1G66170.1	MMD1	Chr1: 24.64	109	46.8
	AT1G33420.1	PHD finger protein	Chr1: 12.12	106	50.0
Hv-Os	Os11t0234200-01	Zinc finger, PHD-type domain	Chr11: 7.13	150	41.3
	Os01t0877500-01	Zinc finger, PHD-type domain	Chr1: 38.08	148	40.5
	Os03t0716200-01	*TIP3*	Chr3: 28.99	106	52.8

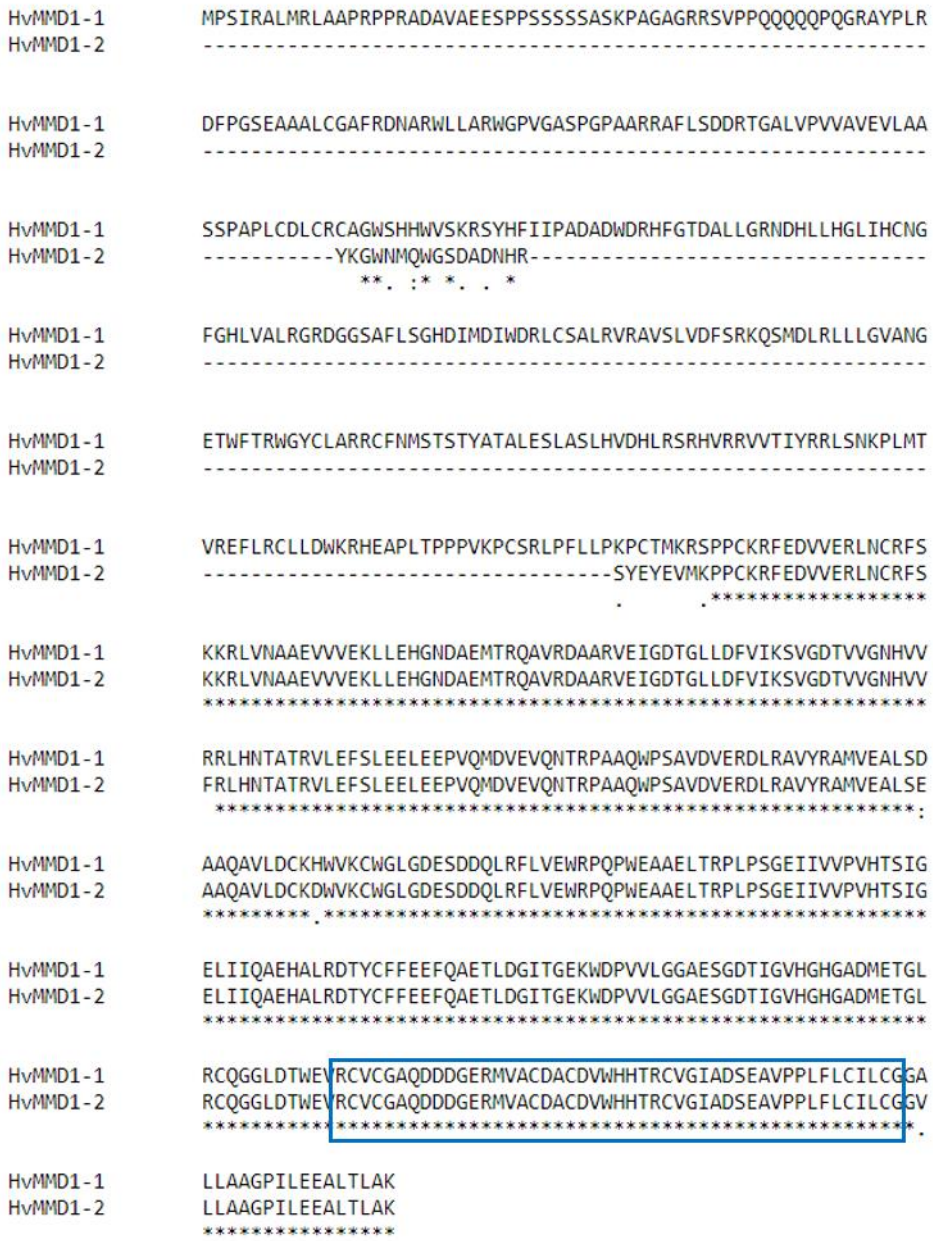

Figure 3.6. Alignment of predicted protein sequences of the putative HvMMD1 *orthologues. All sequences share a high gene identity but the* HvMMD1-1 *sequence is significantly longer than* HvMMD1-2*. Marked in blue is the conserved PHD finger. Alignment through ClustalW.*

Table 3.20. Micro-synteny between barley and rice for annotated genes flanking the putative HvMMD1-1 *orthologue. The barley genes were compared to the rice genome to identify potential orthologues and the gene identity between the best candidate orthologue in rice is given as a percentage. Most potential rice orthologues were located on chromosome Os3.*

	Barley gene	Putative rice orthologue	Gene ID (%)
-7	*HORVU4Hr1G008090*	NA	NA
-6	*HORVU4Hr1G008100*	NA	NA
-5	*HORVU4Hr1G008110*	NA	NA
-4	*HORVU4Hr1G008120*	*Os03g0713600*	88.1
-3	*HORVU4Hr1G008130*	*Os03g0715332*	83.6
-2	*HORVU4Hr1G008140*	NA	NA
-1	*HORVU4Hr1G008150*	*Os03g0715500*	88.6
0	***HORVU4Hr1G008160 (HvMMD1-1)***	***Os03g0716200***	**85.2**
1	*HORVU4Hr1G008170*	*Os09t0386200*	74.0
2	*HORVU4Hr1G008180*	*Os03t0717000*	93.6
3	*HORVU4Hr1G008190*	NA	NA
4	*HORVU4Hr1G008200*	*Os03g0717200*	84.7
5	*HORVU4Hr1G008210*	*Os03g0717700*	87.5
6	*HORVU4Hr1G008220*	*Os03g0717700*	91.3
7	*HORVU4Hr1G008230*	NA	NA

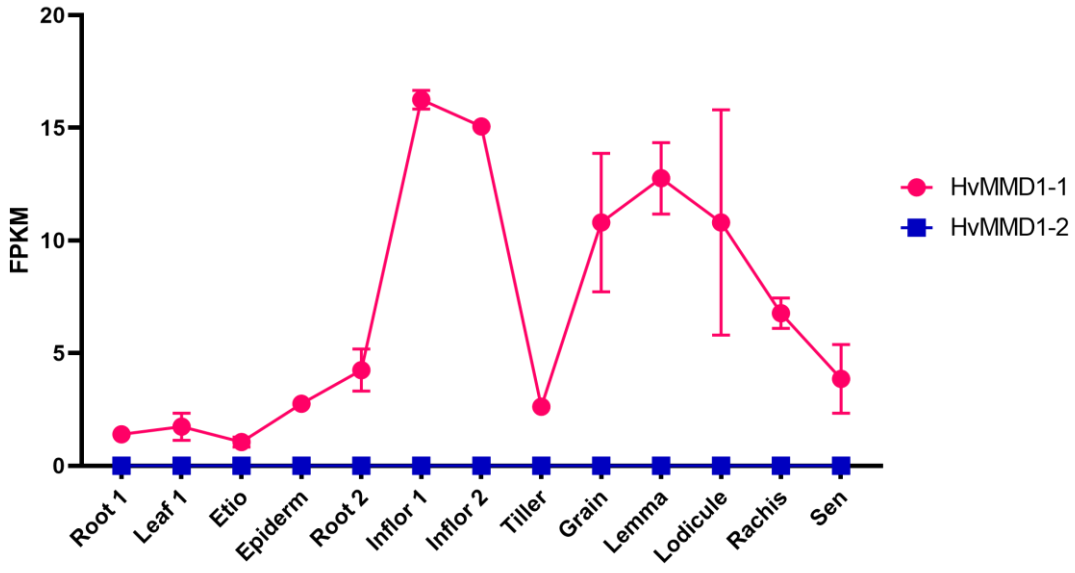

Figure 3.7. Gene expression of putative HvMMD1 *orthologues obtained from BARLEX.* HvMMD1-1 *was preferentially expressed in floral tissues whereas a very low or no expression was found for* HvMMD1-2. *FPKM = Fragments per kilo base of transcript per million mapped fragments. Root 1: Roots from seedlings (10 cm shoot stage), Leaf 1: Shoots from seedlings (10 cm shoot stage), Etio: Etiolated seedling, Epiderm: Epidermal strips, Root 2: Roots, Inflor 1: young developing inflorescence (5mm), Inflor 2: Developing inflorescences (1-1.5 cm), Tiller: Developing tillers, 3rd internode, Grain: Developing grain, Lemma: Inflorescences, lemma, Lodicule: Inflorescences, lodicule, Rachis: Inflorescences, rachis, Sen: Senescing leaves.*

3.3.1.1 Prediction of PHD sequence in the HvMMD1-1 protein and relatedness to *MS1*

There seems to be high sequence similarity and conservation among the *MS1* and *MMD1* orthologues. In *Arabidopsis MMD1* has a high sequence identity with *MS1* with a conserved PHD finger and both genes are involved with male fertility without any noted association with female fertility (Yang et al., 2003, Wilson et al., 2001). Additionally, the barley *HvMS1* and the rice *PTC1* under control of the native *Arabidopsis* promoter of *MS1* can rescue the *ms1* male sterility phenotype (Fernández Gómez & Wilson, 2014; Li et al., 2011) suggesting a conservation of function between barley and *Arabidopsis*.

To investigate the relationship between these genes between Arabidopsis, rice and barley, the protein sequences from the *MS1* and *MMD1* orthologues, as well as the PHD finger proteins identified as highly similar to the MMD1 proteins in the BLAST analysis (Table 3.19) were placed in a phylogenetic tree (Figure 3.8A). This included *MS1*, *MMD1*, *TIP3*, *PTC1*, *HvMS1*, and *HvMMD1-1* along with uncharacterised PHD fingers from Arabidopsis, rice and barley.

The *HvMMD1* orthologues shared a high gene identity and were placed together. There was a clear separation between the *MS1* and *MMD1* protein sequences and the uncharacterised PHD finger proteins suggesting that *HvMMD1-1* is closer related to *MMD1* orthologues than to the *MS1*, *HvMS1* and other PHD fingers. The PHD finger protein identified through BLAST analysis as the sequence with the highest gene identity with the *Arabidopsis MMD1* (Table 3.20) was not placed in the same group as either *MS1* or *MMD1*, further supporting that it was not the best candidate *HvMMD1*.

To further analyse the genes, the protein domains were predicted. In both *MMD1* and *TIP3* the PHD finger is essential for the transcriptional activity of the protein since the PHD facilitates DNA binding (Yang et al., 2003; Yang et al., 2019). Through protein domain prediction tool MotifFinder, it was possible to identify a predicted PHD sequence at the amino acids 612-657 in the *HvMMD1-1*, similar to the PHD positions of *TIP3* and *MMD1* (Figure 3.8B). This together with the gene expression mostly being restricted to the inflorescence (Figure 3.7) the *HvMMD1-1* sequence was hypothesised to be the most likely *MMD1* orthologue candidate in barley.

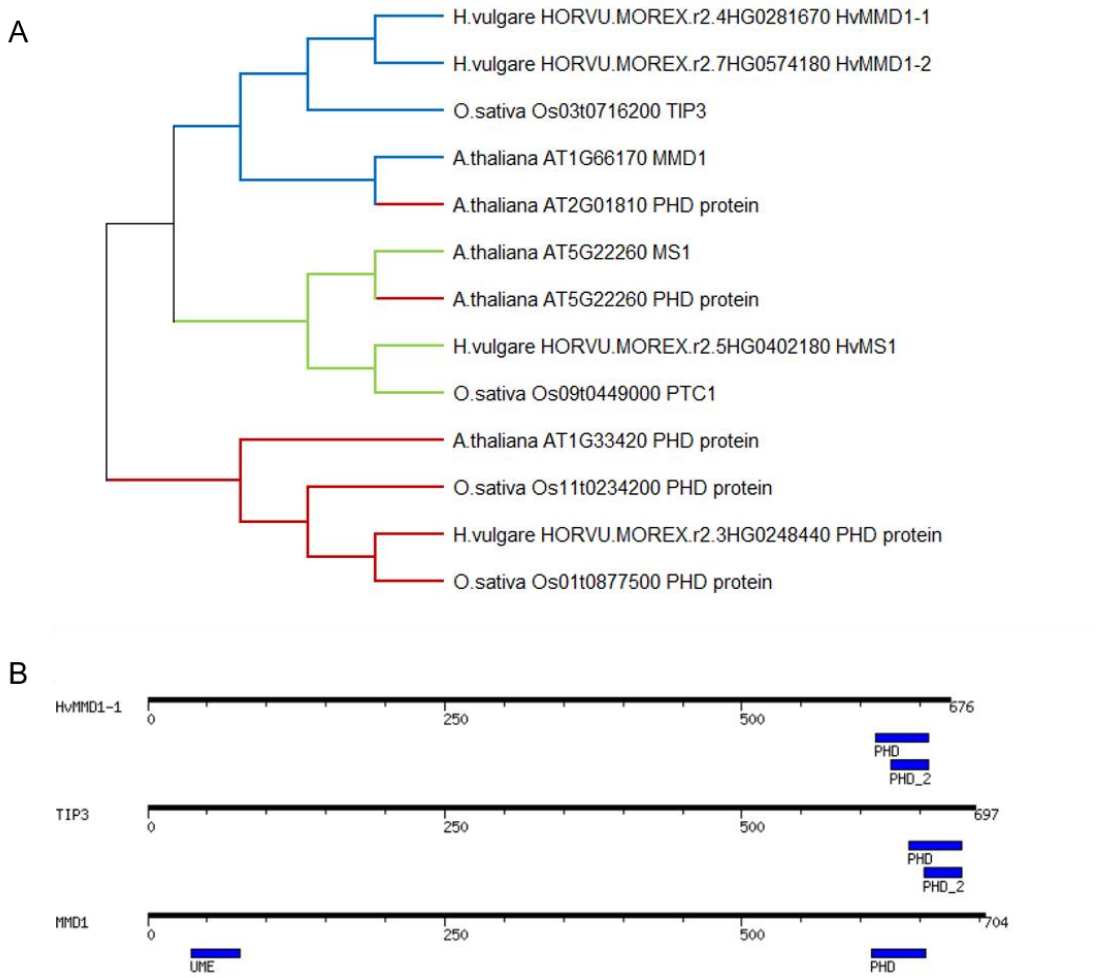

Figure 3.8. Phylogenetic tree of MMD1 *and* MS1 *with respective orthologues and protein domain prediction of* MMD1 *orthologues. A: The* MMD1 *orthologues (branch marked in blue) were separated from the* MS1 *orthologues (*MS1, HvMS1 *and* PTC1, *marked in green), independent of the species, suggesting a separation in sequence similarity between the protein groups. The* HvMMD1 *orthologues shared a high gene identity with the* HvMMD1-1 *and* HvMMD1-2 *being closely related. The PHD protein identified as the sequence with highest similarity to* MMD1 *through BLAST analysis was not closely related to the* MMD1 *orthologues. B: Protein domain prediction from the protein sequences of the* MMD1 *orthologues suggests a conserved PHD finger in the C-terminal of the proteins of* HvMMD1-1, TIP3 *and* MMD1*. Phylogenetic tree made with protein sequences of confirmed orthologues (Yang et al., 2019; Fernández Gómez & Wilson, 2014; Li et al., 2011; Yang et al., 2003; Wilson et al., 2001).*

3.3.1.2 Identification of three putative *HvICE1* orthologues

The *HORVU7Hr1G074490* gene sequence identified in the transcriptome of spikes of HvMS1:OE grown at 15°C and 18°C (José Fernández Gómez, unpublished data) was annotated as an *ICE1* orthologue in the BARLEX database. To identify other possible *HvICE1* candidates and investigate the similarity between orthologues, the *Arabidopsis ICE1* and the rice *OsICE1* were used in BLAST analysis and gene alignments. The protein sequences of *ICE1* and *OsICE1* were compared to *Arabidopsis*, rice and barley to investigate the relatedness of

the sequences. The three sequences with the highest gene identity in the respective genomes are summarised in Table 3.21. As expected the rice genes with the highest gene identity to *Arabidopsis* were the *OsICE1* and *OsICE2*.

In addition to the *HORVU.MOREX.r2.7HG0583410*, named *HvICE1-1*, two other orthologues were identified, *HORVU.MOREX.r2.3HG0260940* named *HvICE1-2* and *HORVU.MOREX.r2.4HG0281900* named *HvICE1-3*, where *HvICE1-1* and *HvICE1-3* share a high level of sequence similarity. Further investigation identified *HvICE1-2* as a possible *ICE2* orthologue through alignment of the *HvICE1-2* protein sequences (Figure S3.1). The *ICE1* and *ICE2* in *Arabidopsis* are part of the bHLH transcription factor family and are the only genes in the family with an absolutely identical bHLH domain sequence (Fursova et al., 2009). Both proteins are involved with cold response through the activation of the *C-REPEAT BINDING FACTORs* (*CBFs*) which initiate cold response, and stomatal patterning however the exact interaction between these proteins is not known (Chinnusamy et al., 2003; Fursova et al., 2009).

Orthologous sequences of *ICE1* and its close homologue *ICE2* were identified based on predictions through Ensembl Plant and through published literature on identified orthologues (Chinnusamy et al., 2003; Deng et al., 2017; Fursova et al., 2009; Kanaoka et al., 2008). The potential *ICE1* orthologues were aligned by ClustalW where the C-terminal sequences were highly similar with an almost identical bHLH domain (Figure 3.9). Further comparisons of the barley homologs revealed an amino acid sequence similarity of *HvICE1-1* and *HvICE1-3* of 75.8% whereas *HvICE1-1* and *HvICE1-2* shared 50.4% similarity.

In rice two orthologues of *ICE1* have been confirmed, named *OsICE1* and *OsICE2*, where both share a high gene identity with the *Arabidopsis ICE1* and contains a conserved bHLH domain (Deng et al., 2017). Previously, one candidate was predicted in barley, named *HvICE1*, for the study of *HvCBF3* expression, however no further studies have been carried out to confirm this candidate (Tondelli et al., 2006). The putative orthologous sequence with the highest identity to *ICE1* is the *HvICE1-1* sequence which is located on chromosome 7H at position 426 Mbp, and corresponds to the gene identified by Tondelli et al., (2006).

HvICE1-1 and *HvICE1-3* share a high gene identity and to investigate these genes further the expression data for the corresponding transcripts were extracted from BARLEX. Both genes are expressed in a similar pattern however *HvICE1-1* has a significantly higher expression with low to no expression of *HvICE1-3* (Figure 3.10). The expression pattern of *HvICE1-2* differed with the highest expression in the grain and the epidermal strips where the other orthologues were not highly expressed. *HvICE1-1* was therefore investigated as the likely orthologue of *ICE1* in further studies.

The *ICE1* orthologous sequences were used to generate a phylogenetic tree in MEGA-X (Kumar et al., 2018) of confirmed and predicted *ICE1* and *ICE2* orthologous genes in monocot and dicot species, using protein sequences without the predicted bHLH domains. Gene sequences from *Arabidopsis*, rice and barley share a highly conserved bHLH domain

(Figure 3.9) however for the remaining sequence, rice and barley share a higher similarity between the *ICE1* and *ICE2* orthologues than with the respective *Arabidopsis* genes (Figure 3.11). There is a clear separation of the monocot and dicot orthologues as well as a separation of the *ICE1* and *ICE2* genes where *HvICE1-1* is more closely related to *HvICE1-3* and *OsICE1,* than to *ICE1* or even *HvICE1-2* and *OsICE2* (Figure 3.11, Figure S1).

This separation of barley homologs together with the differences in gene sequence could be indicative of a separation in function. In further studies *HvICE1-1* and *HvICE1-2* are used as the *ICE1* and *ICE2* orthologues respectively, without any further investigation into *HvICE1-3* due to the high similarity to *HvICE1-1*.

Table 3.21. Gene sequence comparison of ICE1, OsICE1 *and* HvICE1 *orthologues for the identification of a putative* HvICE1 *sequence showing the three best hits from the BLAST analysis. Each protein sequence of* A. thaliana *(At)*, O. sativa *(Os) and* H. vulgare *(Hv) were compared to each other to detect the level of gene identity (%ID).*

Comparisons	Gene	Subject description	Genomic location	Length (bp)	%ID
At-Os	*Os11t0523700-01*	*OsICE1*	Chr11: 18.92	117	72.6
	Os01t0928000-01	*OsICE2*	Chr1: 40.71	112	69.6
	Os01t0928000-01	*OsICE2*	Chr1: 40.71	58	98.3
At-Hv	*HORVU.MOREX.r2.7HG0583410.1*	Putative *HvICE1-1*	Chr7: 378.63	113	72.6
	HORVU.MOREX.r2.3HG0260940.1	Putative *HvICE1-2*	Chr3: 543.47	97	70.1
	HORVU.MOREX.r2.3HG0260940.1	Putative *HvICE1-2*	Chr3: 543.47	58	96.6
Os-At	*AT3G26744.1*	*SCRM*	Chr3: 9.83	104	73.1
	AT3G26744.2	*SCRM*	Chr3: 9.83	104	73.1
	AT3G26744.4	*SCRM*	Chr3: 9.83	104	73.1
Os-Hv	*HORVU.MOREX.r2.7HG0583410.1*	Putative *HvICE1-1*	Chr7: 378.63	101	86.1
	HORVU.MOREX.r2.3HG0260940.1	Putative *HvICE1-2*	Chr3: 543.47	97	70.1
	HORVU.MOREX.r2.4HG0281900.1	Putative *HvICE1-3*	Chr4: 15.90	90	77.8
Hv-At	*AT3G26744.2*	*SCRM*	Chr3: 9.83	113	72.6
	AT3G26744.1	*SCRM*	Chr3: 9.83	113	72.6
	AT3G26744.4	*SCRM*	Chr3: 9.83	113	72.6
Hv-Os	*Os11t0523700-01*	*OsICE1*	Chr11: 18.92	114	86.8
	Os01t0928000-01	*OsICE2*	Chr1: 40.71	117	70.1
	Os11t0523700-01	*OsICE2*	Chr11: 18.92	54	96.3

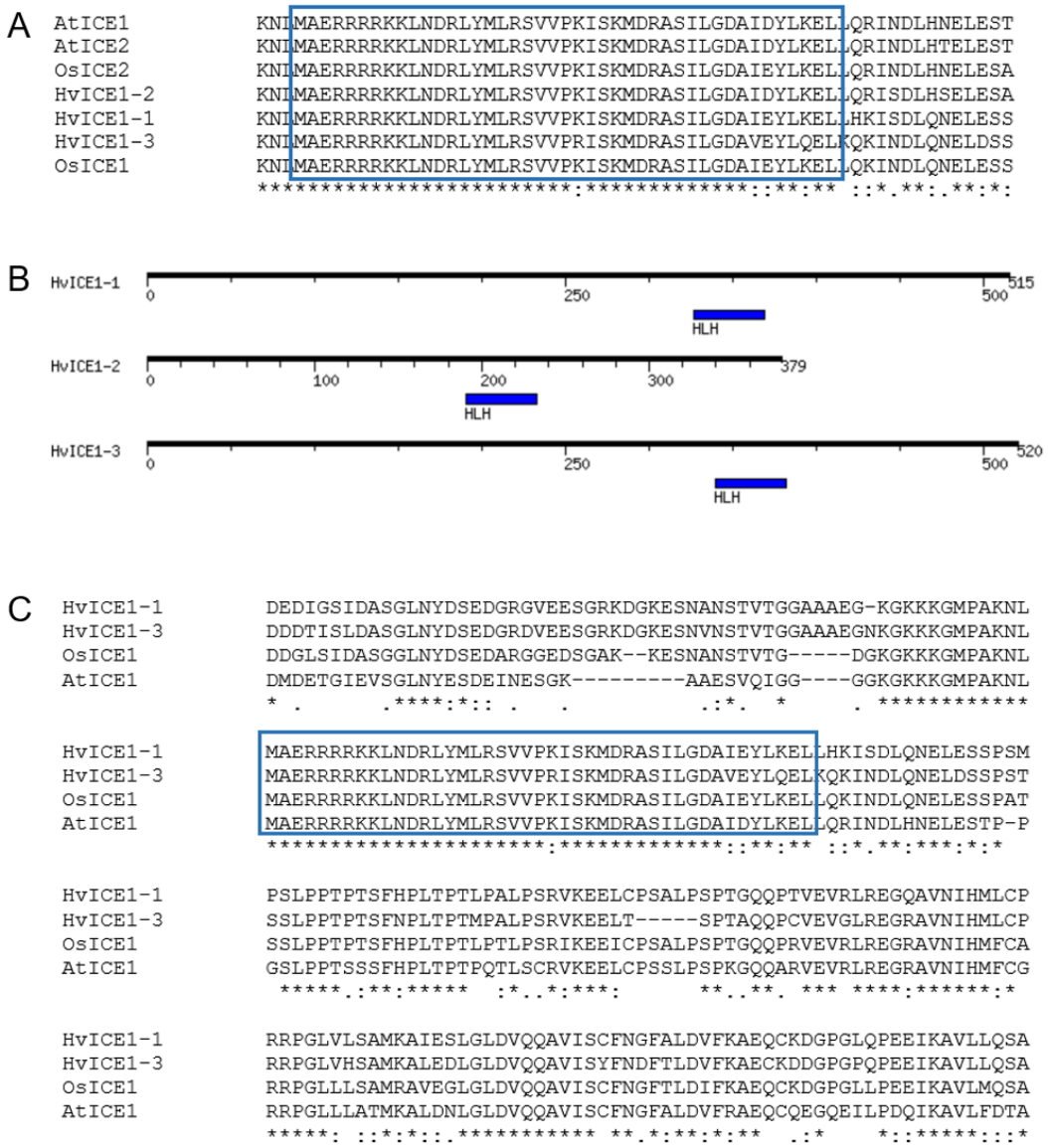

Figure 3.9. Alignment of the conserved bHLH domain in ICE1 *orthologues (A), prediction of bHLH domain in barley homologs (B) and alignment of the C-terminal sequence of the* ICE1 *orthologues in* Arabidopsis*, rice and barley (C). The bHLH domain is highly conserved in all orthologues with a high sequence identity between* ICE1 *orthologues. The identified and predicted protein sequences were used for the alignment.*

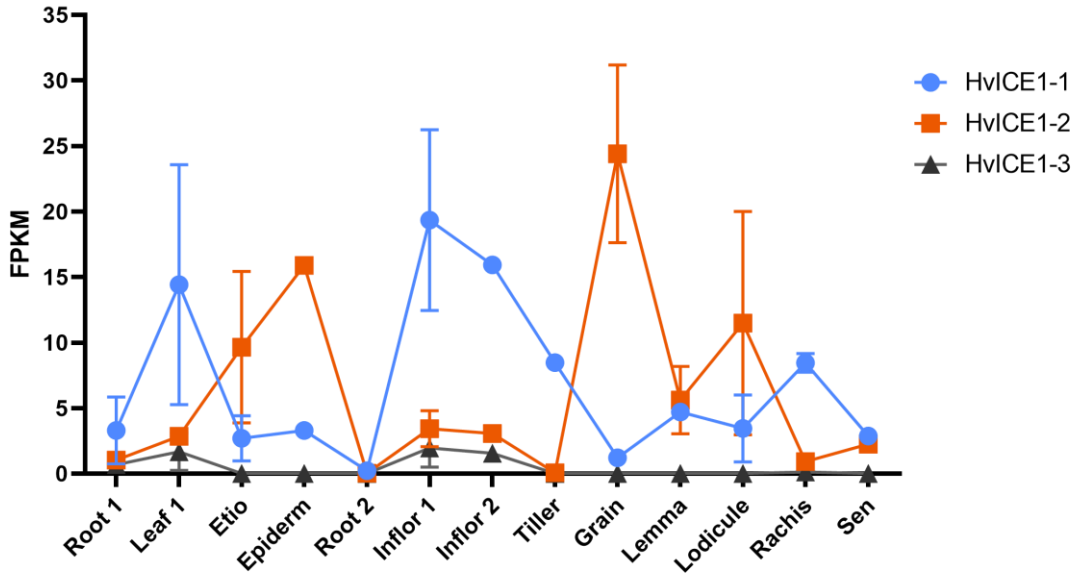

Figure 3.10. Gene expression of the HvICE1 *homologs. Data collected from BARLEX. FPKM = Fragments per kilo base of transcript per million mapped fragments. Embryo: 4-day embryos, Root 1: Roots from seedlings (10 cm shoot stage), Leaf 1: Shoots from seedlings (10 cm shoot stage), Etio: Etiolated seedling, Epiderm: Epidermal strips, Root 2: Roots, Inflor 1: Young developing inflorescences (5mm), Inflor 2: Developing inflorescences (1-1.5 cm), Tiller: Developing tillers, 3rd internode, Grain: Developing grain, Lemma: Inflorescences, lemma, Lodicule: Inflorescences, lodicule, Palea: Dissected inflorescences, palea, Rachis: Inflorescences, rachis, Sen: Senescing leaves.*

3.3.2 Subcellular localisation of HvDEX1, HvMMD1-1 and HvICE1-1

In *Arabidopsis ICE1* and *MMD1* are transcription factors localised to the nucleus (Chinnusamy et al., 2003; Yang et al., 2003), whereas *DEX1* is predominantly localised to the plasma membrane (Ma et al., 2013). To investigate if the subcellular localisation was conserved in the putative barley orthologues *HvDEX1*, *HvICE1-1* and *HvMMD1-1*, the transcripts were coupled to YFP under the control of ZmUbi10 promoter and transiently transformed into tobacco cells (Figure 3.12 , Figure 3.13). The cells were stained with DAPI to confirm nuclear positions and nuclear localisation of *HvICE1-1* and *HvMMD1-1* coupled with YFP (Figure 3.13).

Both transcription factors HvICE1-1:YFP and HvMMD1:YFP were found to be highly expressed in the nuclei of tobacco cells(Figure 3.12 , Figure 3.13). This confirms the nuclear localisation of the transcripts. The signal of HvDEX1:YFP was detected throughout the cells however it accumulated in small vesicles. Since *OsDEX1* is involved with Ca^{2+}-signalling it is possible it is located in the endoplasmic reticulum throughout the cell (Yu et al., 2016).

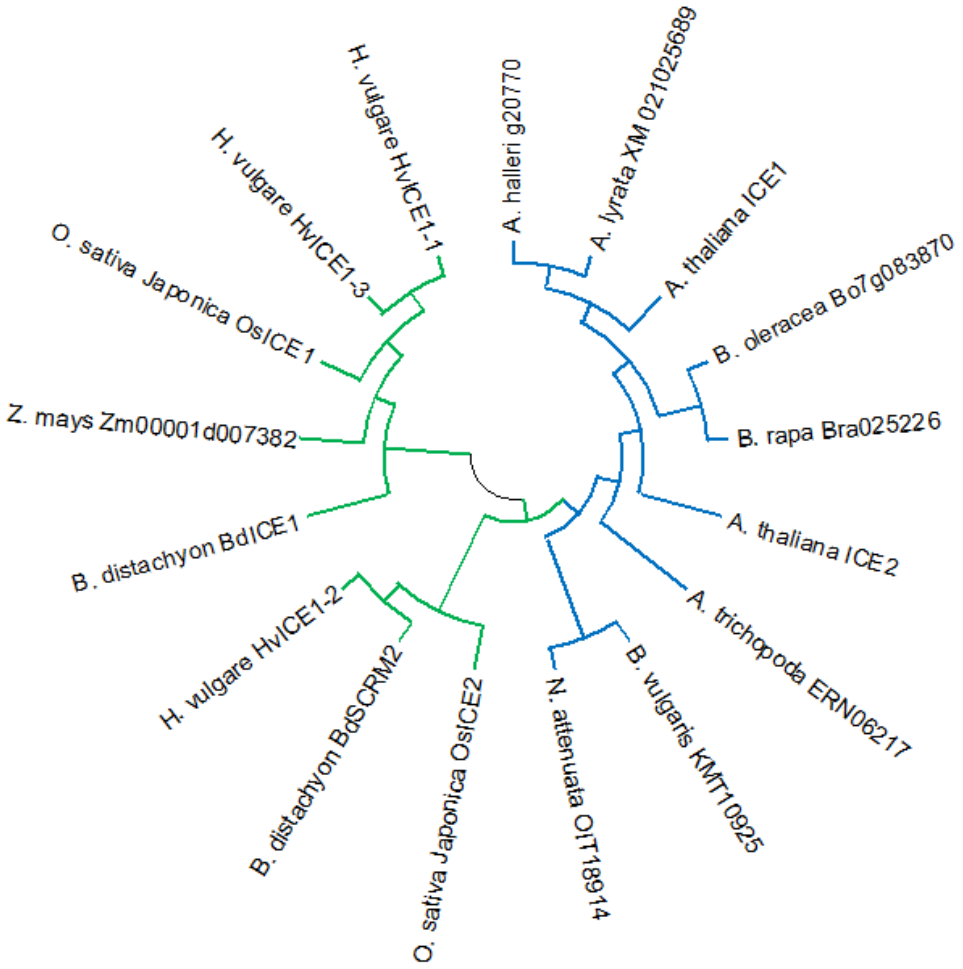

Figure 3.11. Phylogenetic tree of the protein sequences of identified and predicted ICE1 *orthologues without the bHLH domain. Sequences with confirmed function are labelled with the gene name after the sequence i.e.* Arabidopsis thaliana *and* Oryza sativa *with the predicted barley orthologues labelled* HvICE1-1, HvICE1-2 *and* HvICE1-3*. Interestingly the* HvICE1-1 *and* HvICE1-3 *clustered together with OsICE1 whereas* HvICE1-2 *clustered with* OsICE2 *with a clear separation of monocots (green) and dicots (blue). Sequences of* Hordeum vulgare, Oryza sativa *(Liu et al., 2009),* Brachypodium distachyon *(Raissig 2016),* Zea mays *(Jin et al 2018),* Arabidopsis thaliana *(Kanaoka et al., 2008; Chinnusamy et al., 2003),* Arabidopsis halleri, Arabidopsis lyrata, Brassica rapa, Brassica oleracea, Beta vulgaris *and* Nicotiana attenuata *were used to represent monocot and dicot* ICE1 *orthologous sequences.*

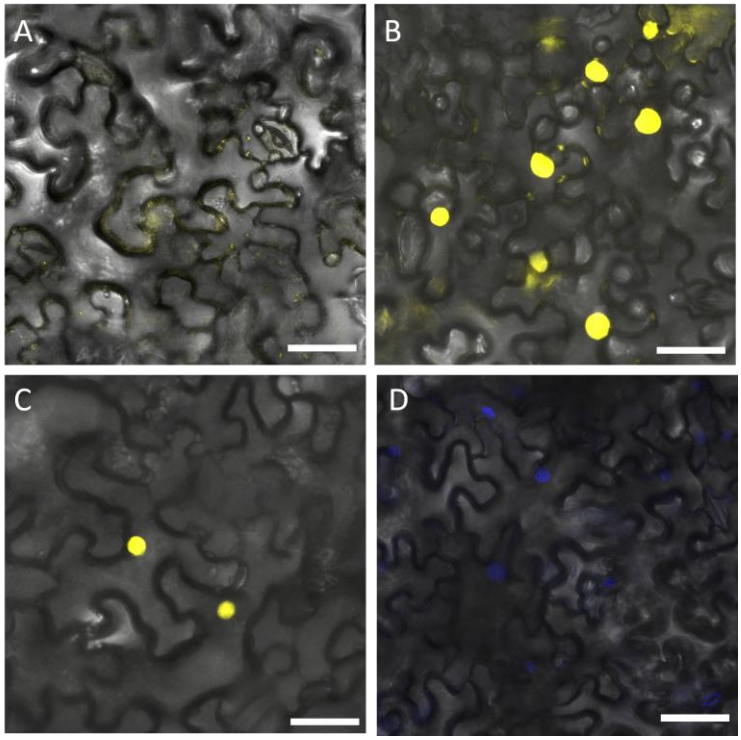

Figure 3.12 . Subcellular location of HvDEX1:YFP (A), HvICE1-1:YFP (B), HvMMD1:YFP (C) and negative control p19 with DAPI staining (D) in tobacco leaf epidermal cells. HvDEX1 *appears to be accumulated in small vesicles throughout the cells whereas* HvICE1-1 *and* HvMMD1-1 *accumulate in the nucleus. Scale bar: 20µm.*

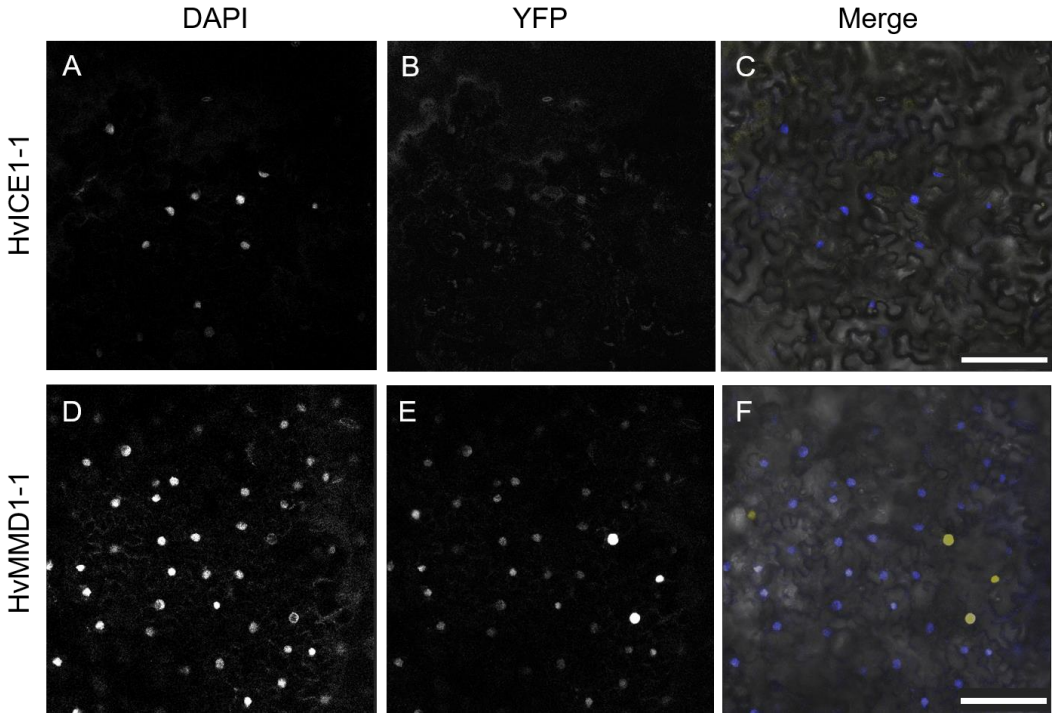

Figure 3.13. Subcellular localisation of HvICE1-1:YFP and HvMMD1-1:YFP in tobacco leaf epidermal cells stained with DAPI to detect nuclear localisation. A: DAPI stain B: HvICE1-1:YFP, C: DAPI and HvICE1-1:YFP merged showing a faint expression of HvICE1-1 *in the nucleus. D: DAPI, E: HvMMD1-1:YFP, F: Merging of DAPI and* HvMMD1-1*:YFP confirmed that HvMMD1-1 was localised to the nucleus. Scale bar 100 µm.*

3.3.3 Generation of constructs used in barley transformation

Investigation of the selected genes, *HvDEX1*, *HvICE1-1* and *HvMMD1-1* was carried out in plants through the transformation of CRISPR gene editing, overexpression of SRDX-silencing constructs for the respective genes. In total 15 constructs were generated, with two CRISPR constructs for *HvDEX1* and *HvMMD1-1* and six for *HvICE1-1,* as well as one overexpression construct per gene and one SRDX-silencing construct for *HvICE1-1* and *HvMMD1-1* (Table 3.22). Each construct was sequenced to ensure that all transgenes were present in the vector used for barley transformation.

The CRISPR constructs were generated either with three sgRNAs in tandem per vector, for *HvDEX1* and *HvMMD1-1*, or with individual sgRNAs per vector, for *HvICE1-1*, in an effort to maximise the mutagenesis efficiency. The sgRNAs were designed to target the beginning of the genes with sgRNA targets T1-6 for HvDEX1 and HvICE1-1 placed in the first exons (Figure 3.12) (Lawrenson et al., 2015). The sgRNA targets T1, T2 and T4 for *HvMMD1-1* were placed prior to the coding sequence of gene in an effort to induce mutations in the promoter region however these sgRNAs were combined in the same vector as targets in the coding sequence (Figure 3.12).

3.3.4 Generation of *HvDEX1*, *HvMMD1-1* and *HvICE1-1* transgenic lines

The protocol developed by (Harwood, 2014, 2019) was used for the stable transformation of barley to generate transgenic lines carrying constructs for CRISPR mediated mutagenesis and the overexpression and silencing of selected genes. Table 3.23 states the number of embryos used for transformation where transformation efficiency ranged from 1-18% success rate. There was a low number of embryos that generated shoots and roots when grown in light, resulting in the low number of generated transgenic lines. All transgenic lines were genotyped for the insertion of the transgenes (Table 3.22) and 100% of the T0 transgenic lines carried the construct of interest.

Transgenic lines transformed with the CRISPR/Cas9 and sgRNAs were genotyped in every generation for the presence of *Cas9*. In the T0 generation all CRISPR transgenic lines were positive for the *Cas9* sequence and the Cas9 was retained in most plants in the T1 generation (Figure 3.13). The transgenic lines positive for the *Cas9* transgene were further genotyped to detect any CRISPR induced mutations. Genotyping for mutations was carried out in the T0, T1 and T2 generation since chimeras in subsequent generations are known to appear from non-mutated T1 generation plants (Hahn et al., 2017). 3-10 plants in each generation for *HvDEX1*, *HvICE1-1* and *HvMMD1-1* were genotyped by amplifying the full-length gene, and the target regions of the sgRNA were sequenced to detect any mutations or heterozygosity in the regions (primers specified in Appendix 1, Table S3.2). Despite the presence of Cas9 in subsequent generations (T1 and T2) no induced mutation could be detected.

Table 3.22. Constructs transformed into barley. For HvDEX1, HvICE1-1 *and* HvMMD1-1 *two types of CRISPR constructs with different sgRNAs, and one overexpression construct with the respective gene CDS coupled to the constitutively active promoter ZmUBI were transformed. For the transcription factors* HvICE1-1 *and* HvMMD1-1 *the CDS under the control of the ZmUbi promoter was coupled to the silencing SRDX sequence in an attempt to silence the genes. The transgenic lines were genotyped for the respective construct by PCR with primers specific to the inserted transgenes.*

Targeted gene	Constructs transformed	Transgenes	Vector	Genotyping
HvDEX1	CRISPR-1	T1+T2+T3 sgRNAs in tandem, Cas9, Hyg	pAGM8031	Cas9 and sgRNA targets
	CRISPR-2	T4, T5, T6 sgRNAs in tandem, Cas9, Hyg	pAGM8031	Cas9 and sgRNA targets
	Overexpression	ProZmUbi:HvDEX1 CDS	pBract214	ProZmUbi:HvDEX1 CDS
HvICE1-1	CRISPR-1	Individual sgRNA T1, T2, T3, and Cas9, Hyg	pAGM8031	Cas9 and sgRNA targets
	CRISPR-2	Individual sgRNA T4, T5, T6, and Cas9, Hyg	pAGM8031	Cas9 and sgRNA targets
	Overexpression	ProZmUbi:HvICE1-1 CDS	pBract214	ProZmUbi:HvICE1-1 CDS
	SRDX silencing	ProZmUbi:HvICE1-1 CDS-SRDX	pBract214	ProZmUbi:HvICE1-1 CDS-SRDX
HvMMD1-1	CRISPR-1	T1+T2+T3 sgRNAs in tandem, Cas9, Hyg	pAGM8031	Cas9 and sgRNA targets
	CRISPR-2	T4, T5, T6 sgRNAs in tandem, Cas9, Hyg	pAGM8031	Cas9 and sgRNA targets
	Overexpression	ProZmUbi:HvMMD1-1 CDS	pBract214	ProZmUbi:HvMMD1-1 CDS
	SRDX silencing	ProZmUbi:HvMMD1-1 CDS-SRDX	pBract214	ProZmUbi:HvMMD1-1 CDS-SRDX

Every generation was genotyped for the insertion of the overexpression or SRDX-silencing transgenes in the genomes of the transgenic lines. Genotyping of the transgenic lines were carried out with primers specific to the individual transgenes (Appendix 1, Table S3.2) to detect the presence of the coding sequences of *HvDEX1*, *HvICE1-1* or *HvMMD1-1* coupled with the ZmUbi promoter for the overexpression construct or with the SRDX sequence for the silencing construct. Figure 3.14 shows an example of genotyping of all the transgenic lines, HvDEX1:OE, HvICE1:OE, HvICE1:SRDX, HvMMD1:OE and HvMMD1:SRDX in the T1 generation with the wild type Golden Promise without the transgene as the negative control. All of the lines transformed with the overexpression or silencing constructs were positive for the insert in the T0 generation and this was retained in most plants in subsequent generations (Figure 3.14). These lines were used for further analysis of the effect of the genes on pollen development and plant morphology as well as expression analysis.

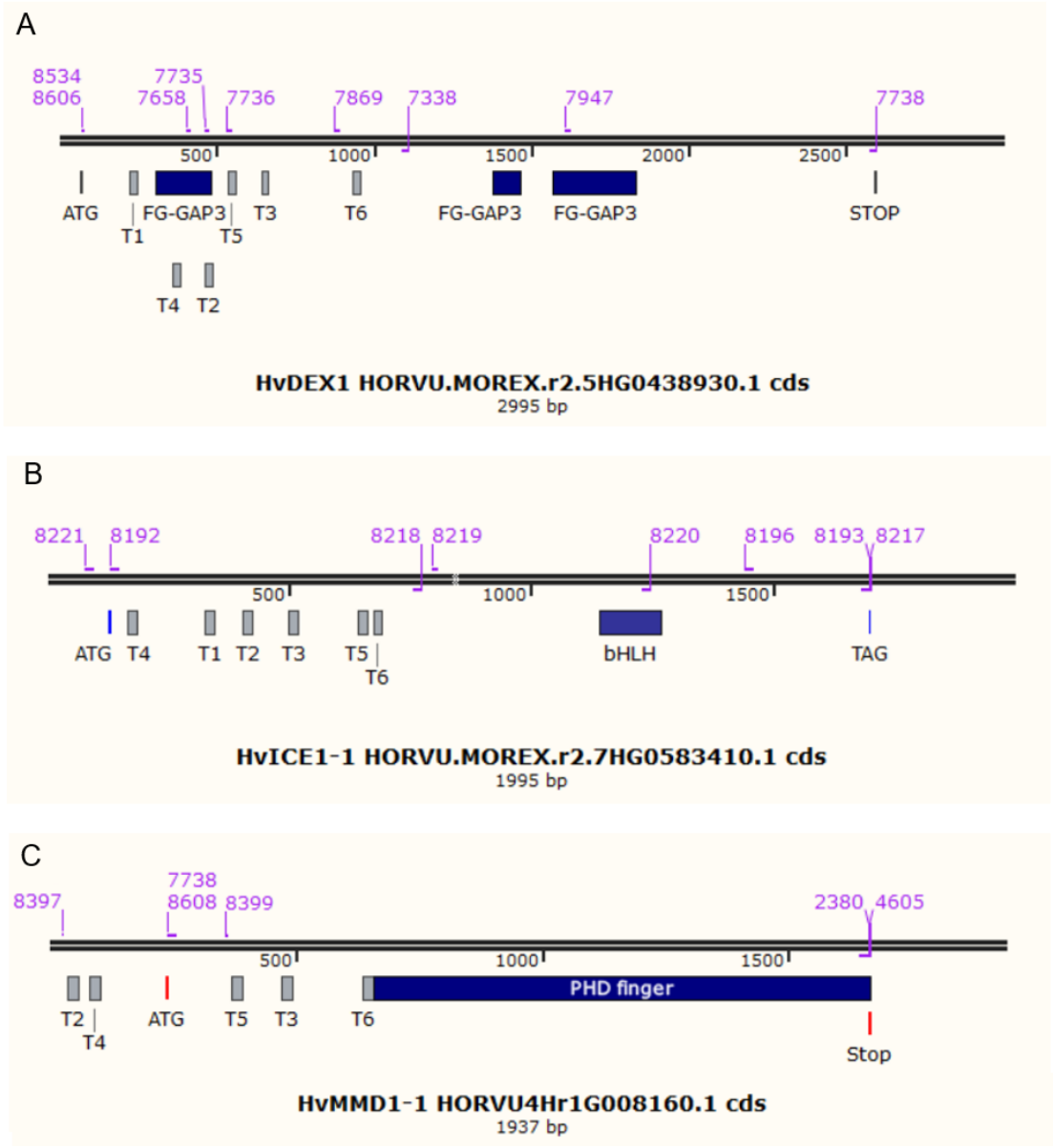

Figure 3.12. Overview of the coding sequences of A: HvDEX1, *B:* HvICE1-1, *and C:* HvMMD1-1 *with predicted functional domains. sgRNA targets for each gene are specified as T1-T6 and are spread out through the beginning of the genes to disrupt gene function. The primers (identified by number) used for amplification of the coding sequences are marked in purple. Primer sequences specified in Appendix 1, Table S3.2.*

Table 3.23. Generated transgenic lines and transformation efficiency per construct. For each construct a minimum of 50 embryos were transformed however the number of generated transgenic lines varied depending on the construct. The overexpression constructs for all lines had the highest transformation efficiency whereas all CRISPR and the HvMMD1-1 SRDX construct had a very low transformation efficiency.

Gene	Construct	Embryos transformed	Transgenic lines generated	Transformation efficiency (%)
HvDEX1	CRISPR	250	8	3.2
	Overexpression	50	3	6.0
HvMMD1	CRISPR	250	7	2.8
	Overexpression	50	8	16.0
	SRDX silencing	100	1	1.0
HvICE1	CRISPR	200	2	1.0
	Overexpression	50	9	18.0
	SRDX silencing	100	4	4.0

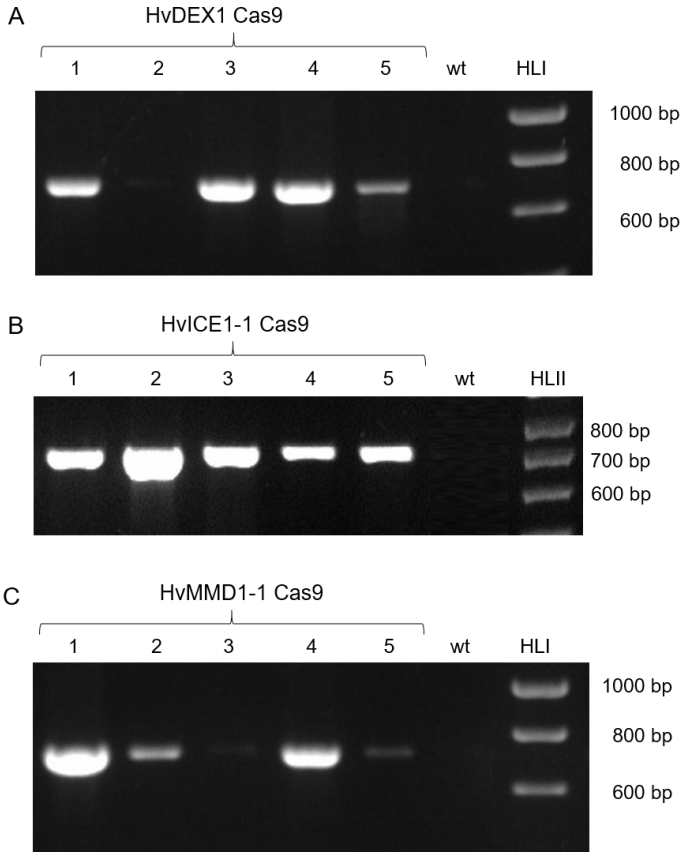

Figure 3.13. Genotyping example of HvDEX1, HvICE1-1 *and* HvMMD1-1 *CRISPR/Cas9 transgenic lines in T1 generation. The primers used for Cas9 screening amplified a region of 717 base pairs. The lines were genotyped for the presence of the Cas9 gene sequence. A: HvDEX1:CRISPR T1-1 plants where plant 1, 3, 4, and 5 had Cas9. B: HvICE1-1:CRISPR T1-1 plants where all plants were positive for the presence of Cas9. C: HvMMD1-1:CRISPR T1-2 plants were all plants were positive for Cas9. Wt: untransformed wild type, Golden Promise. Molecular weight reference markers Hyperladder I (HLI) and Hyperladder II (HLII) (Bioline).*

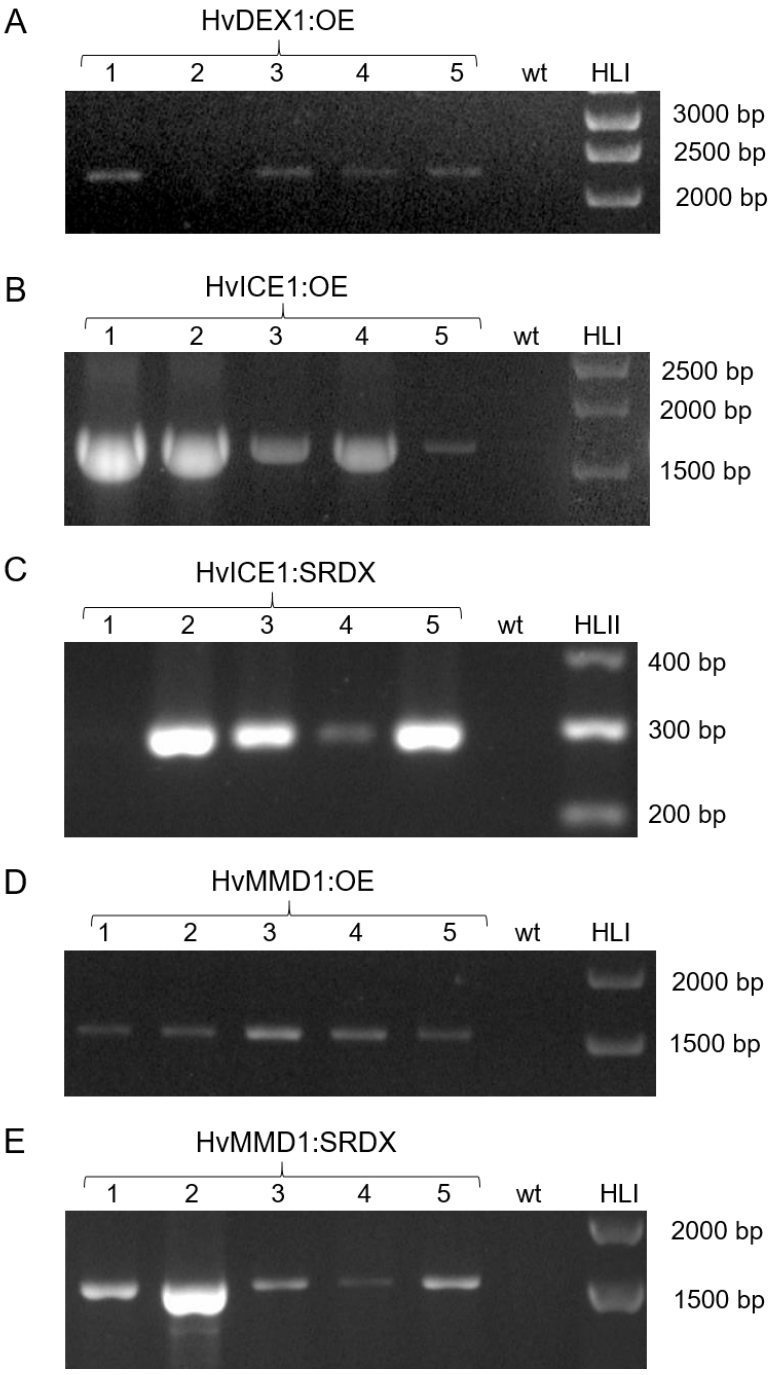

Figure 3.14. Genotyping example of overexpression and silencing transgenic lines in the T1 generation. The wild type (wt) Golden Promise was used as a negative control and did not contain any transgenes. A: HvDEX1 *CDS amplified at 2280 base pairs. The HvDEX1:OE was present in all transgenic plants of the T1-2 line except plant 2. B: All tested plants had the HvICE1:OE transgene (amplicon size 1786 base pairs). C: All plants except plant 1 was positive for the HvICE1:SRDX transgene (amplicon size 298 base pairs). D: HvMMD1:OE was present in all plants (amplicon size 1642 base pairs). E: HvMMD1:SRDX was present in all plants (amplicon size 1465 base pairs). Differences in amplicon intensity was due to differences in gDNA concentration. Molecular weight reference markers Hyperladder I (HLI) and Hyperladder II (HLII) (Bioline).*

3.3.5 Gene expression of the putative orthologues

3.3.5.1 *HvDEX1* expression level in HvDEX1:OE transgenic lines

The level of *HvDEX1* expression was investigated in the transgenic lines carrying the ProZmUbi:HvDEX1 transgene. Two independent transgenic lines, HvDEX1:OE-1 and HvDEX1:OE-2, were grown in control conditions and spikes were collected for RNA isolation in late spike development stage as *OsDEX1* is involved in tapetum degeneration and pollen formation (Yu et al., 2016). One biological replicate was used for each stage for heading (Zadok stage 49, with HvDEX1:OE-1), for spike emergence ¼ out of the last sheath (Zadoks stage 52-53, with HvDEX1:OE-2) and for when the spike had emerged fully from the last sheath (Zadoks stage 58-59, with HvDEX1:OE-2) (Zadoks et al., 1974). All plants were genotyped as containing the transgenes (Figure 3.14) and there was a slightly elevated expression of *HvDEX1* in the HvDEX1:OE-2 line however this was a minor increase which was not statistically significant and it was not detectable in the HvDEX1:OE-1 (at heading) (Figure 3.15) which was also genotyped as positive for the overexpression construct. It is possible that the gene was not overexpressed in the plants tested since it was not possible to determine a significant increase in *HvDEX1* expression in the overexpression lines and no further gene expression analysis was carried out with putatively downstream genes.

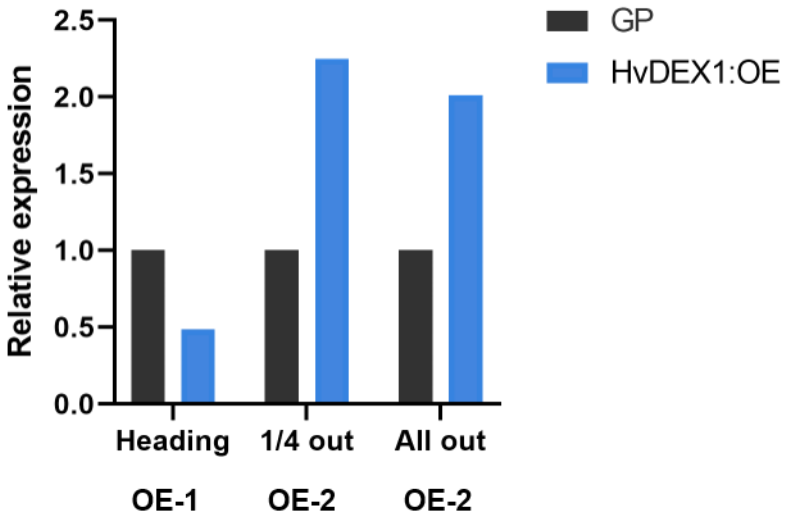

Figure 3.15. Relative expression of HvDEX1 *in HvDEX1:OE transgenic lines in late spike development. The expression of HvDEX1:OE (heading stage) and HvDEX1:OE-2 (1/4 of the spike out of the last sheet and the spike all out of the last sheet) was normalised to two reference genes,* HvTub *and* HvHSP70*, and to the expression of the wild type (GP) for the respective stage.*

3.3.5.2 Expression profile of *HvMMD1* in transgenic lines

The expression of *HvMMD1* was analysed in HvMMD1:OE and HvMMD1:SRDX transgenic lines to determine the level of induced expression of the transgenes. The expression of

HvMMD1 was analysed in one transgenic line with one biological replicate in floral tissues of HvMMD1:SRDX and in three independent HvMMD1:OE transgenic lines with one biological replicate at early spike development stage. All HvMMD1:OE lines had an increased expression level of the *HvMMD1* transcript, between 15-118 times higher than in the wild type, indicating a successful overexpression for these lines. In all stages the HvMMD1:SRDX line the level of *HvMMD1* transcript was increased 50-200 times compared to its expression in the wild type (Figure 3.16). Since the RT-qPCR primers for *HvMMD1* amplifies all *HvMMD1* transcripts including the CDS linked with the SRDX sequence under control of ZmUbi this expression data is an indication that the construct is present and is being expressed at a high level. Due to the lack of biological replicates the results from the expression analysis cannot be used for any statistical analysis and can only be used as an indicator for future studies.

Genes predicted to interact with HvMMD1 based on the function of MMD1 and TIP3 were analysed in spike tissues of the HvMMD1:SRDX-3 line. In the rice *tip3* mutant the pollen development pathway was disrupted and several critical genes had altered expression patterns (Yang et al., 2019). Among the genes affected by altered *TIP3* expression were *GAMYB*, *ETERNAL TAPETUM1* (*EAT1*), *PERSISTENT TAPETAL CELL1 PTC1* (a rice orthologue of *Arabidopsis MS1*), and *UDT1* (the rice orthologue of *Arabidopsis DYT1*) (Yang et al., 2019). In the barley transgenic lines the expression of *HvMMD1* putatively interacting genes was investigated by RT-qPCR with primers from sequences of *GAMYB* (Gubler et al., 1995), *HvMS1* (Fernández Gómez & Wilson, 2014) and predicted barley orthologues of *HvEAT1* and *HvDYT1* as well as *HvMMD1* (Figure 3.16).

In the HvMMD1:SRDX line there was no change in the expression of *GAMYB* compared to the wild type at any spike stage analysed, suggesting that the silencing of HvMMD1 through SRDX-repression does not affect *GAMYB* expression. Interestingly, *HvEAT1* was upregulated in the HvMMD1:SRDX-3 plant at heading stage (Figure 3.16), corresponding to LFE2, where the tapetum is almost degraded (Gomez & Wilson, 2012). *TIP3* is involved with the degeneration of the tapetum whereas *EAT1* is involved with the development of the anther wall and pollen exine (Niu et al., 2013; Yang et al., 2019) and it is possible that the silencing of *HvMMD1* could result in an upregulation of the expression of *HvEAT1* at this stage to compensate for the silenced processes. Detailed study of this is needed to determine the interaction of these genes.

It is also interesting to note the upregulation of *HvDYT1* at the 1.2 cm spike stage and the downregulation of *HvMS1* at the 2 cm stage where the anther walls have formed and differentiation of the sporogenous cells take place (Figure 3.16) (Gomez & Wilson, 2012). Both *HvMS1* and *DYT1*, and its rice orthologue *UDT1* (*Undeveloped Tapetum1*), are involved with tapetum formation early in development (Fernández Gómez & Wilson, 2014; Jung et al., 2005; Zhang et al., 2006) and in the HvMMD1:SRDX line they appear to be upregulated as a result of the inhibition of *HvMMD1*. These differences in gene expression might have compensated for the silencing of *HvMMD1* through the HvMMD1:SRDX construct resulting in maintained fertility however further studies are needed to determine this effect.

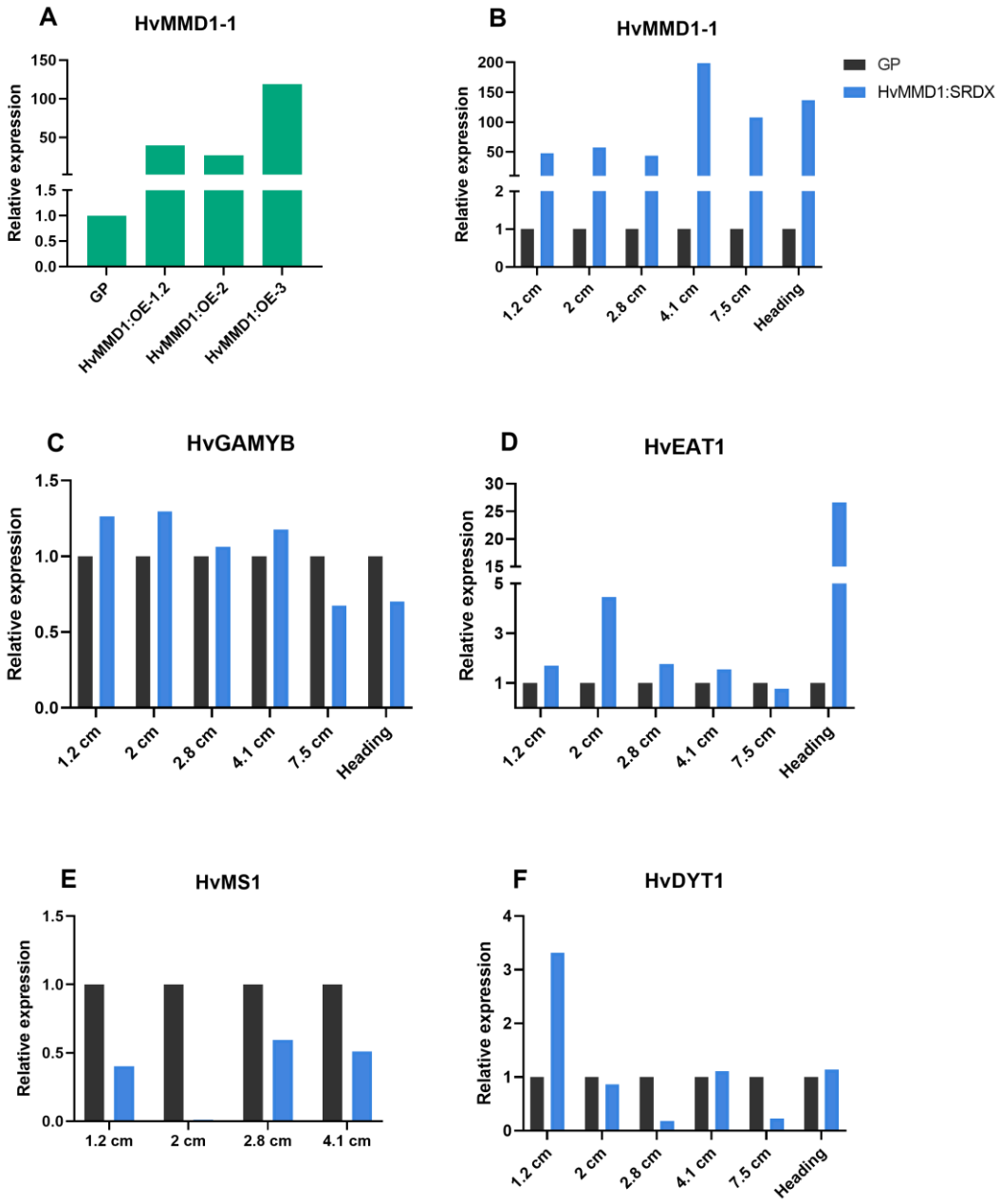

Figure 3.16. Relative expression of HvMMD1-1 *in HvMMD1:OE and HvMMD1:SRDX lines and* HvMMD1-1 *interacting genes in a HvMMD1:SRDX line. One biological replicate was used for HvMMD1:SRDX-3 and HvMMD1:OE lines where each gene of interest were normalised to comparable stage in Golden Promise with two reference genes. A:* HvMMD1-1 *in overexpression lines, B:* HvMMD1-1 *in silencing lines, C:* GAMYB, *D:* HvEAT1, *E:* HvMS1, *F:* HvDYT1.

3.3.5.3 Gene expression of *HvICE1-1*

The expression of *HvICE1-1* was investigated in three independent transgenic lines with three biological replicates for the HvICE1:OE and HvICE1:SRDX genotypes respectively. Leaf tissue from seedlings was used to determine the expression level of the *HvICE1-1* transcript, normalised to two reference genes *HvTubulin* and *HvHSP70*, and compared to the wild type

Golden Promise (GP). The RT-qPCR primers used for the analysis amplified the HvICE1:SRDX transgene as well as the wild type transcript, i.e. both the native *HvICE1-1* and the *HvICE1-1:SRDX*. In all transgenic lines there was a major increase of the *HvICE1-1* transcript compared to the wild type suggesting that the transgenes were expressed (Figure 3.17). These lines were used for further investigation of the effect of *HvICE1-1* on plant morphology and fertility in Chapter 4.

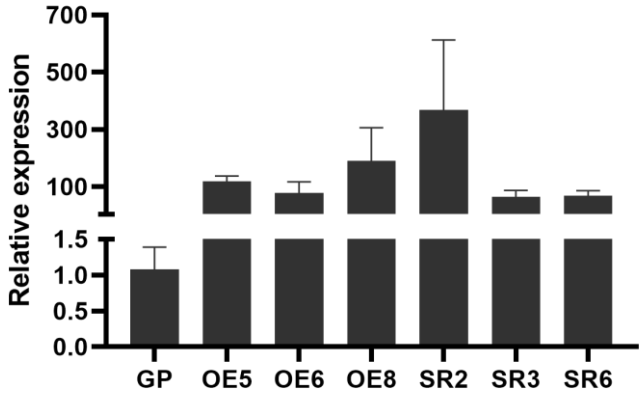

Figure 3.17. Relative expression of HvICE1-1 transgenic lines compared to the wild type GP in seedling leaf tissue. The presence of the HvICE1-1 *was normalised to* HvTubulin *and* HvHSP70 *and to wild type expression. All transgenic lines display an increased expression of* HvICE1-1*.*

3.3.6 Phenotypes of the transgenic lines

The generated transgenic lines were grown under control conditions to investigate the effect of the transgenes on plant morphology. Plants positive for the presence of the CDS of the respective gene under control of the ZmUbi promoter were considered as overexpression lines and plants with the CDS fused with the SRDX sequences were considered to be silencing lines. All analyses were conducted on the T1 generation with three independent lines with two biological replicates (in total six plants per genotype) unless otherwise specified.

The knock-out of the *Arabidopsis dex1* and the rice orthologue *osdex1* did not display any difference in morphology however there has been no analysis of the overexpression of either gene *in planta* (Paxson-Sowders et al., 2001; Yu et al., 2016). General morphology of the HvDEX1:OE lines was not noticeably different from the wild type in terms of plant height, number of tillers, or heading date, suggesting that the transgene ProZmUbi:HvDEX1 did not affect general plant development.

Interestingly, one of the HvMMD1-OE lines, plant T1-5 (from T0-1 plant) displayed differing plant morphology with wider leaves, thick hollow stems, and fewer tillers compared to the wild type. The anthers of this line were compared to the wild type, the anthers from the HvMMD1-OE T1-5 were significantly longer (p-value 1.79E-10) with a 0.8 mm increased average length. The seeds produced from this line were also significantly bigger with a 40% larger grain weight however the seed set was reduced by an average of 22%. No other HvMMD1:OE line displayed a similar phenotype possibly indicating that the increased size was not caused by the overexpression of *HvMMD1-1* but instead was an artefact of the insertion of the overexpression construct into the genome, disrupting other processes. No difference in plant development or physiology was seen in the HvMMD1:SRDX line.

The HvICE1:OE and HvICE1:SRDX lines displayed normal growth and physiology however there was a delay in heading date of 1-2 weeks in the HvICE1:OE lines in comparison to the wild type. In addition, the HvICE1:OE lines developed fewer tillers with an average of only 72% of the number of tillers of the wild type.

To investigate fertility in the transgenic overexpression and silencing lines the viability of the pollen and the seed set was determined (Figure 3.18). As the seed set was analysed in plants grown in different growth cycles it is given as the percentage of the wild type seed set grown in the respective cycle to eliminate factors from varying growth conditions. The results will be discussed for each individual transgenic line.

3.3.6.1 Fertility of the HvDEX1:Overexpression lines

3.3.6.1.1 Pollen viability and seed set of HvDEX1:Overexpression lines

The seed set and pollen viability were measured in two different transgenic lines, HvDEX1:OE-1 and HvDEX1-2, with three biological replicates each in the T1 generation. Interestingly, HvDEX1:OE-1 had a significantly lower seed set (p-value 0.004) but the HvDEX1:OE-2 plants had a significantly higher seed set (p-value 0.025). No difference was found in pollen viability in this generation for any of the lines. Seed set was analysed in subsequent generations from these plants however no consistent difference could be validated for any of the lines. This suggests that there is no effect of the overexpression of HvDEX1 on plant fertility and reproduction.

3.3.6.1.2 Sticky pollen in plant overexpressing HvDEX1

After anthesis when fertilisation had occurred some florets of the HvDEX1:OE-1 generation were identified as sterile as the fertilisation had failed and no seed was developing. Affected florets were compared to fertilised wild type florets of comparable stage through dissection of the pistil and stamens. Both wild type and HvDEX1:OE anthers displayed ruptured anther walls and released pollen, however pollen from the HvDEX1:OE was sticking to the stigma hairs and the lodicules were not enlarged (Figure 3.19). It was hypothesised that the partial sterility in the HvDEX1:OE-1 line could be due to pollen adhesion possibly caused by abnormal pollen coat.

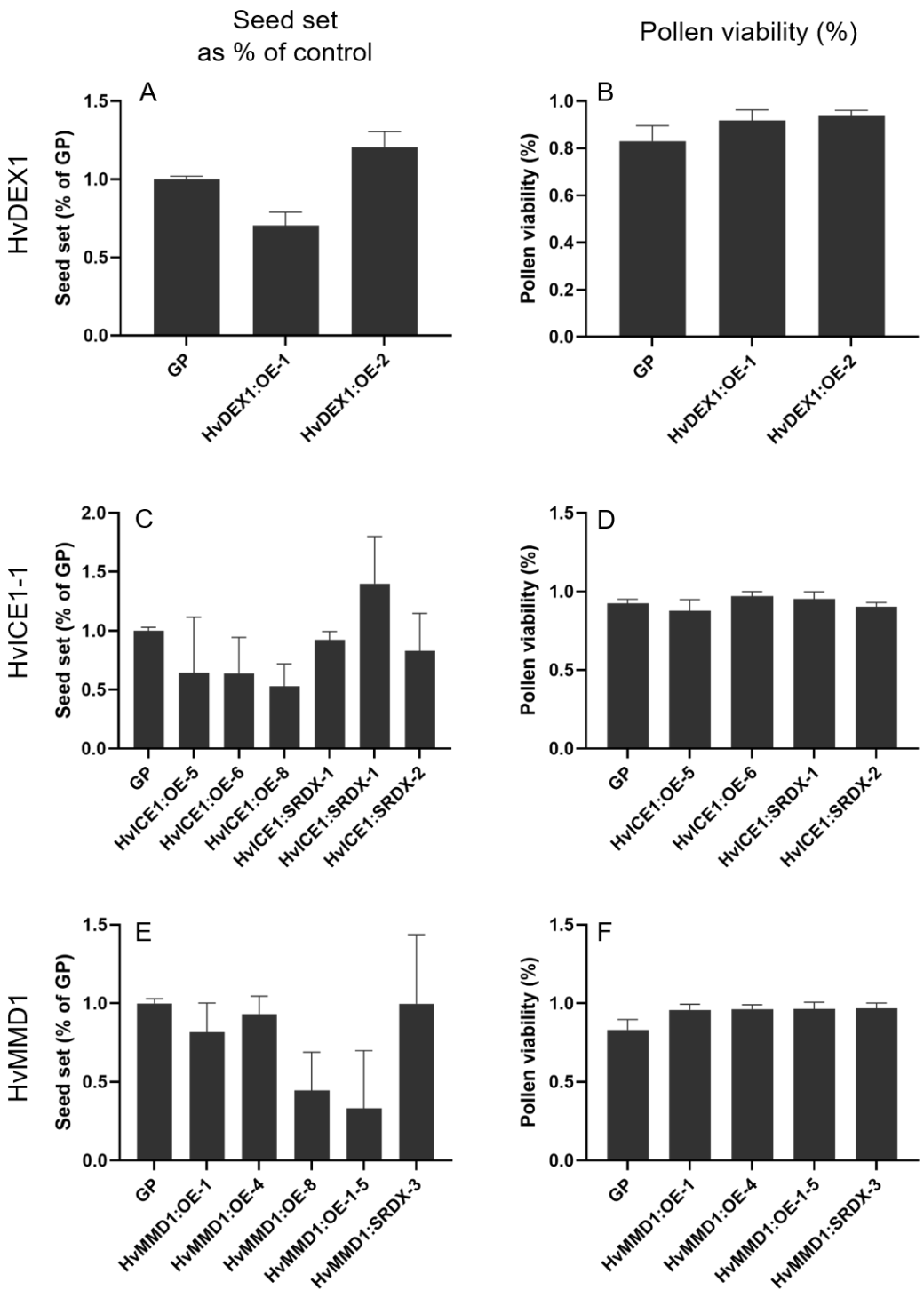

Figure 3.18. Seed set and pollen viability in overexpression and silencing lines for HvDEX1, HvICE1-1 *and* HvMMD1-1*. Seed set for transgenic lines of HvDEX1 (A), HvICE1-1 (C), and HvMMD1-1 (E) is given as the percentage of the GP seed set in corresponding growth cycle. Pollen viability for the lines of HvDEX1 (B), HvICE1-1 (D) and HvMMD1-1 (F) is given as percentage viable of all counted pollen grains.*

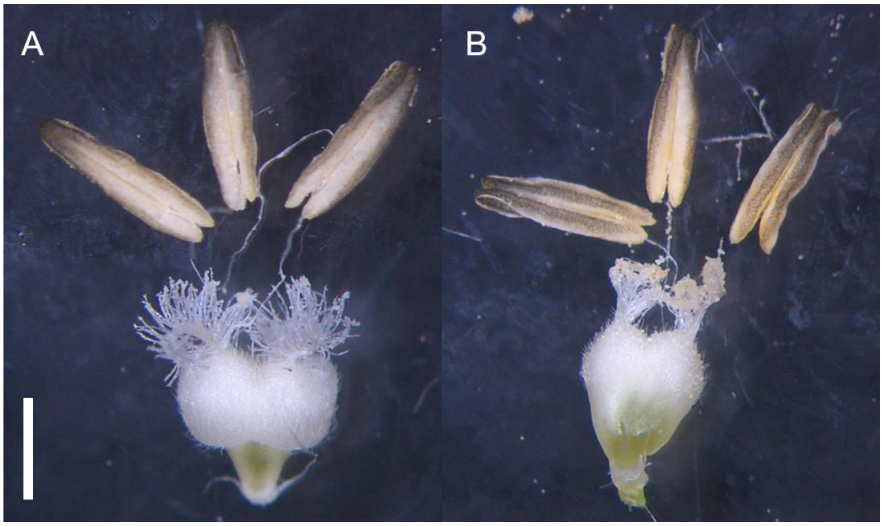

Figure 3.19. Stigma and anthers at pollen release, wild type (A) and HvDEX1-OE T1 (B). Scale bar 1mm.

3.3.6.1.3 Environmental Scanning Electron Microscopy (ESEM) images of HvDEX1 overexpression lines

In *Arabidopsis* and rice *DEX1* and *OsDEX1* are involved with primexine formation and exine patterning (Paxson-Sowders et al., 2001; Yu et al., 2016). To visualise any exine difference caused by the overexpression of *HvDEX1* and to further investigate the pollen adhesion to the stigma, anthers and pollen from were analysed by Environmental Scanning Electron microscopy (ESEM). One transgenic line of the HvDEX1 overexpression line in the T1 generation, HvDEX1:OE-2 was used for the analysis, since this line had been shown to have a slightly elevated level of the *HvDEX1* transcript. Anthers that were yellowing and about to release pollen, stage LFE3, were collected and imaged within 3 h to reduce the dehydration of the pollen grains. No difference was detected in appearance of pollen morphology in the *HvDEX1* overexpression lines in terms of pollen size, or pollen coat (Figure 3.20). It is possible that there is no effect of the ProZmUbi:DEX1 transgene on plant or pollen morphology.

3.3.6.2 Fertility in *HvMMD1-1* overexpression and silencing lines

3.3.6.2.1 Analysis of HvMMD1:Overexpression pollen through ESEM

The *Arabidopsis MMD1* is expressed in early development, specifically in male meiosis, however the closest orthologue in rice, *TIP3* has been shown to affect pollen wall development and exine formation (Andreuzza et al., 2015; Yang et al., 2019). To investigate the effect of *HvMMD1-1* silencing and overexpression on the pollen coat development ESEM analysis was carried out on anthers and pollen from these lines. Samples of the T1 generation of the overexpression line HvMMD1 T1-2-1 and silencing line HvMMD1 T1-3b-4 were collected at anthesis from anthers about to turn yellow and release pollen. Unfortunately, there were problems with the protocol used for attaching the samples to the holder and the grains collapsed and debris accumulated on the surface (Figure 3.21). It was not possible to detect any significant differences between the pollen samples, however since pollen viability and seed set was not affected in these lines the pollen might not be affected by the differential expression of *HvMMD1-1*.

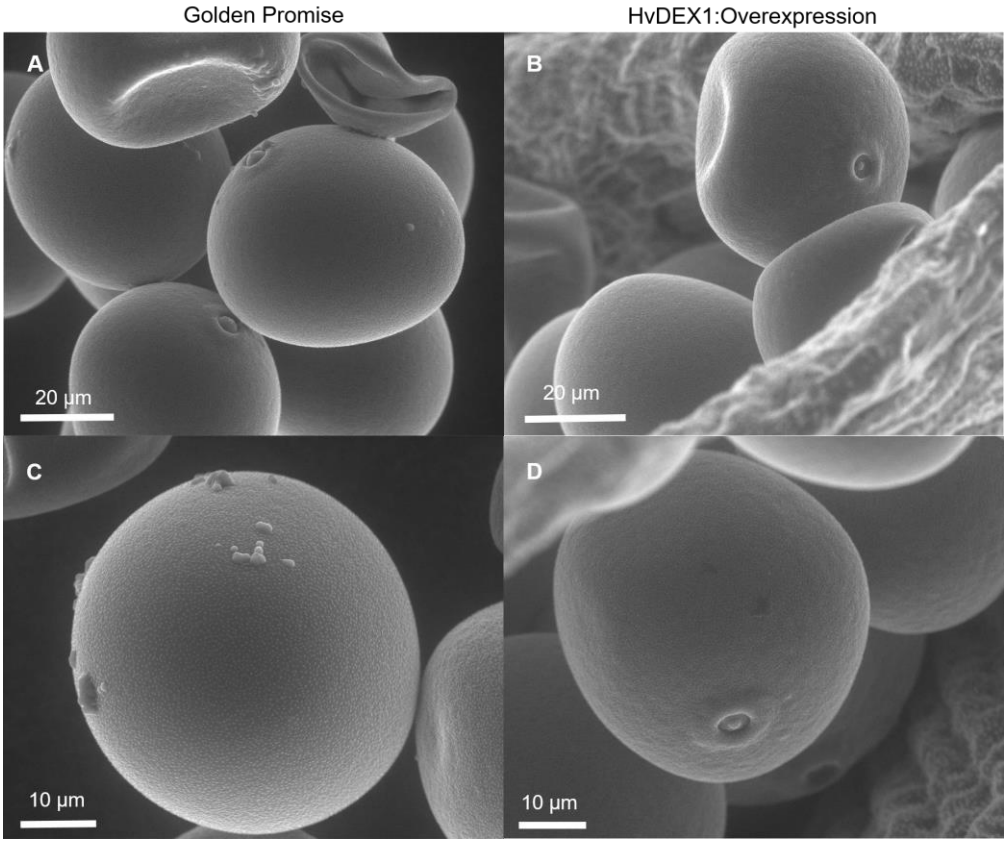

Figure 3.20. ESEM images of mature pollen from Golden Promise (wild type) (A and C) and HvDEX1:Overexpression (B and D) T1 line at stage LFE3 at pollen release from anther.

3.3.6.2.2 Pollen viability and seed set in HvMMD1-1 transgenic lines

Seed set and pollen viability was assessed in three independent transgenic lines in the T1 generation and an additional generation of HvMMD1:OE-1-5 for the overexpression genotype however only one transgenic line was available for the HvMMD1:SRDX genotype (Figure 3.18F). There was no difference in pollen viability for any of the lines but the seed set of HvMMD1:OE-8 was reduced as well as the T2 generation of the HvMMD1:OE-1-5. This suggests that an elevated level of the *HvMMD1-1* or HvMMD1:SRDX transcripts does not affect pollen viability. No consistent effect on seed set could be determined for the *HvMMD1-1* transgenes suggesting that *HvMMD1-1* is not sufficient to alter male fertility in barley.

3.3.6.1 The effect of *HvICE1-1* on fertility

3.3.6.1.1 Pollen viability and seed set in HvICE1-1 *transgenic lines*

For *HvICE1-1* three independent transgenic lines were used for both the overexpression and silencing constructs. No differences were found for pollen viability however there was a lot of variation in seed set for most lines (Figure 3.18D). When the overexpression lines were considered together there was a significant reduction in seed set compared to the wild type GP (p-value 0.0016) but no such difference was found for the silencing lines. These lines were investigated further in relation to cold and drought stress in Chapter 4.

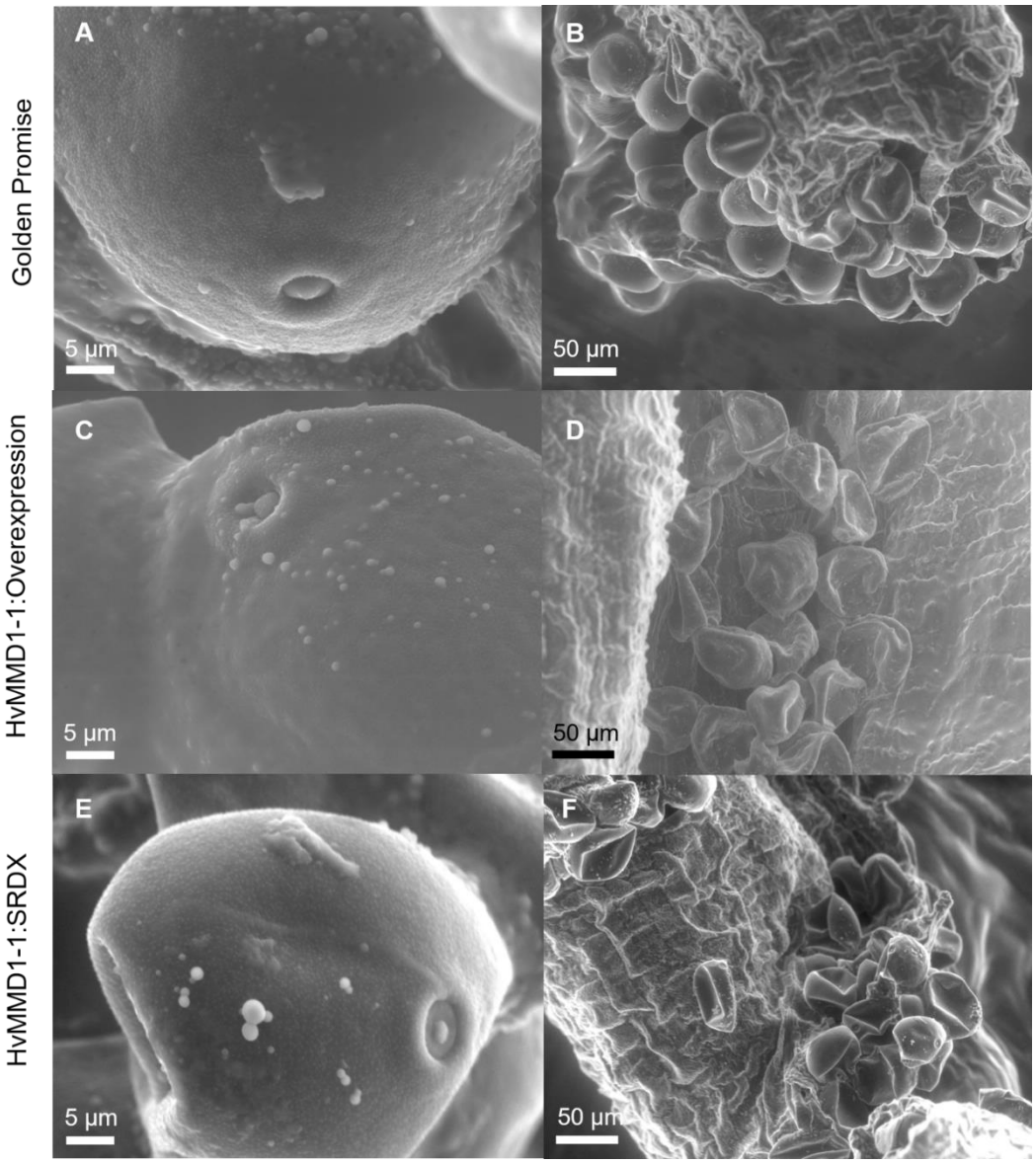

Figure 3.21. ESEM images of pollen from the wild type Golden Promise (A and B), HvMMD1:Overexpression line (C and D), and HvMMD1:SRDX silencing line (E and F) at pollen release stage.

3.4 Discussion

3.4.1 Transferring knowledge from *Arabidopsis* to grasses

Pollen development is essential for reproduction of plants and is controlled by an intricate gene network (Goldberg et al., 1993). Failure to form viable pollen leads to male sterility and forces outcrossing to produce seeds (Chen & Liu, 2014). The aim of this project was to study genes involved in pollen development in barley by identifying barley orthologues of known pollen development genes from *Arabidopsis*. Applying data of the model plant *Arabidopsis* to commercially important crops such as rice, wheat and barley, is a topic of great interest (Devos et al., 1999; Rensink & Buell, 2004; Salse et al., 2002; Spannagl et al., 2010; Zhang et al., 2004) however, direct transfer of gene functions from the dicot *Arabidopsis* to the monocot family has proven difficult due to rapid evolution and disruption of genome structure over the eudicot-dicot divide (Spannagl et al., 2010). To aid the transfer of knowledge between species as diverged as *Arabidopsis* and barley, researchers often combine knowledge from other species such as rice. Therefore, a combination of bioinformatic approaches with different species, mainly *Arabidopsis*, rice, and barley, have been used in this study to find candidate genes.

By comparing potential orthologous from more than two species the predictions can be more robust. Within the monocot family, the resources of the model organism rice are useful as it is closely related to other cereals, including barley. By using this relatedness researchers have been able to compare synteny between multiple cereals on a macro scale (Rensink & Buell, 2004). The usefulness of synteny as a tool for the prediction of gene conservation is sometimes questioned. Spannagl et al., (2010) reports of breakdown of synteny suggesting macro synteny alone is not as useful as previously thought for detailed gene studies. Others suggest that micro-synteny can be conserved between species even without apparent macro-synteny (Devos et al., 1999). When combined with other resources for orthologous gene detection, such as gene identity, protein domain conservation, and expression data, synteny is still considered a central part of comparative studies (Veltri et al., 2016).

In this study three putative orthologues were identified in barley for the *Arabidopsis* genes *DEX1*, *ICE1* and *MMD1*. The barley orthologues *HvDEX1* and *HvMMD1-1* were hypothesised to be involved with pollen development and disruption of these genes through CRISPR, overexpression or silencing were expected to affect fertility. The *HvICE1-1* orthologue was hypothesised to affect fertility and cold tolerance under stress conditions.

3.4.2 Subcellular localisation for functional conservation analysis

Transient expression in tobacco leaves is a widely used technique to rapidly assess the subcellular expression of a gene (Sparkes et al., 2006). In this study the full-length coding sequences of *HvDEX1*, *HvICE1-1* and *HvMMD1-1* were coupled to YFP to investigate if the

expression pattern of the barley orthologues corresponded to the pattern of the *Arabidopsis* genes.

OsDEX1 has been shown to localise to the endoplasmatic reticulum where it is involved with Ca^{2+} homeostasis where OsDEX1:GFP was present in the plasma membranes (Yu et al., 2016). A similar pattern was seen for HvDEX1:YFP where the expressed protein localised to the plasma membrane and vesicles throughout the cell. This suggests that the *HvDEX1* has a conserved expression localisation.

In *Arabidopsis* both *MMD1* and *ICE1* are transcription factors which are localised to the nucleus (Chinnusamy et al., 2003; Yang et al., 2003). This expression localisation was confirmed for the respective putative barley orthologues. Considering these results, the expression localisation of the barley orthologues appears to be conserved.

3.4.3 Generation of CRISPR lines – optimization and number of sgRNA per construct.

The application of targeted mutagenesis through the CRISPR/Cas9 system has become an integral tool for reverse genetic studies in plants (Hassan et al., 2021). Transgenes of the CRISPR/Cas9 gene editing system as well as overexpression or silencing constructs can be introduced into barley through *Agrobacterium* mediated transformation to alter the native expression of a gene (Hiratsu et al., 2003; Lloyd, 2003; Mitsuhara et al., 1996). In barley, transformation is carried out using immature embryos, where the transformation efficiencies in barley has been reported to be 25% on average (Harwood, 2019). However, obtaining a transgenic plant with a desirable mutation vary depending on numerous factors from plant viability to the design of the construct.

One factor to be considered is the number of targets used per construct. In Lawrenson et al., (2015) one or two sgRNAs are used, however, vectors carrying up to 24 individual sgRNAs have yielded stable transformants in plants (Hassan et al., 2021). In this study CRISPR vectors with three sgRNA each, for *HvDEX1* and *HvMMD1-1*, and individual sgRNAs, for *HvICE1-1*, with a total of six sgRNAs per gene were tested without a successful mutagenesis event. Transformation efficiency of CRISPR constructs with sgRNAs for *HvDEX1*, *HvICE1-1* and *HvMMD1-1* was very low with a success rate of 3.2, 2.8 and 1% respectively. In total eight, seven and two transgenic lines carrying CRISPR constructs were generated however no targeted mutations were identified in the T0 generation.

In a study by Howells et al. (2018), the efficiency of CRISPR gene editing was compared between barley and wheat. Gene editing efficiency was found to be higher for barley (15%) than for wheat (5%) with larger deletions and somatic editing however wheat displayed more stable and heritable gene edits (Howells et al., 2018). Barley gene editing was found to

be highly chimeric with possibly several genotypes present in the same tissue and that gene editing continues in several generations (Howells et al., 2018), a feature also discovered in *Arabidopsis* (Castel et al., 2019). The generated T0 CRISPR lines for *HvDEX1*, *HvICE1-1* and *HvMMD1-1* lines with the Cas9 present were therefore grown for a minimum of two generations to detect induced mutations however no mutations were detected.

Determining the cause for this lack of induced mutations is challenging. It could be due to the low number of generated transformants since the documented gene editing efficiency is only 15% and a larger population of transgenic lines would be necessary to identify mutations (Howells et al., 2018). In total 17 transgenic plants were generated where a number of plants from each T0 generation plant were screened in at least two generations however it was not possible to identify any induced mutations.

Another cause for the lack of induced mutations could be due to the sgRNA specificity and design. Optimisation of sgRNA design has been researched for the use with different Cas9-proteins, promoter sequences, sgRNA sequence elements and number of sgRNAs per level 2 construct (Castel et al., 2019; Hassan et al., 2021; Howells et al., 2018). Highest transformation efficiency in wheat was found for transformation events using co-transformation of more than one individual sgRNA level 2 construct containing the Cas9 and a single sgRNA (Howells et al., 2018). In the work presented in this thesis two approaches were tested: *HvDEX1* and *HvMMD1-1* were edited with level 2 constructs containing three sgRNAs, and *HvICE1-1* was edited by co-transformation of three level 2 constructs with only one sgRNA per construct, in total 6 sgRNAs. Unfortunately, since very few transformants were generated for each line it was not possible to determine which of these approaches were superior in barley. For the generation of stably inherited mutations generated through CRISPR targeting multiple transformants would most likely be required.

3.4.4 The use of overexpression and silencing lines for gene function studies

3.4.4.1 Generation of overexpression and SRDX silencing lines

Along with the generation of transgenic lines carrying CRISPR constructs, lines carrying overexpression constructs for *HvDEX1*, *HvMMD1-1* and *HvICE1-1* as well as SRDX silencing constructs for *HvICE1-1* and *HvMMD1-1* were generated. The use of overexpression and silencing lines can be used as a complement to the mutagenesis of the native gene for the study of gene function (Lloyd, 2003; Mitsuda et al., 2011). There are advantages of the use of overexpression and SRDX-silencing lines, such as overcoming functional redundancy or to ensure constitutively silencing effects however it is important to note that observed phenotypes are artificial and not true representations of the functions of the gene (Lloyd, 2003; Mitsuda et al., 2011). Coupling of the target gene to a constitutively active promoter leads to non-specific expression in tissues and developmental stages, potentially disrupting non-related processes. Overexpression and silencing for *HvMMD1-1* and *HvICE1-1* were considered because of potential redundancy in the network.

3.4.4.2 Overexpression of *HvMMD1-1*

The expression of *HvMMD1-1* was analysed in three independent HvMMD1:OE transgenic lines, however only one biological replicate for each line was used. In all lines genotyped as positive for the presence of the HvMMD1:OE insertion there was a significant increase in the *HvMMD1-1* transcript, of 15-118 times the wild type expression level, however only one line, HvMMD1:OE-1-5, displayed a phenotype that deviated from the wild type. In this plant the above ground organs were significantly larger, with wide long leaves, thick hollow stems, longer anthers, and large seeds. This phenotype was only present in one transgenic line despite overexpression of the *HvMMD1-1* transcript in other transgenic lines. It is possible that the phenotype of HvMMD1:OE-1-5 is not due to the effect of the increased level of *HvMMD1-1* but rather is the result of a disruption of other loci caused by the insertion of the overexpression construct.

Multiple transgenic lines are favourable to determine that an observed phenotype is not due to a disruption of an unrelated gene function through insertion of the construct. Unfortunately there was only one successful transformation of the HvMMD1:SRDX so the analysis of the effect of constitutively silencing *HvMMD1-1* could not be definitely determined. The HvMMD1:SRDX line produced was examined in 3 generations, T0-T2, however no difference in phenotype was detected in this line despite a significantly increased expression of the *HvMMD1-1* transcript coupled with the SRDX sequence. Due to the lack of a consistent phenotype related to pollen development, these lines were not analysed further.

3.4.4.3 The identification of the *HvICE1* homologs

One putative orthologue of *ICE1* has previously been identified in relation to the regulation of the barley orthologue of *C-REPEAT BINDING FACTOR* (*HvCBF*) involved with cold response (Tondelli et al., 2006) however there has been no further investigation into the function of *HvICE1* in barley. In this study three gene sequences were identified in barley as potential orthologue candidates to *ICE1* and *ICE2*, named *HvICE1-1*, *-2* and *-3*, where *HvICE1-1* corresponds to the orthologue identified by Tondelli et al. (2006) and through transcriptome analysis of the temperature dependent male fertility HvMS1:OE lines by José Fernández Gómez (unpublished data). This potential redundancy in the network complicates the analysis of the effect of a single gene. To further study the potential *ICE1* orthologue the *HvICE1-1* sequence was selected as the best candidate with barley overexpression and silencing transgenic lines generated.

The transgenic lines, HvICE1:OE and HvICE1:SRDX, were confirmed both with genotyping and expression analysis, where the level of *HvICE1-1* expression was significantly increased in both HvICE1:OE and HvICE1:SRDX lines. To evaluate the effect of differential expression of *HvICE1-1* in barley the lines were grown under optimal barley growth conditions where no difference was seen in growth of the HvICE1-1 lines. There was no difference in pollen viability but there was a reduction in seed set in the overexpression lines, mainly due to a reduction in the number of tillers formed. This lack of phenotype in general physiology

under control conditions enabled further comparisons of the differential expression of *HvICE1-1* under abiotic stresses without disrupted morphology to determine if *HvICE1-1* will provide advantages under abiotic stress conditions.

3.5 Conclusions

In this study three candidate genes were selected for investigation with putative orthologues of *Arabidopsis DEX1*, *ICE1* and *MMD1* identified through bioinformatics analysis. The gene sequences obtained in this study were investigated as orthologues to the *Arabidopsis* and rice pollen development genes to study the conservation between *Arabidopsis,* rice and barley. Transgenic lines overexpressing or silencing the genes were generated however no CRISPR induced mutations were detected. For future generation of CRISPR induced mutant lines multiple sgRNA targets and multiple transformed embryos are needed for a successful mutation event.

Phenotypes of the overexpression or silencing of the *HvDEX1*, *HvMMD1-1* and *HvICE1-1* genes were studied under optimal growth conditions where only one line of the HvMMD1:OE transgenic plants showed a differing phenotype. No consistent effect was seen in the transgenic HvDEX1:OE, HvMMD1:OE and HvMMD1:SRDX lines under control conditions and these genes were not investigated further. *HvICE1-1* was selected for detailed study for the effect of differential expression of *HvICE1-1 in planta* under abiotic stresses and the generated overexpression and silencing lines were used in further experiments detailed in Chapter 4.

Only one putatively orthologue sequence of *DEX1* and *OsDEX1* was identified as a candidate in barley, with high gene identity and confirmed micro-synteny in the genomic region between rice and barley, suggesting that the *HvDEX1* candidate identified is a likely orthologue. The *HvDEX1* overexpression lines generated did not have an elevated expression of the *HvDEX1* transgene similar to the overexpression of *HvICE1-1* and *HvMMD1-1*, possibly suggesting that the transgene was not expressed properly.

In barley three putative orthologues of both *ICE1* and *MMD1* were identified, suggesting a level of redundancy in the barley genome. Overexpression and silencing of *HvICE1-1* and *HvMMD1-1* were generated however knock-out mutations of the native genes would facilitate the determination of the functions of the genes *in planta*. Additionally, to characterise the conserved functions of the genes, it would be interesting to investigate if the genes could bind to and activate predicted downstream genes through yeast-2 hybrid analysis or Chromatin immunoprecipitation analysis.

To further study the candidate genes, the generation of knock-out lines of the genes would facilitate the investigation of the effect of *HvDEX1*, *HvICE1-1* and *HvMMD1*-1 on pollen development. In addition, complementation analysis of the expression of the putative barley

orthologues under control of the native *Arabidopsis* promoter of the respective gene in *Arabidopsis* mutants would further confirm if the function of the barley genes could rescue the mutant phenotypes.

Chapter 4. Effect of differential expression of *HvICE1-1* on cold tolerance, yield and stomatal patterning

4.1 Introduction

4.1.1 *ICE1* is a transcription factor acting as a key regulator in the cold signalling pathway

In this study a potential orthologue of *INDUCER OF CBF EXPRESSION1*/*SCREAM1* (*ICE1*/*SCRM1*) was studied in relation to cold tolerance and spike fertility. An orthologue of *ICE1* was identified as a gene of interest from a transcriptome dataset of the barley *MALE STERILE1* (*HvMS1)* overexpression lines displaying temperature dependent conditional sterility. These lines were sterile under normal growth conditions (15˚C), but fertility could be rescued by growing the plants during flowering at 18˚C or higher (Fernández-Gómez, Talle, & Wilson, 2020). An *ICE1* annotated orthologue, *HvICE1-1,* was identified as differentially expressed in these lines with no expression at 18˚C and a downregulation of 1.5 times at 15˚C in the *HvMS1* overexpression lines compared to the wild type. *HvICE1-1* was recognised as a potential target for further study in pollen development in relation to environmental stress in barley.

ICE1/*SCRM1* is a MYC-like basic helix loop helix (bHLH) transcription factor involved with cold response and stomatal patterning in *Arabidopsis* (Chinnusamy et al., 2003; Kanaoka et al., 2008). In response to low temperatures *ICE1* and its paralog *ICE2* bind to different *C-REPEAT BINDING FACTORS* (*CBFs*) and act as master regulators of cold by inducing the downstream *COLD RESPONSIVE* (*COR*) genes (Chinnusamy et al., 2003; Kim et al., 2015). In stomatal formation ICE1 interact with other bHLH transcription factors by forming heterodimers to initiate stomatal formation (Kanaoka et al., 2008). In addition, ICE1 activates *Flowering Locus C* (FLC), a major repressor of floral transition, to delay flowering under fluctuating environmental stimuli (Wei et al., 2018) and *ice1* knockout mutants lead to reduced fertility and shortened inflorescences (Kanaoka et al., 2008).

In rice the *OsICE1*/*bHLH002* and *OsICE2* have been identified as orthologous to *ICE1* and *ICE2* respectively (Deng et al., 2017), with overexpression of *OsICE1* and *OsICE2* leading to increased cold tolerance in *Arabidopsis* (Deng et al., 2017). Cold tolerance is of great interest in rice since it is highly sensitive to freezing temperatures and little is known about cold signalling in monocots. The cold response pathway related to *OsICE1* has not been widely studied however it has been confirmed that *OsICE1* is involved with cold response in rice (Xia et al., 2020).

4.1.2 The role of ICE1 in cold response

4.1.2.1 ICE1 interaction with *CBF* and cold signalling

Induction of the cold response pathway is under tight control to rapidly protect the plant under changing conditions, whilst preventing unnecessary inhibition of plant growth,

reviewed in Pareek et al. (2017). In response to cold, *ICE1* and *ICE2* are key regulators in the ICE1/2-CBF-COR signalling cascade resulting in the changes in expression of genes involved with metabolism and upregulation of stress responses (Jin et al., 2018; Kim et al., 2015; Lee et al., 2005).

Under cold stress ICE1 induces cold response by binding to the MYC recognition sequences in the *CBF3* promoter (Chinnusamy et al., 2003). The *CBFs* are a family of transcription factors that are activated by cold temperatures and positively regulate the *COR* genes resulting in cold stress response (Stockinger et al., 1997). In *Arabidopsis* six *CBF* paralogs have been identified of which three are involved with cold signalling, *CBF1*, *CBF2* and *CBF3*, where *CBF2* negatively regulate *CBF1* and *CBF3* and vice versa (Choi et al., 2002; Novillo et al., 2004, 2007).

In barley at least twenty *CBFs* are involved with abiotic stresses with a subgroup activated as a result of cold treatment (Skinner et al., 2006). In this subgroup, *HvCBF3* is rapidly induced at low temperatures as the transcript starts to accumulate within 15 min of exposure to cold and overexpression of *HvCBF2* increases cold tolerance in cold acclimated plants (Choi et al., 2002; Jeknić et al., 2014). However, stringent control of the *CBFs* is important as overexpression of these genes can lead to delayed flowering, reduced yield and stunted growth in *Arabidopsis*, *Brassica napus*, rice and barley (Gilmour et al., 2000; Gilmour et al., 2004; Ito et al., 2006; Jaglo et al., 2001; Jeknić, 2014; Liu et al., 1998). Increasing cold tolerance without adverse effects is of great interest for the production of cold tolerant crops.

4.1.2.2 Regulation of ICE1 in the cold signalling pathway

Similar to the *CBFs*, *ICE1* activity is under strict regulation and dependent on the post translational modifications by other proteins. *ICE1* is constitutively expressed throughout the entire plant and is only slightly upregulated by cold suggesting there is always a level of ICE1 present to facilitate a rapid response to changing conditions (Chinnusamy et al., 2003), however ICE1 mediated activation of *CBF3* involves an upstream signalling cascade for its initiation.

Under normal temperatures ICE1 acts as a repressor of *CBF3* by facilitating accumulation of MYB15 which binds to and represses the *CBF3* promoter (Figure 4.1) (Agarwal et al., 2006). At exposure to low temperature, ICE1 is sumoylated by the sumo E3 ligase *SAP AND MIZ1 DOMAIN-CONTAINING LIGASE1* (*SIZ1*) which modifies and stabilises ICE1 which represses the inhibitory effect on MYB15 (Miura et al., 2007). Sumoylation of ICE1 by SIZ1 also promotes the binding of ICE1 to the *CBF3* promoter however the *siz1* knockout mutant does not affect *ICE1* expression (Miura et al., 2007).

In addition to SIZ1 mediated stabilisation, ICE1 is regulated by the interplay of OPEN STOMATA1 (OST1) and HIGH EXPRESSION OF OSMOTICALLY RESPONSIVE GENES 1 (HOS1) competing for the interaction with ICE1 (Ding et al., 2015). *OST1* is involved with ABA signalling and under normal conditions OST1 is bound to and repressed by ABA INSENSITIVE

1 (ABI1) (Figure 4.1) (Yoshida et al., 2006). Under freezing stress OST1 is released from ABI1 to phosphorylate ICE1 which prevents the HOS1 mediated degradation of ICE1 and enhances the binding of ICE1 to the *CBF3* promoter (Ding et al., 2015). HOS1 is one of the main regulators of cold signalling in *Arabidopsis* by direct interaction with ICE1 (Dong et al., 2006). Under cold conditions HOS1 ubiquitinates ICE1 and ICE2, where degradation of ICE1 is detected after 1h, thereby inhibiting binding to the *CBF3* promoter (Dong et al., 2006; Shkryl et al., 2021). Under normal conditions HOS1 does not affect the abundance of ICE1 but overexpression of *HOS1* reduces *ICE1* and *CBF3* expression even at normal temperatures (Dong et al., 2006). In the *hos1* knockout mutants there still was a slight upregulation of *COR* genes under cold stress indicating that there are alternative pathways for cold response (Shkryl et al., 2021).

This interaction of HOS1 with ICE1 seems at least partly conserved in monocots. The ubiquitination of OsICE1 by OsHOS1 also occurs in rice where OsHOS1 is prevented from phosphorylating OsICE1 during cold stress if OsMAPK3 phosphorylates OsICE1 (Lourenço et al., 2013; Zhang et al., 2017). In addition, several orthologous genes of the ICE-CBF-COR pathway have been identified in Triticeae (Jin et al., 2018) suggesting that the cold sensing pathway is highly conserved and under strict regulation. Plants susceptible to cold and exhibiting cold signalling defects have been found to produce less pollen and have a higher pollen sterility with cold stresses during meiosis and pollen maturation being extra detrimental (Sharma & Nayyar, 2016). Studying interactions in the *ICE1* regulatory system in barley is important for the understanding of cold tolerance in relation to fertility in cereal crops.

4.1.2.3 Cold signalling and implications for floral development

Cold sensing also has implication for plant fertility where genes involved with the cold signalling pathway may affect plant growth and flowering progression. Similar to how *CBFs* can affect flowering, *HOS1* is also involved with regulation of flowering time in relation to vernalisation (Mouradov et al., 2002). In *Arabidopsis* the *hos1* mutant flowers earlier and the expression of the *FLOWERING LOCUS C* is reduced indicating that *HOS1* has a repressing function in flowering (Ishitani et al., 1998; Lee et al., 2001).

In the cold signalling pathway the expression of *JASMONATE ZIM-DOMAIN*1 (*JAZ1*) affects ICE1 activity by directly binding to and repressing both ICE1 and ICE2 under normal temperatures (Hu et al., 2013). This effect is inhibited during cold stress by the activation of *CORONATINE INSENSITIVE1* (*COI1*) through jasmonic acid (JA) signalling which inhibits JAZ1 binding to ICE1 and ICE2 (Hu et al., 2013). The inhibition of JAZ1 by COI1 in response to cold actively supresses the *FLOWERING TIME LOCUS T* and leads to delayed flowering (Zhai et al., 2015). This interaction of the cold response signalling pathway and the flowering pathway and its implication for flowering time is of interest to improve cold hardiness while maintaining fertility.

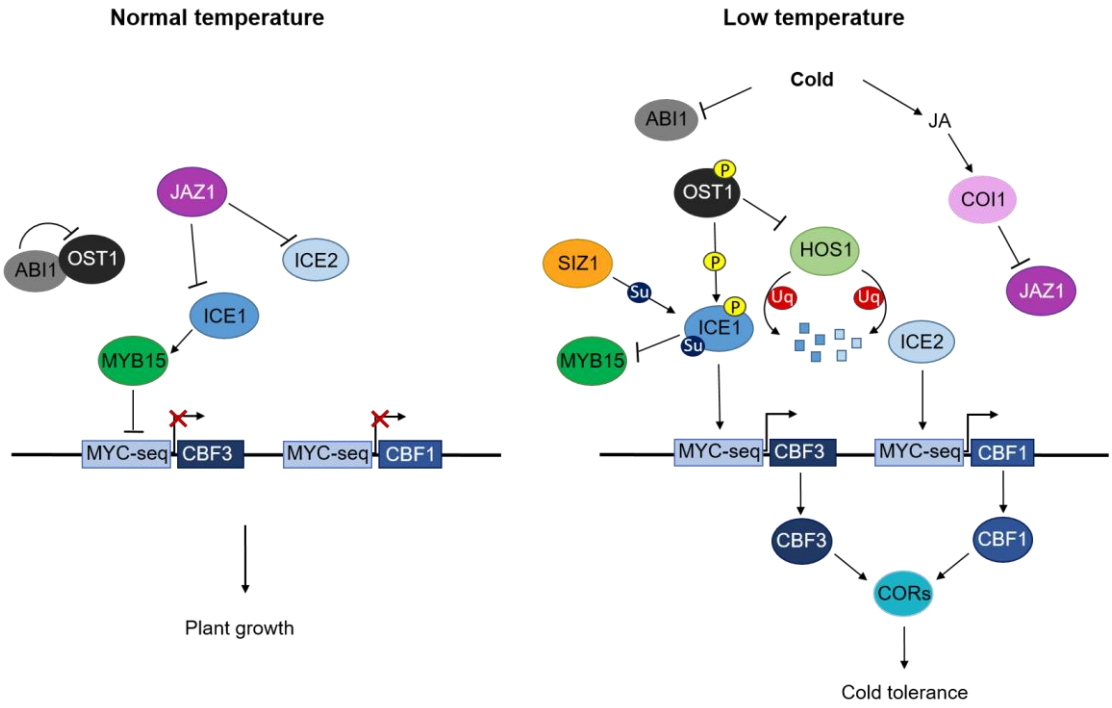

Figure 4.1. Regulatory network of ICE1 *mediated cold signalling in* Arabidopsis*. Under normal temperatures ICE1 facilitates MYB15 accumulation which represses CBF signalling. At cold temperatures ABI1 is prevented from interacting with OST1 causing OST1 to be free to phosphorylate ICE1 and inhibit HOS1 mediated ubiquitination of ICE1. ICE1 is also sumoylated by SIZ1 and prevents MYB15 accumulation and interaction with the CBF3 promoter to activate its expression leading to cold tolerance. ABI1: ABA INSENSITIVE 1, CBF: C-REPEAT BINDING FACTOR, CORs: COLD RESPONSIVE, HOS1: HIGH EXPRESSION OF OSMOTICALLY RESPONSIVE GENES1, ICE1/2: INDUCER OF CBF EXPRESSION1/2, JA = jasmonic acid, JAZ1: JASMONATE ZIM-DOMAIN1, OST1: OPEN STOMATA1, P =phosphorylation, SIZ1: SAP AND MIZ1 DOMAIN-CONTAINING LIGASE1, Su =sumoylation, Uq = ubiquitin. Adapted from Pareek et al., (2017), Ding et al., (2015), and Hu et al., (2013).*

4.1.3 ICE1 interacting genes in stomatal patterning

In addition to its influence on cold response *ICE1* is involved with stomatal patterning. Stomata are pores on the epidermal leaf surface where gaseous exchange occur as a part of photosynthesis and they are critical for plant growth and the water cycle in the plant (Harrison et al., 2020). Comprised of two guard cells, with flanking subsidiary cells in grasses, these pores can open and close in response to external stimuli to improve requirements for photosynthesis, reduce water loss, or prevent leaf damage (Franks & Farquhar, 2007; Hepworth et al., 2018; Raissig et al., 2016).

ICE1/SCRM affects stomatal patterning by forming heterodimers with the bHLH transcription factors SPEECHLESS (SPCH), MUTE, AND FAMA where ICE1 acts downstream of SPCH but upstream of MUTE and FAMA (Figure 4.2) (Kanaoka et al., 2008). In the nucleus, ICE1 dimerises strongly with MUTE and FAMA where the expression level of *ICE1* and *ICE2* appears to influence stomatal differentiation (Kanaoka et al., 2008). Overexpression of *ICE1*

in *Arabidopsis* yields an increase of *FAMA* expression and stomatal formation whereas a knockout mutant of *ice1* significantly reduces the stomatal density with a complete lack of stomata in the *ice1ice2* double mutant (Kanaoka et al., 2008; Pillitteri et al., 2011; Putarjunan et al., 2019).

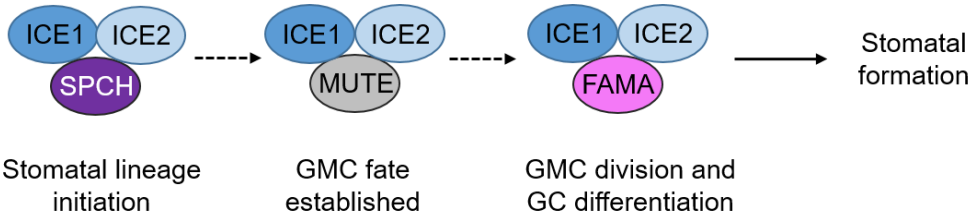

Figure 4.2. The simplified interaction of ICE1 and ICE2 with the bHLH factors SPCH, MUTE and FAMA required for stomatal formation in Arabidopsis. Stomatal cell fate is initiated by SPCH interacting with ICE1 and ICE2, with establishment of guard mother cells (GMCs) with MUTE and further guard cell (GC) differentiation by the interaction of ICE1 and ICE2 with FAMA. Adapted from Raissig et al., (2016),and Kanaoka et al., (2008).

4.1.3.1 Gene network associated with stomatal formation in grasses

Formation of guard cells and the flanking subsidiary cells that regulates the opening and closing of the stomata, as well as the stomatal density is critical for respiration. Stomata in grasses are initiated at the leaf base and are formed in straight lines in contrast to the scattered pattern seen in dicots. Grasses have the ability to open and close stomata very rapidly, a mechanism attributed partly to the additional subsidiary cells on either side of the guard cells and might be one of the causes of the success of grasses (Franks & Farquhar, 2007).

In addition to the difference in morphology between dicot and monocot stomata, there appears to be differences in the gene network regulating stomatal formation. In the wheat relative *Brachypodium* the *ICE1* orthologues, *BdICE1* and *BdSCRM2*, are involved with stomatal formation but act non-redundantly and a knockout of *BdICE1* leads to loss of stomata (Raissig et al., 2016). *BdICE1* can act independently of *BdSPCH1* and *BdSPCH2* in contrast to the signalling in *Arabidopsis* where *ICE1* acts downstream and interacts with *SPCH* (Kanaoka et al., 2008; Raissig et al., 2016). The *Osice1* knockout in rice resulted in an absence of stomata whereas a *Osice2* knockout showed no stomatal defects (Wu et al., 2019). Also, the bHLH transcription factors *OsSPCH*, *OsMUTE* and *OsFAMA* interact with *OsICE1* at different stages in stomatal development with *OsICE1* interacting with *OsSPCH* to initiate stomatal formation, with *OsMUTE* to form guard cells, and with *OsFAMA* for later maturation (Wu et al., 2019). In barley a reduction of stomatal frequency has been shown to improve drought tolerance however there has been no studies on the molecular pathways of stomatal formation (Hughes et al., 2017). Investigation of the impact of the *HvICE1-1* orthologue in barley in relation to stomatal formation is of interest.

In barley few genes have been studied in terms of stomatal formation but the overexpression of the *EPIDERMAL PATTERNING FACTOR* (*HvEPF1*), an orthologue of *EPF1* involved with stomatal formation through stabilisation of SPCH, was found to reduce stomatal density (Hughes et al., 2017; Simmons & Bergmann, 2016). This reduction in density was analysed in terms of yield under control and drought conditions where a reduction in the number of stomata improved drought stress without adverse effect on yield (Hughes et al., 2017). It is possible *HvICE1-1* has an effect on drought tolerance as it was first identified as a candidate close to a QTL involved with both cold and drought tolerance (Tondelli et al., 2006). In addition, in tea plant *ICE1* was identified as one out of 10 genes upregulated under both drought and cold stress (Samarina et al., 2020). Further investigation into the correlation between ICE1, stomatal formation, and possible drought tolerance is needed.

4.1.4 The interplay of stomata and cold in photosynthesis

4.1.4.1 Photosynthesis parameters for the estimation of photosystem efficiencies

Photosynthesis is dependent on the gaseous exchange facilitated by the stomata as well as abiotic stress factors. Excess light energy not used in photosynthesis can be emitted in several different pathways such as chlorophyll fluorescence, photochemistry (photochemical quenching, qP), or heat (non-photochemical quenching, NPQ) to protect the photosystems (Maxwell & Johnson, 2000). By measuring these parameters it is possible to estimate the efficiency of the photosystem I and II (PSII) of plants subjected to different growth conditions. Recovery of photosynthetic properties without permanent damage to the photosystems after periods of cold tress is a valuable agronomic trait (Dai et al., 2007; Gray et al., 2003).

By measuring the chlorophyll fluorescence in the absence of light (F_o), at maximum light (F_m) and at steady state light conditions (F_t) the efficiency of photosystem II (ϕ_{PSII}) can be evaluated. This measures the quantity of light absorbed by the chlorophyll and used in photochemistry, and in extension the rate of photosynthesis. The ϕ_{PSII} can further be used to calculate the linear electron transport rate (ETR), where the amount of light being used by the PSII is calculated, and the overall photosynthetic capacity.

In contrast to the estimation of the ETR, it is also possible to measure how many reaction centres are open by calculating photochemical quenching, qP. The efficiency of PSII (ϕ_{PSII}) and the amount of PSII that are open (qP) under specific conditions can be used to calculate the maximum efficiency of the PSII by calculating F_v/F_m. In barley the values for the maximum efficiency of the PSII is 0.84, with lower values indicating inhibition of photosynthesis through stress (Dai et al., 2007).

4.1.4.2 Cold response genes and photosynthesis

The effect of stomatal or cold sensing genes on photosynthesis has partly been investigated in *Arabidopsis* by looking at *ICE1* related genes however no study has been conducted on the

influence of *ICE1* on chlorophyll fluorescence of leaf tissue. In a transcriptome analysis of the *ICE1*/*SCRM* overexpressing mutant, *scrm-D,* no difference in the transcription of genes predicted to be related to photosynthesis, carbohydrate or central tricarboxylic acid metabolism genes was detected (Pillitteri et al., 2011). However, *ICE1* belongs to a subgroup of bHLH transcription factors with *ICE2*/*SCREAM2*, *bHLH093* and *bHLH061* where the *bhlh093*/*bhlh061* double mutant show impaired light sensing and photoperiod disruption resulting in impairment in inflorescence development, indicating a possible connection between this group of bHLH factors and photosynthesis (Poirier et al., 2018).

The interplay between cold and light response genes in grasses is however not widely studied. Low temperatures are known to reduce light-induced electron transport rates and freezing tolerance in cereals is connected to photosynthesis capacity after cold acclimation (Dai et al., 2007; Dal Bosco et al., 2003; Kubien et al., 2003). In barley there is a connection between cold-regulated, *COR,* genes and photosynthesis, where a *cor14b* mutant is dependent on chloroplast development for its expression (Dal Bosco et al., 2003). Expression of the cold-regulated gene *COR14b* is increased as a result of both cold induction and short light pulses, indicating an overlapping gene network between temperature and light responses (Crosatti et al., 1999). Further investigation of chlorophyll fluorescence found that the maximum efficiency of PSII not affected under non-lethal freezing stress but the effective quantum yield of photochemical energy conversion in PSII (ϕPSII) decrease after freezing treatment, as did NPQ (Dai et al., 2007).

In this study, HvICE1:OE and HvICE1:SRDX lines were generated (Chapter 3) and analysed for differences in chlorophyll fluorescence under cold stress to determine any effect of *HvICE1-1* on photosynthesis capacity. In *Arabidopsis ICE1* is involved with stomatal patterning and the cold signalling pathway with related genes showing impaired photosynthetic capacity. A potential *HvICE1* orthologue was originally isolated in the temperature dependent sterile *HvMS1* overexpression line. The *HvICE1-1* candidate was differentially expressed in HvMS1:OE lines, with a 1.5 times higher expression in the sterile anthers at 15°C than in the fertile anther at 18°C. Here, the implication of the potential *ICE1* orthologue candidate *HvICE1-1* was studied in relation to cold and drought tolerance to investigate abiotic stress response in relation to fertility and stomatal formation. Finally, the expression of predicted *HvICE1-1* interacting genes was analysed to determine conserved functions of *HvICE1-1* in the barley cold signalling network.

4.2 Methods

4.2.1 Seed germination test

Transgenic seeds carrying the HvICE1:OE and HvICE1:SRDX constructs were generated (described in Chapter 3). To test the difference in germination of the *HvICE1-1* lines compared to wild type (Golden Promise (GP)), seeds from three individual transgenic lines for each genotype were used. In total 150, 148, and 110 seeds were used to study germination of GP, HvICE1:OE and HvICE1:SRDX lines respectively. Seeds were sterilised as described in section 2.1 and placed in the dark at 21˚C on moist filter paper. After 5 days the number of germinated seeds were counted.

4.2.2 Growth conditions and stresses

All experiments were carried out in growth room at control conditions of 16 h light 15˚C and 8 h dark 12˚C unless specified otherwise. Seeds were sterilised (section 2.1) and germinated seeds were moved to soil or vermiculite. For all experiments carried out in soil the plants were grown in nutrient rich Levington M3 soil under well-watered conditions until the beginning of the respective treatment unless otherwise specified.

4.2.2.1 Cold stresses

For the chilling treatments the seedlings were grown in control conditions in germination trays of 150 ml soil per seedling until the 2-3 leaf stage. Varying durations and severities of cold treatments were conducted as summarised in Table 4.1. In the freezing survival experiment (Experiment 1C, Table 4.1) the seedlings were placed at +4˚C for cold acclimation for 24 h before cold treatment of -12±2˚C for 30 min. The seedlings were then returned to control conditions and survival was assessed after 14 days.

In the long cold stress experiment (Experiment 2C, Table 4.1) seedlings were grown in 10 cm pots at control conditions for three weeks until the third leaf stage before the application of the cold treatment of constant +6˚C with 12 h photoperiod. The seedlings were then returned to control conditions for five days before being moved back to 6˚C for 24 h after which leaf tissue was collected for RNA isolation. The plants were then transferred to 2 L pot for the remaining growth period. Three plants were used for each genotype in each condition, however only one independent transgenic line was analysed. Stomatal imprints from the mid-section of mature leaves (section 4.2.4) of cold treated and control lines were collected at the same point as the collection of leaf tissue for RNA isolation (section 2.8).

A similar cold treatment was conducted during spike development (Experiment 3C, Table 4.1). Plants were grown in control conditions with three plants in each 5 L pot until spike stages 37-LFE1 when the spikes were 2-4 cm long (Gomez & Wilson, 2012). The plants were then exposed to +6˚C for three days at 16 h photoperiod before being returned to control conditions until harvest. For both HvICE1:OE and HvICE1:SRDX one independent transgenic line was used with three biological replicates for each treatment group.

In experiment 4C (Table 4.1) seedlings were grown in control conditions in germination trays of 150 ml soil per seedling until the 2-3 leaf stage. The seedlings grown in control conditions were placed in the dark for 15h before the start of the treatments in an effort to reduce differences in light conditions and decrease diurnal effects (Pillitteri et al., 2011). The seedlings were then moved to -1 (±1)˚C and were sampled for leaf tissue at 0 h, 30 min and 2 h for RNA isolation. After 24 h the seedlings were returned to control conditions with normal light levels at 15˚C to recover and the controls were returned to light. After 4 h of recovery the photosynthetic measurements were carried out as specified in section 4.2.3. For each treatment six wild type seedlings were used, for HvICE1:OE six seedlings from three different transgenic lines (18 per treatment) and for HvICE1:SRDX 3-6 seedling from three different transgenic lines were used (15 per treatment).

Table 4.1. Cold experiments conducted with the HvICE1-1 lines. All plants were grown in control conditions before and after the application of the cold treatment.

Experiment	Temperature/ Duration of cold treatment	Lines used	Stage of cold stress	Pot size	Sampling
1C	+4°C for 24 h -16˚C for 30 min	HvICE1:OE-5 HvICE1:OE-6 HvICE1:OE-12 HvICE1:SRDX-1 HvICE1:SRDX-2 HvICE1:SRDX-3 Golden Promise	2-3 leaf stage	150ml pots	Survival assessment
2C	+6˚C for 3 weeks 5 days control 24 h 6˚C	HvICE1:OE-5 HvICE1:SRDX-1 Golden Promise	3 leaf stage	10 cm pot	Stomatal imprint, Stomatal conductance, Gene expression analysis
3C	+6°C for 3 days	HvICE1:OE-1 HvICE1:SRDX-1 Golden Promise	37-LFE1 stage	3 plants per 5L pot	Fertility assessment
4C	24 h dark adaption 0 to -3˚C for 30 min and 2 h	HvICE1:OE-5 HvICE1:OE-6 HvICE1:OE-8 HvICE1:SRDX-2 HvICE1:SRDX-3 HvICE1:SRDX-6 Golden Promise	2-3 leaf stage	150ml pots	Photosynthesis measurement, Gene expression analysis

4.2.2.2 Drought stresses

To test the water management of the different HvICE1-1 lines in terms of fertility, a drought stress was applied at three different developmental stages, seedling stage, early tillering, and at spike development.

In the first drought experiment (Experiment 1D, Table 4.2) the seedlings were grown in germination trays with 150 ml wet vermiculite supplemented with 0.5x Hoaglands pH 6 once per week, using a modified protocol from Cai et al. (2020). For each treatment six seedlings of each genotype was used, with three different transgenic lines for HvICE1:OE (18 per treatment), two different transgenic lines for HvICE1:SRDX (12 per treatment), and six wild type seedlings. Drought stress was applied by watering each seedling with 8-10 ml of 0.5x Hoaglands with 20% polyethylene glycol (PEG) daily for 12 days. Controls were watered with an equivalent volume of 0.5x Hoaglands daily. At the end of the drought stress stomatal imprints were taken for each plant on the middle section of a mature leaf on the abaxial side. The biomass of the roots and shoots were weighed.

Two drought stress experiments were conducted with plants grown in soil with three plants per genotype used with one independent transgenic line for HvICE1:OE and HvICE1:SRDX. The exposed soil in the pots were covered with cling film to reduce evaporation. For the drought stress at early tillering (Experiment 2D, Table 4.2), the seedlings were grown in 10 cm pots until early tillering stage, Zadoks stage 2 (Zadoks et al., 1974), when water was withheld for 5 days. The controls were kept well-watered by watering to saturation with subsequent drainage. The pots were weighed daily and fertility was evaluated through seed count.

Table 4.2. Drought experiments conducted on the HvICE1-1 lines. All plants were grown in control conditions before and after the application of the drought stress.

Experiment	Duration of drought	Lines used	Stage of drought stress	Pot size	Sampling
1D	12 days	HvICE1:OE-5 HvICE1:OE-6 HvICE1:OE-8 HvICE1:SRDX-2 HvICE1:SRDX-3 Golden Promise	3 leaf stage	150 ml vermiculite	Stomatal imprint, Root:Shoot ratio
2D	5 days	HvICE1:OE-5 HvICE1:SRDX-6 Golden Promise	Early tillering	10 cm pots	Fertility assessment
3D	9 days	HvICE1:OE-1 HvICE1:SRDX-1 Golden Promise	37-LFE1	2 L pots	Fertility assessment

Drought stress during spike development was applied at the same stage as the second cold stress, at spike development stage 37-LFE1 (Experiment 3D, Table 4.2). The plants were grown in 2 L pots until water was withheld for 9 days where the controls were kept well-watered. The pots were weighed every three days and fertility was evaluated through seed count.

4.2.3 Photosynthesis measurement with Fluorcam

To estimate the difference in photosynthetic capacity of the HvICE1-1 lines under control and cold stress the chlorophyll fluorescence was measured using a FluorCam CF Imager (FC800-222, Photon Systems Instruments, Drasov, Czech Republic) according to McAusland et al. (2019). Seedlings that underwent the chilling treatment of 1(±1)˚C in the dark for 24 h (Experiment 4C, Table 4.1) were returned to control conditions (+15˚C with light) to recover for 4 h. Three biological replicates of three independent transgenic lines (Golden Promise, HvICE1:OE 5, 6, 8 and HvICE1:SRDX 2, 3 6) were used for control and cold treated samples. The middle section of mature leaves was placed on wet filter paper between two glass plates with the adaxial side up. The plates were dark adapted for 1h before the measurement of the variable (F_v) and the maximum (F_m) fluorescence in dark adapted state to generate the maximum quantum yield of PSII (F_v/F_m) (Maxwell & Johnson, 2000). The F_m' (maximum fluorescence in light adapted state), F' (steady state level of fluorescence), and F_o (minimum fluorescence in dark adapted state) were then measured at different light intensities of 10, 20, 30, 40, 80, and 100 % corresponding to 21.2, 142.5, 271.7, 395.4, 901.9, and 1147.9 µmol s^{-} m^{-2} measured with LI250-A light meter (Licor, United states). The measurements were used to calculate quantum yield of PSII (Φ_{PSII}), non-photochemical quenching (NPQ), proportion of open PSII (qP) and the electron transport rate (ETR) using the equations stated in **Error! Reference source not found.** (Maxwell & Johnson, 2000).

Table 4.3. Description of equations used for the calculation of photosynthesis parameters. Where PFD *is the amount of light available and* a *is the absorption factor for barley (0.84)* (Dai et al., 2007).

Parameter	Description	Formula
$\boldsymbol{F_v/F_m}$ $\boldsymbol{(QY_{max})}$	Maximum quantum yield of PSII	$(F_m - F_o)/F_m$
Φ_{PSII}	Efficiency of PSII	$(F'_m - F')/F'_m$
$\boldsymbol{NPQ}$	Non-photochemical quenching	$(F_m - F'_m)/F'_m$
$\boldsymbol{qP}$	Photochemical quenching	$(F'_m - F')/(F_m' - F'_o$
$\boldsymbol{ETR}$	Electron transport rate	$\Phi_{PSII} \times PFDa \times (0.5)$

4.2.4 Stomatal imprints

The stomata were visualised by making stomatal imprints of the leaf surface of the barley plants. On the abaxial or adaxial side a thin layer of clear nail polish was added to the middle section of the leaf tissue. When the polish was completely dry the imprint was lifted with clear tape and placed on a glass microscopy slide. Stomatal imprints were imaged using a Leica DMRB microscope, 10x/0.3 PH1 PL Fluortar, Leica EC2 Camera Driver 3.0.0.25, V00.70, in the Leica Application Suite Version 4.12.0, Build :86 (Leica Biosystems, Germany). Three biological replicates of three independent transgenic lines were used (Golden Promise, HvICE1:OE-5,6,8 and HvICE1:SRDX-2,3,6). Five images were taken of each imprint, spanning 2 cm^2 of leaf tissue. Images were processed in ImageJ 1.52a (National Institutes of Health, USA) (Schneider et al., 2012) to count the number of stomata to estimate stomatal density.

4.2.5 Stomatal conductance

Stomatal conductance was measured on the abaxial and adaxial sides of a mature and the top leaf developed in cold or control conditions. For each of the genotypes, wild type, HvICE1:OE and HvICE1:SRDX, three biological replicates from one independent transgenic line were used for each condition tested (Experiment 2C, Table 4.1). All measurements were carried out in the middle of the light period at 15˚C over 3 days with a SC-1 Leaf porometer, Decagon Device Inc. 2365 NE Hopkins Ct. Pullman, WA 99163 USA. The porometer was equilibrated to 15˚C for at least 30 min before the start of the sampling.

4.2.6 Gene expression

Relative gene expression analysis was carried out as specified in the general methods section (section 2.10). Absolute gene expression was calculated through the use of a standard curve of the C_t values obtained from RT-qPCR of *HvICE1-1* templates of known concentrations. The standard curve was generated by measuring the amplification rate of a dilution series of the *HvICE1-1* coding sequence from 0.1 ng/µl to $1x10^{-9}$ ng/µl. The template was amplified from cDNA before purification with PCR clean-up as in (section 2.4) and the concentration was determined with NanoDrop Spectrophotometer 2000 (Thermo Scientific). Using the molecular weight of the *HvICE1-1* coding sequence of 1572 bp with a molecular mass of 660 g/mol per base pair, the starting template concentration (C_o) was calculated for each DNA concentration (ng/µl) with Equation 4.1:

$$\log(C_o) = \frac{(ng/\mu l \times N_A)}{(1572 \times 660\, g/mol \times 10^9)}$$

Where C_o is the starting template concentration and N_A is Avogadro's number (6.022×10^{23}). The starting template concentration and the corresponding C_t value was plotted and a linear regression line was fitted to generate the standard curve as the reference for the absolute quantification of the *HvICE1-1* transcript (Figure 4.3). The equation of the linear regression line was used to calculate the quantity of *HvICE1-1* transcript in test samples.

Absolute expression was analysed in tissues collected from the wild type Golden Promise. Seeds were sterilised as in (section 2.1) before germination on filter paper for the collection of germinating embryos or in compost for remaining sampling. The stages sampled are

specified in Table 4.4 and includes root and leaf tissues from mature and developing plants as well as germinating embryos. Samples were collected and immediately frozen in liquid nitrogen. RNA extraction was carried out as described in section 2.8.

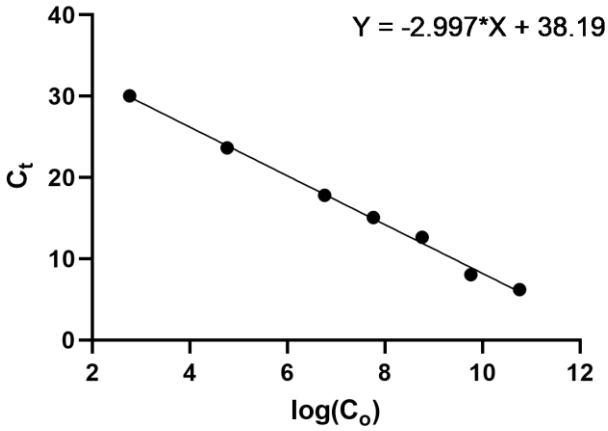

Figure 4.3. Standard curve for the quantification of HvICE1-1 *transcript in RT-qPCR. The template concentration was plotted against the corresponding C_t and a linear regression line was fitted with the slope equation displayed in the graph.*

Table 4.4. Collection of plant tissue for absolute expression analysis of HvICE1-1 *throughout the plant. Plants were grown at 15/12˚C with 16h photoperiod. Samples were immediately frozen in liquid nitrogen.*

Tissue	**Collection time after germination**
Root	
Seedling - 1 cm from seed, 3 roots/rep	6 days
Mature - 1-2 cm from tip	4 weeks
Tip from mature - 0-0.5 cm from tip	4 weeks
Shoot	
Developing shoot - 3 cm from coleoptile	2 weeks
Mature leaf - midsection of mature leaf	6 weeks
Seed	
4 day germinating embryo	4 days

4.3 Results

4.3.1 Expression of the *HvICE1-1* transcript and putatively interacting genes in wild type tissues in control conditions

4.3.1.1 Expression of *HvICE1-1* throughout the plant

From the expression pattern of the *HvICE1-1* transcript publicly available on BARLEX, *HvICE1-1* was identified as expressed in all tissues with a high level of transcript detected in the seedling leaf, developing inflorescence and developing grain (Figure 4.4A). To further investigate the *HvICE1-1* expression in the wild type Golden Promise (GP), additional tissues were analysed for the presence of *HvICE1-1* through analysis of the absolute expression in root and leaf tissue as well as germinating embryo. Tissues were collected from three biological replicates and the absolute expression of *HvICE1-1* was calculated based on the standard curve generated from the *HvICE1-1* template as described in section 4.2.6.

In the wild type under control conditions the *HvICE1-1* transcript was present in all tissue types tested, i.e. root tissue of seedlings, mature roots, root tips of mature plants, leaf tissue of developing shoots and of mature leaves, as well as germinating embryos. This level of expression of *HvICE1-1* in all tissues corresponds to the expression pattern previously reported in *Arabidopsis* where there is a low level of consistent expression of *ICE1,* possibly as a safeguard to enable a rapid cold response (Chinnusamy et al., 2003). A similar level of expression was found in the different root tissues investigated and in the germinating embryo but there was a higher expression in the developing leaf tissue compared to the mature leaf (Figure 4.4B).

4.3.1.2 Identification of HvICE1-1 putatively interacting genes

In barley three *HvICE1* homologs were identified, *HvICE1-1*, *HvICE1-2* and *HvICE1-3*, where *HvICE1-1* was predicted to be the best candidate as the *ICE1* orthologue, and *HvICE1-2* as a possible *ICE2* candidate (Chapter 3). *HvICE1-3* shared a high gene identity with *HvICE1-1* and was not investigated since it was not possible to distinguish between the proteins (Chapter 3, Figure 3.9). To study the effect of the differential expression level of *HvICE1-1 in planta* and its effect on other genes, the genes known to interact with *ICE1* in *Arabidopsis* were identified and putative orthologues were detected in barley using bioinformatic approaches as described in section 3.2.1 and 3.2.2. Putative orthologues in barley of genes of interest were identified through BLAST analysis of the *Arabidopsis* and rice orthologues to the barley genome. The gene sequences with the highest gene identity to the *Arabidopsis* and rice orthologues were selected.

In *Arabidopsis* the main regulators of *ICE1* were identified to be *HOS1*, which represses *ICE1*, and *SIZ1*, which is required for the activation of *ICE1* (Dong et al., 2006; Miura et al., 2007). In barley only one orthologue (HORVU.MOREX.r2.4HG0284290.1, HvHOS1) was found for HOS1 and OsHOS1 (Table 4.5). For SIZ1 and OsSIZ1, the best barley orthologue candidate was HORVU.MOREX.r2.1HG0010970.1, HvSIZ1 (Table 4.6). OST1 is needed for the activation of ICE1 through phosphorylation (Ding et al., 2015) however it was not possible to detect an orthologue in barley and it could not be investigated in the HvICE1-1 lines.

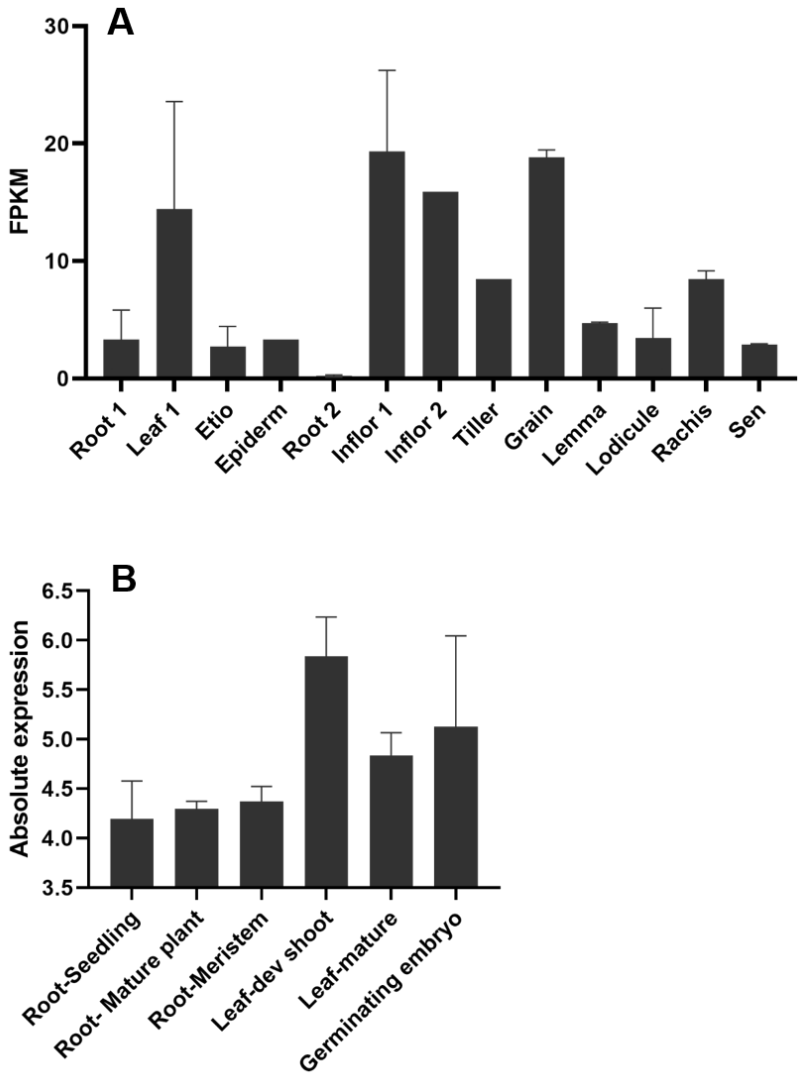

Figure 4.4. Expression profile of HvICE1-1*. A. Quantitative expression of* HvICE1-1 *(*HORVU.MOREX.r2.7HG0583410.1*) throughout the plant obtained from BARLEX, and B. of absolute expression in additional tissues.* HvICE1-1 *show a level of expression in all tested tissues with an elevated level in leaf seedling, developing inflorescence and developing grain. Absolute expression of* HvICE1-1 *confirms an elevated expression level in leaf tissue of the seedling with a constant expression in root tissues. FPKM = Fragments per kilo base of transcript per million mapped fragments. Root 1: Roots from seedlings (10 cm shoot stage), Leaf 1: Shoots from seedlings (10 cm shoot stage), Etio: Etiolated seedling, Epiderm: Epidermal strips, Root 2: Mature roots, Inflor 1: young developing inflorescence (5mm), Inflor 2: Developing inflorescences (1-1.5 cm), Tiller: Developing tillers, 3rd internode, Grain: Developing grain, Lemma: Inflorescences, lemma, Lodicule: Inflorescences, lodicule, Rachis: Inflorescences, rachis, Sen: Senescing leaves.*

Table 4.5. BLAST analysis of HOS1 *orthologues. The confirmed gene in* Arabidopsis *(*AtHOS1*) and the orthologue in rice (*OsFAMA*) predicted through EnsemblPlants, were used to identify a putative orthologue in barley.* HORVU.MOREX.r2.4HG0284290.1 *(marked in green) was identified as the only orthologue to* AtHOS1 *and* OsHOS1*.*

	Ranking	Best barley candidate	Percentage of identical matches	Alignment length
AtHOS1	1	HORVU.MOREX.r2.4HG0284290.1	47.059 %	714
OsHOS1	1	HORVU.MOREX.r2.4HG0284290.1	75.966 %	932

Table 4.6. BLAST analysis of SIZ1 *orthologues. The confirmed gene in* Arabidopsis *(*AtSIZ1*) and the orthologue in rice (*OsSIZ1*), were used to identify a putative orthologue in barley.* HORVU.MOREX.r2.1HG0010970.1 *was identified as the best orthologue to* AtSIZ1 *and* OsSIZ1*.*

	Ranking	Best barley candidate	Percentage of identical matches	Alignment length
AtSIZ1	1	HORVU.MOREX.r2.1HG0010970.1	51.631 %	889
	2	HORVU.MOREX.r2.3HG0275680.1	47.727 %	836
	3	HORVU.MOREX.r2.5HG0385900.1	48.459 %	714
OsSIZ1	1	HORVU.MOREX.r2.1HG0010970.1	79.585 %	867
	2	HORVU.MOREX.r2.3HG0275680.1	54.588 %	850
	3	HORVU.MOREX.r2.3HG0275680.1	49.206 %	63

In addition, two putative downstream genes, *HvCBF3* and *HvFAMA*, were selected for gene expression analysis. *HvCBF3* has been shown to be involved with cold tolerance and in *Arabidopsis CBF3* is directly activated by *ICE1*, which made this gene an interesting target for the investigation of *HvICE1-1* interactions (Chinnusamy et al., 2003; Choi et al., 2002). Among the genes involved with stomatal formation, *SPCH*, *MUTE*, and *FAMA*, the *HvFAMA* was selected for analysis in the HvICE1-1 lines as the *FAMA* orthologue is involved in the last step of stomatal formation and might be affected in stomatal formation defects (Kanaoka et al., 2008). *FAMA* and the predicted rice orthologue, *OsFAMA*, were used to identify *HORVU.MOREX.r2.1HG0058670.1* as the best candidate *HvFAMA* (Table 4.7).

Table 4.7. BLAST analysis of FAMA *orthologues. The confirmed gene in* Arabidopsis *(*AtFAMA*) and the orthologue in rice (*OsFAMA*) predicted through EnsemblPlants, were used to identify a putative orthologue in barley.* HORVU.MOREX.r2.1HG0058670.1 *(marked in green) was identified as the best orthologue to* AtFAMA *and* OsFAMA*.*

	Ranking	Best barley candidate	Percentage of identical matches	Alignment length
AtFAMA	1	HORVU.MOREX.r2.1HG0058670.1	48.157 %	407
	2	HORVU.MOREX.r2.4HG0338430.1	45.045 %	222
	3	HORVU.MOREX.r2.6HG0501920.1	43.220 %	236
OsFAMA	1	HORVU.MOREX.r2.1HG0058670.1	68.564 %	404
	2	HORVU.MOREX.r2.4HG0338430.1	46.614 %	251
	3	HORVU.MOREX.r2.6HG0514270.1	45.783 %	249

4.3.1.3 Expression of HvICE1-1 putatively interacting genes in HvICE1:OE and HvICE1:SRDX lines

To investigate the impact of the overexpression of *HvICE1-1* and the SRDX-tagged *HvICE1-1* transcript the gene expression of HvICE1-1 putatively interacting genes was analysed in leaf tissue of the HvICE1-1 lines as well as the wild type. The gene expression was analysed by RT-qPCR in seedling leaf tissue of plants grown in control conditions at 15˚C, with three biological replicates per line and three independent transgenic lines for HvICE1:OE (OE-5, OE-6 and OE-8) and HvICE1:SRDX (SR-2, SR-3 and SR-6).

As expected the *HvICE1-1* transcript was increased in the HvICE1:OE and HvICE1:SRDX lines as the RT-qPCR primers amplified all expression of the *HvICE1-1* transcript, including the transcript with the SRDX tag. This confirms that the transgenes were expressed. The expression of the *HvICE1-2* orthologue however was not significantly different in any of the lines suggesting that the level of *HvICE1-1* does not affect the expression of *HvICE1-2*.

Interestingly, there was no significant difference in the level of *HvHOS1*, *HvSIZ1*, *HvCBF3* or *HvFAMA* in any of the lines tested (Figure 4.5). Most surprising was the lack of effect on the putatively downstream gene *HvCBF3*. In *Arabidopsis ICE1* binds to the promoter of *CBF3* and activates its expression however an intricate regulatory pathway including *OST1*, *HOS1* and *SIZ1* is required for the induction of *CBF3* (Chinnusamy et al., 2003; Ding et al., 2015; Miura et al., 2007). Previous work has also shown that *HvCBF3* is not detectable at optimal growth conditions and requires stimuli such as cold or mechanical agitation for its expression (Choi et al., 2002).

A possible explanation for this lack of induction of putatively *HvICE1-1* interacting genes could be that *HvICE1-1* is not sufficient to initiate long term effects on these genes, but rather requires interactions with other proteins to induce changes in these genes. It is also possible that *HvICE1-1* affects other genes not tested or that the interactions of *ICE1* is not conserved in the putative signalling pathway in barley. It is however interesting to evaluate

the effect of differential expression of *HvICE1-1* on physiological qualities in barley and the level of cold response.

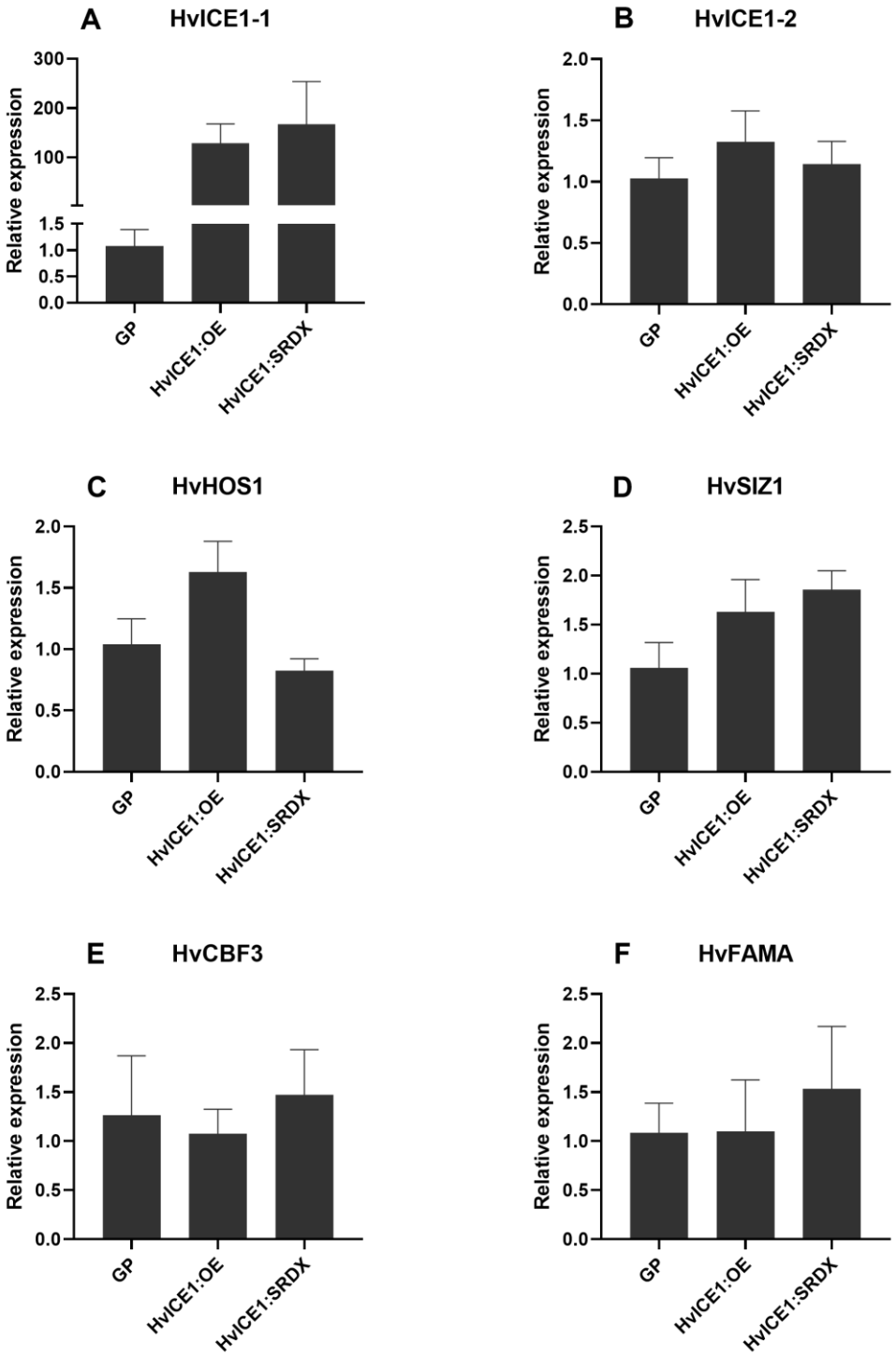

Figure 4.5. Gene expression of HvICE1-1 *and HvICE1-1 putatively interacting genes in wild type (GP), HvICE1:OE, and HvICE1:SRDX lines in control conditions. The* HvICE1-1 *transcript was significantly increased in both transgenic lines however no difference were found for the other genes in the HvICE1:OE and HvICE1:SRDX lines. Error bars = SEM.*

4.3.2 General physiology and seed germination of HvICE1-1 transgenic lines

Several generations of transgenic lines were studied to determine the effect of SRDX silencing or overexpression of *HvICE1-1*. The T0 generation of the HvICE1:OE and HvICE1:SRDX were grown in the early summer of 2020, preventing detailed phenotyping of a variety of traits due to restricted access to growth facilities as a consequence of COVID-19.

The HvICE1:OE and HvICE1:SRDX plants were genotyped to ensure the transgenes were maintained as described in Chapter 3 (section 3.3.4). The expression of the HvICE1:OE and HvICE1:SRDX constructs in the respective transgenic lines were verified in Chapter 3 (section 3.3.4) where transgenic lines genotyped as positive for the transgene also displayed an increased level of the *HvICE1-1* transcript and were therefore considered as expressing the construct of interest.

In the T0 generation anther length and pollen viability was investigated with no detectable difference between the HvICE1-1 lines and the wild type Golden Promise. For the silencing genotype seed set data was only available for HvICE1:SRDX-1 and -6 in the T0 generation with both lines showing a reduction in seed set and seed size (Figure 4.6). In the T0 generation only the HvICE1:OE-2 line showed a reduction in seed set of the nine overexpression lines produced. It is worth mentioning that the T0 generation might not be indicative of the behaviour of the transgenic lines as it is generated from calluses from immature embryos.

4.3.3 Seed set of HvICE1:OE and HvICE1:SRDX generations

Seed set was investigated in subsequent generations in individual experiments to study the effect of abiotic stresses on seed set in the HvICE1 transgenic lines. HvICE1:SRDX consistently showed no reduction in seed set but the HvICE1:OE lines differed occasionally in control conditions, mostly due to high degree of variation within the population. In an effort to improve the comparisons between wild type and HvICE1-1 OE and SRDX lines the seed set from all experiments were combined. To account for variance between growth conditions the seed set was given as percentage of the wild type within the experiment. Here there was a clear decrease in seed set in HvICE1:OE lines (p-value 0.0016) but no difference for the HvICE1:SRDX lines (Figure 4.7). The number of tillers for the lines were counted in each experiment where HvICE1:OE had on average only 72% of the tillers of the wild type whereas HvICE1:SRDX lines had 102%. The reduction in seed set seen for the HvICE1:OE was most likely due to a reduction in number of tillers formed. In addition the date to heading was measured in the T1 generation where the HvICE1:OE lines were 1-2 weeks later than GP however no other physiological differences were detected.

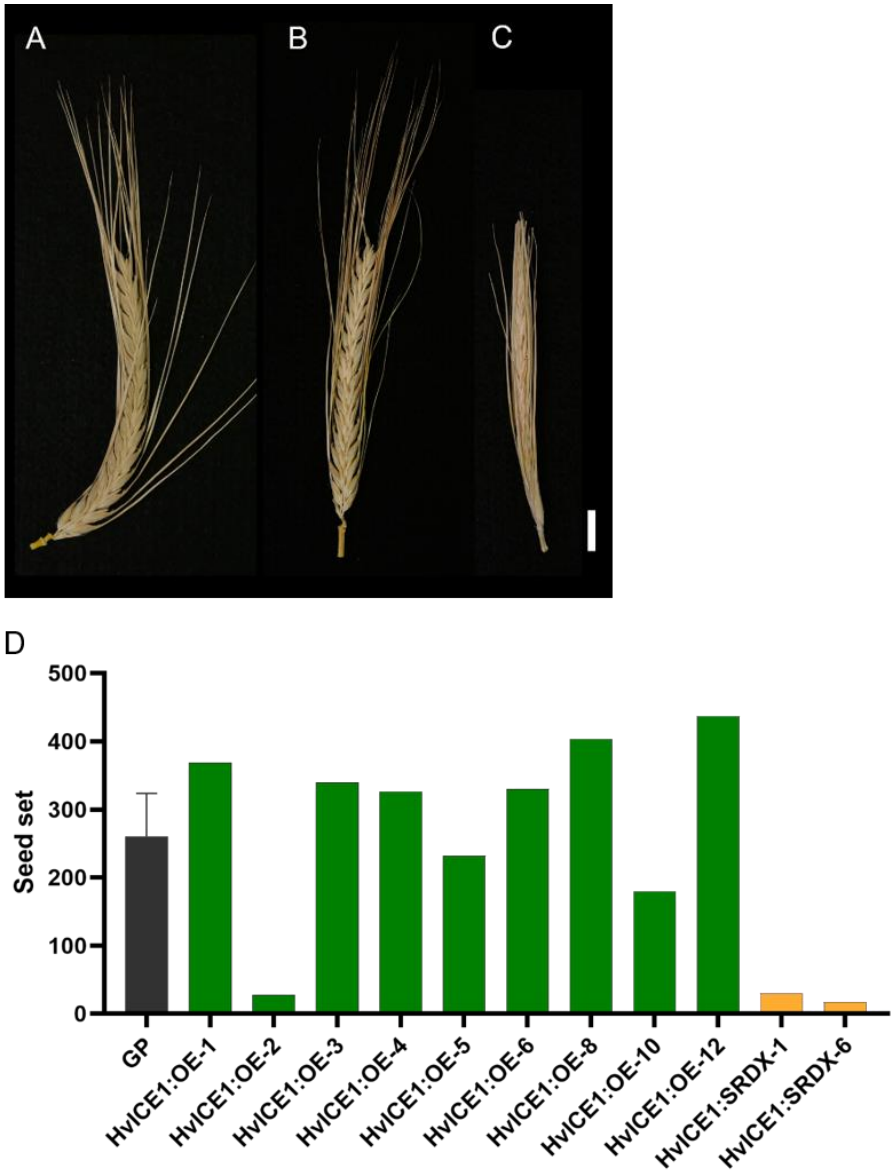

Figure 4.6. Spikes of the fully fertile Golden Promise (A), and the T0 generation of the partially sterile HvICE1:OE-2 (B) and HVICE1:SRDX-6 (C). (D) Seed set of HvICE1:OE-2 and HvICE1:SRDX-1 and -6 was markedly reduced compared to the wild type whereas no difference was found for HvICE1:OE-5 and -10. Scale bar = 1cm.

4.3.4 Seed germination of HvICE1 transgenic seeds

In *Arabidopsis ICE1* has been shown to interact with *ABSCISIC ACID INSENSITIVE5*, to regulate seed germination where ICE1 promotes germination by supressing abscisic acid signalling (Hu et al., 2019). The loss of function mutant *ice1* showed ABA hyposensitivity with a reduced germination rate (Hu et al., 2019). To test whether *HvICE1-1* could affect seed germination in barley, seeds from HvICE1:SRDX and HvICE1:OE T0 generation were compared to the germination rate of the wild type. Silencing of *HvICE1-1* was hypothesised to decrease germination rates however all genotypes had a high degree of germination, 95, 85 and 91% germination for wild-type, HvICE1:OE and HvICE1:SRDX, without any significant difference associated with the different levels of HvICE1 expression. Differential expression

of *HvICE1-1* in these lines does not appear to affect seed germination however it is possible that the transcription factor silencing function of the SRDX sequences is not a true equivalent of a *HvICE1-1* knock-out mutant.

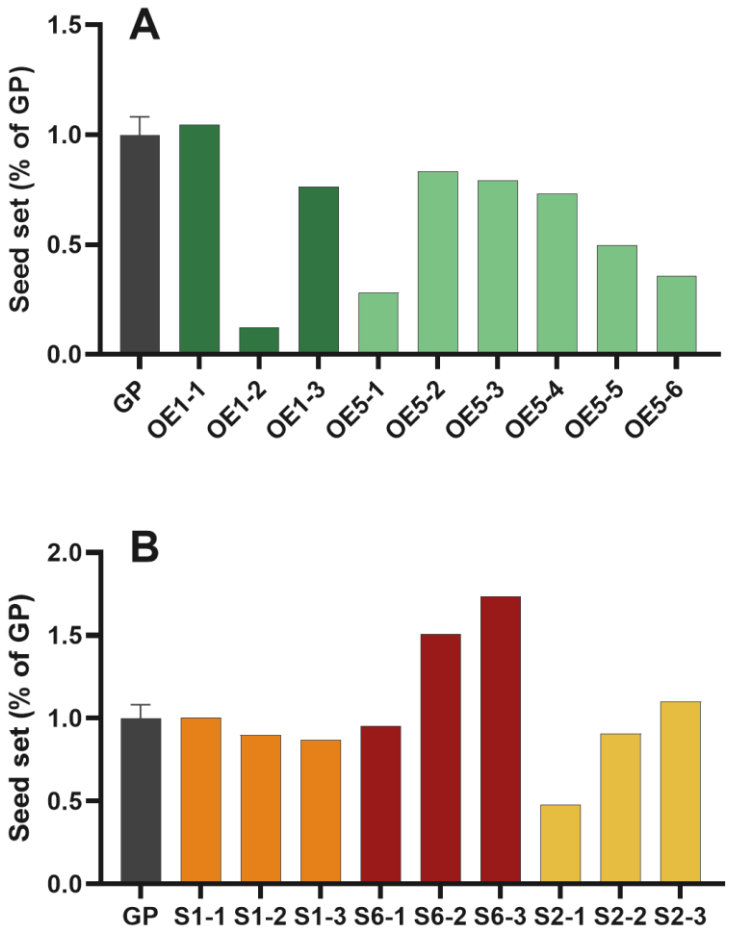

Figure 4.7. Seed set of HvICE1:OE (A) and HvICE1:SRDX (B) individual transgenic plants. Seed set was determined in the T1 generation of HvICE1:OE lines from plants of lines OE1 and OE5, and for HvICE1:SRDX lines from plants of the S1, S6 and S2 T1 generation. The seed sets are compared in multiple growth cycles and are given as percentage of the wild type seed set of the corresponding trial.

4.3.5 Stomatal density at different levels of *HvICE1-1* expression

To evaluate the effect of differential expression of *HvICE1-1* on stomatal formation in barley the number of stomata in mature leaf tissue was counted. Stomatal imprints of the abaxial and adaxial side were used to count the number of stomata at five sections of each leaf to estimate stomatal density of the leaf.

The stomatal density was reduced on the abaxial side for all HvICE1:OE and HvICE1:SRDX lines, however it was not significant for HvICE1:OE-5 (Table 4.8, Figure 4.8). In addition, there was a difference between the HvICE1-1 lines and the wild type in the ratio of stomatal density of the adaxial and abaxial side where the wild type had a higher stomatal density on the abaxial side whereas the opposite was true for the HvICE1 transgenic lines. The ratio of the number of stomata on the abaxial compared to the adaxial was significantly lower in the HvICE1:SRDX lines (ratio abaxial:adaxial of 1.13 and 0.78 for GP and HvICE1:SRDX respectively). It is possible that the silencing of *HvICE1-1* leads to a redistribution of the formation of stomata between the abaxial and adaxial side.

Table 4.8. Stomatal density of wild type (GP), HvICE1:OE and HvICE1:SRDX lines on the abaxial and adaxial leaf side. The stomatal density of each line was compared to the wild type using a Student t-test to estimate the effect of the independent line (T-test genotype). A minimum of 280 stomata were counted per line. Significant differences (p-values>0.05) are highlighted in green.

		Stomata/mm²	***No. counted***	***T-test genotype (p-values)***
Adaxial	GP	24.02	484	-
	HvICE1:OE-5	20.77	453	0.086
	HvICE1:OE-6	12.93	282	1E-06
	HvICE1:OE-8	18.62	406	0.031
	HvICE1:SRDX-2	13.66	298	5E-06
	HvICE1:SRDX-3	16.55	361	0.001
	HvICE1:SRDX-6	15.64	341	3E-04
Abaxial	GP	19.58	427	-
	HvICE1:OE-5	28.57	623	4E-04
	HvICE1:OE-6	16.28	355	0.024
	HvICE1:OE-8	23.07	503	0.08
	HvICE1:SRDX-2	18.43	402	0.491
	HvICE1:SRDX-3	21.28	464	0.281
	HvICE1:SRDX-6	19.35	422	0.89

4.3.6 Seedling survival during freezing stress

To investigate if overexpression or silencing of *HvICE1-1* could affect seedling survival during freezing stress, seedlings at 2-3 leaf stage were cold acclimated at 4˚C for 24 h before a freezing shock of -12˚C for 30 min. The seedlings were then returned to control conditions of 15/12˚C day night temperatures of 16 h photoperiod for 14 days before evaluation of survival and recovery. Three independent transgenic lines of HvICE1:OE and HvICE1:SRDX were used, as well as the wild type Golden Promise, with six biological replicates per line.

The wild type showed high survival, with five out of six plants surviving however recovery was slow and the average height of the seedlings decrease slightly (Figure 4.9). In contrast,

the HvICE1:OE lines exhibited 100% survival with HvICE1:OE-5 and HvICE:OE-6 recovering and showing more growth than the wild type. The HvICE1:OE-12 seedlings were slightly younger at the start of the cold treatment compared to the other lines which could have affected the reduced recovery seen in this line. The HvICE1:SRDX-1 seedlings had a survival rate of 60% with poor recovery and a seedling size smaller than prior to the cold treatment. However, the other HvICE1:SRDX seedlings, displayed 100% survival with recovery to pre-cold treatment seedling size, but was still shorter than the HvICE1:OE lines. It is possible that overexpression of *HvICE1-1* leads to increase cold tolerance and silencing of *HvICE1-1* results in cold sensitivity however the effects are not clear.

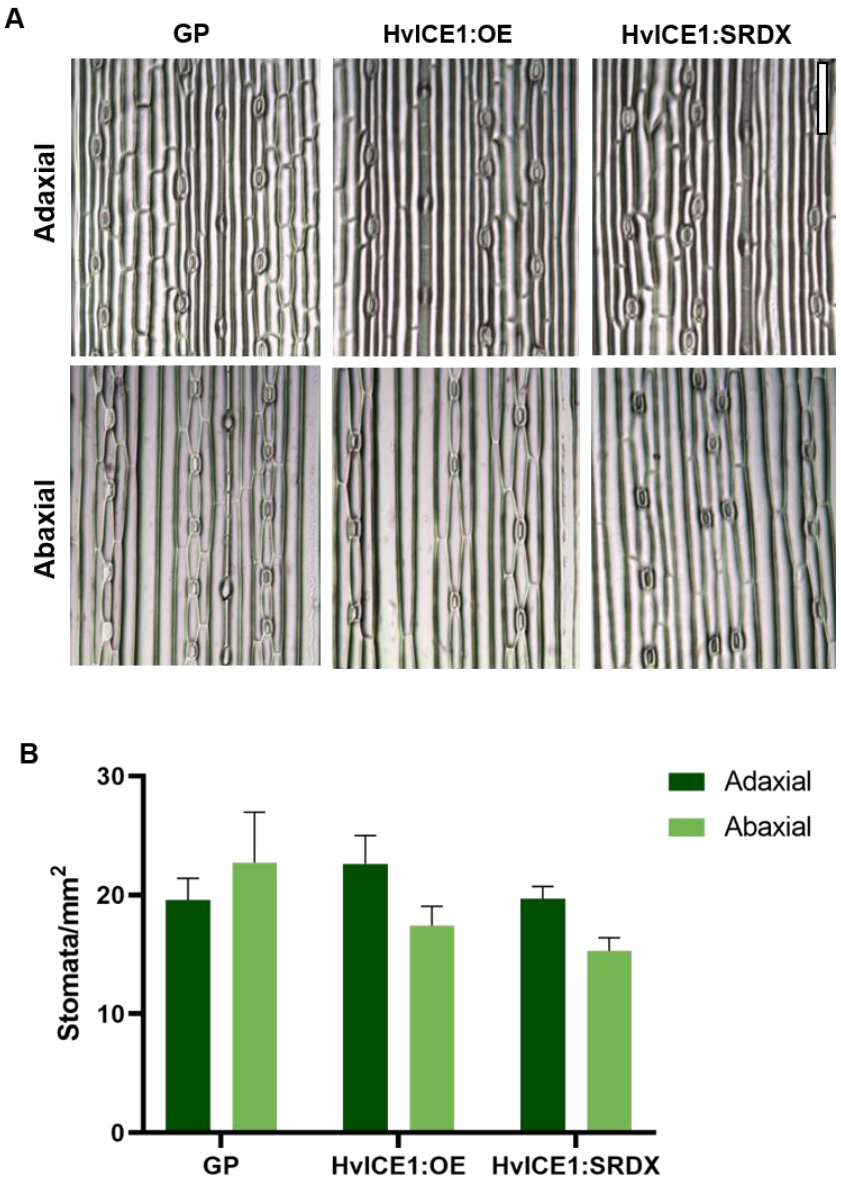

Figure 4.8. Stomatal pattern and density on the abaxial and adaxial side of the leaves of control, HvICE1:OE and HvICE1:SRDX lines. A. The stomatal patterning did not markedly differ between the lines although HvICE1:SRDX tended to have more stomata in double rows. B. The stomatal density on the abaxial side was reduced in all HvICE1 transgenic lines compared to the wild type. Both HvICE1:OE and HvICE1:SRDX lines had a higher stomatal density on the adaxial side compared to the abaxial side, a ratio not seen in the wild type. Scale bar: 200 µm

Figure 4.9. Seedlings of wild type, HvICE1:OE and HvICE1:SRDX lines before (A) and after (B) exposure to freezing stress of -12˚C for 30 min. Survival and recovery was estimated after 14 days in control conditions. The overexpression lines (images 1, 3, 5) showed 100% survival with great recovery for HvICE1:OE 5 and 6 however OE-12 showed more leaf damage. The HvICE1:SRDX lines (images 2, 4, 6) showed 100% survival of the HvICE1:SRDX-2 and -3 but -1 showed recovery of only 60% with poor recovery. The wild type (image 7) had 83% survival with good recovery. Scale bar in blue = 2 cm.

4.3.7 Effect of *HvICE1-1* on stomatal patterning and stomatal conductance under long term cold stress on seedlings

To investigate the function of *HvICE1-1* in barley, the transgenic lines with the overexpressing or silencing constructs were exposed to cold treatments at different developmental stages. The four cold experiments described in Table 4.1 will be considered separately due to differences in cold stress severity and duration.

4.3.7.1 Seed set of HvICE1:SRDX-1 not affected by cold treatment

The HvICE1-1 plants were subjected to a period of long mild cold stress, of 6˚C for 21 days, during seedling development to simulate a decrease in temperature in early development. In this experiment six biological replicates of one transgenic line per genotype were used. Due to constraints in growth rooms there was also a change in photoperiod between the treatments with control conditions of 16h/8h light/dark cycle and cold treatment at 12h light/dark cycle for the cold treatment.

After the cold treatment the seedlings were returned to control conditions for the remaining time of the growth cycle. Cold treated seedlings of all genotypes, including the wild type, displayed delayed growth compared to the control group and subsequently the heading date was delayed. Within the cold treated group the heading date was 2-7 days later for both HvICE1:OE-5 and HvICE1:SRDX-1 lines compared to the wild type.

Total seed set and fertility was determined by counting the number of fertile and sterile spikelets per spike, of all spikes for each plant. Long term cold treatment resulted in a decrease in seed set in the wild type, mainly due to a reduction in number of tillers, with a smaller decrease in fertility (p-values seed set: 0.003 and fertility: 0.024) (Table 4.9). The HvICE1:OE-5 plants displayed a reduction in seed set compared to wild type under both normal conditions and cold treatments but no difference was found between the treatments (Table 4.9, Figure 4.10). The spikelet fertility of all genotypes was reduced after a period of cold stress but the HvICE1:OE-5 plants had a significantly lower fertility than the wild type. This effect was not seen in the HvICE1:SRDX-1 plants were there was no difference in seed set between the growth conditions, or compared to the wild type in control conditions. Despite the reduction in fertility for HvICE1:SRDX-1 between the growth conditions there was no difference in total seed set for this genotype, which can be attributed to an increased number of tillers. It is possible that the silencing of *HvICE1-1* results in some degree of cold tolerance in terms of fertility whereas a constant overexpression of *HvICE1-1* inhibits seed set.

To further investigate the effect of *HvICE1-1* on cold tolerance in relation to seed set a shorter cold treatment was carried out during spike development. From 15˚C control conditions the plants were exposed to three days of 6˚C to simulate a cold snap during early flowering. No difference was seen in seed set between the genotypes in different conditions. It is possible that the cold treatment was not sufficient to induce any changes in fertility.

Table 4.9. Comparisons of the seed set and spikelet fertility of the HvICE1 lines and the wild type Golden Promise (GP) in control and cold conditions. The overexpression and silencing lines were compared to GP within each treatment group to determine the effect of the genotyped, and each genotype was compared between the two treatments to determine the effect of the treatment. Comparisons were carried out with the student t-test and p-values smaller than 0.05 are highlighted in green.

Conditions	Lines compared	p-value	
		Seed set	Fertility
Control	GP to HvICE1:OE-5	0.013	0.024
	GP to HvICE1:SRDX-1	0.408	0.330
Cold treated	GP to HvICE1:OE-5	0.021	8×10^{-4}
	GP to HvICE1:SRDX-1	0.107	0.637
Control vs. Cold treated	GP	0.003	0.024
	HvICE1:OE-5	0.271	0.036
	HvICE1:SRDX-1	0.771	0.003

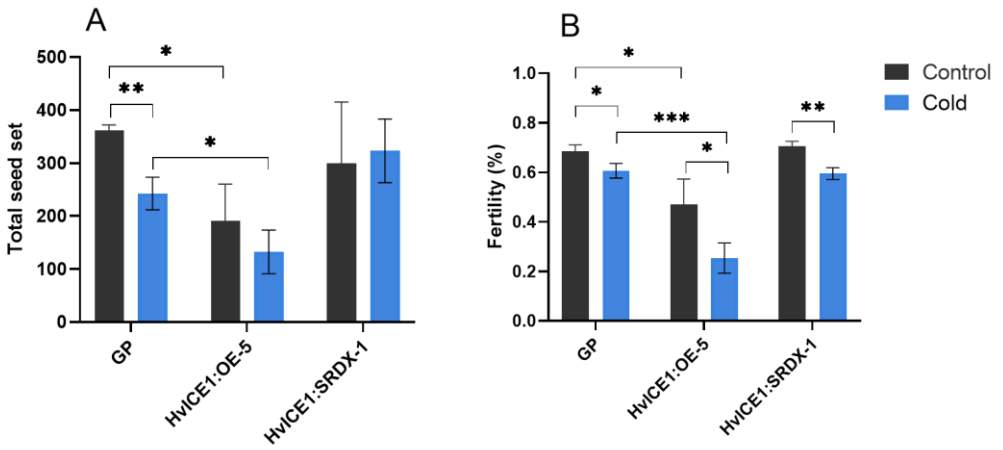

Figure 4.10. Total seed set and spikelet fertility in long term cold stress at seedling stage compared to control conditions. Seed set was reduced in the wild type (GP) after the cold stress and in both conditions of HvICE1:OE-5 however there was no reduction in the HvICE1:SRDX-1 plants. The spikelet fertility was determined by counting the number of fertile and sterile spikelets per spike. Fertility was reduced in all genotypes after cold treatment however only HvICE1:OE showed a reduction in fertility in comparison to the wild type.

4.3.7.2 Stomatal density is reduced after long term cold treatment

To test the effect of *HvICE1-1* on stomatal formation, the stomata were studied in leaves developed at 6˚C in the HvICE1:OE-5 and HvICE1:SRDX-1 lines in comparison to the wild type. Stomatal imprints covering 2 cm^2 of the middle section of young leaves were used to count the number of stomata on the abaxial and adaxial leaf sides. Five images of each imprint were taken at representative regions, covering 7.3 mm^2 with 351-617 stomata counted for each sample group (Table 4.10).

After the long-term cold treatment stomatal density was markedly reduced in all genotypes on both the abaxial and the adaxial side but no differences were found between the genotypes (Table 4.10, Figure 4.11). In this experiment there was no significant difference in the stomatal density between the abaxial and adaxial side, in contrast to earlier experiments. Only HvICE1:SRDX-1 plants had a significantly increased stomatal density compared to the wild type under cold treatment but HvICE1:SRDX in control conditions and HvICE1:OE in both treatment groups displayed similar trends. An explanation for the difference in the outcome of the stomatal density between the experiments could be the reduced number of samples and that only one transgenic line per genotype was used in this experiment, reducing the statistical significance of any effects.

Table 4.10. Stomatal density on the adaxial and abaxial side of wild type (GP), HvICE1:OE-5 and HvICE1:SRDX-1 under control and cold treatment. 367-617 stomata were counted per line in a comparable area to estimate the stomatal density. The stomatal densities of HvICE1:OE-5 and HvICE1:SRDX-1 were compared to the wild type for the respective treatment (T-test genotype) to estimate the effect of the genotype. Stomatal density was also compared between the treatments for each genotype to determine the effect of the treatment (T-test treatment) where all lines showed a reduction in stomatal density after cold stress.

	Treat-ment	***Genotype***	***Stomata /mm²***	***No. counted***	***T-test genotype***	***T-test treat-ment***
Adaxial		GP	26	567		
	Control	HvICE1:OE-5	27.56	601	0.101	
		HvICE1:SRDX-1	28.29	617	0.031	
		GP	17.88	390		6.88E-07
	Cold	HvICE1:OE-5	19.90	434	0.092	1.37E-06
		HvICE1:SRDX-1	19.95	435	0.079	2.28E-07
Abaxial		GP	23.89	521		
	Control	HvICE1:OE-5	23.98	523	0.092	
		HvICE1:SRDX-1	23.62	515	0.079	
		GP	16.10	351		2.23E-07
	Cold	HvICE1:OE-5	16.83	367	0.465	7.02E-08
		HvICE1:SRDX-1	18.02	393	0.102	6.89E-05

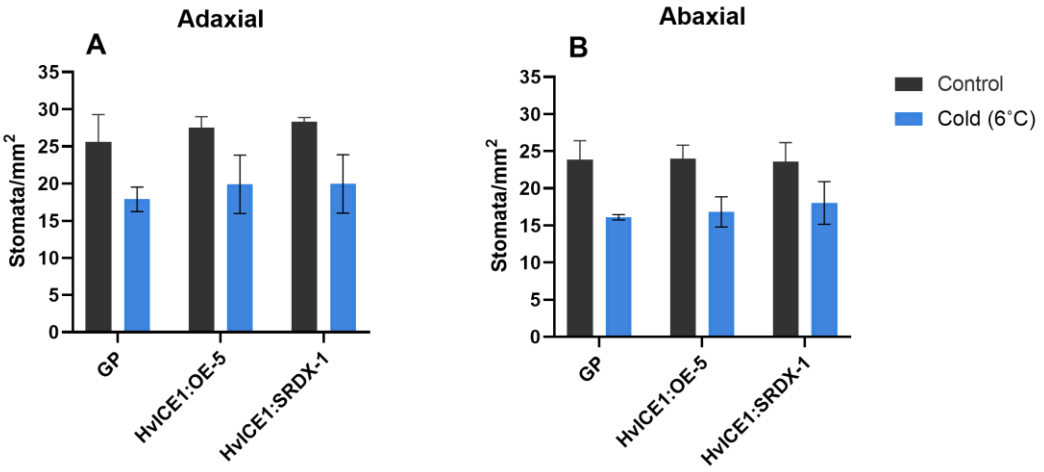

Figure 4.11. Stomatal density of wild type (GP), HvICE1:OE-5 and HvICE1:SRDX-1 on the adaxial (A) and abaxial (B) side of leaf grown in control conditions or at 6°C cold stress. All lines showed a significant decrease in stomatal density on the adaxial and abaxial leaf side at 6°C compared to plants grown in control conditions.

4.3.7.3 Stomatal conductance is reduced in HvICE1:OE-5 in control conditions

Stomatal conductance was measured to analyse the stomatal function in the HvICE1-1 lines and to determine any effects of differential expression of HvICE1-1 lines during cold treatment. The stomatal conductance was measured on the abaxial and adaxial side of a young leaf fully developed in either control conditions or under cold treatment. Measurements were taken in the middle section of young leaves once per day for three days in the middle of the light cycle on plants grown in either control or in three weeks of +6˚C. All plants were measured in control conditions to avoid potential differences in stomatal opening due to differing humidity levels of the growth rooms.

In all lines tested, HvICE1:OE-5, HvICE1:SRDX-1, and wild type, the stomatal conductance on the adaxial side was higher compared to the abaxial side in both treatments (Figure 4.12). On the abaxial side of the leaves there was no difference in stomatal conductance between the lines for either growth condition. Stomatal conductance was however lower on the adaxial side of the HvICE1:OE-5 plants in control conditions compared to the wild type (p-value 0.011) but this effect was not seen in the cold treated plants. Since no difference was seen in stomatal density between HvICE1:OE-5 and the wild type, the difference in stomatal conductance in control conditions could be due to the degree of openness of the stomata. Stomatal opening and closing is a mechanism employed by plants to rapidly protect against external stresses such as changes in temperatures (Franks & Farquhar, 2007) and might explain the difference seen in HvICE1:OE-5. Again, only one transgenic line per genotype was used but these results indicate that there might be an effect of *HvICE1-1* on stomatal formation and function.

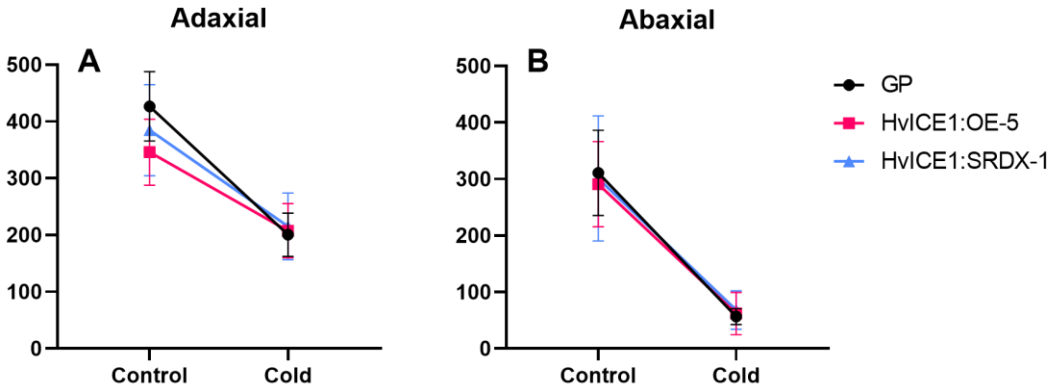

Figure 4.12. Stomatal conductance in HvICE1:OE-5, HvICE1:SRDX-1, and wild type in control and cold treated plants. Conductance was measured over three days on the adaxial (A) and abaxial (B) side of a three biological replicates of young leaves developed in the respective growth condition. No difference was found between the lines in the different conditions except for HvICE1:OE-5 which displayed a lower conductance under control conditions than the wild type.

4.3.7.4 Gene expression of *HvICE1-1* related genes under long cold stress in leaf tissues

The expression of genes potentially affected by *HvICE1-1* were investigated in the long-term cold treated seedlings to determine any effect of the HvICE1-1 lines in control or long term cold acclimated plants. Leaf tissue in the cold treated seedlings was collected after 21 days of cold acclimation at +6˚C, 5 days of 15˚C control conditions, and another 24 h of +6˚C to induce cold response. Expression of *HvICE1-1*, *HvICE1-2*, *HvHOS1*, *HvSIZ1*, *HvCBF3*, and *HvFAMA* was analysed to see potential effects of *HvICE1-1* overexpression and silencing under long term cold treatment. Three biological replicates for HvICE1:OE-5, HvICE1:SRDX-1 and the wild type were used for each treatment, and the expression of the genes of interest were normalised to two reference genes and to the wild type in control conditions.

In the wild type the expression of *HvICE1-1* was significantly reduced after 24 h of cold treatment, with a decrease of 58.5%. As expected, in both the HvICE1:OE-5 and HvICE1:SRDX-1 plants there was a significantly higher expression level of the *HvICE1-1* transcript but there was not a significant increase after cold stress due to the level of variation in the samples (Figure 4.13A). Previous studies of *ICE1* orthologues have found an upregulation of *ICE1* in *Arabidopsis* after 2 h of 0˚C cold stress, and an upregulation of *OsICE1* after 8h of 4˚C (Chinnusamy et al., 2003; Verma et al., 2020). In barley, the putative *ICE1* downstream target, *HvCBF3*, was upregulated after 15 min but was no longer elevated after 24 h indicating that *HvCBF3* expression is no longer being induced (Choi et al., 2002). It is possible that the *HvICE1-1* transcript is no longer elevated after 24 h of cold stress which is why no induction was seen in the cold treated plants.

Here, there was no difference in the expression of the *HvICE1-1* putative homolog *HvICE1-2* in any of the lines or growth conditions suggesting that *HvICE1-2* is not affected by the expression of *HvICE1-1* or that any cold induced differences in *HvICE1-2* expression could not be detected after 24h (Figure 4.13B).

To further investigate the cold response in the wild type and the HvICE1-1 transgenic lines the potential *HvICE1-1* regulators *HvHOS1* and *HvSIZ1* were investigated. It was not possible to detect a change in *HvHOS1* expression between the control and cold treated plants in the wild type and the HvICE1:SRDX-1 plants due to the level of variation in the samples, however in the HvICE1:OE-5 seedlings there was a significant reduction of *HvHOS1* in the cold stressed plants (Figure 4.13C). The expression of *HvSIZ1* appeared to be reduced in the cold treated plants however the difference was not significant (Figure 4.13D). The overall expression of *HvSIZ1* under control conditions was significantly reduced in the HvICE1:OE-5 plants but this could not be determined for the HvICE1:SRDX-1 plants.

In *Arabidopsis HOS1* acts as a repressor of *ICE1* under normal growth conditions, but is prevented from interacting with *ICE1* during cold stress although its expression is not reduced (Dong et al., 2006; Miura et al., 2007). A similarly controlled regulation could be in place in for the *HvICE1-1* and *HvHOS1* putative orthologues, however detailed molecular studies are needed to confirm the direct interaction of the proteins.

SIZ1 in *Arabidopsis* activates *ICE1* through sumoylation in response to cold but similar to *HOS1*, its expression is not affected by cold treatment (Miura et al., 2007). In the HvICE1:OE-5 plants the initial level of *HvSIZ1* suggests a reduction in expression however it was not possible to determine a further reduction in the cold treated seedlings.

It is possible that the regulation of *HvICE1-1* by the putative regulators *HvHOS1* and *HvSIZ1* is not dependent on expression levels but rather on post transcriptional modifications. The trends seen in this cold stress experiment need to be further confirmed with additional transgenic lines and with further cold stress inductions to determine the short-term effect of cold stress on barley seedlings.

4.3.7.5 *HvICE1-1* putative downstream targets

The *HvCBF3* expression was analysed in all lines and growth conditions, however the lack of reproducibility between the samples prevented any detailed analysis of the expression. Interestingly, for the putative stomatal formation gene *HvFAMA*, all lines showed a decrease in *HvFAMA* transcript after 24 h of cold treatment, independent of the level of *HvICE1-1* (Figure 4.13E).

From the gene expression analyses of the *HvICE1-1* related genes in long term cold treated plants it was hypothesised that *HvICE1-1* influences the expression of *HvHOS1* and *HvSIZ1* however no significant effects were found for *HvICE1-2* under these growth conditions. In addition, *HvFAMA* appeared to be repressed after cold treatment.

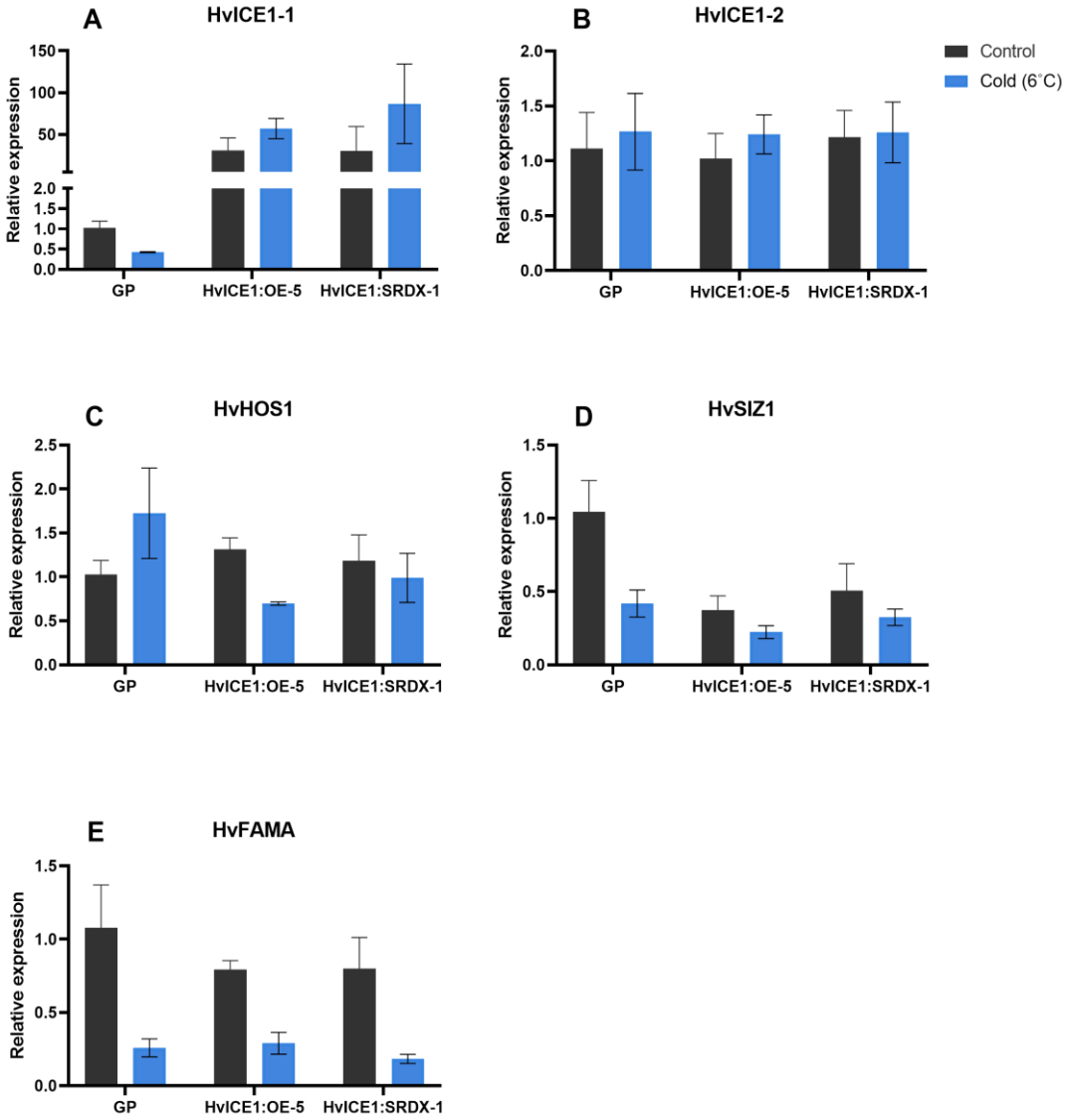

Figure 4.13. Relative gene expression as measured by RT-qPCR in leaf tissue after long term cold stress. Each line and gene was normalised to two reference genes and to the wild type of the control treatment with three biological replicates of one transgenic line. A. The expression of HvICE1-1 *was elevated in both HvICE1-1 lines and a decrease was seen in the wild type after cold treatment. B. No difference was found for* HvICE1-2 *in any condition. C. The expression of* HvHOS1 *was reduced in non-cold stressed HvICE1:OE-5 plants but no other effect was seen. D. The expression of* HvSIZ1 *was reduced in the control conditions of HvICE1:OE-5 compared to the wild type however no other differences were significant. E.* HvFAMA *was reduced in response to cold in both HvICE1-1 lines. Error bars = SEM.*

4.3.8 The effect of a short chilling stress on *HvICE1-1* overexpression and silencing seedlings

The effect of overexpression and silencing of *HvICE1-1* on barley was further investigated by exposing seedlings to a short period of chilling stress. Seedlings were grown in control conditions until the 2-3 leaf stage when they were exposed to 0-3˚C for 24 h to simulate a cold snap at seedling stage. Gene expression analysis was carried out on leaf tissue collected after 0 h, 30 min and 2 h of cold stress and photosynthesis measurements were carried out after a period of recovery to identify any differences in photosynthetic capacity between the lines. Here, three biological replicates of three independent transgenic lines for each genotype were used.

4.3.8.1 Gene expression analysis in chilling stressed seedlings

Similar to the expression analysis carried out on the HvICE1-1 transgenic lines under a long-term cold stress the gene expression of putative *HvICE1-1* interacting genes were investigated after a short period of chilling stress. The expression of the genes of interest were analysed in three independent transgenic lines as an average of three biological replicates to determine if the independent lines displayed similar trends in gene expression (Figure 4.14). Comparable trends in gene expression in response to cold treatment was seen for most independent lines, however variations in the biological replicates within the transgenic lines decreased the statistical significance of detected differences in some of the individual transgenic lines (Figure 4.14). In the following analysis the independent transgenic lines of the HvICE1:OE and HvICE1:SRDX genotypes are considered together to visualise trends of the different genotypes and any deviations in the independent lines are noted (Figure 4.15). For each time point the same set of plants were sampled to compare the effect of the cold treatment on individual plants. The expression of each gene was normalised to two reference genes, *HvTub* and *HvHSP70*, and to the expression of the wild type in control conditions.

4.3.8.2 The expression of the *HvICE1-1* and *HvICE1-2* homologs in cold stressed seedlings

The expression of *HvICE1-1* was analysed in the cold stressed plants to determine the level of cold induced expression and to detect any overexpression of *HvICE1-1* or expression of the SRDX-tagged *HvICE1-1* transcript. In the long-term cold stress on seedlings the level of *HvICE1-1* was reduced after 24 h of cold treatment in the wild type however no difference was found after 30 min or 2 h of cold stress, possibly due to the level of variation in the samples (Figure 4.15A). The level of *HvICE1-1* in the HvICE1:OE and HvICE1:SRDX lines was, as expected, significantly higher compared to the wild type in the control and the two cold treatments. The expression of *HvICE1-1* was not significantly altered after 30 min of cold stress in the HvICE1:OE but was markedly reduced after 2 h. It was however not possible to detect a significant difference in *HvICE1-1* level between the treatments in the HvICE1:SRDX lines, similar to the trends in the wild type (Figure 4.15A).

These results in addition to the trends seen in the long term cold stress experiment suggests that *HvICE1-1* in the wild type is not initially affected but might be reduced after a longer period of cold stress. It is also evident that the *HvICE1-1* expression is highly elevated in the

HvICE1:OE and HvICE1:SRDX lines however the regulation of *HvICE1-1* in response to cold requires further studies.

The *HvICE1-2* was identified as a homolog to *HvICE1-1* and a potential orthologue of *ICE2*, a gene which can induce cold response through the activation of downstream *CBF* genes (Kim et al., 2015). In the long-term cold stress no difference in *HvICE1-2* expression was found in any line under any growth condition, but after 30 min of cold stress a potential increase of *HvICE1-2* was found in the wild type but with a lot of variation in the transcript level (Figure 4.15B). In the HvICE1-1 transgenic lines the *HvICE1-2* expression did not change significantly but compared to the wild type the HvICE1:OE showed a significantly lower level of *HvICE1-2* after 30 min of cold stress. It is possible that the increased level of the *HvICE1-1* transcript in the HvICE1:OE lines affects the rapid cold response of *HvICE1-2.* Further studies are needed to determine the specific interaction of *HvICE1-1* and *HvICE1-2* in the cold signalling pathway.

4.3.8.3 Effect of *HvICE1-1* on putatively interacting genes under a short chilling stress

To study the regulation of *HvICE1-1* under a short chilling stress the putative orthologues of two of the major *HvICE1-1* regulators, *HvHOS1* and *HvSIZ1*, were analysed in relation to *HvICE1-1* in the short chilling stress.

In the wild type the expression of *HvHOS1* was not significantly altered after 30 min or 2h of cold stress, similar to the trend seen after 24h cold stress (Figure 4.15C). In *Arabidopsis HOS1* is rapidly reduced after 30 min of cold stress but recovers within 1h to pre-stress levels (Lee et al., 2001), a response not seen in any of the barley lines. In the HvICE1:OE lines, however, there was a minor reduction in *HvHOS1* expression after 30 min of cold stress and a significant reduction after 2h. In the HvICE1:SRDX lines there was no significant change after 30 min but a reduction after 2 h, similar to what was seen in the other genotypes. Together it suggests that the *HvHOS1* expression is not significantly altered by cold in the wild type under the conditions tested but that the overexpression or silencing of *HvICE1-1* leads to a reduction of *HvHOS1* after 2h of cold stress.

SIZ1 acts as an activator of *ICE1* through sumoylation which stabilises and enables *ICE1* binding to the *CBF3* promoter (Miura 2017) which generated interest in the putative *HvSIZ1* orthologue in the HvICE1-1 transgenic lines. All genotypes, wild type, HvICE1:OE and HvICE1:SRDX displayed a similar expression pattern of *HvSIZ1* in response to cold and there was no significant difference in *HvSIZ1* expression at the different time points for the different lines (Figure 4.15D). There was no induction of *HvSIZ1* in the HvICE1:SRDX after 30 min but after 2 h of cold stress there was a significant increase compared to the control conditions. In the long-term cold stress there was a lower level of *HvSIZ1* in the HvICE1:OE-5 plants in the control conditions but this could not be confirmed in this experiment with any of the transgenic lines or the HvICE1:OE-5 line used in both experiments. Together the experiments show that there appears to be an effect of cold on *HvSIZ1* expression long term however it is not clear whether *HvSIZ1* interacts with *HvICE1-1*.

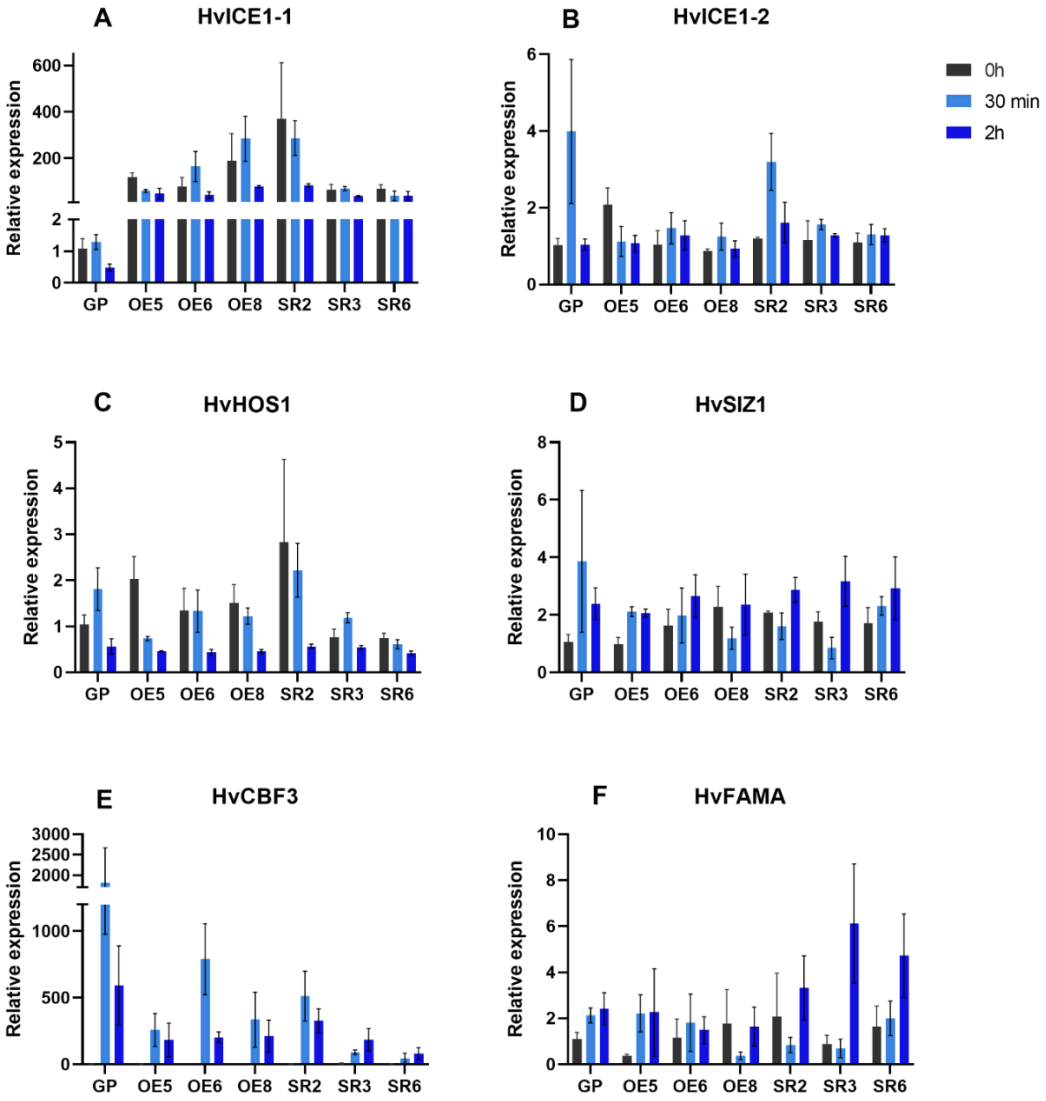

Figure 4.14. Gene expression data of genes of interest in individual transgenic lines with three biological replicates at 0h, 30 min and 2h of cold stress. The individual lines from the same genotype did not display any significant difference from each other and were therefore analysed as average of the genotype (Figure 4.15). Each line and gene is normalised to two reference genes, HvTub *and* HvHSP70*, and to the wild type of the corresponding treatment. Error bars = SEM.*

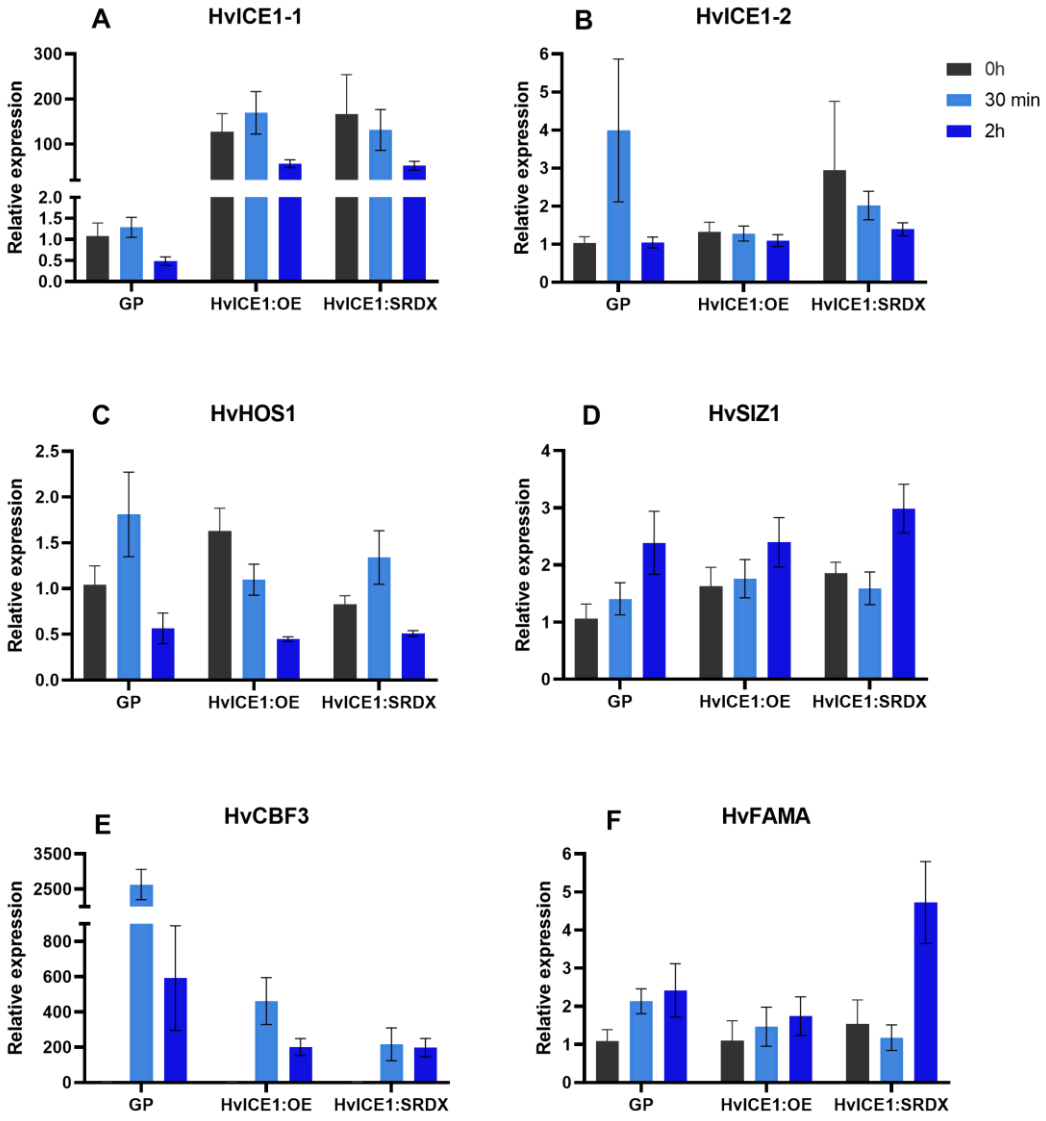

Figure 4.15. Relative gene expression after 30 min and 2 h chilling stress. Each line and gene is normalised to two reference genes, HvTub *and* HvHSP70*, and to the wild type of the corresponding treatment. For HvICE1:OE and HvICE1:SRDX three biological replicates of three transgenic lines are combined. A. The expression of* HvICE1-1 *was elevated in all transgenic lines. B.* HvICE1-2 *in the transgenic lines was not significantly affected by cold. C. In the OE lines the* HvHOS1 *expression was reduced after cold treatment, with no difference in the wild type. D.* HvSIZ1 *was not affected by cold in the wild type but showed a significant increase after 2h of cold stress in both HvICE1:OE and HvICE1:SRDX lines. E. The expression of* HvCBF3 *was induced in all lines at 30 min of cold stress. F.* HvFAMA *was increased after 2 h of cold stress in the HvICE1:SRDX lines. Error bars = SEM.*

For the putative *HvICE1-1* downstream target *HvCBF3*, there was a distinctly higher level of *HvCBF3* in the wild type after 30 min and 2 h of cold stress, with a 1300 and 300 times higher expression respectively, indicating that *HvCBF3* is strongly induced by cold in the wild type (Figure 4.15E, Table 4.11). A similar effect was seen in in both the HvICE1:OE and HvICE1:SRDX lines however the induction was significantly lower than in the wild type

without any difference between the two HvICE1-1 genotypes although the induction was smaller in the HvICE1:SRDX lines (Table 4.11). Interestingly the *HvCBF3* expression was not higher in the HvICE1:OE lines compared to the wild type suggesting that *HvICE1-1* is not sufficient to constitutively increase the *HvCBF3* expression. There appears to be some interaction between the *HvICE1-1* and the *HvCBF3* however since the overexpression and especially the HvICE1:SRDX lines had a significantly lower level of *HvCBF3* than the wild type after 30 min of cold stress.

Table 4.11. Fold change in HvCBF3 *expression levels in response to cold treatments in wild type, HvICE1:OE and HvICE1:SRDX. The strongest induction of* HvCBF3 *was seen in the wild type at 30 min of cold stress with a smaller induction in the HvICE1:OE and HvICE1:SRDX lines.*

Genotype	**Fold change of HvCBF3 expression between treatments**		
	0 h to 30 min	0 h to 2 h	30 min to 2 h
Wild type (GP)	1384	312	0.22
HvICE1:OE	430	167	0.39
HvICE1:SRDX	15.2	13.9	0.92

Finally, when investigating the expression of *HvFAMA* in the cold stressed plants, there was no detectable difference in either genotype in control conditions or after 30 min of cold stress but after 2 h of cold there was a significant increase in *HvFAMA* expression in the HvICE1:SRDX lines (Figure 4.15). In the long term cold stress *HvFAMA* was suppressed in all lines after 24 h. This suggests that *HvFAMA* is not affected in short time cold stress in the wild type and but there might be an interaction between *HvICE1-1* and *HvFAMA*.

The results from the relative gene expression analysis was combined in a heat map to illustrate the effect of cold stress on the wild type, HvICE1:OE and HvICE1:SRDX (Figure 4.16). In summary, the *HvICE1-1* transcript was elevated in both HvICE1:OE and HvICE1:SRDX lines confirming the expression of the transgenes. *HvICE1-1* in the wild type was not affected but a short cold stress but was reduced after 24h. There was no effect on *HvICE1-2* expression in control conditions in any of the lines but there was a reduction in the HvICE1:OE lines after 30 min of cold stress.

The putative regulator *HvHOS1* was not affected by cold treatment in the wild type but in the HvICE1:OE lines there was a reduction in *HvHOS1* after 30 min, 2 h and 24 h of cold treatment with only slight reduction in the HvICE1:SRDX lines after 2 h of cold stress (Figure 4.16). Another putative regulator *HvSIZ1* showed similar pattern of expression in all lines with only minor increases in expression after cold stress. The putative downstream target *HvCBF3* was highly induced by a short cold treatment in all lines but with a reduced induction in the HvICE1:OE and HvICE1:SRDX lines. *HvFAMA* expression was reduced in response to a long cold stress and induced in HvICE1:SRDX after 2 h cold stress.

		Cold stress			
		0 h	30 min	2h	24 h
HvICE1-1	wt	1.08	1.29	0.49	0.43
	OE	103.93	169.34	56.63	56.99
	SR	166.71	147.67	58.77	86.65
HvICE1-2	wt	1.03	3.99	1.04	1.27
	OE	1.32	1.28	1.10	1.24
	SR	2.95	2.02	1.39	1.26
HvHOS1	wt	1.04	1.81	0.57	1.72
	OE	1.63	1.10	0.45	0.70
	SR	0.83	1.34	0.51	0.99
HvSIZ1	wt	1.06	3.86	2.39	0.42
	OE	1.63	1.76	2.40	0.22
	SR	1.86	1.59	2.99	0.32
HvCBF3	wt	1.26	2627.38	592.18	-
	OE	1.07	461.43	201.77	-
	SR	14.39	216.52	198.45	-
HvFAMA	wt	1.09	2.13	2.42	0.26
	OE	1.10	1.47	1.74	0.29
	SR	1.53	1.18	4.72	0.18

Figure 4.16. Heat map of relative gene expression of HvICE1-1 *related genes in response to cold stress in wt (Golden Promise), HvICE1:OE and HvICE1:SRDX transgenic lines. The expression of* HvICE1-1 *was elevated in the HvICE1:OE and HvICE1:SRDX lines but was reduced after a longer period of cold stress. In response to cold stress the expression of* HvCBF3 *was increased in all lines with the strongest increase in the wild type.*

4.3.9 Photosynthesis efficiency in relation to *HvICE1-1* and cold stress

Low temperature stress induces the cold signalling pathway and severely impairs plant growth and development (Kim et al., 2015) and the effect of *ICE1* has previously not been investigated in relation to photosynthetic efficiency. Further analysis of the effect of *HvICE1-1* on cold tolerance was carried out by measuring the photosynthetic efficiency of the HvICE1-1 transgenic plants after a period of chilling stress. The efficiency of photosystem II was studied in wild type, HvICE1:OE and HvICE1:SRDX lines after a 24 h period of +0-3˚C chilling stress in the three independent transgenic lines with three biological replicates.

The quantum yield was measured at various light levels to visualise photosystem efficiencies (ϕPSII) at different light intensities. This was used to calculate the electron transport rate (ETR) to estimate the overall photosynthetic capacity. The maximum quantum yield (QYmax) of photosystem II (PSII) for each of the lines was calculated through F_v/F_m. The statistical outcome of the comparisons between wild type and the HvICE1:OE or HvICE1:SRDX are summarised in Table 4.12 and between control conditions and cold treatments are summarised in Table 4.13.

4.3.9.1 Quantum yield and electron transport rate in HvICE1-1 transgenic lines

There was no difference in maximum quantum yield between the lines or between the treatments indicating that the overexpression or silencing of *HvICE1-1* did not affect the maximum photosynthetic capacity (Figure 4.17A). The variation seen in the HvICE1:OE and HvICE1:SRDX cold treated samples are due to individual leaves in the sampling, independent of line effects.

Quantum yield (ϕPSII) was increased in the HvICE1:OE lines compared to the wild type at most light levels in control conditions but was reduced at some light levels after cold stress indicating an effect of the level of *HvICE1-1* on photosystem efficiency (Figure 4.17B, Table 4.12, Table 4.13). In the HvICE1:SRDX lines the quantum yield was slightly lower for certain light levels after cold stress however not consistently. The electron transport rate (ETR) was higher in the HvICE1:OE lines at most light levels in control conditions but was reduced to below wild type levels after a period of cold stress. In response to cold the wild type also displayed reduced ETR but the HvICE1:SRDX was not affected at most light levels.

Together this suggests that the silencing of HvICE1:SRDX does not affect the quantum yield or the ETR under control conditions but might offer an advantage under cold stress. In contrast the overexpression of *HvICE1-1* appears to increase the photosynthetic efficiency and the ETR under control conditions but lead to a stronger reduction in response to cold stress.

4.3.9.2 *HvICE1-1* effect on photochemical and non-photochemical quenching

In addition to measuring the efficiency of PSII, the amount of open reaction centres were estimated by calculating the photochemical quenching (qP). Photochemical quenching influence the operating efficiency of the PSII and is important for the protection at high light levels (Baker et al., 2001). In response to cold the qP of the wild type and the HvICE1:OE lines decreased significantly at most light levels but HvICE1:SRDX only showed some reduction at 20 and 30% light levels (Figure 4.17E, Table 4.13). When comparing the lines to the wild type there was an increase in qP in the HvICE1:OE lines in control conditions with a significant reduction after cold stress whereas HvICE1:SRDX displayed a similar level of qP to the wild type (Table 4.13). Together these measurements of photochemical quenching suggests that HvICE1:OE is more susceptible to cold stress and HvICE1:SRDX maintains a level similar to the wild type in control conditions and at these cold stress conditions.

The level of non-photochemical quenching (NPQ) at different light levels did not change depending on genotype (Figure 4.17D, Table 4.12) indicating that the level of *HvICE1-1* did not affect NPQ in normal condition or under cold stress. When comparing the performance of the genotypes between control and freezing stress there was an increase in NPQ for both HvICE1:OE and HvICE1:SRDX but no statistically significant change in the wild type lines (Table 4.13). The *HvICE1-1* overexpression and silencing lines display an increase in heat dissipation in response to cold stress, possibly due to an increase in light protective mechanism or to the light damage itself.

Through these measurements all genotypes displayed a similar QY_{max} suggesting there is no penalty for a high level of *HvICE1-1* expression in terms of maximum photosystem efficiency. In all parameters measured the HvICE1:OE lines displayed the biggest change in response to cold with a reduction in ϕPSII, ETR, and qP as well as a higher NPQ for most light levels in comparison to the wild type. In contrast, the HvICE1:SRDX lines only deviated from the wild type performance at certain light levels and showed similar cold induced responses as the wild type.

Table 4.12. Comparisons of photosynthesis parameters between wild type and HvICE1-1 transgenic lines of qP, NPQ, QY, ETR, and QYmax. For each light level the photosynthetic measurement of HvICE1:OE or HvICE1:SRDX was compared to the wild type to determine any difference in photosynthetic capacity at specific light levels. For each light level a t-test was performed between the wild type and transgenic plants and p-values less than 0.05 are highlighted in green.

		LIGHT %	**10**	**20**	**30**	**40**	**80**	**100**
Parameter	**Treatment**	**Light (µmol/sm²)**	**21.2**	**142.5**	**271.7**	**395.4**	**901.9**	**1148**
qP	CONTROL	HvICE1:OE	0.268	0.088	0.128	0.001	0.001	0.001
		HvICE1:SRDX	0.097	0.271	0.118	0.213	0.351	0.169
	COLD	HvICE1:OE	0.213	0.203	0.042	0.037	0.045	0.282
		HvICE1:SRDX	0.437	0.410	0.153	0.068	0.031	0.059
NPQ	CONTROL	HvICE1:OE	0.834	0.842	0.224	0.232	0.416	0.499
		HvICE1:SRDX	0.432	0.913	0.309	0.175	0.212	0.219
	COLD	HvICE1:OE	0.590	0.864	0.861	0.710	0.478	0.292
		HvICE1:SRDX	0.672	0.920	0.773	0.895	0.768	0.557
QY	CONTROL	HvICE1:OE	0.538	0.019	0.132	0.005	0.011	0.005
		HvICE1:SRDX	0.642	0.010	0.195	0.279	0.410	0.223
	COLD	HvICE1:OE	0.132	0.094	0.024	0.019	0.030	0.060
		HvICE1:SRDX	0.376	0.324	0.154	0.045	0.033	0.059
ETR	CONTROL	HvICE1:OE	0.538	0.019	0.132	0.005	0.011	0.005
		HvICE1:SRDX	0.642	0.010	0.195	0.279	0.410	0.223
	COLD	HvICE1:OE	0.132	0.094	0.024	0.019	0.030	0.060
		HvICE1:SRDX	0.376	0.324	0.154	0.045	0.033	0.059
QYmax	CONTROL	HvICE1:OE	0.439					
		HvICE1:SRDX	0.500					
	COLD	HvICE1:OE	0.139					
		HvICE1:SRDX	0.354					

Table 4.13. Comparisons of the photosynthetic measurements between control and cold treated samples at for qP, NPQ, QY, ETR and QYmax. For each light level a t-test was performed between the control and cold treated plants and p-values less than 0.05 are highlighted in green.

		LIGHT %	10	20	30	40	80	100
Parameter	**Genotype**	**Light (µmol/sm²)**	**21.2**	**142.5**	**271.7**	**395.4**	**901.9**	**1148**
qP	GP		0.284	0.000	0.449	0.028	0.013	0.007
	HvICE1:OE		0.077	0.002	0.003	0.002	0.005	0.199
	HvICE1:SRDX		0.297	0.001	0.033	0.105	0.275	0.448
NPQ	GP		0.170	0.592	0.058	0.065	0.131	0.253
	HvICE1:OE		0.023	0.269	0.003	0.026	0.254	0.838
	HvICE1:SRDX		0.016	0.451	0.000	0.001	0.020	0.110
QY	GP		0.027	0.000	0.435	0.052	0.016	0.005
	HvICE1:OE		0.094	0.009	0.001	0.001	0.005	0.037
	HvICE1:SRDX		0.666	0.047	0.051	0.058	0.226	0.512
ETR	GP		0.027	0.000	0.435	0.052	0.016	0.005
	HvICE1:OE		0.094	0.009	0.001	0.001	0.005	0.037
	HvICE1:SRDX		0.666	0.047	0.051	0.058	0.226	0.512
QYmax	GP	0.029						
	HvICE1:OE	0.107						
	HvICE1:SRDX	0.685						

4.3.10 Effect of *HvICE1-1* on drought – stomatal patterning and root-shoot ratio

Water management during drought stress is essential, with stomatal density on a leaf influencing how much water is released through respiration (Harrison 2019). To further study the effect of *HvICE1-1* in barley the transgenic HvICE1 lines were subjected to drought stress at different stages of development. No difference had been found in the number of stomata formed under control or cold treatment for any of the genotypes tested (Figure 4.18) however it is possible that other abiotic stresses resulting in reduced water availability might influence stomatal patterning.

4.3.10.1 Stomatal density under drought stress

Stomatal densities of the transgenic lines were studied to determine any effect of *HvICE1-1* on drought resistance in terms of water management through stomatal formation. The number of stomata were counted on leaf tissue from seedlings developed under control or drought stress conditions. Drought was applied by watering with nutrient solution containing 20% PEG to simulate osmotic induced drought whereas controls were watered with nutrient solution only. In the control and induced osmotic drought three biological replicates of three independent transgenic lines of HvICE1:OE and two lines of HvICE1:SRDX were used.

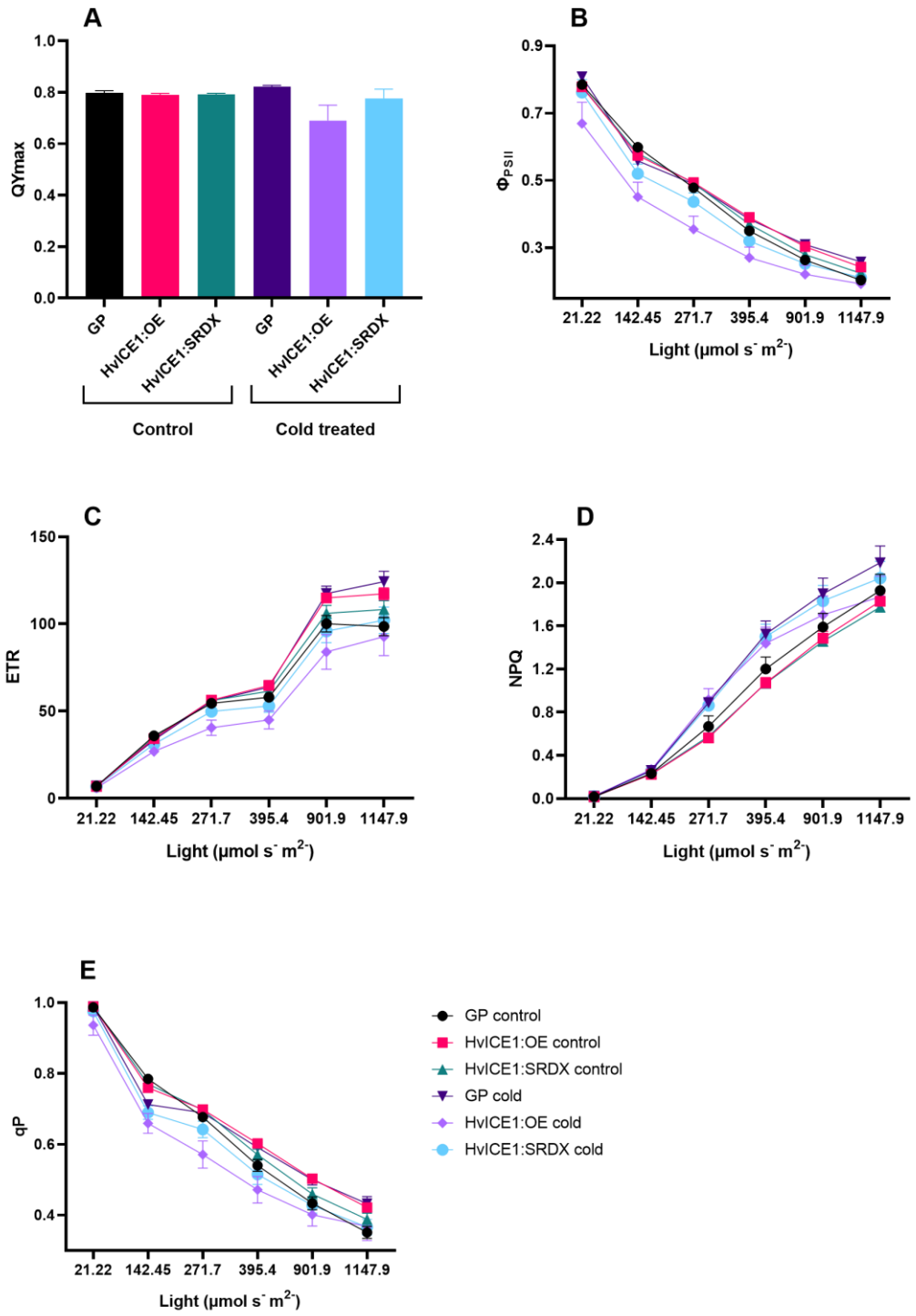

Figure 4.17. Photosynthetic measurements at different light levels of HvICE1-1 lines under control or cold stress conditions. A. There was no difference in QYmax between the lines or the treatment with the variation in the cold stressed transgenic lines due to individual leaves. B. Photosystem efficiency, C. Electron transport rate, D. Non-photochemical quenching, E. Photochemical quenching. The biggest difference was seen in the cold treated HvICE1:OE which displayed a lower ϕPSII, ETR and qP as well as a higher NPQ for most light levels. Error bars = SEM.

In previous experiments the stomatal density differed between the lines on the abaxial side, and in this experiment leaf imprints on the adaxial side of one mature leaf from six plants were imaged to estimate stomatal density and the number of counted stomata per line is specified in (Table 4.14). In control conditions the stomatal densities were compared for the lines grown in compost (section 4.3.5) and in nutrient supplemented vermiculite in the drought experiment to detect differences caused by growth conditions. Seedlings of comparable stages of the same lines of the same generation were compared. Interestingly, there were significant differences between almost all lines between the growth conditions (Table 4.15). The wild type and the HvICE1:OE lines generally had a higher stomatal density when grown in compost, except HvICE1:OE-6, whereas the HvICE1:SRDX lines had a higher density when grown in vermiculite. It is possible that the growth conditions impacted the formation of stomata due to differences in water or nutrient availability or in the ability of the root to obtain water.

To further investigate the possible effect of *HvICE1-1* on water management during drought stress, the weight of roots and shoots in the different lines were measured in the seedlings after growth in control conditions or under drought stress. The overall biomass was reduced in the plants subject to drought stress but it was not specific to genotype (Figure 4.19). There was no difference in biomass for either shoot or roots in any of the lines and there was no difference in the root to shoot ratio suggesting that the effect of vermiculite on stomatal density might not be due to genotype specific effects on the root biomass.

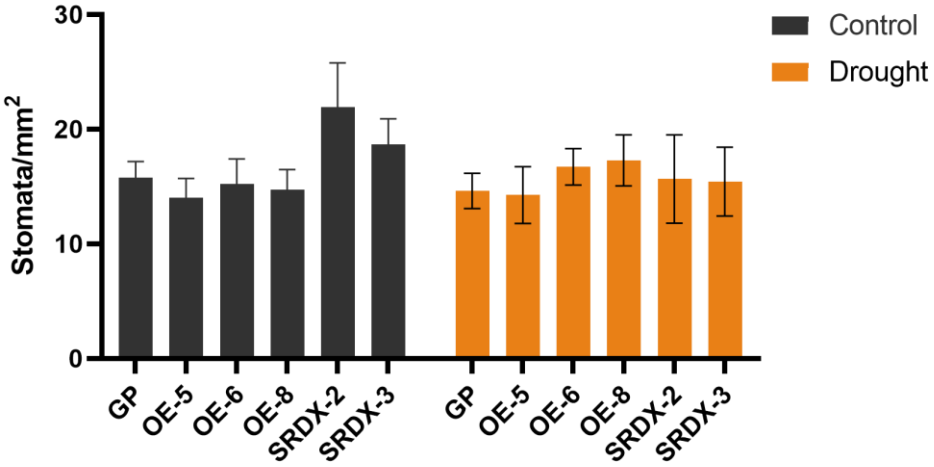

Figure 4.18. Stomatal density in wild type (GP), HvICE1:OE and HvICE1:SRDX lines at control or drought stress grown in vermiculite. The stomatal density was significantly higher in the HvICE1:SRDX lines under control conditions with no difference in the HvICE1:OE lines. Error bars = SEM.

Interestingly, under control conditions in vermiculite both HvICE1:SRDX lines had a significantly higher stomatal density compared to the wild type, which is the opposite of what was seen for lines grown in compost. Compared to the wild type, silencing of *HvICE1-1* lead to a significant increase in stomata (p-value 0.008) under control conditions whereas no difference was seen in drought conditions. The overexpression of *HvICE1-1* appeared to not influence the stomatal density in control or drought conditions. When comparing the performance of the lines between treatments the overexpression lines did not differ, but the silencing lines displayed an adaptation to drought by a reduction in stomatal density to wild type levels (Figure 4.18). The regulation of *HvICE1-1* appears to be important for the formation of stomata in barley seedlings and dependent on growth conditions as well as temperature.

Table 4.14. Stomatal count in control and drought stressed seedlings. At least 600 stomata were counted per line over a comparable area to estimate stomatal density. The HvICE1-1 lines were compared to the wild type (GP) within each treatment group (T-test genotype) to estimate the effect of the genotype. The lines were also compared between the treatments i.e. drought stressed to control for each individual line (T-test treatment) to estimate the effect of the drought stress on each line. The HvICE1:SRDX lines had a higher stomatal density in control conditions which was reduced under drought stress. Two lines of HvICE1:OE showed an increase in stomatal density after a period of drought stress.

		Stomata/mm²	***No. counted***	***t-Test genotype***	***t-Test treatment***
Control	GP	15.75	687		
	HvICE1:OE-5	14.01	611	0.085	
	HvICE1:OE-6	15.20	663	0.621	
	HvICE1:OE-8	14.74	643	0.301	
	HvICE1:OE	14.65	1917	0.202	
	HvICE1:SRDX-2	21.92	956	0.004	
	HvICE1:SRDX-3	18.66	814	0.023	
	HvICE1:SRDX	20.29	1770	0.008	
Drought	GP	14.63	638		0.22
	HvICE1:OE-5	14.26	622	0.7648	0.842
	HvICE1:OE-6	16.74	730	0.0416	0.198
	HvICE1:OE-8	17.29	754	0.0368	0.052
	HvICE1:OE	16.10	2106	0.18	0.053
	HvICE1:SRDX-2	15.66	683	0.5561	0.019
	HvICE1:SRDX-3	15.43	673	0.5730	0.061
	HvICE1:SRDX	15.54	1356	0.531	0.002

Table 4.15. Stomatal density of seedlings grown in compost and vermiculite under control conditions. There was a significant difference in stomatal density for each line between the growth conditions, except HvICE1:SRDX-3.

Genotype	Stomata/mm^2		t-Test (p-value)
	Vermiculite	Compost	
GP	15.75	24.02	4E-07
HvICE1:OE-5	13.65	20.77	3E-11
HvICE1:OE-6	15.20	12.93	0.0123
HVICE1:OE-8	14.74	18.62	0.0037
HVICE1:SRDX-2	21.92	13.66	4E-08
HVICE1:SRDX-3	18.66	16.55	0.0828

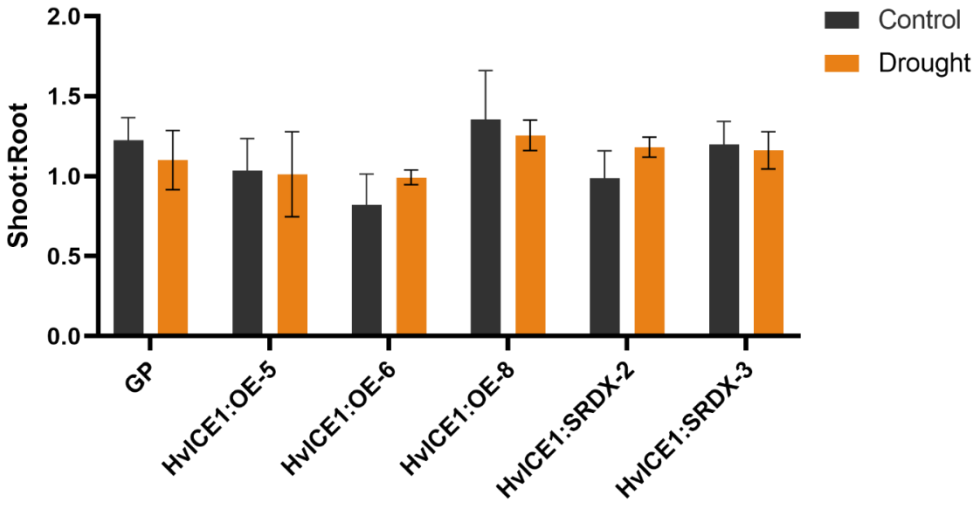

Figure 4.19. Shoot to root ratio in seedlings in control conditions and after drought stress in wild type (GP), HvICE1:OE and HvICE1:SRDX lines. There was no significant difference in the biomass ratio of the different genotypes.

4.3.10.2 Seed set in drought stressed HvICE1-1 lines at flowering

Drought stress was applied during flowering by withholding water from compost grown plants. The drought experiment with plants in 2 L pots was started at LFE1-LFE2 when spikes were 3-4 cm long where water was withheld for 12 days. Plants grown as control were kept well-watered. The weight of the plants was measured to monitor any differences in water usage throughout the drought treatment. No effect on morphology was detected in the amount of water used between GP, HvICE1:SRDX and HvICE1:OE (Figure 4.20).

After the completion of the drought stress at flowering the plants were returned to normal watering regimes for the duration of the growth cycle before seed set analysis. All experiments are carried out with three biological replicates with one transgenic line, HvICE1:OE-5 and HvICE1:SRDX-2, per genotype. Previous experiments suggest that

overexpression or silencing of *HvICE1-1* reduces yield (section 4.3.3) however no difference in seed set was found between the genotypes under control conditions possibly due to the level of variation in the samples (Figure 4.21). When exposed to drought the HvICE1:OE-5 plants displayed a significantly reduced seed set compared to the wild type but no difference was found between drought stressed plants and control plants within the HvICE1:OE-5 genotype. No difference was found for the HvICE1:SRDX lines. This suggesting that overexpression of *HvICE1-1* is not favourable for drought resistance however the level of variation in the HvICE1:OE-5 plants prevented any analysis in the control conditions.

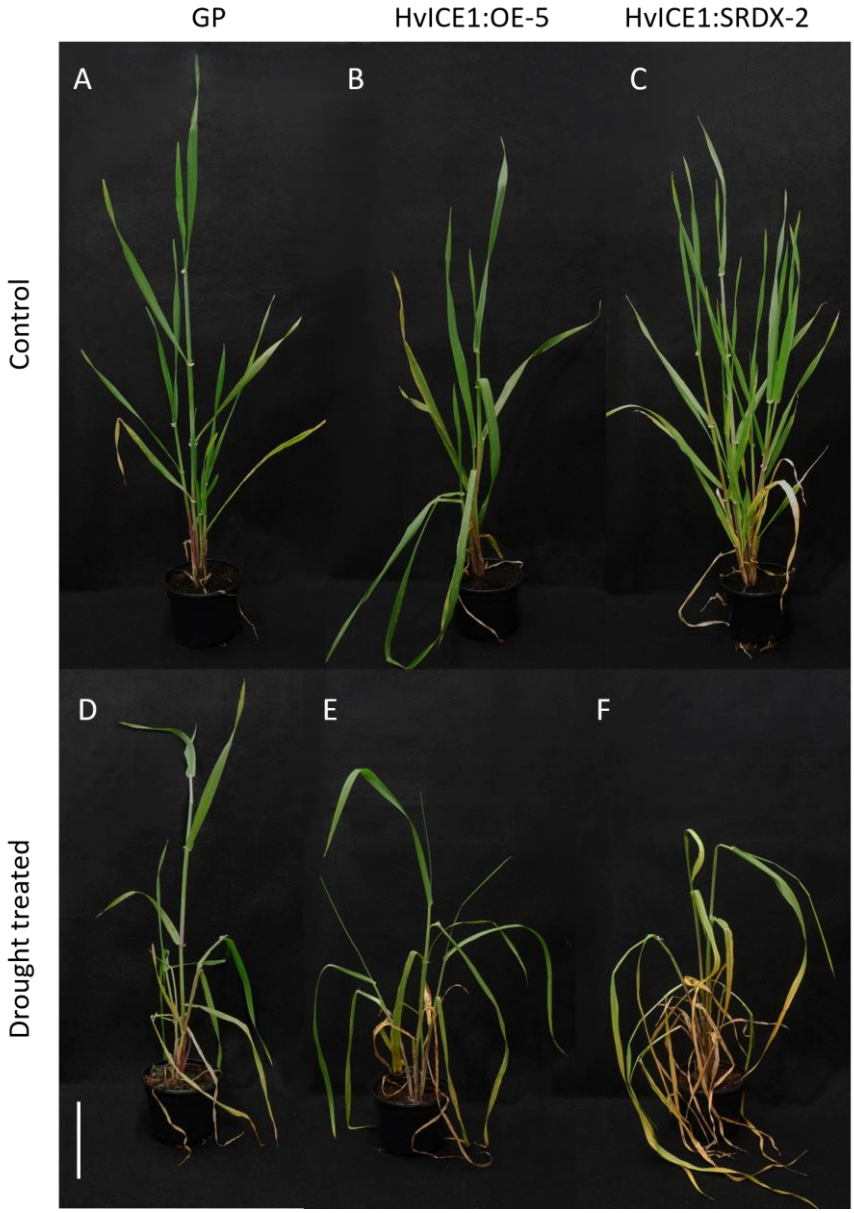

Figure 4.20. Effect of drought on wild type (GP), HvICE1:OE-5 and HvICE1:SRDX-2 plants. Plants were grown in compost where the controls were kept well-watered (A-C) and the drought was applied by withholding water for 12 days (D-F). Scale bar 10 cm.

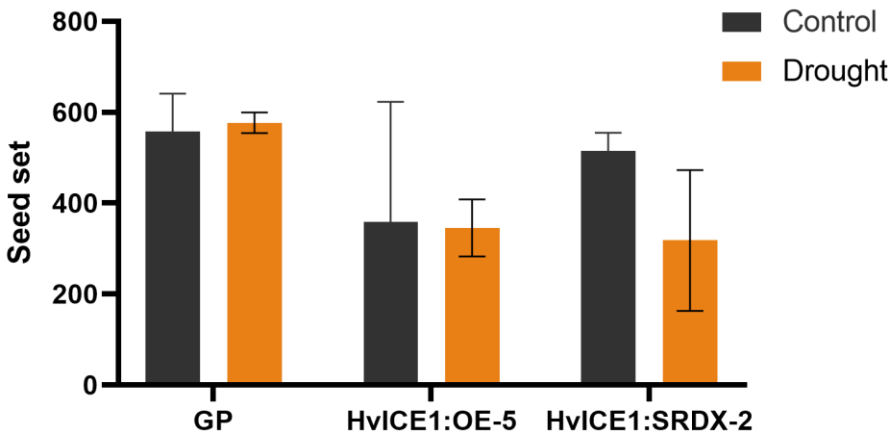

Figure 4.21. Seed set in wild type (GP), HvICE1:OE-5 and HvICE1:SRDX-2 under drought stress during flowering. No differences were found in seed set between the lines due to the level of variation in the samples.

4.4 Discussion

4.4.1 Expression of *HvICE1-1* related genes in cold response

Cold sensing and response is critical for plant survival and is under stringent control (Beck et al., 2007; Pareek et al., 2017). With this highly controlled signalling pathway with overlapping sensory pathways, it is important to consider a variety of parameters such as duration and temperature as well as photoperiod and acclimation time for the study of cold response.

In control conditions *HvICE1-1* was found to be expressed in all tested tissues with similar expression levels in roots, shoots, spikes and embryos (Figure 4.4). This is similar to the expression pattern in *Arabidopsis* where *ICE1* is expressed continuously, possibly to enable rapid cold responses (Chinnusamy, 2003). In barley after a long-term cold stress there was a reduction of *HvICE1-1* in wild type whereas *HvICE1-2* seemed to be unaffected. Interestingly, there was no significant difference in *HvICE1-1* expression in the HvICE1:OE-5 and HvICE1:SRDX-1 plants after 24 h of cold stress.

For gene expression analysis of putatively *HvICE1-1* interacting genes, two different types of cold experiments were conducted with varying lengths to study the effect of *HvICE1-1*. Cold stress was carried out under similar light conditions with the exception of a difference in photoperiod whereas chilling stress was conducted under dark conditions to remove diurnal effects (Pillitteri, 2011). In both treatments there was no acclimation period.

In response to a short chilling stress *HvICE1-1* was not significantly altered in response to cold however there seemed to be a decrease after 2 h. This trend was consistent between the genotypes suggesting that *HvICE1-1* is not induced by cold at the time points tested but is inhibited after longer cold stress. In addition, the *HvICE1-2* expression was not significantly altered by the cold stress, in any of the genotypes tested, possibly due to the level of variation in the samples.

The effect of differential expression of *HvICE1-1* was studied by investigating the expression of predicted *HvICE1* regulators *HvHOS1* and *HvSIZ1* genes. There was no detectable difference in *HvHOS1* or *HvSIZ1* expression in the wild type however after 2h of cold induction the putative repressor *HvHOS1* was reduced and the putative activator *HvSIZ1* was increased suggesting that these genes are involved with the cold response (Figure 4.15) (Dong et al., 2006; Miura et al., 2007). It is possible that initially elevated levels of *HvICE1-1* lead to an increase of *HvHOS1* but this effect subsides in long term cold stress and in constitutively elevated levels *of HvICE1-1*. In control conditions in the long term cold stress *HvSIZ1* appeared to be reduced in the HvICE1:OE-5 and HvICE1:SRDX-1 plants compared to the wild type but this effect was not seen in the corresponding control conditions of the short term cold stress experiment. It is possible that the presence of the *HvICE1-1* transcript is not sufficient to alter the putative regulators in every condition.

The putative *HvICE1-1* downstream target *HvCBF3* is induced very rapidly in response to cold where a first increase is detectable after 15 min of cold stress with maximum reached at 2 h and a return to pre-cold stress after 24 h indicating that timing of analysis is important (Choi,

2002). In this study, *HvCBF3* was upregulated after initial cold stress in the wild type and stayed elevated after 2 h (Figure 4.15). In the HvICE1:OE and HvICE1:SRDX lines there was also an induction however it is not as pronounced, without a reduction at 2 h in HvICE1:SRDX. Consistently higher levels of the *HvICE1-1* transcript could be sufficient to interfere with the rapid response of *HvCBF3* explaining why the *HvCBF3* induction was a lot smaller in the HvICE1:OE plants. The silencing of *HvICE1-1* in the HvICE1:SRDX lines did not appear to fully repress the expression of *HvCBF3* although its induction in the HvICE1:SRDX lines was markedly reduced compared to the wild type (Figure 4.15). Together this suggests that HvICE1-1 is involved with the control of the cold response gene *HvCBF3* however other genes might be involved either with the regulation of *HvCBF3* or the activity of *HvICE1-1*. Further studies of a complete knock out of the *HvICE1-1* gene would provide more information of the interaction of *HvICE1-1* and *HvCBF3* and the role of *HvICE1-1* in the cold signalling pathway.

4.4.2 Effect of differential expression of *HvICE1-1* in seed set and general physiology

Abiotic stresses that cause water deficiency, such as drought, cold and salinity, induces specific and unspecific responses in plants with both cold and drought stresses causing osmotic changes and decreased water potential in plant cells (Beck et al., 2007; Samarina et al., 2020). To investigate the function of *HvICE1-1* in barley and its effect on plant physiology under abiotic stress, the transgenic lines overexpressing *HvICE1-1* or constitutively silencing *HvICE1-1* were compared to wild type (Golden Promise) to investigate the influence of *HvICE1-1* on plant morphology. The function of *HvICE1-1* in stomatal patterning in monocots and the effect of differential expression of *HvICE1-1* on water usage, especially in relation to fertility was investigated.

4.4.2.1 Seed set in HvICE1-1 plants under abiotic stress conditions

A reduction in stomatal density in barley has been shown to increase drought tolerance but has no effect on yield (Hughes et al., 2017). The *Arabidopsis ice1* knockout mutant did not have a reduced seed set however the overexpressing *scrm-D* mutant displayed reduced fertility under control conditions (Chinnusamy et al., 2003; Kanaoka et al., 2008). A study in *Brachypodium* has shown that a knockout of *BdICE1* leads to loss of stomata without a reported reduced seed set in the *Bdice1* and *Bdscrm2* double mutant (Raissig et al., 2016). In *Arabidopsis ICE1* has been shown to influence male fertility by affecting anther dehydration and pollen viability (Wei et al., 2018) and to investigate whether differential expression of *HvICE1-1* could affect yield in barley the seed set was counted in several generations and under different abiotic stresses.

The first T0 generation of the transgenic lines had a strong reduction in seed set in the HvICE1:OE and HvICE1:SRDX lines which may be a consequence of the stress conditions involved with the transformation protocol. In subsequent generations, the HvICE1:OE lines displayed a reduction in seed set in control conditions and under abiotic stresses, with no difference detected for HvICE1:SRDX lines for any stress conditions compared to the wild type. In the long term cold stress experiment there was a reduction in seed set for the

HvICE1:OE lines in both control conditions and after cold treatment (Figure 4.10) and drought stress at tillering caused a significant reduction in comparison to the wild type.

Interestingly, this reduction in seed set does not appear to be an effect of stomatal density as overexpression of *HvICE1-1* does not influence stomatal density (Figure 4.11). Similarly, an increase in stomatal density in the silencing lines does not affect seed set in control conditions. This effect of either increased or decreased expression of *HvICE1-1* on fertility is consistent with previous results in *Arabidopsis* however not in connection to stomatal density (Chinnusamy et al., 2003; Kanaoka et al., 2008). It is possible that the overexpression of *HvICE1-1* is not sufficient to alter stomatal density but affects other developmental processes that can affect fertility, by inhibiting growth as the number of tillers produced in the HvICE1:OE lines was reduced in these lines.

4.4.3 The influence of *HvICE1-1* on stomatal formation

Stomatal formation is initiated in *Arabidopsis* by *ICE1* and *ICE2* interacting with bHLH transcription factors *SPCH*, *MUTE* and *FAMA* to form heterodimers (Kanaoka et al., 2008). To test whether *HvICE1-1* could influence stomatal patterning or density, the stomata was imaged in HvICE1:OE and HvICE1:SRDX lines on leaf tissue in seedlings. Kanaoka et al. (2008) identified the *ice1* knockout mutant to be sufficient to reduce the number of stomata formed and the double mutant *ice1ice2* displayed a complete lack of stomata. Additionally, constitutively expression of *ICE1* results in a significant increase in stomata in *Arabidopsis* (Pillitteri et al., 2011; Putarjunan et al., 2019). Here, the overexpression of *HvICE1-1* in barley did not affect stomatal density in control conditions or in response to abiotic stresses such as drought or a long-term cold treatment, indicating that *HvICE1-1* is not sufficient to initiate stomatal formation in barley. Interestingly, the silencing of *HvICE1-1* lead to an increase in stomatal density under control and drought conditions with change in stomatal density ratio between the adaxial and abaxial side of the leaf.

In *Arabidopsis ICE1* binds directly to the promoter of *FAMA* and is involved with stomatal guard cell formation (Wei et al., 2018), and in *Brachypodium* the expression of *BdICE1* acts to establish stomatal fate but *BdSPCH2* is the major regulator (Raissig et al., 2016). In barley, the expression of *HvFAMA* was significantly reduced after a short chilling stress but no difference was found between the genotypes, suggesting that the reduction of *HvFAMA* in long term cold treated plants was unrelated to *HvICE1-1* expression and possibly not directly affected by *HvICE1-1*.

ICE1 and *ICE2* are redundant heterodimerisation partners of *SPCH*, *MUTE*, and *FAMA*, and are required for stomatal development in *Arabidopsis* suggesting that the interplay of the *ICE1* and *ICE2* transcription factors with other bHLH proteins might be important (Raissig, 2016). In barley no difference in expression of the *HvICE2* candidate *HvICE1-2* was detected in any genotype in control or long term cold treated plants indicating that *HvICE1-2* is not affected by *HvICE1-1* at the time points measured.

Despite an increase in stomatal density in the HvICE1:SRDX lines there was no difference in stomatal conductance between HvICE1:SRDX and the wild type (Figure 4.12). HvICE1:OE however, did have a lower stomatal conductance than the wild type despite no significant difference in stomatal density. Since *ICE1* is involved with stomatal initiation and not the opening and closing of the stomata the conductance was measured in the same conditions to remove any influence of the growth conditions and only measure differences in conductance dependent on stomatal density. Measurement in control conditions for all plants gives a more accurate representation of the number, size, and activity of the stomata since all available stomata should be open in the same conditions.

4.4.4 Differences in chlorophyll fluorescence and photosynthesis parameters in HvICE1-1 lines during cold stress

Cold and freezing stress severely impairs photosynthesis in the leaf resulting in reduced plant growth and potential loss of yield (Baker & Rosenqvist, 2004). Cold tolerant varieties able to reduce the detrimental effect of a period of cold stress are therefore of interest and can be identified by measuring parameters indicating the efficiency of the photosystems (Baker 2004 and others).

Excess light not used in photosynthesis can be harmful and needs to be emitted through one of several pathways such as chlorophyll fluorescence, photochemistry (qP), and heat (NPQ). By measuring these parameters it is possible to estimate the efficiency of the photosystems under different light and growth conditions (Murchie & Lawson, 2013).

A previous study in barley found that a range of photosynthesis parameters changed in response to cold but the detrimental effects were mitigated to a higher degree in a cold tolerant variety (Dai et al., 2007). They found no difference in the maximum quantum yield of the photosystem (QY_{max}) but the quantum yield of the photosystem II (ϕPSII) decreased and the non-photochemical quenching (NPQ) increased after cold stress with only minor changes in the electron transport rate (ETR) and photochemical quenching (qP) (Dai et al., 2007).

No difference in QY_{max} was seen between any lines or conditions indicating that the maximum efficiency is not affected by the expression of *HvICE1-1* or that the cold stress was detrimental (Figure 4.17, Table 4.12, Table 4.13). The HvICE1:SRDX plants rarely differed from the wild type in photosynthesis parameters suggesting that the SRDX-tagged *HvICE1-1* did not significantly affect quenching or photosystem efficiency. The HvICE1:OE lines however outperformed the wild type with a more efficient PSII under control conditions but was more susceptible to cold stress. In addition the ETR was higher in the HvICE1:OE lines under control conditions with a strong reduction in cold treated plants, an effect not seen in HvICE1:SRDX lines (Figure 4.17). The amount of open photosystems (qP) decreased in all lines at both conditions when the light level increased. At cold stress both control and HvICE1:OE showed a reduction at most light levels however the HvICE1:SRDX lines displayed no major change.

There was no change in NPQ between the lines within treatment groups but both HvICE1:OE and HvICE1:SRDX had higher NPQ during cold stress. The NPQ value gives the efficiency of heat dissipation which can be affected by light-induced damage or of the light protective mechanism. An increase of NPQ could be an indication that there is an increase in light protective processes or damage.

Since the QY_{max} was constant in the lines the reduction in efficiency of the photosystems, especially a higher light levels might indicate that *HvICE1-1* inhibits maximum photosynthesis. Lack of inhibition of the photosynthetic rate and no reduction in photochemical quenching in the silencing lines exposed to cold could indicate a faulty cold response network. Together this suggests that there is a slight advantage to the overexpression of *HvICE1-1* under control conditions in terms of photosystem efficiency however cold stress affects these plants more severely than the HvICE1:SRDX and wild type.

4.5 Conclusion

In this study the function of *HvICE1-1* was tested *in planta* using overexpression and SRDX-tagged *HvICE1-1* transgenes in barley. Similar to *ICE1* in *Arabidopsis* the native *HvICE1-1* was found to be expressed throughout the plant with a higher level in the leaf tissue. The overexpression of *HvICE1-1* lead to reduced fertility by reducing the number of tillers produced but silencing of *HvICE1-1* had no effect on yield.

It was also shown that *HvICE1-1* influence stomatal formation and that growth conditions affect the stomatal density in the genotypes tested. In contrast to the function of *ICE1* in *Arabidopsis*, *HvICE1-1* was not sufficient to alter the expression of *HvFAMA* involved in stomatal formation under control conditions suggesting that other genes are necessary for the regulation of stomatal formation in barley. Investigation of other bHLH barley orthologues involved with stomatal formation in *Arabidopsis* could be a way to determine the effect of *HvICE1-1* on stomatal initiation and differentiation.

Interestingly, an increase in stomata was not present after drought stress in the HvICE1:SRDX possibly due to inhibition of stomatal formation through a separate pathway. In addition, there seems to be no effect of *HvICE1-1* on the expression of the stomatal transcription factor *HvFAMA*, indicating that the signalling pathway of stomatal formation is different in barley. Instead *HvICE1-1* is most likely involved in cold sensing as silencing of *HvICE1-1* appear to impair the cold sensing ability as the photosynthetic rate is not reduced during cold stress.

Through gene expression analysis in cold stressed seedlings of the putative *HvICE1-1* regulators *HvHOS1* and *HvSIZ1* it was shown that these genes are affected by the expression of *HvICE1-1* however not in control conditions. Detailed molecular studies of the physical interaction of the proteins are needed to confirm any conserved interaction and to determine the exact relationship between *HvHOS1*, *HvSIZ1* and *HvICE1-1*.

Chapter 5. Analysis of gene bank mutant populations for the identification of male sterile traits in barley

5.1 Introduction

5.1.1 Mutant populations for gene identification

Before the onset of *in planta* gene editing techniques the use of forward genetics was instrumental for the discovery of novel phenotypes and characterisation of gene functions (The International Barley Genome Sequencing Consortium, 2012; Druka et al., 2011; Talamè et al., 2008). Induced or spontaneous mutations collected and stored at gene banks with phenotype data attached is a valuable resource for morphological studies. Barley mutant collections have aided mapping of genes in the genome and the study of genetic diversity between cultivars however genetic resources has been a limiting factor of usage (Caldwell et al., 2004; Druka et al., 2011; Falk et al., 2001).

An aspect complicating detailed comparisons of mutant lines is the differences in genomic background of the mutant collections (Druka et al., 2011). For the identification of the genetic component behind a trait it is important to remove background influence from the original cultivar by reducing the size of the region containing the trait of interest (Hospital, 2001).

In the 1980s a project was launched with the objective to gather a range of barley mutants from programs from around the world and introduce them into a common background (Druka et al., 2011; Wolfe & Franckowiak, 1991). The mutant lines were repeatedly backcrossed into the cultivar Bowman to generate near isogenic lines (NILs) where only the region containing the mutant trait was introgressed into Bowman to simplify comparisons between the lines (Druka et al., 2011; Lundqvist, 2014). Based on morphological and physiological features the mutants were categorised into groups to simplify the usage of the lines (Lundqvist, 2014). This collection of 881 mutant lines was deposited at the Nordic Genetic Resource Center (NordGen, https://sesto.nordgen.org) and is freely available for research purposes (Druka et al., 2011; Lundqvist, 2014).

The mutant categories are described in the International Database for Barley Genes and Barley Genetic Stocks (https://www.nordgen.org/bgs/index.php) detailing phenotypes, chromosome mapping locations, and mutant background history. The Bowman mutant collection with over 4000 alleles has been used for a range of morphological and genetic studies on 2-rowed spring barley. In floral development the mutant collections has led to the investigation of the floral bract growth mutant *THIRD OUTER GLUME1* (*TRD1*) phenotype in barley (Houston et al., 2012), studying of the effect of *INTERMEDIUM-C* (*INT-C)* gene on lateral floret development (Ramsay et al., 2011), and phenotyping of alleles of early flowering time locus (Zakhrabekova et al., 2012).

One of the mutant groups is categorised as male sterile genic (msg) mutants and consists of 50 independent lines carrying traits resulting in male sterility. These lines exhibit full female fertility but varying degree of abnormal anther sizes, filament elongation, and pollen defects (Franckowiak et al., 2015). Detailed studies of the nature of the male sterility have however not been conducted and no further effort has been made to identify the genetics behind the traits.

5.1.2 Mapping of male sterile traits with marker array

Exploitation of the germplasm stored at gene banks is limited by the lack of genotyping data of the accessions (Wambugu et al., 2018). Druka et al. (2011) set out to genotype the BW-lines using an array containing 1536 Single Nucleotide Polymorphism (SNP) markers, based on the Illumina GoldenGate Assay, to identify the introgressed region (Close et al., 2009; Druka et al., 2011). With the aid of the marker data the region containing the mutant trait was mapped to a chromosome and to a region flanked by two SNP markers associated with the trait for each Bowman line (Druka et al., 2011).

The density of markers needed to map loci of interest is determined by the decay of linkage disequilibrium (LD) of a species, i.e. the level of degradation of coinheritance of two loci (Rafalski, 2002). Low level of LD requires high resolution of markers to accurately determine associated markers whereas species with higher LD and coinheritance can be mapped with a lower density of markers (Rafalski, 2002). The LD of elite barley cultivars differs based on multiple factors including germplasm origin, whether the cultivar is 2-rowed or 6-rowed, and depending on the chromosome where the loci is located (Yadav et al., 2021; Zhou et al., 2012; Rafalski, 2002). LD has been found to extend up to 50 cM for specific loci however LD over moderately long distances of 0-20 cM appears to be more common (Bengtsson et al., 2017; Zhou et al., 2012; Malysheva-Otto et al., 2006). Together this indicates that a relatively low marker density can be used to identify and track associated markers in barley. However, markers associated with a mutant trait mapped to a large introgressed region can be vulnerable to LD decay and poor coinheritance of associated markers and mutant traits.

In this project, six male sterile NILs from the Bowman (BW) population were analysed for male sterility caused by pollen development related genes (Table 5.1). Markers previously associated to the male sterile trait were evaluated for coinheritance of the mutant trait and complemented with the 50k iSelect marker array (Bayer et al., 2017) to screen for additional markers in the introgressed region. Selected lines were grown in different conditions for a morphological analysis of the male sterile traits to understand the underlying cause of the sterility. The aim was to link the male sterility trait to the genetic component causing the phenotype.

Table 5.1. Selected lines from the male sterile genic (msg) mutant category from the Bowman (BW) population chosen for further investigation. Each line had been backcrossed to generate NILs where an introgressed region containing the trait of interest had been mapped to a chromosome. For each line two associated SNP markers, SNP1 and SNP2, had been identified and mapped to a location. The distance between the SNPs indicates the size of the region where the trait is most likely located.

Line name and ID	Back-ground	Back-crosses	Chrm	SNP marker (BOPA1)		SNP position	Region size (Mbp)	Region size (cM)
BW545 - msg1.ca	Clho 5368	7	1H	1	2577-1122	397.2	15.8	4.84
				2	7800-594	381.3		
BW546 - msg10.ay	Compana	6	7HS	1	1213-1959	41.8	498	33.04
				2	3140-491	539.8		
BW554 - msg2.cb	Compana	6	2HL	1	3576-2715	494.3	401	18
				2	4065-397	93.0		
BW579 - msg42.db	Betzes	5	3HS	1	4593-2007	32.6	472	39.85
				2	ABC08184-2-1-35	504.8		
BW588 - msg50.hm	Berac	6	7H	1	1674-468	525.2	103	57.57
				2	7397-854	628.4		
BW591 - msg8.ch	Betzes	5	5HL	1	Consensus GBS0531-1	659.7	76	0.35
				2	12756-233	583.3		

5.2 Materials and methods

5.2.1 Selection of lines for analysis

From the mutant collection of NILs with associated markers, six lines from the male sterile genic annotation were selected for detailed analysis of the male sterility trait. Lines from the mutant collection were selected based on the purity of the NILs i.e. number of backcrosses, as well as seed availability, and the reliability of the markers associated with the region. Lines backcrossed five or more times were preferred to ensure a clean background (Hospital, 2001).

The markers were evaluated based on the correspondence between the historical mapping and markers identified through SNP genotyping. Prior to the SNP mapping with the Illumina GoldenGate markers the mutant trait had been mapped to a chromosome based on the coinheritance of genes with easily identified morphological expression (Druka et al., 2011). These genes had historically been mapped to specific chromosome and were used as indicators of the position of the mutant trait (Druka et al., 2011). Lines where this historical mapping corresponded with the genetic SNP mapping were favoured.

Taken together these criteria resulted in six lines chosen for further analysis. In all of the lines the traits originated from a spontaneous mutation and segregate in a monofactorial recessive manor i.e. the homozygotes wild type, heterozygotes, and homozygous mutant segregate in a 1:2:1 ratio where only homozygous mutants displayed male sterility (Druka et al., 2011; Franckowiak et al., 2015).

5.2.2 Seed sterilisation and growth conditions

Seeds were sterilised as described in general methods (section 2.1) and were treated with the fungicide REDIGO PRO, Bayer CropScience, according to the manufacturer's description, in the first growth cycle and sown in germination trays with John Innes compost number 1. Few seeds germinated and after two weeks the seedlings were transferred to 1 litre pots with John Innes Number 3 (Westlands, UK).

To improve germination in the second growth cycle the seeds were not treated with the REDIGO PRO fungicide but were sterilised and cold treated before germination on filter paper as described in general methods (section 2.1). Germinated seedlings were placed in germination trays with John Innes potting compost number 1. After two weeks the seedlings were transferred to 5 litre pots with John Innes Number 3 (Westlands, UK) with three seedlings per pot.

Plants maintained in the glasshouse were grown in John Innes potting compost number 3 and plants in the growth room were grown in John Innes potting compost number 1 due to availability. Plants were grown in glasshouse at 20-25˚C for 16 h daytime and 15˚C for 8 h

night. All seeds, 10 seeds per line, were provided by NordGen (https://www.nordgen.org/en/).

5.2.3 DNA extraction, genotyping and screening with the 50k marker array

gDNA extraction and genotyping of the BW-lines was carried out with the REDExtract-N-Amp Plant PCR kit, Sigma Aldrich, as described in general methods (section 2.4). The plants were genotyped with allele specific PCR for the two associated SNPs (Table 5.1) using primers specific to either the Bowman or the introgressed region (mutant) genotype of the allele for each marker (Table 5.2). To confirm the genotype, plants positive for the mutant SNP were sequenced. A region containing the SNP was amplified using primers specified in Table 5.3 before being sequenced using the Eurofins TubeSeq service described in general methods (section 2.6). Sequences of all primers are stated in Appendix Table S5.1.

For further genotyping DNA was extracted from 100 mg leaf tissue using the ISOLATE II Plant DNA kit (Bioline). Genomic DNA from selected plants was screened using 16,376 markers from the 50k Illumina Infinium iSelect genotyping array (Bayer et al., 2017) at RAGT Seeds Ltd.

Table 5.2. Primers used for allele specific amplification of SNPs. For each line the two markers, SNP1 and SNP2, were genotyped with a primer specific to either allele, named Bowman for wild type and mutant for the genotype of the introgressed region. Primer sequences of the primer numbers are stated in Appendix Table S5.1.

Line	SNP	Primer number		Common	Size of amplicon (bp)
		Bowman	Mutant		
BW545	1	7997	7998	7712	197
	2	7999	8000	7714	134
BW546	1	8001	8002	7724	160
	2	8003	8004	7718	177
BW554	1	8006	8005	7692	206
	2	8007	8008	8028	129
BW579	1	8010	8009	7696	180
	2	8011	8012	8029	134
BW588	1	8013	8014	7728	195
	2	8015	8016	7729	195
BW591	1	8018	8017	7704	81
	2	8019	8020	7731	151

Table 5.3. Primers used for amplification of the SNP region before sequencing. The SNP1 and SNP2 regions were amplified to confirm the genotype after allele specific PCR. Primer sequences of the primer numbers are stated in Appendix 1, Table S5.1.

Line	SNP	Primer number		Size of amplicon (bp)
		Forward	Reverse	
BW545	1	7711	7712	322
	2	7713	7714	270
BW546	1	7715	7724	314
	2	7717	7718	313
BW554	1	7725	7692	405
	2	7726	7727	328
BW579	1	7695	7696	333
	2	7697	7698	376
BW588	1	7728	7700	507
	2	7729	7730	329
BW591	1	7703	7704	208
	2	7731	7732	256

5.2.4 Phenotyping and collection of anthers for imaging

Phenotyping of the BW-lines was carried out on individual plants based on their genotype. All traits were measured during late spike development (Zadok stage 70 (Zadoks et al., 1974)) to compare mature plants and spike development. Plant height was measured from the base of the tillers to the extended spikes. Growth stage of spikes was determined based on the position of the spike in the last sheath based on the staging system in Gomez & Wilson (2012). The level of leaf necrosis, apparent waxiness and growth stature was visually assessed in comparison to Bowman. Fertility was assessed by counting fertilised spikelets and seeds after harvest. All traits were compared to Bowman to determine the influence of the introgressed region in the Bowman background.

Anthers from fertile and sterile spikelets were collected after anthesis and imaged directly using a Zeiss IV Stemi SV 6 microscope with Axiocam ERc 5s camera (Zeiss, Germany) and processed with ZEN Imaging Software (Zeiss, Germany).

5.2.5 Backcrossing to Bowman

To rescue male sterility in the BW-lines, manual pollination was carried out with pollen from Bowman. Spikes with anthers at anthesis stage were collected and the top third of the spikelet was cut diagonally to expose the anther. The spikes were placed in sunlight for 5 min to allow the anthers to dry slightly and extrude from the spikelet. The spikes of the sterile plant were placed in a transparent plastic bag (15x5 cm) and the top was cut to open. One of the Bowman spikes with the extruded anthers was placed inside the bag and shaken to release pollen. The spike was removed, and the bag was sealed. Spikelets of different stages, from just before pollen release to the swelling of the ovary, were pollinated.

5.2.6 Heat stress experiment

Selected lines were exposed to a period of heat stress during flowering to investigate the effect of heat stress on fertility. The homozygous wild type line BW554-1 with partial sterility, and the homozygous mutant line BW591-6, which had a low number of average seeds per spike were grown at constant 15˚C with 16 h photoperiod in growth room. During early spike development, LFE1-LFE3 (Gomez and Wilson, 2012) the plants were subjected to a three day period of 30˚C without irrigation before being returned to pre-stress conditions. Plants were also grown at 20-25˚C with 16 h photoperiod in greenhouse. Fertility was assessed through seed set counting.

5.3 Results

5.3.1 Germination in first generation of BW-lines

From the BW-mutant population six lines were chosen for analysis of the male sterile trait, based on the purity of the NILs, seed availability, and the reliability of the SNP markers associated with the region (Table 5.1). Ten seeds per line were provided by NordGen and were planted however the germination frequency was low for all of the lines including the cultivar Bowman, ranging from 60% to only 30% for BW579 (Table 5.4). This might have been due to treatment of the seeds with the fungicide REDIGO PRO which decreases the germination of seeds with poor germination (REDIGO PRO SDS, Bayer Crop Science).

5.3.2 Identification of few homozygous mutants in selected lines

Individual plants were genotyped through allele specific PCR for the two associated SNPs of each line (Table 5.1). The SNP1 and SNP2 for each line were genotyped as either wild type (Bowman), mutant (non-Bowman) or heterozygous, where mutant genotypes were confirmed with sequencing of the region covering the SNPs associated with the trait. The genotype of some of the markers differed between SNP1 and SNP2 for each line indicating that the entire region did not have the same genotype. This was especially prevalent in BW546 where the SNP1 and SNP2 flanked a substantial region of 498 Mbp/33 cM where linkage disequilibrium is unlikely to be maintained.

For the lines BW545, BW554, and BW588 a high proportion of the plants were homozygous wild type, which is not consistent with a 1:2:1 segregating population. One explanation for this lack of heterozygosity may be that the seed stocks were maintained as selfed individuals i.e. the original fertile lines would have been heterozygous or homozygous wild type (Robbie Waugh, personal communication). A portion of the seeds distributed from the seed stock could therefore be homozygous wild type for the trait of interest.

Table 5.4. Genotyping and germination result of first growth cycle. Only one letter is used to indicate the genotype of both SNPs where both SNP carried the same genotype. Where the SNPs differed, the genotype is indicated as SNP1/SNP2. Genotype code: B = Bowman, M = mutant, H, heterozygote, NA = Unsuccessful genotyping and (-) = missing plant.

Plant	BW545	BW546	BW554	BW579	BW588	BW591	Bowman
1	B/H	H/M	B	B/NA	B	-	B
2	B	H/B	B	B/NA	B	M/NA	B
3	B	H/B	B	H/NA	B	M	B
4	B	B/H	B	-	B	M	B
5	B	B	-	-	B/M	M	B
6	-	B	-	-	B	M/NA	B
Germination (%)	**60**	**60**	**40**	**30**	**60**	**50**	**60**

5.3.3 Phenotyping of physiology and fertility in selected BW-lines

To investigate the effect of the mutant introgressed region, plants from each line were phenotyped for a range of morphological and physiological traits. Height of main tiller, awn length, maturity of spikes and fertility among other traits were assessed post-anthesis (Zadok stage 70, (Zadoks et al., 1974)), relative to Bowman. Lines where no plants had been genotyped as homozygous mutant were not prioritised and only one plant was investigated for these lines, BW545, BW546, BW554, BW579, and BW588 (Table 5.5). Three Bowman plants were phenotyped as control as well as all five plants of BW591 genotyped as mutant for at least one of the markers associated with the male sterile trait. Due to the small sample size and lack of homozygous mutants it was not possible to determine if the observed differences were significant. However, differences in traits were used to select lines for further investigation.

There were minor differences in overall height and development progress between the individual plants where BW554-1 was slightly shorter than Bowman and had less developed spikes at the time of phenotyping. BW588-5 and BW591-2 out of all plants, including the BW591 lines, were taller and BW588-5 were more developed than Bowman (Table 5.5). Other physiological traits such as apparent waxiness, leaf necrosis, number of tillers, and plant stature for each plant were visually assessed to be similar to Bowman.

5.3.4 Analysis of anthers collected from sterile and fertile spikelets

Anthers were analysed directly after anthesis (Waddington stage 10, pollination (Waddington et al., 1983)). In plants with varying degrees of fertility multiple anthers from the different phenotypes were collected and imaged. Anthers from the fully sterile spike in BW554-1 was compared to anthers from a spike with both sterile and fertile spikelets. In the fully sterile spike (554-1A S) the anthers were significantly smaller compared to the sterile (554-1B S) and fertile (554-1C F) anthers of the semi-sterile spike (Figure 5.1), however, neither of the sterile anthers seemed to be releasing any pollen.

The anthers of the fully sterile BW579-3 (Figure 5.1) were elongated but had not swelled like the fertile anthers of Bowman and had not opened to release any pollen. In the homozygous mutant BW591-4 there was no noticeable difference between the sterile and fertile spikelets regarding size and rupture of the anther wall to release pollen. The sterile anthers of BW591-5 were longer than the fertile anther from the same spike but had opened to released pollen (Figure 5.1). The most significant difference between the spike morphology between the fertile and sterile spike was seen in BW591-6 where the sterile anthers were shorter and less swollen, the anther wall was not ruptured, and no pollen was released.

Table 5.5. Phenotypes and genotypes of individual plants of selected BW-lines. Each plant was phenotyped for plant height, growth stage of spike in late spike development, and fertility. Fertility was determined for some spikes by assessing the number of fertilised spikelets. BW579-3 was the only plant displaying complete sterility. Genotype given as wt (Bowman), het (heterozygous) and mut (non-Bowman) for either both SNPs or for SNP1/SNP2.

Line	Genotype	Height of main tiller (cm)	Growth stage of spike	Fertility
Bowman	wt	55	spikes almost out of last sheath	Yes
545-1	het	55	spikes fully in or half out of last sheath	Yes
546-1	het	45	spikes out of last sheath and filling	Yes
554-1	wt	40	spikes mostly in last sheath	1 sterile spike
579-3	het	50	spikes half in last sheath	No, full sterility
588-5	mut/wt	65	spikes have elongated peduncle	Yes
591-2	mut	75	spikes half out of last sheath, or with elongated peduncle	Yes
591-3	mut	55	spikes almost out of last sheath	Yes
591-4	mut	55	spikes half out of last sheath, or with elongated peduncle and many younger spikes	3-4 sterile spikelets in 3 spikes
591-5	mut	55	spikes almost out of last sheath	Yes
591-6	mut	55	spikes almost out of last sheath	2 sterile spikes

5.3.5 Spike development and seed set

Spike development and seed set was similar in all lines with a few exceptions in individual plants. Only BW579-3 displayed complete sterility even as heterozygote for only one associated marker (Figure 5.2). The plant was backcrossed to Bowman but it was not possible to rescue the sterility and no seeds were produced, suggesting that the plant might also have been female sterile.

Seed set was markedly reduced in BW554-1 and BW554-4, both genotyped as homozygous wild type for the SNP markers however the remaining BW554 lines with identical genotypes had seed sets comparable to Bowman (Figure 5.2). The markers associated with the mutant trait in the BW554 line flanks a region of 401.3 Mbp/18cM which spans most of chromosome 2H (Table 5.1). Due to its size the region is vulnerable to linkage disequilibrium decay meaning that individual plants could carry different sizes of introgressed regions contributing to differences in phenotypes. More markers in the introgressed region are necessary to accurately genotype and track the underlying trait for the mutant phenotype.

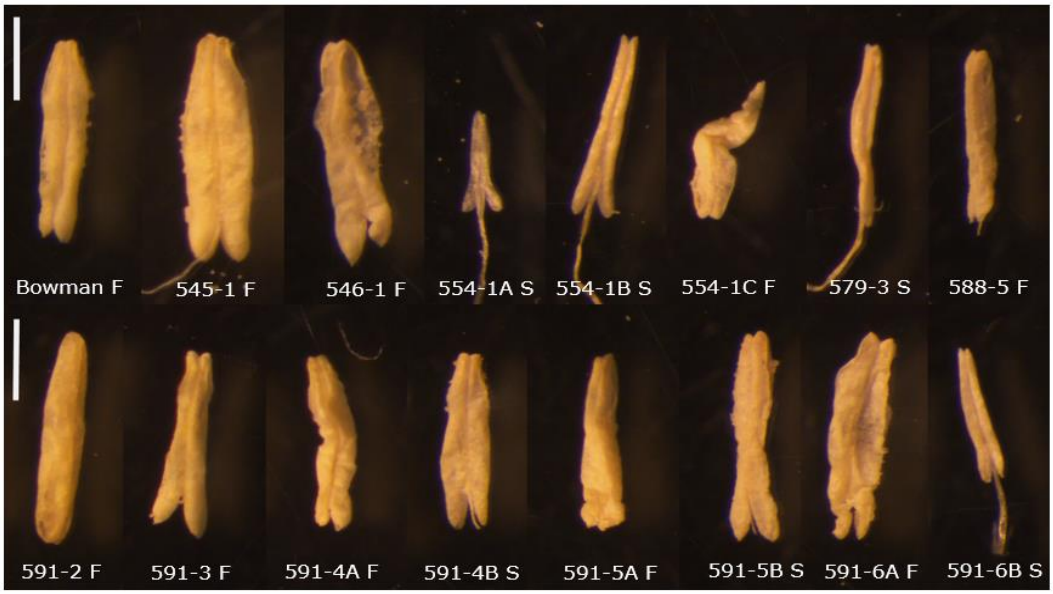

Figure 5.1. Anthers collected from spikelets of individual plants of different BW-lines. From each plant five anthers were collected from different spikes and a representative anther is shown. Anthers are marked as sterile (S) or fertile (F) after the line name, where anthers coming from the same plant but of different fertility are marked A, B, C. Scale bar 1 cm.

5.3.6 Effect of heat stress on sterility

To investigate the reduced seed set seen in BW554-1 in the first growth cycle, the progeny of this plant was subjected to a short heat stress in controlled conditions to replicate the heat stress event in the greenhouse in the first growth cycle. In early spike development in the first growth cycle with BW554-1 there was a period of elevated temperatures due to a heat wave in the greenhouse. This heatwave, where temperatures, were raised to 30˚C daytime from the normal 20-25˚C conditions, lasted for 3 days and might have influenced fertility, possibly causing the reduction in seed set seen in BW554-1. Heat stress during spike development and flowering could severely impact cereal reproduction and lead to loss of yield (Barnabás et al., 2008).

The timing of the increased temperature in the early spike development was thought to have caused some of the observed partial sterility in the BW-lines. A temperature-controlled experiment was performed where plants were grown in a growth room at constant 15˚C before a three-day heat stress of 30˚C and compared to plants grown in greenhouse conditions at 20-25˚C. Seeds from BW554-1 were selected due to its reduced seed set. BW591-6 seeds were also tested as this line had been genotyped as mutant and had the lowest seed set among the BW591 plants.

In all growth conditions BW591-6 had the highest seed set with no noticeable difference between Bowman and BW554-1. All lines showed an increase in seed production when grown at 15˚C with a subsequent decrease in fertility after the three-day heat stress for Bowman. This lack of reduction in heat stress in the BW554-1 and BW591-6 lines indicate that the heat stress event during the first growth cycle might not have been the cause for the reduction in fertility (Figure 5.3). No other change in morphology was noted.

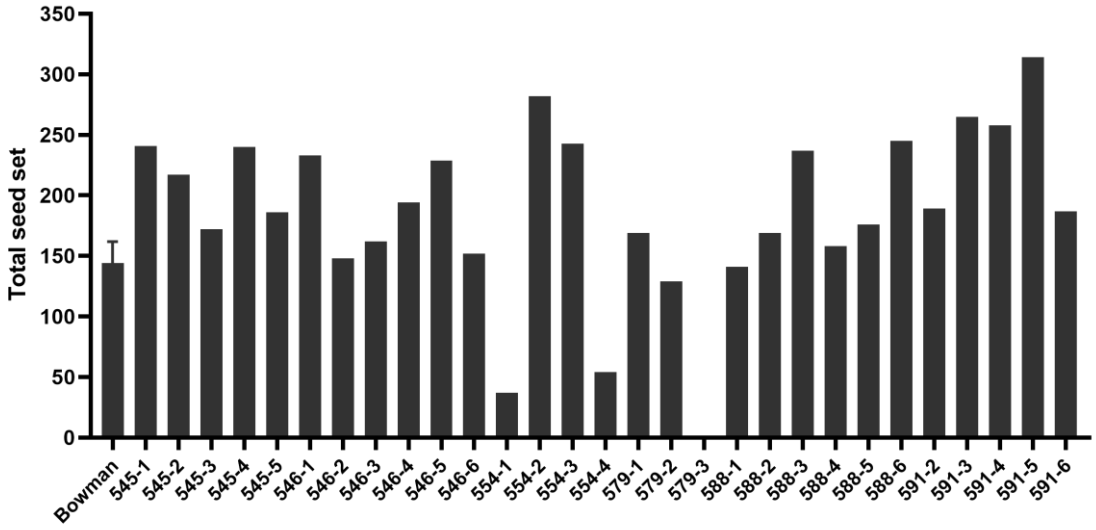

Figure 5.2. Total number of seeds produced per plant. BW554-1 and BW554-4 has a significantly reduced seed set compare to Bowman and remaining BW554 plants. Only BW579-3 displayed total sterility with no seeds produced.

5.3.7 Identification of additional markers using a 50k genotyping array

To further map the region containing the male sterile trait the lines were screened with 16,376 markers in the 50k Illumina Infinium iSelect genotyping array at RAGT Seeds Ltd. DNA from an individual plant from each line was used to screen for introgressed regions in the Bowman background and possibly identify new markers associated with the male sterile trait. Due to a lack of phenotype in most plants the marker array was used to detect if any non-Bowman regions were present and whether these could be used for further investigation or be found to not influence fertility.

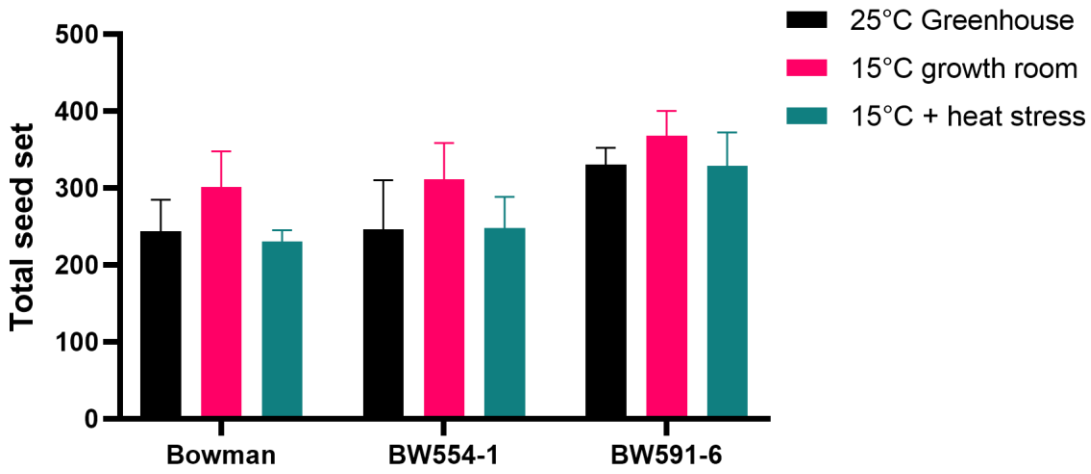

Figure 5.3. Seed set of Bowman, BW554-1 and BW591-6 at three growth conditions. Highest seed set for all lines were seen in plants grown in 15˚C with Bowman showing a slight reduction after a period of heat stress. The BW554-1 and BW591-6 were not significantly affected by the heat stress.

Plants were selected for screening based on previous genotyping in the first growth cycle, where mutant genotypes for at least one marker were favoured, i.e., BW545-1, BW546-1, BW579-3, BW588-5, and BW591-6 (Table 5.4). Where all plants displayed a homozygous wild type (Bowman) genotype the plant with the lowest fertility was selected to investigate if any introgression was present in the genome i.e., BW554-1 (Figure 5.4).

Individual plants from the different lines were compared to Bowman to identify introgressed regions. New markers genotyped with a non-Bowman genotype were considered to be introgressed along with the mutant trait from the cultivar that carried the original mutant phenotype. Markers with a non-Bowman genotype were identified in all lines except the homozygous wild type BW554-1, indicating that no introgression was present in this line. The non-Bowman markers identified in the remaining BW-lines were almost exclusively located in the region around the SNP1 or SNP2 for each line, previously predicted to contain the mutant trait by Druka et al. (2011).

Using allele specific PCR the BW545-1 was genotyped as Bowman for SNP1 and heterozygous for SNP2 which was partly confirmed with the additional markers. SNP1 was not included in the 50k array however SNP2 and all 11 markers between and surrounding the region of SNP1 and SNP2 were identified as heterozygous. In total a region of 27Mbp was identified as non-Bowman in heterozygous form for BW545-1 indicating that the progeny of BW545-1 could be segregating for the mutant trait (Figure 5.4).

In the sterile BW579-3 a large region of non-Bowman genotype was identified on chromosome 3H between the associated SNP1 and SNP2 (Figure 5.4). Here the SNP1 was confirmed to be heterozygous and the SNP2 to be homozygous non-Bowman which had not been determined in previous genotyping. In the 50k array 468 new markers were identified in this region with an overall 3% difference in marker genotype. An additional 22% difference was found for heterozygous markers between BW579-3 and Bowman. This shows that a large region had been introgressed into the Bowman background which could contain the sterility trait and could be mapped further. Unfortunately, no seeds were produced from this plant however other seeds in the seed stock could carry similar introgressions.

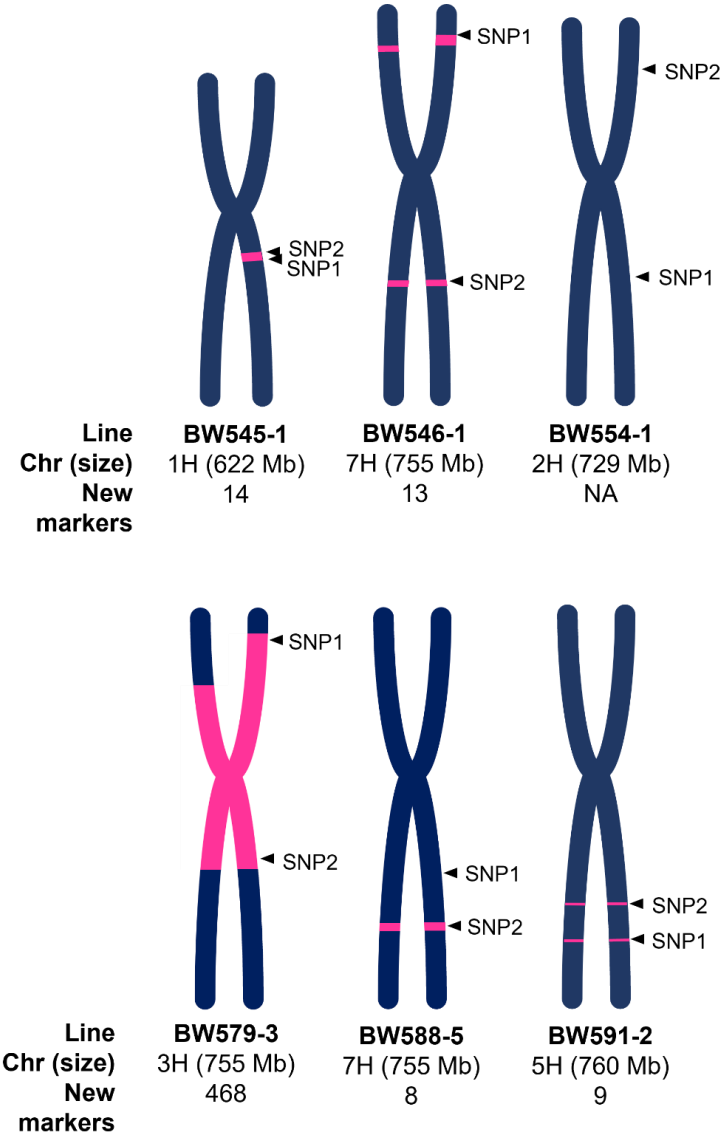

Figure 5.4. Overview of introgressions on the affected chromosomes in individual plants of the BW-lines. Plants were screened with the 50k array for markers with a non-Bowman genotype to identify new markers for further mapping of the male sterile trait. The locations of the SNP1 and SNP2 associated with the mutant traits are indicated on the chromosomes where the Bowman genotype is marked in blue and non-Bowman is marked in pink. The new markers were identified within the region corresponding to the non-Bowman (pink).

The BW546-1, BW588-5 and BW591-2 were genotyped as homozygous mutant for at least one of the associated SNPs through allele specific PCR. This was confirmed with the 50k array where small regions of non-Bowman were identified as introgressed at the site of the associated markers in these plants (Figure 5.4). However, the region between these markers were exclusively of the Bowman genotype. It is possible that the mutant donor is identical with Bowman in this region and therefore cannot be detected, or there has been two smaller introgressions, or recombination events at the location of the associated markers. However, since there was no sterile phenotype for BW546-1, BW588-5, and BW591-2 the homozygous non-Bowman markers, i.e. BW546-1 SNP2, BW588-5 SNP2, and both SNPs for BW591-2, could be assumed to no longer be linked with the sterile trait. Additionally, in lines where the region between the SNPs were wild type, i.e. BW546, BW588, and BW591, any fine mapping of the region is made difficult due to lack of markers linked to the mutant trait.

5.3.8 Screening of fertility in segregating lines

Due to the small sample of available seeds and low germination, the fertility of the BW-lines could not be accurately determined in the first growth cycle. It was also not possible to detect a fully introgressed region for both associated markers in BW545, BW554 and BW588 with only some mutant genotypes detected in the remaining lines. Therefore, additional seeds were requested from NordGen for all lines however only BW545, BW546, BW579, BW588 were available. These seeds were planted to screen for any observable sterility. However, no consistent sterility was observed and there was no reduction in seed set for any of the lines.

BW545-1 had been genotyped as heterozygous for SNP2 with a 27 Mbp confirmed introgressed region between SNP1 and SNP2. To investigate whether this region could influence fertility in homozygous form the progeny of the segregating BW545-1 was analysed. The homozygous BW545-2 and Bowman were used for controls however none of the lines were genotyped due to COVID-19 lab closure. Instead, fertility was assessed by seed set where only a slight reduction was found in the progeny of BW545-1. All plants, eleven from BW545-1, twelve from BW545-2 and three from Bowman, were able to set seeds indicating that none of the lines were fully male sterile. It is possible that none of the plants were homozygous mutant or that the trait only confers partial sterility. The lines could be investigated further with more plants or for the cause of partial sterility in flower development.

5.4 Discussion

5.4.1 Mutation breeding and the sensitivity of male reproductive fertility

The BW-collection of mutations has been used for the identification and investigation of multiple genes affecting general morphological traits in addition to having increased the understanding of the inflorescence development in barley. Usage of the BW-lines has led to the identification of new alleles of *DISRUPTED MEIOTIC cDNA 1* (*HvDMC1*) in the developing inflorescence (Colas et al., 2019), increased knowledge of the pleiotropic effects of *SIX-ROWED SPIKE* and *CENTRORADIALIS* due to the interplay of alleles (Bi et al., 2019; Bull et al., 2017) and to the identification of the barley *BLADE-ON-PETIOLE 1* and *2* involved in spike architecture (Jost et al., 2016). The comparisons of mutations from different sources in a common genetic background has simplified the analysis of the effect of individual mutations.

Identification of male sterile traits from mutant collections can be especially difficult due to the influence of abiotic factors and the sensitivity of the reproductive development. Pollen development requires an intricate machinery of genetic components and environmental cues to form viable pollen. The fertility of the stamens in a variety of plants is particularly vulnerable to abiotic stresses such as heat, drought, and photoperiod (Chen & Liu, 2014; Kim & Zhang, 2018; Smith & Zhao, 2016). Finding the underlying genetic component behind the male sterile trait from a population of spontaneous mutants could therefore be difficult as the sterility could be strongly dependent on growth conditions.

5.4.2 Lack of mutant genotypes in the seed stock

In this study selected BW-lines in the male sterile genic (msg) mutant category at the NordGen seed bank were analysed for male sterility. Mutants in the msg category had been classified as carrying a recessive male sterile trait, i.e. it is maintained as a fully fertile heterozygotes (Franckowiak et al., 2015). For the analysis of these lines 10 seeds were provided per line from NordGen. In general the germination rate was low in the first growth cycle, 30-60%, possibly due to the effect of REDIGO PRO, a fungicide which can cause germination inhibition (REDIGO PRO SDS, Bayer). Out of the seeds that germinated few seeds carried a mutant genotype or displayed male sterility which prevented further analysis of this trait in the mutant lines. Only one plant, BW579-3, genotyped as having a large introgression of non-Bowman DNA on chromosome 3H, exhibited sterility however it was not possible to rescue the fertility with pollen from Bowman resulting in loss of the line.

The plants were genotyped using allele specific PCR, where primers were designed to only amplify one allele, either the Bowman or the mutant allele. However, the primers designed for the mutant alleles could not be accurately tested for the lines were no mutant genotype was present for one or both of the associated SNPs, which was the case for BW545, BW554, BW579 and BW588. Individual plants from these lines were instead genotyped through sequencing which confirmed there was no mutant allele present. Therefore there was no positive control to ensure the primers for the mutant alleles were working properly for

screening of the plants in subsequent generations. Due to the cost of sequencing multiple plants for two markers, and due to the lack of a sterile phenotype, the genotyping was only carried out in the first generation.

Lines genotyped as heterozygous for at least one of the associated markers were analysed in a subsequent generation to possibly identify homozygous mutant genotypes. This second generation was not genotyped as no sterility was found. It is possible that there were no homozygous mutants in this population and that is why no fully sterile phenotype was identified.

To explain this lack of male sterile phenotypes in the mutant lines it is important to consider how the lines were generated, mapped, and maintained. The BW-lines were generated by repeated backcrosses of the mutant lines with Bowman, where homozygous mutants were used for phenotyping and mapping with SNPs (Druka et al., 2011). The stocks provided by NordGen are maintained as selfed series of the fertile plants i.e. they contain homozygous wild types and segregating heterozygotes (Robbie Waugh, personal communication). It is possible that the majority of the seed stock consists of homozygous Bowman seeds with only some heterozygous mutant lines in the population. This together with the low amount of seeds provided for analysis and low germination rate could explaining why plants from BW545, BW554 and BW588 were genotyped with a high proportion as homozygous Bowman.

5.4.3 Temperature induced sterility

During early spike development in the first growth cycle there was a period of three days of high temperature and drought. Severe heat stress during early pollen development has been shown to be detrimental for barley spike reproduction and induces sterility (Abiko et al., 2005; Barnabás et al., 2008; Sakata et al., 2000). Some of the sterility in the homozygous wild type BW554-1 and BW554-4, was believed to have been caused by the heat stress event since the wild type Bowman was unaffected and fully fertile. Among the homozygous mutant BW591 plants the BW591-6 had the lowest seed set and was also included in the heat stress experiment to determine if the mutant phenotype in this line could be enhanced by a heat stress event.

To test this hypothesis the progeny of BW554-1 and BW591-6 were subjected to three different growth conditions, constant 15˚C, constant 15˚C with three days at 30˚C and no irrigation, and 20-25˚C greenhouse conditions. However, only Bowman showed a significant decrease in seed set after the heat stress indicating that the temperature change in the first growth cycle might not have affected the seed set in the BW554-1 and BW591-6 lines.

One possibility for this lack of repeated display of sterility in BW554-1 which carried a mutant introgression could be that the heat stress was too short or applied at the wrong

stage. The stage of when the heat stress is applied is crucial for the plants ability to handle the stress. In a comparison of heat stress applied at different stages Sakata et al. (2000) showed that the barley spike is most sensitive to heat from early stage until meiosis of pollen mother cells but at later stages the plant was able to partially recover fertility. It is possible that the BW-lines were exposed to the heat stress too late in development. Additionally, the overall higher temperature in the greenhouse over a prolonged time might have weakened the plants making them more susceptible to the heat stress.

5.4.4 Identification of new markers for fine mapping of the mutant region

Using the 1k Illumina GoldenGate array the mutant traits were mapped to specific regions in Bowman with genetic material from the original donor (Close et al., 2009; Druka et al., 2011). The markers used for the genotyping of the msg lines had a low density and the regions associated with the sterility trait, especially in the BW546, BW554, and BW579 lines, flanked regions of substantial sizes increasing the possibility of recombination events occurring between the markers and breaking up the region. This decay of linkage disequilibrium between associated markers could explain the difference in genotype between SNP1 and SNP2 in some lines.

Despite the lack of a male sterile phenotype in most lines, individual plants were screened with more markers to estimate the level of a non-Bowman genome introgressed into the lines. One plant from each line that was homozygous mutant, heterozygous for one or two markers, or displayed some degree of sterility was genotyped with the 50k Illumina Infinium iSelect genotyping array at RAGT Seeds Ltd. For all lines, except for BW544 where no non-Bowman markers were found, it was possible to identify more markers in the region predicted to contain the mutant trait.

It is possible however that some markers associated with the mutant trait were not detected if the marker carried the same genotype for the introgressed region and Bowman. The genomic background of the donor of the mutant allele could be highly similar to Bowman however due to lack of pedigree information available on the mutant donors Clho 5368, Compana, Betzes and Berac (Table 5.1) it is difficult to determine the overlap of the Bowman and donor genome. The 50k Illumina genotyping array might not be specific enough to distinguish between the genomes however the new markers that were identified for some the lines could be a useful resource for further mapping of the trait of interest if a strong male sterile phenotype could be identified.

The plant BW579-3 was the only plant identified to be completely sterile; both female and male fertility was affected with no viable seeds produced. The fully sterile plant BW579-3 was genotyped and shown to contain a large proportion of non-Bowman DNA on

chromosome 3H with most of the region being homozygous for the non-Bowman markers. It is therefore possible that the trait conferring sterility was present in homozygous form and was located in the region identified to contain non-Bowman DNA in homozygous form. Further screening of this line with more seeds could be useful for the identification of additional sterile plants.

5.4.5 Conclusion

The use of collections of mutant NILs is a good source of novel traits, however male sterility is affected by numerous biotic and abiotic components and is therefore difficult to characterise. A clear phenotype is essential for the mapping of the region containing the male sterile trait to narrow down the potential candidate genes that could infer the male sterile trait. Different conditions could be tested for the lines however the initial phenotype was identified in similar conditions as in this study where no stable phenotype was detectable. It is possible that the mutant trait is no longer present in the seed stock due to the maintenance of only fertile plants or it is present in only a small proportion of heterozygotes. Further screening of a large amount of seeds in several generations would be required to identify and map any potential male sterile traits.

Chapter 6. Genome-wide association studies of anther length and extrusion in hexaploid winter wheat

6.1 Introduction

6.1.1 The use of anther traits in hybrid breeding

Hexaploid bread wheat is principally self-pollinating, retaining pollen within the cleistogamous floret. For hybrid seed production an effective pollen donating parent is required with good pollen production and shedding qualities (Boeven et al., 2018; Whitford et al., 2013). One way to estimate the pollen donor quality of a plant is to measure anther length and anther extrusion. Anther size is used as an estimate for pollen production due to a positive correlation between the length of the anther and pollen number and mass (Beri & Anand, 1971; De Vries, 1974; Milohnic & Jost, 1970; Nguyen et al., 2015). Pollen shedding outside of the floret has been attributed to filament length and anther extrusion as florets with longer filament and more extrusion result in more outcrossing (Beri & Anand, 1971; Muqaddasi et al., 2016; Muqaddasi, Pillen, et al., 2017). As a self-pollinator, bread wheat has relatively small anthers and a low production of pollen, making it hard to find cultivars with good pollen donor traits for hybrid breeding (Nguyen et al., 2015). Identifying the underlying genetic component of anther length and anther extrusion is therefore of interest for future breeding.

Anther extrusion is the combination of the floret opening and the elongation of the filament and is responsible for the spreading of pollen outside of the floret (Pinthus & Levy, 1983a). Anther extrusion is a promising trait for breeding as it is highly heritable and has been shown to be controlled by multiple loci with varying effect (Boeven et al., 2016; Buerstmayr & Buerstmayr, 2015, 2016; He et al., 2016; Lu et al., 2013; Muqaddasi et al., 2016; Muqaddasi, Pillen, et al., 2017; Skinnes et al., 2010). This complexity in anther traits is further displayed by the intricate correlation of other traits tied to pollen production and spreading.

Anther extrusion have been found to be linked with higher resistance to Fusarium head blight (Buerstmayr & Buerstmayr, 2015) and anther length has been shown to be positively correlated to grain weight (Song et al., 2018). Previous studies have also found a connection between anther length and extrusion, pollen grains per anther, and pollen mass (Langer et al., 2014; Milohnic & Jost, 1970; Nguyen et al., 2015). In addition, some studies have found a positive correlation between plant height and pollen mass in wheat (Langer et al., 2014) and between plant height and pollen shed outside of the floret (Beri & Anand, 1971) however it remains to be confirmed in further studies. These potential correlations between anther length, extrusion, and plant height and the understanding of the complexity of the genetic background controlling anther traits is of importance to understand wheat floral biology.

6.1.2 Genome wide association study in diverse wheat populations for identification of markers associated with anther traits

To investigate the complexity of anther traits in wheat, and potentially identify the underlying genetics behind anther properties, three different populations were analysed in genome-wide association studies (GWA studies). GWA studies are essential tools for genomic research and are used to identify loci associated with a trait and estimating the effect of the loci on the trait of interest. In the last decade GWA studies have been used for the detection of the underlying genetic component of biotic and abiotic stress responses as well as quality traits of importance for agronomic traits and yield (Saini et al., 2022a). Previous studies of anther length and extrusion has led to the identification of loci of interest however differences in germplasm origin or marker density appear to influence the outcome (Adhikari et al., 2020; El Hanafi et al., 2021; Muqaddasi et al., 2016; Muqaddasi et al., 2017; Song et al., 2018). Further association studies and analysis of population structure are needed to confirm if previously identified regions are involved with anther traits and if there is genetic diversity in wild relatives that can be used for breeding in elite cultivars.

6.1.2.1 Wheat populations used for GWAS

The populations used for the GWA studies are summarised in Table 6.1 and were selected for analysis based on population structure and level of genetic diversity. The Yellowhammer population consists of 427 elite winter wheat varieties compiled by a consortium led by the National Institute of Agricultural Botany (NIAB) with the intent to contain as much diversity as possible in terms of disease resistance, mainly yellow rust resistance. The germplasm is mainly European, with a strong representation of variates developed in the United Kingdom. The population was genotyped with the 35k Axiom wheat breeders array, containing 35 143 single nucleotide polymorphism (SNP)- based markers specifically designed to detect genetic differences between elite hexaploid wheat (Allen et al., 2017).

The Piko x Julius (PxJ) population is a bi-parental mapping population generated by KWS UK to map anther extrusion. Piko has been used extensively as the pollen donor in hybrid breeding programs due to its long anthers and high anther extrusion (Boeven et al., 2018) whereas KWS Julius is an elite variety with low to average anther extrusion. Bi-parental mapping populations are a relatively simple way to map traits of interest (Singh & Singh, 2015). By crossing two inbred, highly homozygous lines with diverging phenotypes, the location of the quantitative trait loci (QTL) behind the trait can be mapped. With a normal rate of recombinations of about one or two per chromosome the number of markers needed to detect QTLs can be as low as a few hundred however, due to the low number of recombinations, the bi-parental populations have low mapping precision (Scott et al., 2020).

The third population used for GWAS was the Breeders Observation Panel (BOP). The 95 lines in the BOP were generated by introgression of the wheat wild relatives *Amblyopyrum muticum* and *Triticum urartu* into elite wheat varieties to increase the genetic diversity of the hexaploid wheat genome (Grewal et al., 2021; Grewal et al., 2018; King et al., 2017, 2019). Hexaploid wheat was formed via two hybridisation events – *T. urartu* (AA genome) x

Ae. speltoides (BB genome) followed by the tetraploid x *Ae. Tauschii* (DD genome) (Marcussen et al., 2014). The genomic diversity in the modern day wheat is therefore a result of only 10 000 years of genomic mutation and some outcrossing to e.g. tetraploid wheat (Charmet, 2011). The lack of genetic diversity in modern wheat has been identified as a significant problem for future breeding opportunities (King et al., 2017; Winfield et al., 2016). Generation of introgression lines through the recombination with alien wheat relatives could introduce more genetic diversity in the wheat genome, however identification of introgressions relies on screening with markers for alien material.

Table 6.1. Summary of populations used in the GWA studies of anther traits. Three populations, the elite cultivars of Yellowhammer, the bi-parental mapping population Piko x Julius, and the alien introgressions of BOP, were individually screened with population specific markers. Yellowhammer was sampled in 4 replicates and genotyped by the consortium with the 35k Axiom array. Piko x Julius was generated and genotyped with markers from the Axiom array by KWS UK and sampled in two consecutive generations. Three replicates of BOP was sampled with genotyping conducted by Grewal et al., (2020, 2021a, 2021b) and King et al (2017).

Population name	**Type of population**	**Sampling location**	**Year sampled**	**Measured traits**	**Number of lines**	**Markers**
Yellow-hammer	Elite varieties	Field trial at KWS UK and RAGT UK	2020 and 2021	Anther length, anther extrusion, plant height	427 lines	19704 SNP markers from the Axiom 35k array
Piko x Julius	Bi-parental mapping population	Greenhouse at KWS UK	2018 and 2019	Anther length	475 plants	2113 SNP markers
Breeders observation panel	Alien introgression	Field trail at KWS UK and Limagrain UK	2020 (partial) and 2021	Anther length, anther extrusion, plant height	32 *A. muticum* + 63 *T. urartu*	484 + 115 KASP markers

6.1.2.2 Genotyping of the wheat populations

Differences in marker coverage, marker type, and genotyping method can influence the outcome of GWA studies. Suitability of the genotyping platform for the detection of significant associations depends on i) the specificity of the markers, ii) whether they detect differences between elite variates or between wheat wild relatives, and iii) of the density and chromosome coverage of the markers. Each population was genotyped with a different set of markers based on availability and suitability to the population structure.

6.1.2.2.1 35k Axiom elite cultivar markers used in the Yellowhammer population

The Yellowhammer population consisted of 427 elite cultivars chosen for their diversity in disease resistance. The breeding of elite hexaploid bread wheat has resulted in a lack of genetic diversity and difficulties in identifying molecular markers to detect any variation. The Breeders 35k Axiom array was specifically designed for the genotyping of elite varieties (Allen et al., 2017) and is publicly available at CerealsDB (https://www.cerealsdb.uk.net/cerealgenomics/CerealsDB/indexNEW.php).

6.1.2.2.2 KASP markers for the alien introgression lines in BOP

The BOP consists of lines with two different types of alien introgression where two wild relatives, *A. muticum* and *T. urartu*, were independently crossed to hexaploid wheat (Grewal et al., 2021; King et al., 2019). The lines were genotyped with Kompetitive allele specific PCR (KASP) markers specifically designed to detect polymorphisms between the wild relative and wheat (Grewal et al., 2020, 2021a, 2021b; King et al., 2017).

The KASP markers used to genotype the lines were specifically designed to capture the individual wild relative genomes, i.e. the *A. muticum* lines were not genotyped with the markers for *T. urartu* and vice versa (Grewal et al., 2020, 2021a, 2021b; King et al., 2017). The *A. muticum* and *T.urartu* lines in the BOP were therefore treated as separate populations resulting in small sample sizes and few markers, reducing the statistical power of any associated markers (

Table 6.2). However, the population carries a lot of genetic diversity which previously has not been analysed for anther traits. In addition, the lines were backcrossed three times to hexaploid wheat cultivars to generate relatively homogenous backgrounds and multiple lines carrying similar or equal introgressed regions (Grewal et al., 2021a; King et al., 2019). The population is therefore of interest to detect genetic diversity currently not present in the modern hexaploid wheat.

	Markers	**Anther length (NOBS)**			**ANTHER extrusion (NOBS)**		
Population	**Total**	**KWS**	**LG**	**Total**	**KWS**	**LG**	**Total**
A. muticum	484	68	27	95	30	62	92
T. urartu	154	134	58	192	31	60	91

Table 6.2. Markers and phenotype observations in the BOP. The A. muticum and T. urartu populations were treated as separate populations due to differences in species specific markers and number of observations. NOBS: number of phenotypic observations.

	Markers	Anther length (NOBS)			Anther extrusion (NOBS)		
Population	**Total**	**KWS**	**LG**	**Total**	**KWS**	**LG**	**Total**
A. muticum	484	68	27	95	30	62	92
T. urartu	154	134	58	192	31	60	91

6.1.2.2.3 Markers for the Piko x Julius population

The PxJ population was phenotyped as two consecutive generations (F4 and F5) however these generations were not genotyped. These plants had been selected based on anther traits in previous generations and had been genotyped as homozygous in QTL regions of interest after repeated selfing. The lines collected had varying sizes of recombined regions and were genotyped with 2113 markers in the F3 generation with further fine mapping with 19 markers in 6 different regions of interest. Additional markers were used in regions on chromosomes 1B, 3A, 3B, 4D, 5B and 5D as these regions were hypothesised to contain QTLs involved in anther length based on preliminary studies carried out by Nicholas Bird at KWS UK. The following generations (F4 and F5) were not genotyped since the regions of interest were identified as fixed and only the background segregated (Nicholas Bird, personal communication). Every line was assumed to have the same genotype in all generations, e.g. marker data from PxJ_10H was copied to all subsequent PxJ_10H derivates. This approach assumes no crossover or segregation occurred in later generations e.g. 10H-3 or 10H-3-2, and adds identical values for all replicate lines derived from the same original cross. Piko is not one of the elite variates included in Yellowhammer but KWS Julius is part of the population and was genotyped with the 35k Axiom array. It is therefore interesting to compare the markers identified in both populations to further validate the associated regions.

6.1.2.3 The importance of model and method selection for GWAS

6.1.2.3.1 GWAS models

In GWA studies the markers spread throughout the genome are analysed for association with a phenotype by a regression analysis for each individual marker. This process is computationally intensive which has created a need for models that improve computational efficiency and statistical accuracy of predicted associations (Huang et al., 2018). For the selection of statistical methods used in a GWAS it is important to consider the conditions in the underlying algorithms for the accuracy of the identification of associated markers.

The traditional Mixed linear model (MLM) requires intense calculation power but are proven to be effective in analysing population structure by taking into account relatedness and

other factors that might skew results (Zhou & Stephens, 2013). In this method markers are tested against the confounded kinship in the population and is very computationally intensive (Zhou & Stephens, 2013). All the methods that improves computational speed has similar or the same statistical power as MLM since it is based on kinship but calculated differently (Huang et al., 2018).

BLINK is one of the most recent models developed to increase statistical power and decrease computation time (Huang et al., 2018). The model is a multi-loci test method that works on markers instead of bins by adding linkage disequilibrium information, markers that are in strong disequilibrium with the most significant markers are excluded, and kinship is not derived from markers (Huang et al., 2018).

In BLINK these properties exclude the assumption that associated markers are evenly distributed across the genome, which is assumed in other models, and together this leads to more statistical power, reduction of false negatives and positives, and increased speed compared to previous methods (Huang 2018). In an evaluation of models used for GWAS in wheat, BLINK is superior, however due to its recent release it has not been applied in other GWAS studies on anther traits (Saini et al., 2022a; Wang & Zhang, 2020). BLINK has been implemented in the Genomic Association and Prediction Integrated Tool (GAPIT) software package which is widely used to perform GWAS, genomic predictions and to compare and select the best model for the available data (Wang & Zhang, 2020).

6.1.2.3.2 Principal component analysis for population structure

As part of a GWAS a principal component analysis (PCA) is conducted. PCA is a tool to reduce the dimensions in a large set of variables while retaining the most amount of information to estimate population structure and sample ancestry in genetic datasets (Price et al., 2006). The purpose of PCA is to reduce the number of variables of a data set while preserving as much information as possible by grouping potentially correlated values into uncorrelated variables, principal components (PCs).

In this study wheat populations were screened for anther extrusion and anther length to identify the underlying genetic component controlling these traits. Molecular markers were used to detect loci associated with anther traits for use in future hybrid breeding. Genetic diversity in European elite bread wheat and the correlations between anther extrusion, anther length and plant height were investigated. This constitutes the most detailed analysis of anther length in hexaploid wheat that has been conducted.

6.2 Materials and methods

6.2.1.1 Growth conditions and field trials

The Yellowhammer and the Breeders observation panel (BOP) were grown in field at the breeding companies KWS UK and RAGT Ltd in Cambridgeshire, UK, and at Limagrain Ltd in Suffolk, UK. Lines were grown in randomised plots in two-rowed (at RAGT Ltd) and five-rowed (at KWS UK) observation plots and were sampled in May-June of 2020 and 2021. The Piko x Julius (PxJ) population were grown in pots in greenhouse at KWS UK. PxJ was sampled in June 2018 and in May 2019 by KWS (Nicholas Bird). Field trials were treated according to local best practice.

6.2.1.2 Phenotyping of anther traits

6.2.1.2.1 Anther length measurement

Anthers from each line were collected just before the onset of anthesis when the anthers turned yellow but had not yet released pollen. Anthers from 4-5 spikelets on 2-3 spikes were collected with a minimum of 10 anthers per line. The anthers were collected from the middle section of the spike from the lateral florets and placed in Clarke's solution fixative of 75% (v/v) ethanol and 25% (v/v) acetic acid (John-Bejai, 2017). Anthers were imaged with a stereomicroscope (Stemi SV 6, Zeiss IV, Germany) where 9-15 anthers were measured for each line and replicate, and analysed with ImageJ 1.52a (National Institutes of Health, USA) (Schneider et al., 2012).

6.2.1.2.2 Anther extrusion

Anther extrusion was estimated by counting anther retention per floret. From each line five spikes were collected after anthesis but before the seed was bigger than a third of the floret. The spikes were kept at 4˚C until analysed to prevent drying. In bread wheat each floret forms three anthers and the level of anther extrusion was assessed by counting the remaining anthers in each floret and subtracting the retained anthers from the maximum of three. For each spike the outermost two florets of the middle six spikelets were counted. Anther extrusion was averaged in five spikes over 12 spikelets (in 2020, total of 60 spikelets) and 6 spikelets (in 2021, total of 30 spikelets) for each line and calculated as percentage of missing anthers.

6.2.1.2.3 Plant height

Each observation plot was measured for plant height at KWS UK and Limagrain by the respective company. Height data was recorded for Yellowhammer 2020 and 2021 at KWS UK, and for the BOP at KWS in 2021 and Limagrain in 2021.

6.2.1.3 Population analysis and GWAS

6.2.1.3.1 Statistical analysis

To estimate the fixed effect of the genotype on a trait it is important to account for the random effects of differing growth conditions in different trials and years (Bradshaw, 2016). This can be done by calculating Best Linear Unbiased Estimator (BLUE) values for each genotype and trait to account for non-genetic variance in replicates in different sampling locations and years. The BLUEs were calculated using the Linear Mixed Models function in the Mixed Models (REML) in GenStat (Version 21.1, 2020, VSN International) where genotype was treated as fixed effects and sampling year and site as random effects. Genetic, residual, and sampling variances for anther length and anther extrusion in the different populations were calculated in the lmer4 R package (Bates et al., 2015).

Correlations between anther traits and plant height were estimated with Pearson's correlation coefficient in R, gglot2 package (Wickham, 2016), which compares the ratio between the covariance of two variables and the product of their standard deviations.

The coefficient of additive genetic variance (CV_A) was calculated to estimate genetic variability in the traits of interest using Equation 6.1:

$$CV_A = \frac{\sqrt{V_A}}{\bar{X}}$$

where V_A is additive genetic variance and $\bar{X}$ is the estimated mean (BLUEs) of the trait (Houle, 1992).

Broad sense heritability, which estimates the effect of the genotype on the phenotypic variation, for each trait was calculated using the BLUE values for each line with Equation 6.2:

$$h^2 = \frac{\sigma_G^2}{\sigma_G^2 + (\sigma_e^2/n)}$$

where σ_G^2 is the genotypic variance, σ_e^2 is the residual variance, and *n* is the number of independent replicates (Gioia et al., 2017).

Principal components analysis (PCA) for the estimation of population structure was carried out with the built in feature of R package GAPIT (3.0) (Wang & Zhang, 2020). The PCA of GAPIT was used to determine the optimal number of PCs to use for each population.

6.2.1.3.2 GWAS

Association analyses were performed using the BLINK and MLM algorithms implemented in GAPIT R package (3.0) (Huang et al., 2018; Wang & Zhang, 2020). The GAPIT model selection was used to determine the optimal method for analysis where BLINK was selected for all

analyses except for both anther traits for BOP *T. urartu* where MLM was a better fit for the data. Quality control of the genotyping data was carried out to reduce the risk of false positives. SNPs with low call rates, SNPs displaying rare variants, and individuals with a lot of missing data are commonly removed (Pavan et al., 2020). SNPs with a low rate of alternative alleles may be due to genotyping errors or the loci might be rare enough that there is no statistical power of any association to these loci. Minor allele frequency was set to <0.05, and markers with >10% missing data were removed (Pavan et al., 2020). The significance level for associated markers was determined by the Bonferroni correction where the p-value limit (0.05) is divided by the number of SNPs (Table 6.3). This significance level was used to avoid false positives however this stringent approach could exclude true discoveries. As a complement the false discovery rate (FDR) adjusted p-value was calculated using the built in function in GAPIT 3.0 (Wang & Zhang, 2020). This reduces the number of false negatives and positives by calculating the expected proportion of false positives among all the positive markers (Benjamini & Hochberg, 1995).

Table 6.3. Significance level threshold determined by Bonferroni correction and false discovery rate (FDR) for associated markers identified through GWAS.

Population	Significance level	FDR-adjusted level
Yellowhammer	2.77E-06	2.63E-05
Piko x Julius	2.54E-05	8.88E-05
BOP A. muticum	1.59E-04	6.49E-04
BOP T. urartu	3.25E-04	5.56E-04

6.2.1.3.3 Molecular markers used to genotype each population

Genotyping of the Yellowhammer population was conducted by a consortium led by the National Institute for Agricultural Botany (NIAB) using the Axiom 35k array encompassing 35,143 SNP markers available at CerealsDB (Allen et al., 2017). The Piko x Julius population was genotyped by KWS using a subset of 2113 markers from the Axiom dataset.

The *A. muticum* population in the BOP was genotyped with 484 KASP markers (Grewal et al., 2020; King et al., 2017). The 115 KASP markers used for the screening of the *T. urartu* population were developed by (Grewal et al. 2021a, 2021b) with physical positions in the genome based on Ling et al. (2018).

After marker quality control specified above the markers used were as follows: 18053 markers in Yellowhammer, 1971 markers in PxJ, and 315 and 154 markers in the BOP for the *A. muticum* and *T. urartu* subpopulations (Appendix 1, Table S6.1)

6.2.1.3.4 *Candidate gene analysis*

The regions identified as associated with anther traits in the Yellowhammer population were investigated for candidate genes. The location of the associated markers from CerealsDB (https://www.cerealsdb.uk.net/cerealgenomics/) was used to investigate the genomic region surrounding the marker using EnsemblPlants (Howe et al., 2021). Genes located close to the associated marker and within the span of the flanking non-associated markers were investigated for known orthologous genes in other species, mainly *Arabidopsis thaliana* and *Oryza sativa*, and for gene ontology predictions for the biological process of the gene. Candidate gene analysis was carried out in the Yellowhammer population only due to higher marker density and smaller candidate regions.

6.3 Results

6.3.1 Correlation between plant height, anther length, and anther extrusion in elite varieties and alien introgression lines

6.3.1.1 Population structure and replicability between sites and years

Anther traits were evaluated in multiple environments (locations and years) for all populations. The Yellowhammer population was sampled for anther extrusion and anther length in two consecutive years in two different sites at KWS UK and RAGT UK for a total of four independent replicates. The Breeders observation panel (BOP) was sampled for anther length in 2020 and for anther length and extrusion in 2021 at KWS UK and Limagrain UK. The bi-parental Piko x Julius (PxJ) mapping population was phenotyped for anther length as two consecutive generations in 2018 (F4 generation) and 2019 (F5 generation), with 210 and 265 individual lines in the respective years.

To estimate replicability for the traits and genetic variation, the broad sense heritability and coefficient of additive genetic variation (CV_A) was calculated (Table 6.4). Best linear unbiased estimator (BLUE) values were calculated for each trait in each population to account for random effects. BLUE-adjusted means were used as the estimated phenotypic value for each line in further analyses. Anther length varied from 1.89-4.93 mm in the PxJ population, making it the most diverse, and anther extrusion was most varying in the Yellowhammer lines with a range of 1.53-86.25%.

The broad sense heritability was high for both anther extrusion and anther length traits in the BOP, 0.74 and 0.87, and Yellowhammer populations, 0.91 and 0.85 respectively, with a slightly lower heritability in the Piko x Julius population, 0.63, indicating these traits have a strong genetic basis (Table 6.4).

The CV_A was higher for anther extrusion than for anther length and plant height indicating that there is more genetic variability for anther extrusion, which is also seen in the range of trait values (Table 6.4). The variability in anther length was very low for all populations with only minor differences between lines. Anther length was not the primary selection target when the populations were generated which might explain why there is very little variation in this particular trait.

In the BOP lines the alien introgressions were backcrossed to only three cultivars (Pavon 76, Paragon, and Chinese Spring) to generate a comparable population which could explain the very low CV_A for plant height among the BOP lines since the diversity of the background population was low.

Table 6.4. Phenotypic observations, broad sense heritability and additive genetic variance for the populations. The heritability was estimated to be high for all traits indicating a strong genetic component. Genetic variability was found to be low for anther length and plant height but medium to high for anther extrusion. NOBS: Number of observations, CV_A: coefficient of variation.

Trait	Population	NOBS	Herit-ability	CV_A	Min (mm)	Max (mm)	Mean (mm)
Anther length	**Yellowhammer**	1481	0.85	0.06	2.97	4.68	3.69
	BOP	287	0.87	0.07	3.12	4.61	3.90
	Piko x Julius	475	0.63	0.08	1.89	4.93	4.16
					(%)	**(%)**	**(%)**
Anther extrusion	**Yellowhammer**	1613	0.91	0.62	1.53	86.25	22.71
	BOP	183	0.74	0.47	1.67	89.44	30.75
					(cm)	**(cm)**	**(cm)**
Plant height	**Yellowhammer**	840	0.86	0.13	58.5	140	75.6
	BOP	191	0.59	0.07	44.5	99	83.7

6.3.1.2 Correlations between anther length, anther extrusion, and plant height

To investigate any potential correlation between anther traits and plant height the Pearson's correlation coefficient was calculated for each combination of traits summarised in (Table 6.5, Figure 6.1). In the correlation analysis the BOP lines were treated as one population due to the common genetic background. In addition, different traits are compared within the individual lines which are not affected by the difference in alien introgression.

A medium correlation was found for anther extrusion and plant height in both the Yellowhammer and BOP populations, with a correlation coefficient of 0.45 and 0.36 respectively (Figure 6.1, Table 6.5). Interestingly, there was little to no correlation between anther length and plant height. In addition, there was little to no correlation between extrusion and length. Both of these latter correlations (anther length-plant height and anther extrusion-anther length) were higher in the Yellowhammer population than in the BOP with the Yellowhammer population generally being more diverse in terms of anther extrusion and plant height than the BOP population.

Table 6.5. Pearson's correlation coefficient between anther length, anther extrusion, and plant height in Yellowhammer and BOP populations. Confidence interval = 95%

	Yellowhammer	BOP
Extrusion - Height	0.452	0.354
Length - Height	0.199	0.031
Extrusion - Length	0.135	0.005

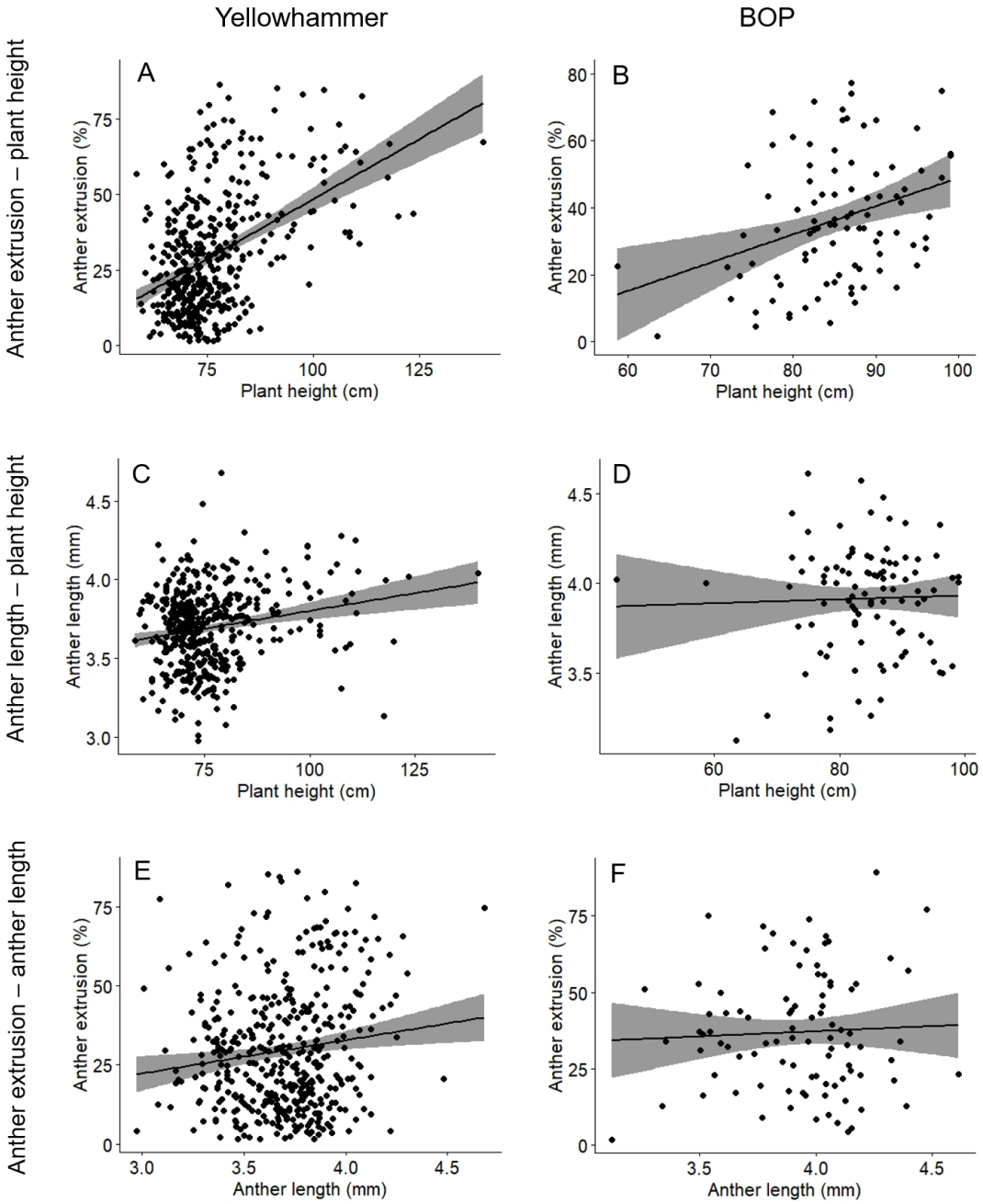

Figure 6.1. Correlation plots of anther extrusion, anther length, and plant height in the Yellowhammer and BOP populations. Anther extrusion and plant height displayed a medium correlation in Yellowhammer (A) and BOP (B) but there was a low to no correlation for anther length and plant height in both Yellowhammer (C) and BOP (D), and for anther extrusion and anther length in Yellowhammer (E) and BOP (F).

6.3.1.3 Distribution of traits

For all populations the distribution of anther length, anther extrusion and plant height were displayed in histograms (Figure 6.2). Anther length in Yellowhammer displayed a normal distribution with a skewed distribution for anther extrusion and plant height towards reduced extrusion and lower plant height. In contrast to the normal distribution of the anther length in Yellowhammer, the Piko x Julius anther length was skewed towards longer anthers with a higher average than the Yellowhammer population.

Interestingly, the anther extrusion in *A. muticum* lines was heavily skewed towards low extrusion in comparison to *T. urartu* lines which displayed a normal distribution. These populations consisted of few samples which could skew the results however this difference is not seen in anther length or plant height, suggesting that it is only the anther extrusion that is affected. This difference in anther extrusion between the *A. muticum* and *T. urartu* lines could be due to an underlying component in the introgressed regions.

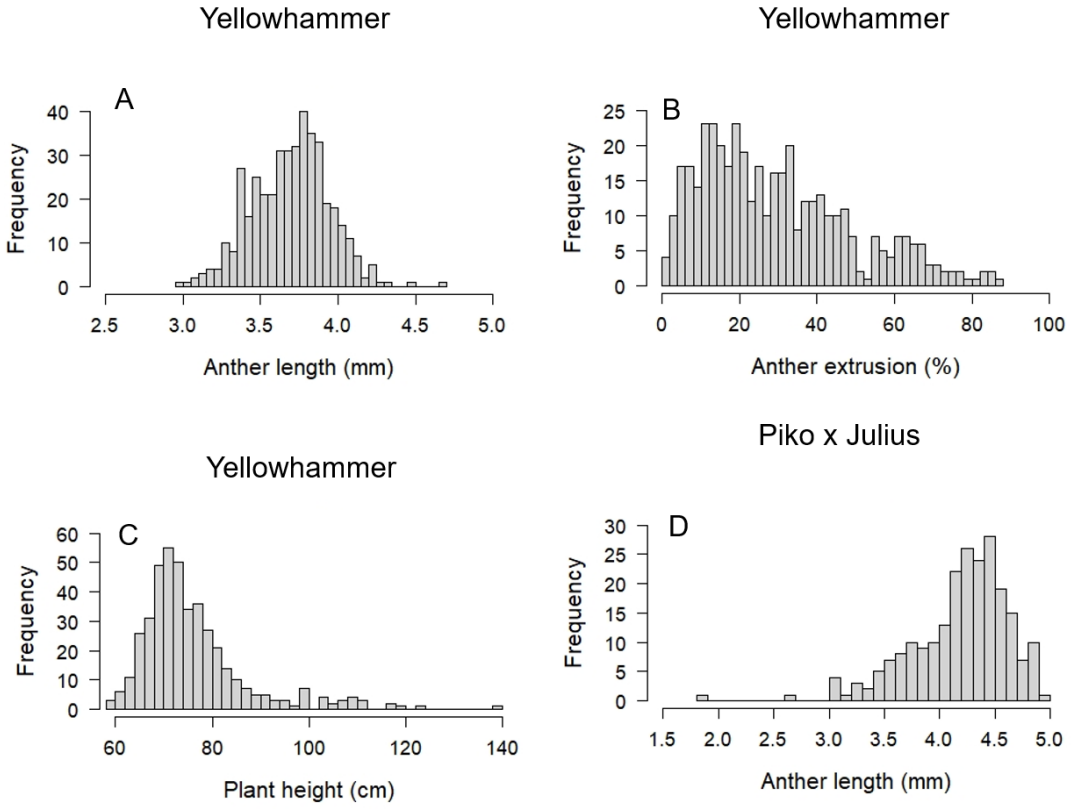

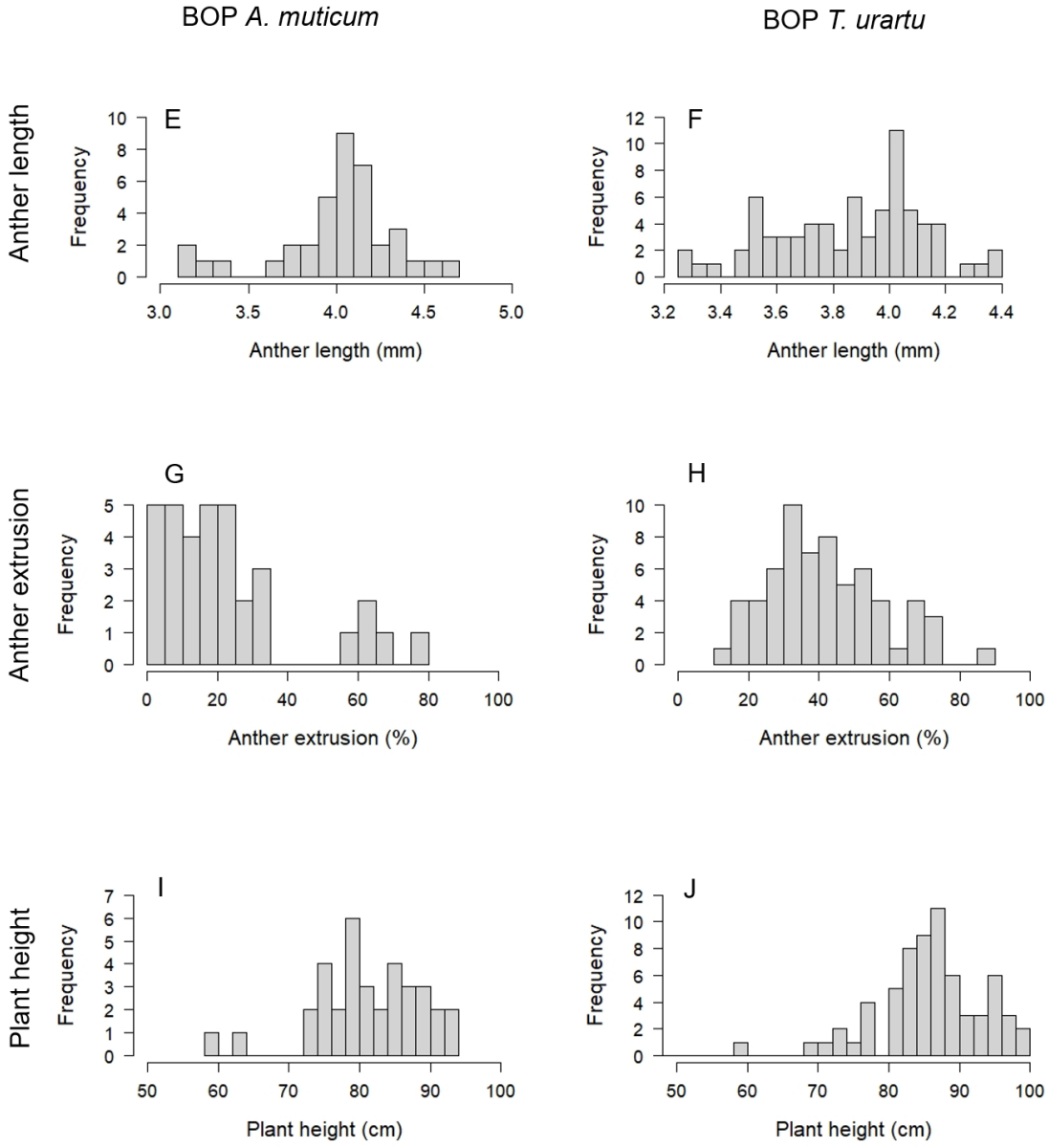

Figure 6.2. Histograms of the distribution of anther length, anther extrusion and plant height in Yellowhammer (A-C), Piko x Julius (D) and BOP (E-J). Yellowhammer anther extrusion (B) and plant height (C) display a skewed distribution with a preference for low extrusion and shorter plant height. Unlike the normal distribution in Yellowhammer (A) the anther length in Piko x Julius (D) is skewed towards longer anthers. The distribution for BOP traits was divided between then A. muticum (E, G, I) and T. urartu lines (F, H, J). Most traits (E-J) display a slightly skewed normal distribution except for anther extrusion in BOP A. muticum (G) where there is a strong bias for low extrusion.

6.3.1.4 Effect of germplasm on anther extrusion and length in Yellowhammer

The lines of the Yellowhammer population were selected to incorporate as much diversity as possible in regards to disease resistance traits from elite cultivars developed mainly in Europe. Genetic diversity differs between geographical origins where germplasm origin can affect ratios of phenotype traits (Huang et al., 2002). Elite cultivars carry less diversity than landraces with breeder and farmer preferences further affecting genetic diversity in specific traits (Würschum et al., 2017). The Yellowhammer population was therefore analysed for a potential germplasm origin effect on anther traits.

Anther traits were not a direct target in the development of this panel and a random distribution was expected in terms of anther length and extrusion. This provided an opportunity to analyse the correlation between germplasm origin and anther traits in commercially available cultivars developed in Europe without any bias. The germplasms were categorised into regions of Northern Europe (Sweden, Denmark, Lithuania), Central Europe (France, Germany, The Netherlands, Belgium, Czech Republic, Italy) Other (Canada, USA, Unknown) based on where the lines had been developed. The BLUEs for each trait and lines were plotted in violin plots to display the distribution of the population (Figure 6.3). Most of the lines had been developed in the UK or Central Europe with a much smaller proportion developed in the other regions. This difference in representation complicates the analysis however, it is possible to compare the two major regions.

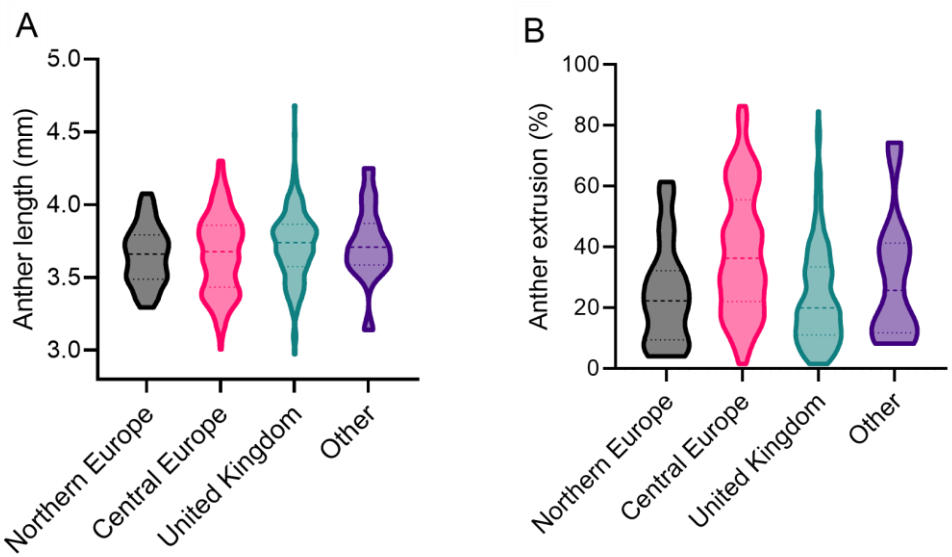

Figure 6.3. Violin plots of the distribution of anther length (A) and anther extrusion (B) in relation to germplasm origin. Dashed lines in bold indicates median value with other dashed lines indicating quartile lines. Northern Europe (Sweden, Denmark, Lithuania), Central Europe (France, Germany, The Netherlands, Belgium, Czech Republic, Italy) Other (Canada, USA, Unknown).

For anther length there seems to be no difference between the regions in terms of distribution but the cultivars from the United Kingdom appear to contain the most diversity (Figure 6.3A). This however could be due to the overrepresentation of cultivars from this region. In addition, there is no bias for either long or short anthers with a similar distribution in all germplasms. For anther extrusion however, there seems to be a preference for higher extrusion in the lines developed in Central Europe compared to the other regions with an overall bias for all regions towards low extrusion (Figure 6.3B).

6.3.1.5 PCA and QQ plots for population analysis

To determine the presence of any distinct population clustering, principal component analysis (PCA) was conducted to determine the optimal number of principal components (PCs) to use in further GWAS analysis. One PC was identified for the Yellowhammer but no genetically distinct populations were found for the BOP or PxJ populations resulting in an optimal 0 PC. To investigate if there was any segregation in germplasm origin in the subpopulations identified in Yellowhammer the lines of the subpopulations were grouped according to the country where they were developed. Lines developed in the UK were overrepresented in the smaller population with a major frequency of French germplasm in the larger population (Figure 6.4). This suggests that there is a difference in the genetic background in these lines.

Quantile-quantile plots (QQplots) were used to investigate if the models applied in the GWAS would be stringent enough to account for population structure through the correlation between observed and expected p-values (-log10(p)). The BLINK model was a good fit for all analyses except for both anther traits in the BOP *T. urartu* population where MLM was better suited (Figure 6.5). In the QQplots of the BOP lines the observations did not adhere as stringently to the expected line with more noise and outliers possibly due to the reduced number of phenotypic observations (Figure 6.5). In the QQplot for anther extrusion in the *T. urartu* lines there are outliers which do not fit the observed-expected trend line however none of these diverged significantly to be detected as false positives and BLINK was still a better model than MLM (Figure 6.5).

For anther extrusion in the Yellowhammer population both MLM and BLINK models were tested. In the QQplot the data points continuously deviated slightly from the trend line in the BLINK model indicating a overfitting problem with this model. The MLM was a better fit for the data (Figure 6.6) however no markers were identified as significant. MLM is a robust model however false negatives is an inherent problem this model, especially for traits controlled by multiple loci (Wang et al., 2016). For further analysis the BLINK model results were used for Yellowhammer anther extrusion however identified markers with lower significance level than the FDR threshold will not be considered.

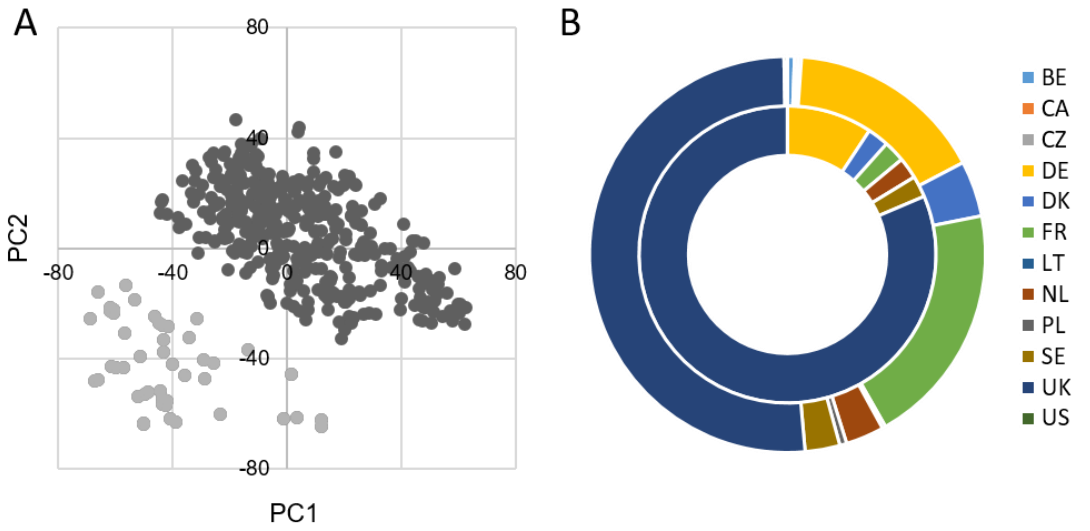

Figure 6.4. Principal component analysis of the Yellowhammer population indicating two genetically distinct subpopulations (A) (dark and light grey) and the distribution of countries in these subpopulations where the dark grey corresponds to the outer circle and light grey to the inner circle (B). BE: Belgium, CA: Canada, CZ: Czech Republic, DE: Germany, DK: Denmark, FR: France, LI: Lithuania, NL: The Netherlands, PL: Poland, SE: Sweden, UK: United Kingdom, US: United States

6.3.2 GWAS of anther traits in wheat populations

6.3.2.1 Identified anther extrusion and anther length associated markers

All markers identified through GWA studies as being associated to anther length and anther extrusion are summarised in Table 6.6. The markers for the different BOP lines will be discussed separately because of the difference in marker data and population structure, but due to the overlap between the Yellowhammer and Piko x Julius data these will be considered together as complements of each other.

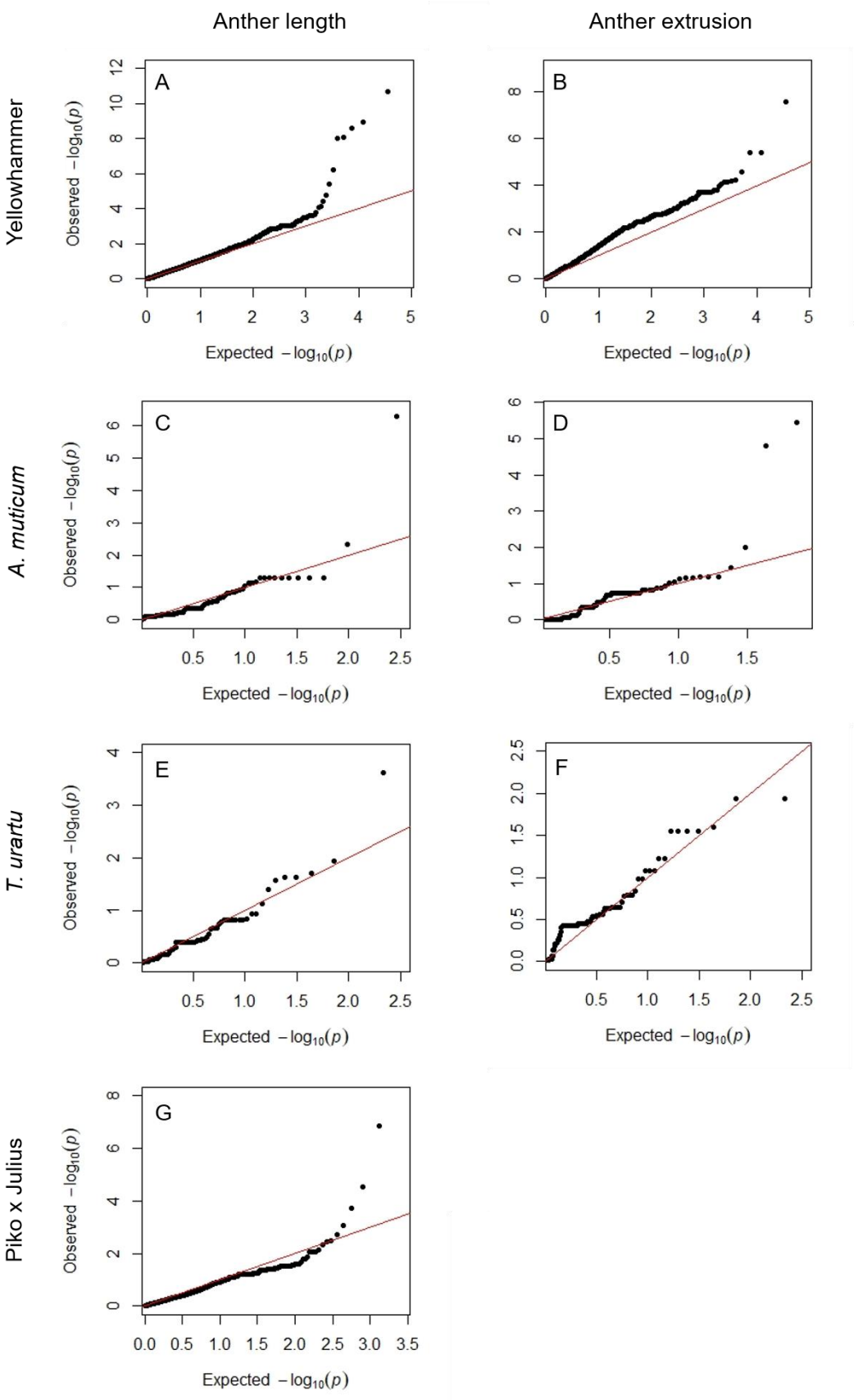
Anther length
Anther extrusion
Yellowhammer
A. muticum
T. urartu
Piko x Julius
A
B
C
D
E
F
G
Observed $-\log_{10}(p)$
Expected $-\log_{10}(p)$

Figure 6.5. QQ plots of expected versus observed p-values of the different traits in the populations as predicted by BLINK. Anther length and anther extrusion in Yellowhammer (A and B) aligned well with a slight deviation in the anther extrusion. Due to the lack of replicates in the BOP (C-F) there are more deviations from the fitted lines, however the BLINK model is acceptable. A: Yellowhammer anther length, B: Yellowhammer anther extrusion, C: A. muticum *anther length and D anther extrusion, E:* T.urartu *anther length and E anther extrusion, G: Piko x Julius anther length.*

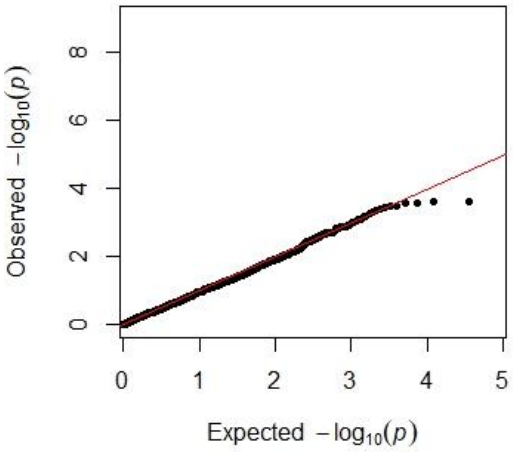

Figure 6.6. QQplot of Yellowhammer anther extrusion with the MLM model. The model is a good fit for the data however the data is under fitted and no significant markers were detected using this model.

6.3.2.2 Markers associated with anther length in elite varieties

Eight markers were identified to be associated to anther length (FDR adjusted p-value<0.05) in the Yellowhammer population (Table 6.6, Figure 6.7). Of particular interest are the markers located on chromosome 4D, AX-94569284 and AX-94547815. There is no physical position available for marker AX-94547815, however based on consensus it is located on the short arm of 4D (CerealsDB). This region has previously been hypothesised to be related to anther traits as the *Reduced height* (*Rht*)-genes are located in this region (Pearce et al., 2011). The *Rht* negative alleles were introduced into elite wheat varieties to reduce plant height during the Green Revolution in an effort to minimise lodging and achieve a higher harvest index (Hedden, 2003). Several studies investigating anther traits have either confirmed (Boeven et al., 2016; Buerstmayr & Buerstmayr, 2016; He et al., 2016; Lu et al., 2013; Muqaddasi, Reif, et al., 2017; Okada et al., 2019) or rejected (Adhikari et al., 2020; El Hanafi et al., 2021; Song et al., 2018) an association of anther traits and *Rht*-genes. In this study no markers associated to anther extrusion was found on chromosome 4D however two markers for anther length were found in this region in Yellowhammer and one in PxJ.

One of the major dwarfing genes *Rht-D1* (formerly *Rht2*) is located on the short arm of chromosome 4D at 19.19 Mbp (Pearce et al., 2011). The Yellowhammer markers associated to anther length on 4D are both located close to the telomeric region of the chromosome with AX-94569284 at 38.45 Mbp. Since Piko carries the tall stature *Rht-D1a* allele (Okada et al., 2021) and KWS Julius carries the dwarfing allele *Rht-D1b* the resulting recombinant lines in the bi-parental population were investigated for anther length at this locus.

In the PxJ population one anther length associated marker, we70502s01, was located at 26.35 Mbp at 7.16 Mbp apart from the *Rht-D1* locus. There is a possibility that we70502s01 is not tightly linked to the *Rht-D1* locus, however this is the first marker available on the 4D chromosome and is the best approximation for the locus. The other marker identified on 4D, we85435s01, is located a significant distance apart at 365.85 Mbp, with only seven markers located between these markers with a 70% allele identity in this region, resulting in a highly similar genotype in this region. There was a significant difference in anther length in lines genotyped as Piko compared to KWS Julius for both markers and no difference in anther length was found between the markers. Unfortunately, 4D is the chromosome with the lowest coverage with only 271 and 12 markers in the Yellowhammer and PxJ populations respectively over a total of 648 Mbp. This low coverage might explain why markers in PxJ located far apart were both identified as associated with anther length. However, none of the seven markers between the markers were identified in the GWAS to be associated with anther length.

The only other chromosome with more than one marker associated to anther length is 1B. Two markers in the Yellowhammer population were estimated to be associated with anther length, AX-94640607 and AX-94430026, located 582.72 Mbp apart with 1451 other non-associated markers in between.

No markers were found to be linked to anther length on chromosome 1B in the PxJ population despite 146 PxJ markers in this region. The genotype of Piko and KWS Julius is available in the 35k Axiom sequencing array used for the Yellowhammer population, enabling a more detailed comparison of the genotype of both parents in this region. Based on the marker positions there were 1392 markers in this region with genotyping data in the CerealsDB genotyping dataset. This region is 88.3% homozygous between Piko and KWS Julius, indicating that this region is mostly fixed and contains little genetic diversity that could be used in an association analysis.

Table 6.6. Markers identified as associated to anther length and anther extrusion in all populations. FDR (false discovery rate)-adjusted p-value, NOBS: number of observations. YH: Yellowhammer, PxJ: Piko x Julius.

Population	SNP	Chromo-some	Position (Mbp)	p-value	FDR-adjusted p-value	NOBS
Anther length						
YH	AX-94640607	1B	57.44	9.72E-09	3.51E-05	395
YH	AX-94430026	1B	640.16	1.64E-05	0.037	395
YH	AX-94455100	2A	529.95	1.08E-09	9.7E-06	395
YH	AX-94601538	3D	548.55	5.79E-07	1.74E-03	395
YH	AX-94569284	4D	38.45	8.79E-09	3.51E-05	395
YH	AX-94547815	4DS	NA	3.63E-06	3.56E-07	395
YH	AX-95239116	6D	291.96	1.97E-11	1.45E-05	395
YH	AX-94649073	7D	585.56	2.41E-09	9.37E-03	395
PxJ	BS00179633	4B	638.75	3.02E-05	0.02	181
PxJ	BS00166010	4D	26.35	1.87E-11	3.68E-08	181
PxJ	BS00022113	4D	365.85	1.38E-07	1.36E-04	181
BOP A. muticum	WRC1404	1B	5.08	3.09E-07	9.72E-05	37
BOP T. urartu	WRC0599	5A	59.55	2.80E-04	0.043	71
Anther extrusion						
YH	AX-94875635	1B	564.91	3.98E-06	0.024	395
YH	AX-94826225	2A	763.05	3.82E-06	0.024	395
YH	AX-94929452	2B	139.92	2.69E-08	4.85E-04	395
BOP A. muticum	WRC1427	2A	0.05	6.14E-05	6.44E-03	33
BOP A. muticum	WRC2084	4B	0.13	1.67E-05	2.63E-03	33
BOP A. muticum	WRC0952	7D	2.12	1.82E-09	5.74E-07	33

In addition, three markers, AX-94601538 on 3D, AX-95239116 on 6D, and AX-94649073 on 7D, were isolated as linked to anther length in the Yellowhammer population but no markers were found for these positions in PxJ. The genotype for Piko and KWS Julius differ for these markers according to CerealsDB indicating that there is genetic diversity at these loci. However, the PxJ marker coverage for chromosome 3D (770 Mbp) and 6D (712 Mbp) is only 8, 48, and 42 markers respectively, where no markers were in the regions identified in the Yellowhammer dataset. Interestingly, one marker was identified in PxJ but not in

Yellowhammer, we77630s01 located on chromosome 4B at 638.75 Mbp. Markers corresponding to this locus in the Yellowhammer were present in the GWAS however was not associated to anther length.

6.3.2.2.1 Candidate gene analysis

The loci of the eight markers were investigated for candidate genes involved with anther length. Genes located closer to the associated marker than to the closest flanking markers were considered as candidates. No characterised genes or known functions were available for any of the candidate genes however gene ontology predictions of biological processes of the genes and predicted orthologues in *Arabidopsis* and rice (*Oryza sativa*) were used to identify genes of interest (Table 6.7).

One of the candidate genes, TraesCS4D02G062800, for marker AX-94569284 on chromosome 4D had two rice orthologues containing the *Ole e 1* allergens domain. This domain is involved in pollen physiology and pollen tube emergence (Carlos et al., 2011) however these domains were not predicted for the wheat candidate gene.

Another candidate gene, TraesCS7D02G472300, detected for AX-94649073 on chromosome 7D, was predicted to be involved with pollen recognition in pollen-pistil interaction for self-incompatibility recognition and expressed in the endosperm and pericarp of the seed (data collected from Ensembl, Howe et al., 2021). This gene could be interesting for further analysis regarding pollen development and recognition in wheat.

In the locus around marker AX-94430026 on chromosome 1B, one candidate gene was predicted to be orthologous of several Sulfotransferases (SOTs) in *Arabidopsis*. The SOT family members have diverse functions and the *SOT16*, *SOT17* and *SOT18* genes can be induced by a variety of plant hormones such as jasmonic acid, are expressed throughout plant tissues and developmental stages in *Arabidopsis*, including floral tissues and stamens, as reviewed by Hirschmann et al. (2014). Not a lot is known about these proteins in plants however *BrSOT16* and *BrSOT18* are highly expressed in stamens (Zang et al., 2009), making them interesting targets for further investigation.

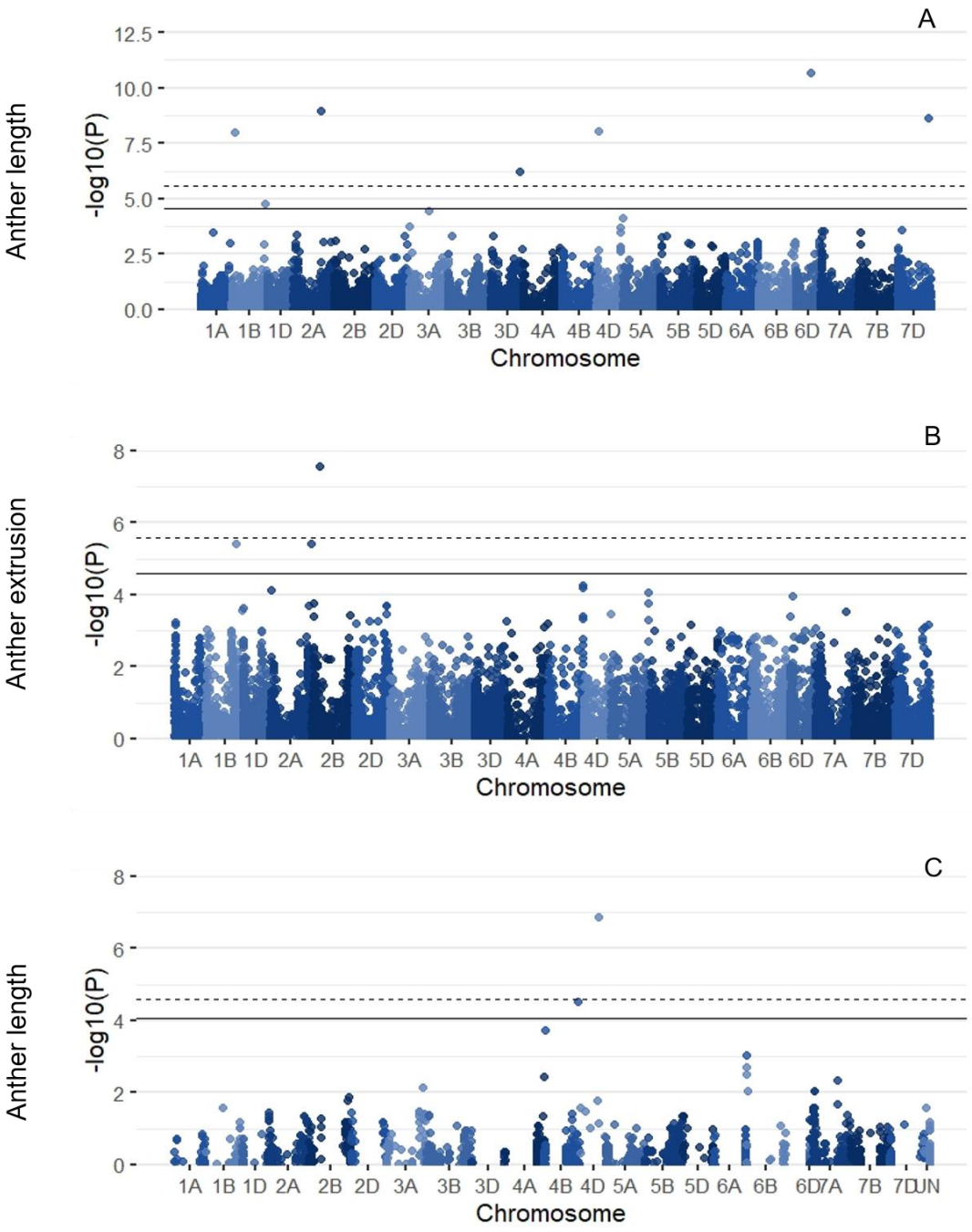

Figure 6.7. Manhattan plot of markers identified as associated to Yellowhammer anther length (A) and anther extrusion (B), and anther length in the Piko x Julius population (C). Significance threshold levels given as FDR (unbroken line) and Bonferroni (dashed line) corrected levels. Markers above the FDR significance threshold were considered associated to the trait of interest with eight markers identified for anther length and three markers for anther extrusion in Yellowhammer and three markers in Piko x Julius.

Table 6.7. Candidate genes for markers identified for anther length and extrusion. Genes at the loci corresponding to the identified associated marker were analysed for predicted function with dedicated gene ontology (GO) terms, and with predicted orthologues through Ensembl. Highlighted in green are predictions related to pollen properties.

Marker	Candidate genes	GO term	Orthologues Gene name	Description of gene
Anther length				
1B AX-94640607	TraesCS1B02G073400	NA	NA	
	TraesCS1B02G073500	NA	NA	
	TraesCS1B02G073600	NA	FBL19 AT4G30640	SCF-dependent proteasomal ubiquitin-dependent protein catabolic process
			SKIP1 AT5G57900	SCF-dependent proteasomal ubiquitin-dependent protein catabolic process
1B AX-94430026	TraesCS1B02G414800	GO:0006508: proteolysis	NANA AT3G1270,	Aspartic proteinase NANA, chloroplast
			Os05g0557100	Peptidase A1 domain containing protein
	TraesCS1B02G414900	NA	AT1G74100 SOT16, AT1G18590 SOT17, AT1G74090 SOT18	Response to jasmonic acid stimulus involved in jasmonic acid and ethylene-dependent systemic resistance
	TraesCS1B02G415000	NA	NA	
	TraesCS1B02G415100	NA		
	TraesCS1B02G415200	GO:0043248: proteasome assembly	AT3G15180	ARM repeat superfamily protein
			Os05g0557200	Armadillo-type fold domain containing protein
2A AX-94455100	TraesCS2A02G308200	NA	AT5G08630	DDT domain-containing protein
	TraesCS2A02G308100	NA	AT4G09150	T-complex protein 11
3D AX-94601538	TraesCS3D02G436900	GO:0006468: protein phosphorylation	NA	
	TraesCS3D02G437000	GO:0030246: carbohydrate binding	NA	
4D AX-94569284	TraesCS4D02G062800	NA	Os10g0206500	Pollen Ole e 1 allergen/extensin domain containing protein
			Os10g0208600	Pollen Ole e 1 allergen/extensin domain containing protein
	TraesCS4D02G062900 GRF1-interacting factor1	GO:0008283:cell population proliferation	GIF1 AT5G28640	
		GO:0009955: adaxial/abaxial pattern specification	OsGIF3 Os03g0733600	
		GO:0048825: cotyledon development		

6D	TraesCS6D02G206200	NA	NA	
AX-95239116	TraesCS6D02G206300	NA	AT2G20240	GPI-anchored adhesin-like protein
			AT4G28760	Methyl-coenzyme M reductase II subunit gamma
			AT5G43880	Methyl-coenzyme M reductase II subunit gamma
7D	TraesCS7D02G472300	GO:0006468: protein phosphorylation	NA	
AX-94649073		GO:0048544: recognition of pollen		
	TraesCS7D02G472400	GO:0030833: regulation of actin filament polymerization	ARPC3 AT1G60430	Actin-related protein 2/3 complex subunit 3
		GO:0034314: Arp2/3 complex-mediated actin nucleation		
	TraesCS7D02G472500	NA	NA	

Anther extrusion

1B	TraesCS1B02G337300	NA	NA	
AX-94875635	TraesCS1B02G337400	GO:0009658: chloroplast organization	NA	
		GO:0010438: cellular response to sulfur starvation	NA	
		GO:0010439: regulation of glucosinolate biosynthetic process	NA	
	TraesCS1B02G337500	NA	NA	
2A	TraesCS2A02G561300	GO:0006355: regulation of transcription	NA	
AX-94826225	TraesCS2A02G561400	GO:0006355: regulation of transcription	NA	
	TraesCS2A02G561500	NA	NA	
	TraesCS2A02G561600	NA	NA	
	TraesCS2A02G561700	GO:0006355: regulation of transcription	NA	
	TraesCS2A02G561800	GO:0006355: regulation of transcription	NA	
	TraesCS2A02G561900	NA	NA	
	TraesCS2A02G562000	NA	NA	
2B	TraesCS2B02G167100	NA	Os07g0645000	Allergen V5/Tpx-1 related family protein
AX-94929452				

6.3.2.3 Markers associated with anther extrusion in elite varieties

In the Yellowhammer population three markers were identified to be associated with anther extrusion. The markers were located on three different chromosomes, 1B, 2A and 2B. Other markers were close to the significance level (Figure 6.7B) however due to the distribution of data in the QQplot for the BLINK model these markers were not considered as significant as they might be false positives.

The regions surrounding these markers were analysed for candidate genes involved with anther extrusion with three, eight and one candidate genes located in the marker regions on 1B, 2A and 2B. None of these genes had a characterised function or relevant predicted functions or orthologues (Table 6.7).

6.3.2.4 Markers in the alien introgression lines

6.3.2.4.1 A. muticum *markers for anther length and extrusion*

The BOP lines were considered as separate from the Yellowhammer and PxJ populations but were further divided into lines with introgressions from *A. muticum* and *T. urartu* based on available marker data and population structure. Manhattan plots of the associated markers for the subpopulations of the BOP illustrates the low coverage of the genome (Figure 6.8).

In the *A. muticum* introgression lines one marker was identified for anther length and three for anther extrusion. The marker for anther length, WRC1404, was located on chromosome 1B. Lines genotyped as non-wheat for this markers did not have any introgressions confirmed by the marker data (Grewal et al., 2021a, 2021b) or genome in situ hybridisation analysis (Grewal et al., 2020) of the *A. muticum* genome but they were all missing most of chromosome 1B (a deletion of 550 Mbp out of 799Mbp total 1B chromosome). Other markers in this region with the same genotype did not show any association. The anther length of the six lines with this deletion at the location of WRC1404 is significantly shorter (p-values of 0.0017) than the average of the entire population of 36 lines possibly indicating that this deletion has a negative effect on anther length (Table 6.6).

The discrepancy of surrounding markers not being associated should not be an effect of the GWAS model since BLINK tests associated markers based on other markers and not kinship. In addition, it does not assume that associated markers are spread evenly in the genome, two factors that might otherwise skew the results. It is possible that a deletion of the 1B chromosome will reduce the length of anthers since lines with the deletion are significantly shorter. However, only one marker out of 17 in this region were predicted to be associated to anther length.

The three markers, WRC1427, WRC2084 and WRC0952, identified as associated with anther extrusion in the *A. muticum* population were all located on different chromosomes, 2A, 4B and 7D. Each of these had few lines with a validated wild relative introgression and there

was no difference in anther extrusion between the whole *A. muticum* population and the lines positive for either marker. Most likely these markers represent false positives due to the small sample size and low marker coverage.

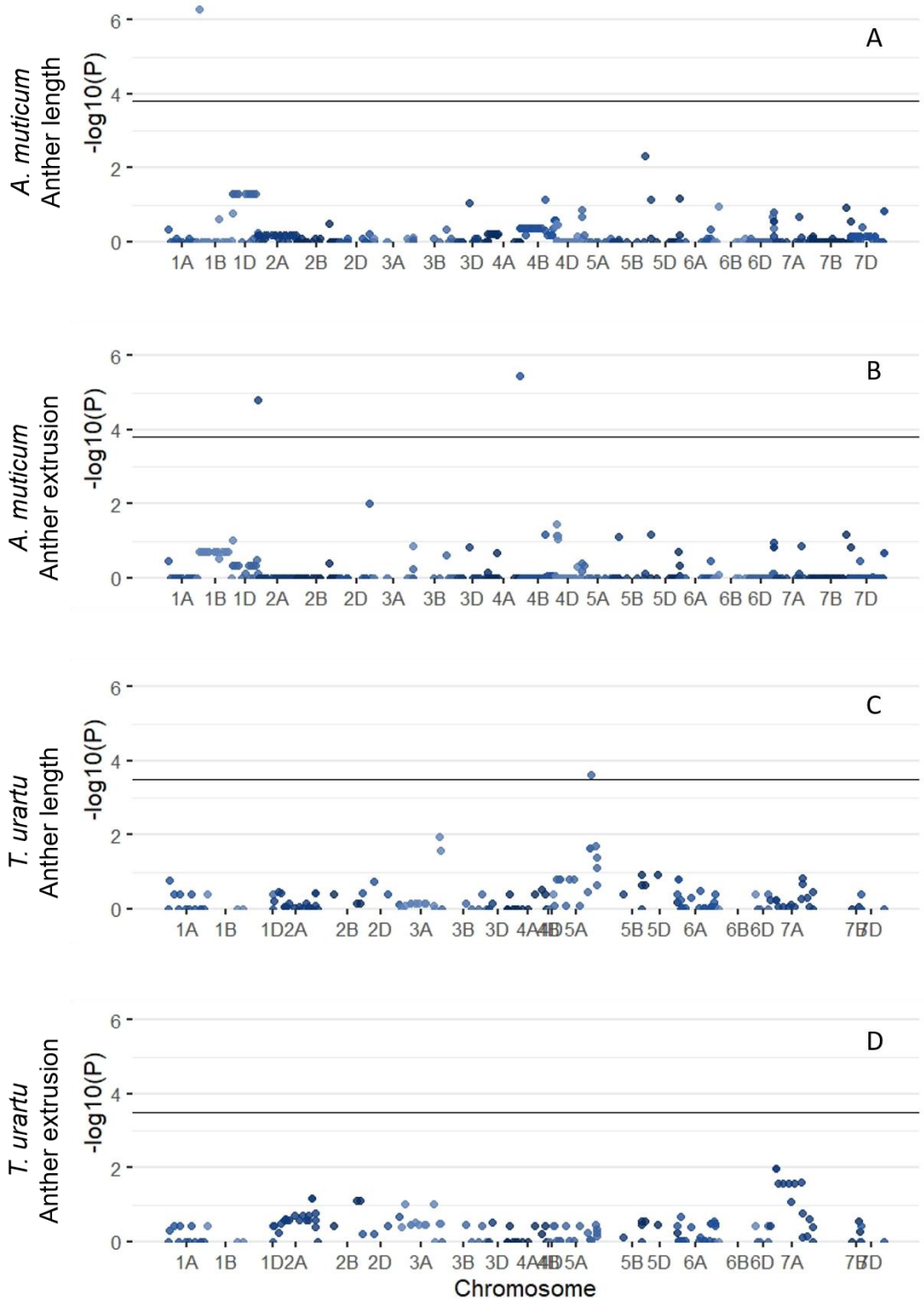

Figure 6.8. Manhattan plots of anther trait associated markers in BOP. Anther length in A. muticum *(A), anther extrusion in* A. muticum *(B), anther length in* T. urartu *(C), and anther extrusion in* T. urartu *(D). All plots display a low marker density in all chromosomes.*

6.3.2.4.2 Anther length associated marker in T. urartu *population*

In the *T. urartu* population only one marker was associated with anther length, WRC0599 on chromosome 5A at position 595.5 Mbp. In total 17 lines out of the 73 lines (23.3%) in this subpopulation were positive for a *T. urartu* introgression at this locus. These lines carried six introgressions (5A.5 – 5A.10) of different sizes detected by WRC0599, in addition some lines had multiple introgressions on chromosome 5A (Figure 6.9) (Grewal et al., 2021a). The lines with an introgression at WRC0599 at 595 Mbp did not have introgressions on other chromosomes. When all lines were considered together the anther length was significantly shorter compared to the entire *T. urartu* population (p-value 0.0012). No difference was found in plant height between the lines that were positive for the introgression at WRC0599 compared to all the lines in the *T. urartu* population.

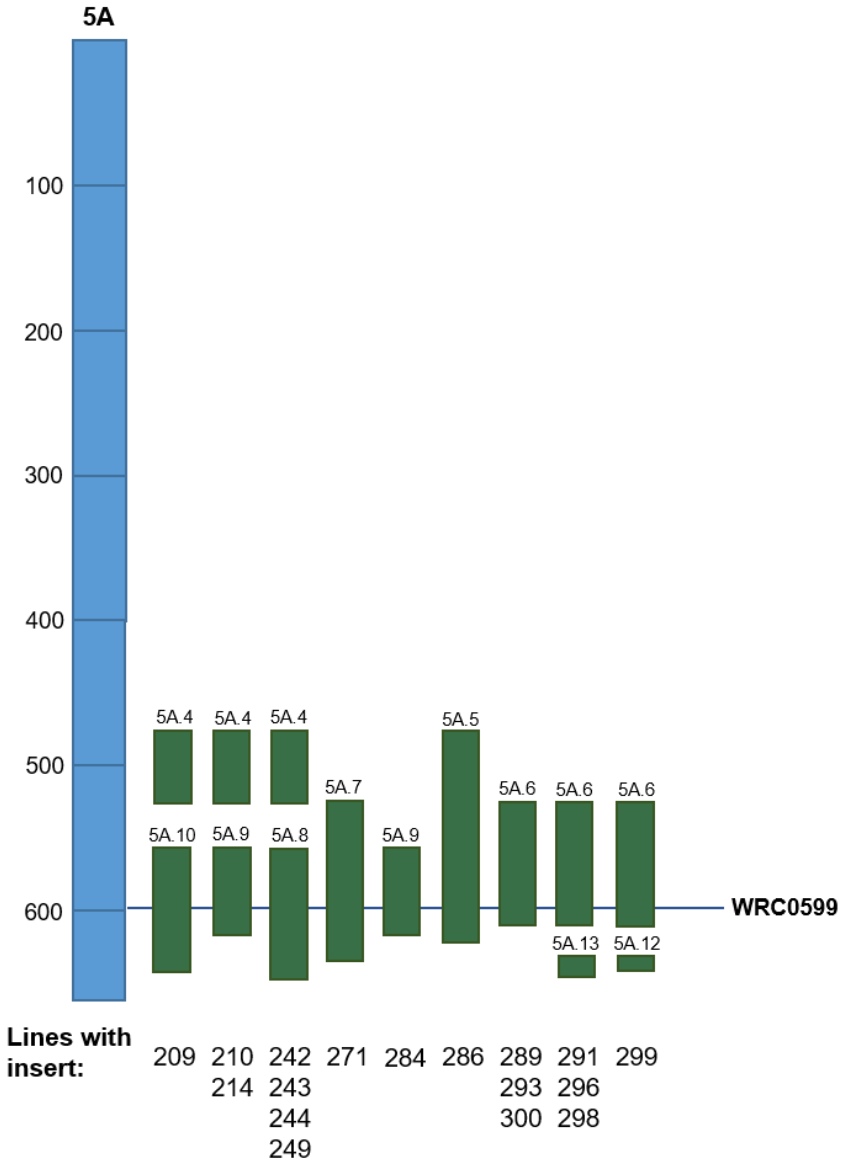

Figure 6.9. Overview of introgressions from T. urartu *on chromosome 5A in the BOP lines. Lines with introgressions at the position of marker WRC0599 (at 595 Mbp) had shorter anthers compared to the rest of the BOP population. The lines did not have any introgressions on other chromosomes. Details of introgressions 5A.4-5A.13 are available in Grewal et al. (2021b).*

6.3.2.5 Comparisons of anther traits for specific introgressed regions

In addition to the conducted GWAS the lines were analysed to see if any particular introgression from the *T. urartu* or *A. muticum* genome was more likely to have an impact on anther length or extrusion. Lines with similar introgressions, of either *A. muticum* or *T. urartu*, were compared to the rest of the populations to determine if any regions from the wild relatives contributed to higher extrusion or longer anthers.

It was not possible to determine if any regions contributed to longer anthers however two regions were found for anther extrusion. All lines with an introgression on chromosome 7D were among the five lines with highest extrusion. These lines had a significantly higher extrusion than the rest of the *A. muticum* population (p-value 1.9E-5) with an average of 49% higher extrusion. This introgression spanned most of chromosome 7D, and only three lines had an introgression of the *A. muticum* genome in this region however, since all lines displayed very high extrusion compared to the remaining population it is still worth investigating further.

Similarly, all lines with an introgression from *T. urartu* on the short arm of 3A had a significantly higher extrusion (p-value 0.004) with 17.6% higher extrusion than the remaining population. This introgression was identified in 8 out of 61 lines and correlates to a relatively small region however due to the low coverage the exact size of the introgression could not be determined. It is possible that an introgression from *A. muticum* on chromosome 7D and from *T. urartu* on chromosome 3A can lead to higher extrusion. Further investigation and fine mapping in these regions can be carried out to identify candidate regions or genes related to anther extrusion.

6.4 Discussion

6.4.1.1 Anther traits in hexaploid bread wheat

Anther traits have long been of interest for hybrid breeding since a good pollen donor is a requirement for crossing of elite parents (Boeven et al., 2018; Whitford et al., 2013). For this purpose the pollen donor should preferentially produce a large quantity of pollen and be able to spread viable pollen outside of the cleistogamous floret. Anther length is a valuable measurement for the identification of wheat plants with high pollen production as there is a positive correlation between pollen mass and anther length (De Vries, 1974; V. Nguyen et al., 2015) whereas anther extrusion is a good indication of the ability to spread pollen (Pinthus & Levy, 1983b).

Traditionally anther length has not been a trait of interest for breeding due to the difficulty in high-throughput phenotyping and selection. Anther extrusion on the other hand, has previously been studied as either counted, where the number of retained anthers in florets are counted, or visual extrusion, by in field scoring of the extent of extruded anthers, making it possible to screen multiple lines in field. In this study, the genetic variation in hexaploid wheat was found to be very low for anther length in comparison to extrusion. Similar results have been found in comparable multi-line studies (Langer et al., 2014; Skinnes et al., 2010; Song et al., 2018) suggesting that there is not much usable genetic diversity for anther length.

6.4.1.2 Correlations between anther length, anther extrusion, and plant height

Previous studies have investigated wheat flowering traits as diverse as duration of floret opening and openness, stigma length, pollen shedding (El Hanafi et al., 2021), spikelet sterility and density (Song et al., 2018), days to heading and spikelet numbers (Okada et al., 2021) and many more in attempts to find correlations between floral traits and underlying genetic components. When investigated together many of these traits have also been found to be correlated indicating a high complexity in wheat floral traits worth investigating further (Boeven et al., 2016; El Hanafi et al., 2021; Okada et al., 2021; Song et al., 2018).

Beri & Anand (1971) found a modest positive correlation (0.298) between anther size and plant height and hypothesised that taller plants produced more pollen which generated interest in finding the loci potentially affecting both traits. Since then, other studies have looked into anther length (Okada et al., 2019; Song et al., 2018; De Vries, 1974) however, only Okada et al. (2019) investigated anther length in relation to plant height, where a modest correlation was confirmed. Several studies have instead focused on the relationship between anther extrusion, filament length, and plant height, and found a modest to strong positive correlation between these traits (Boeven et al., 2018; Buerstmayr & Buerstmayr, 2016; Langer et al., 2014), a low correlation (Boeven et al., 2016) or no correlation (Beri & Anand, 1971).

In this study no correlation was found between anther length and plant height, but a medium correlation was found for anther extrusion and plant height for both the Yellowhammer and BOP populations. In addition, there seems to be no correlation between anther length and anther extrusion in either investigated population in this study. This lack of consistency between studies is an obvious problem and will be addressed together with the associated markers identified through the GWAS.

6.4.2 GWA studies targeting anther traits in wheat

6.4.2.1 Anther length and anther extrusion associated markers in elite cultivars

In the last few decades the decrease in sequencing costs and the increase in available markers have made it possible to conduct genome wide association studies in wheat with larger populations (Gupta et al., 2019). GWA studies are an important genomic research tool for the identification of the genetic regions underlying traits of interest. It is only recently GWA studies have been attempted in hexaploid wheat to find loci related to anther traits and comparing studies can be challenging as the markers and populations used in the individual studies can differ greatly (Saini et al., 2022a).

Here, GWA studies were conducted on the elite cultivar population Yellowhammer, the Piko x Julius bi-parental population, and the Breeders observation panel of wild relative introgression lines, to identify loci involved with anther length and anther extrusion. The accuracy of the predictions from GWA studies depends on the population size, number of markers used for the genotyping and the genetic diversity in the population. The Yellowhammer population consisted of 427 genetically diverse individuals genotyped with a high density marker array which makes it suitable for GWAS. The Piko x Julius and BOP populations however had few individuals and a low marker coverage significantly reducing the statistical power of the predictions from the analyses. It is worth considering the identified associated markers however it is important to highlight the problems associated with these populations.

In total eleven markers were identified to be associated with anther length in elite cultivars with two markers in the BOP introgression lines. For anther extrusion three markers were found in elite cultivars with an additional three in the BOP. Other studies have previously identified loci associated to anther length (El Hanafi et al., 2021; Song et al., 2018) and extrusion (Adhikari et al., 2020; Boeven et al., 2016; El Hanafi et al., 2021; Muqaddasi et al., 2016; Muqaddasi et al., 2017; Skinnes et al., 2010) however there is little overlap in identified regions. Here, all loci identified for anther length and extrusion in the elite cultivars were novel indicating a presence of underutilised loci for future breeding and research into anther development.

6.4.2.2 Effect of population germplasm and marker density on identified markers

6.4.2.2.1 Marker density differences in GWA studies

Difference in marker coverage between GWA studies could contribute to the differing results found between studies on anther traits in wheat (Saini et al., 2022a). Compared to other major crops the wheat genome is very large and consists of three sub-genomes with a combined size of about 17 giga bases which was fully annotated only recently (IWGSC, 2018). Multiple molecular marker assays for the use in GWA studies, genomic selection or breeding have been developed to detect difference among elite varieties or wild species (Sun et al., 2020). Still the marker coverage in GWA studies in hexaploid wheat for the study of anther traits has remained fairly low ranging from 27197 markers in (Muqaddasi, Reif, et al., 2017) to only 2575 markers in (Muqaddasi et al., 2016). In this study 19704 were used to detect associated marker in the elite variety population Yellowhammer with 2113 markers in the Piko x Julius mapping population. This difference in coverage and in the type of marker data used could explain differences in detected associated markers between studies. Future development and application of higher density genotyping arrays in hexaploid wheat elite cultivars will enable more detailed studies to potentially identify the loci controlling anther traits in different populations.

6.4.2.2.2 Germplasm origin effect as a factor in GWA studies

Differences between studies could be due to linkage disequilibrium structure differences in populations with varying germplasm origin (Kraft et al., 2009). In terms of germplasm origin it is necessary to investigate population structure to identify ancestral relationships where repeated measures are crucial (Kraft et al., 2009; Pavan et al., 2020). Germplasm origin have been found to significantly affect other traits such as plant height and rooting depth where breeder preference and local adaptation have influenced the genetic diversity present in regional germplasms (Huang et al., 2002; Narayanan et al., 2014; Würschum et al., 2017).

Differences in GWA studies related to anther traits might be influenced by the germplasms used in the analysis where traits could be genotype dependent (Okada et al., 2019). GWA studies on anther traits have primarily focused on elite variates for the identification of loci present in commercially available cultivars and for the high marker density available for genotyping of elite cultivars. These elite cultivars have usually been developed in a certain region e.g. Chinese cultivars (Song et al., 2018), Western European (Boeven et al., 2016), Middle east and North African (El Hanafi et al., 2021), and Mexican (Adhikari et al., 2020) which potentially could affect the genetic diversity present in the populations and subsequently the detection of associated markers. The lines in the Yellowhammer population were mostly developed in Western Europe with most cultivars generated in UK. As seen in Figure 6.3 there is a difference in genetic diversity even within European breeding programs with a difference in distribution of anther extrusion between regions. The genetic diversity in the population analysed could therefore influence the detected loci.

6.4.2.3 Candidate genes and regions of interest

6.4.2.3.1 Identification of candidate genes related to pollen properties

For the associated markers identified in this study a candidate gene analysis was conducted to explore the novel loci identified for anther length and extrusion. The region surrounding the loci identified in the Yellowhammer population were analysed for candidate genes with predicted functions in pollen development. Markers surrounding the significant markers could be in linkage disequilibrium (LD) with the significant marker which could increase the region available for candidate gene detection. The average LD decay for wheat is 8 Mb (Pavan et al., 2020) however in wheat LD differs between chromosomes and between genomes with a higher LD around the centromeres where there are fewer recombination events and a particularly high LD on chromosome 4D (Aleksandrov et al., 2021, Dadshani et al., 2021). Therefore the region containing potential candidate genes associated with anther length and extrusion could be extended however in this study only genes located closer to the associated marker than to the next available non-associated markers were investigated to reduce the number of candidate genes. The identified markers from BOP and Piko x Julius were not used for predictions of candidate genes because the low marker density led to vast associated regions with too many possible genes.

Of special interest are the markers identified on 4D (AX-94569284) and 7D (AX-94649073) associated with anther length in Yellowhammer. One of the candidate genes for the region on 4D was predicted to have an orthologue in rice, *Ole e 1*, involved with pollen tube formation and pollen allergens (Fernández-González et al., 2020). A candidate gene on 7D was predicted to be involved with pollen recognition in self incompatibility systems making it an interesting gene for further studies in wheat. These functions and orthologues are predicted, whereas further detailed studies in wheat are necessary to investigate the possible effect of these genes on anther length. No candidate genes of interest for pollen development were identified for anther extrusion.

6.4.2.3.2 Markers on 4D associated with anther length and their relation to Rht-D1

In this study two markers in the Yellowhammer and one in PxJ were found on 4D to be associated with anther length but no markers were found to be associated with anther extrusion in the regions of the *Rht* genes. The markers identified on 4D are located close to the telomeric region of the chromosome in both Yellowhammer and PxJ population, AX-94569284 at 38.45Mbp and we39240s01 at 113.76Mbp, where the *Reduced height*, *Rht-D1* gene involved with plant height and the *TEOSINTE BRANCHED1* (*TB1-D1*) gene involved with inflorescence architecture (Dixon et al., 2018) are located. The *Rht* genes were extensively used in the Green Revolution to generate cultivars with reduced height without adverse effects on yield (Würschum et al., 2017). There are differing accounts of whether the loci with the *Rht* genes and *TB-D1* affect anther length or extrusion where some confirm the association of *Rht* with anther extrusion (Boeven et al., 2016; He et al., 2016; Okada et al., 2019, 2021) whereas others have found no effect of any *Rht* genes on anther length (El Hanafi et al., 2021; Song et al., 2018).

The parents Piko and KWS Julius carry different alleles for *Rht-D1* located at 19.19 Mbp, with Piko carrying the tall stature allele *Rht-D1a* (Okada et al., 2021) and KWS Julius the *Rht-D1b* dwarfing allele. A bi-parental population with Piko and Gladius, a semi-dwarf with medium sized anthers, previously confirmed the association of Piko's *Rht-D1a* allele with greater anther length and higher extrusion (Okada et al., 2021). The lines with the *Rht-D1a* allele in the bi-parental Piko x Julius recombinant population had significantly longer anthers indicating that *Rht-D1* might be involved with anther length in PxJ. However, no evidence was found to support *Rht*-genes influence on anther extrusion in the investigated populations. Further fine mapping of this region is needed to determine the potential influence of the Rht genes on anther traits.

In this study there is little to no correlation between anther length and plant height, which is interesting in light of the possible influence of *Rht-D1* on anther length (Zanke et al., 2014). A clear correlation between anther length and plant height would have further supported the influence of the height gene *Rht-D1* on anther length and this lack of correlation could possibly be explained by looking at genes influencing plant height. In a GWA study on plant height in winter wheat varieties Zanke et al. (2014) found there might be multiple loci influencing plant height aside from the *Rht*-genes. With multiple loci controlling plant height a lack of correlation between plant height and anther length is not necessarily discrediting the interaction of the *Rht* genes on anther length or extrusion.

6.4.2.3.3 The 1B region for anther length

On chromosome 1B two markers were identified as associated to anther length and one to anther extrusion in Yellowhammer. Previous studies have identified markers related to anther extrusion on chromosome 1B (Adhikari et al., 2020; Boeven et al., 2016; El Hanafi et al., 2021; Muqaddasi et al., 2016) but only Song et al. (2018) investigated and found one marker related to anther length.

Analysis of candidate genes in the region of the associated markers that could be involved with anther length yielded three and five predicted genes for the markers AX-94640607 and AX-94430026 respectively. There was no pollen related function predicted for any of the genes or their predicted orthologues (Table 6.7) however detailed studies of these genes have not been carried out.

In the Piko x Julius population no markers were found on chromosome 1B since this region was genetically identical between the parents Piko and KWS Julius and does not contain any diversity that could be detected. Bi-parental populations are very useful for mapping traits of interest however, the detection of loci related to a trait requires highly diverse parents of different genotypes (Singh & Singh, 2015). Where both parents have the same genotype some important loci that influence a trait can be missed since the population is not diverse enough to isolate any association (Singh & Singh, 2015).

In general, loci detected as associated to anther length or extrusion in the Yellowhammer population but not in the Piko x Julius population could be due to lack of genetic diversity present in the bi-parental population or poor marker density in the predicted regions. Interestingly, one marker, we77630s01 located on 4B, was isolated in the PxJ population with no corresponding region in Yellowhammer. The Yellowhammer population is more genetically diverse and should encapsulate any variation present in the PxJ. It is possible it is a false positive since this region was not significant enough to be associated to anther length in the Yellowhammer population or that the associated allele is underrepresented in Yellowhammer and therefore removed in minor allele frequency quality control.

6.4.2.4 Markers associated to anther length and extrusion in the BOP

The lack of genetic diversity present in hexaploid wheat has been recognised as a significant problem and introgression from wild relatives has been identified as a way to possibly introduce new material that could prove useful for breeding (King et al., 2017; Winfield et al., 2016). The lines in the Breeders Observation Panel (BOP) contains varying sizes of introgressions from the wheat wild relatives *Amblyopyrum muticum* and *Triticum urartu*, and were generated to increase the genetic diversity in bread wheat (Grewal et al., 2018; King et al., 2017). Although both *A. muticum* and *T. urartu* were included in the BOP they were treated as separate subpopulations due to the marker availability used for the genotyping of the introgressions. Markers used for the genotyping of these subpopulations were specifically designed to detect each wild relative i.e. the *A. muticum* markers were not used for the *T. urartu* population and vice versa. Each subpopulation therefore contained very few individual lines and had low marker density, preventing any detailed analysis of specific genes or loci. Instead, the populations were used with the intent to discover regions containing genetic diversity in relation to anther traits currently not present in the modern hexaploid wheat. This approach of finding associated markers in small but genetically distinct populations is therefore a first step in the mapping of regions of interest. Identified regions can be fine-mapped to find candidate genes involved in anther development that might be of use for future breeding.

6.4.2.4.1 Markers isolated in the A. muticum *population*

The *A. muticum* population was very small with only 33 and 37 phenotype observations for anther extrusion and anther length respectively. The four markers identified as associated to anther traits in this subpopulation has some problems that reduces the likelihood that these are true discoveries. The marker associated with anther extrusion on chromosome 1B does not correspond to an introgressed region but rather a deletion on 1B and the markers for anther length had low minor allele frequencies or very few observed phenotypes where no difference were found for lines positive for an alien introgression compared to other lines in the population. These markers were therefore considered as likely false positives and were not investigated further.

6.4.2.4.2 The effect of the 5A region in the T. urartu *population*

In the *T. urartu* population one marker was found to be associated with anther length. The WRC0599 marker on 5A was significantly associated to anther length when using the BLUE values as well as individual replicates in the GWAS (data not shown), further strengthening its possible influence on anther length. In the *T. urartu* population 23.3% of the lines had an insert at this locus where these lines had significantly shorter anthers. No associated markers were found in the Yellowhammer population on chromosome 5A however previous studies found 5A to be of interest for anther length in elite varieties (El Hanafi et al., 2021; Song et al., 2018). However, directly comparing this introgression population with elite variates such as the lines in Yellowhammer and PxJ is complicated due to the differences in population structure, sample numbers, and marker density. A bigger population and better marker coverage would be necessary to narrow down the region of interest to identify a reasonable number of candidate genes that could be analysed further through detailed genetic studies of the candidate genes from the wild relative or of orthologous in hexaploid wheat using gene manipulation techniques.

Additional regions of interest were identified by comparing specific introgressions between the lines. Introgressions from the *T. urartu* genome on chromosome 3A and most of chromosome 7D from *A. muticum* resulted in significantly higher extrusion. Fine mapping of these regions to possibly identify the regions contributing to the increased anther extrusion could be valuable as a breeding target.

6.5 Conclusion and future work

Anther trait diversity is important for future hybrid wheat breeding and the genetics behind anther development and pollen dispersal properties is of great interest. In this study elite cultivars and wild relative introgression lines were studied to detect loci involved with anther traits. Eleven novel genomic regions were identified as associated to anther length and three regions were found for anther extrusion in elite cultivars indicating that anther traits could be controlled by a number of loci in hexaploid wheat. Candidate genes identified in these loci are of interest for further investigation to possibly identify novel genes involved with anther development in hexaploid wheat.

The repository of genetic diversity in wheat wild relatives is currently being explored to identify regions of interest with additional loci found to be associated with anther length and extrusion in the introgression lines. Here, a region on chromosome 5A in the *T. urartu* genome is identified as a candidate for added genetic diversity of anther length. Further fine mapping of this region and other loci identified as associated with anther traits is of interest to isolate candidate genes and explore the genetic diversity in wild wheat relatives.

Chapter 7. General discussion

7.1 The use of anther traits for enhanced breeding

Yield stability and improvement provide crucial challenges for future plant breeding in the face of growing demand and increase in extreme weather conditions. The study of the developmental biology of cereal flowers as well as traits affecting yield through abiotic stress responses is necessary for the generation of plants able to withstand such environmental stress, but also to deliver increased yields.

Through heterosis, hybrid breeding has the potential to generate varieties with higher yield, and improved stress responses, but large scale production of hybrids require systems enabling reliable, continued crosses of two elite varieties (Kim & Zhang, 2018; Longin et al., 2012; Mühleisen et al., 2014). Qualities resulting in a good pollen donor, such as high pollen production and spreading, is required for the male parent, whereas the female parent has to be prevented from self-pollination through inhibition of the release of viable pollen. In this project, traits aligned to both these goals have been studied in wheat and barley to get a better understanding of the challenges of hybrid breeding.

7.2 Pollen development genes in barley and validation of identified orthologues

The gene regulatory network controlling pollen development has been widely studied in model species, such as *Arabidopsis* and rice, however the transfer of knowledge to temperate monocot crops like barley and wheat has been slow. Identification of orthologous genes of interest from the *Arabidopsis* or rice molecular pathway can be used to investigate the conservation of gene function and to further study the function of the gene in cereal crops of agronomic importance.

Bioinformatic approaches are useful for the identification of gene sequences of potential orthologues, and for prediction of subcellular localisation or gene function (Duran et al., 2009). Once gene sequences and functions have been predicted, validation of identified target genes can be accomplished *in planta* through altered levels of gene expression using overexpression lines, gene silencing or knock-out mutations to disrupt gene functions (Curtin et al., 2017; Ioannidis et al., 2009). With the discovery of the CRISPR/Cas9 gene editing system and the implementation of plant transformation protocols, the possibilities for targeted gene mutagenesis for the study of genes have revolutionised crop research (Zhang et al., 2017).

The CRISPR/Cas9 gene editing system has the possibility of recognising specific target sequences, and introduce single or double stranded breaks to potentially introduce mutations (Zhang et al., 2017). The system is reliant on the transformation of the sequences of the Cas9 protein along with the sgRNAs into the plant, but for some species there is no transformation protocol available or only certain cultivars are susceptible for

transformation, severely reducing the usefulness of the system (Botella, 2019). *Agrobacterium* mediated transformation of immature embryos is the most efficient transformation system for barley, however Golden Promise is the only cultivar which is widely used, and it requires lengthy cultivation of immature embryos with low transformation efficiencies with average success rates of 25% (Harwood, 2019). In addition, the success of the mutagenesis in the transgenic plants depends largely on the design and number of sgRNA per transformation as well as the type of Cas9 used (Castel et al., 2019; Lawrenson et al., 2015).

Efforts to maximise gene editing efficiencies through sgRNA target optimisation has been carried out in *Arabidopsis* (Castel et al., 2019), however this has only been analysed in individual studies for barley. In a study on a phytoene desaturase gene (*HvPDS*) involved in the carotenoid pathway, using one sgRNA per transformation, the efficiency of the Cas9 induced mutagenesis in transgenic lines was 15%, with six out of forty transgenic plants exhibiting mutations (Howells et al., 2018). In another study on *HvPM19* involved with abscisic acid signalling, three out of thirteen, and one out of ten transgenic plants exhibited stably inherited mutations, resulting in gene editing efficiencies of 23% and 10% with two individual sgRNAs used for the transformation (Lawrenson et al., 2015). The difference in efficiency between the number of sgRNAs transformed into barley has not been extensively evaluated and multiple transgenic lines with different sgRNA design and gene targets are required to optimise CRISPR induced mutagenesis protocols in barley.

In this project CRISPR sgRNA targets were generated for three genes of interest, *HvDEX1*, *HvICE1-1* and *HvMMD1-1*. In two separate vectors three sgRNAs in tandem were used for *HvDEX1* and *HvMMD-1*, and for *HvICE1-1* three sgRNAs in independent vectors were co-transformed, resulting in six targets transformed per gene. In total 17 transformants were produced which were positive for the Cas9 transgene, however no CRISPR induced mutations were identified. The low transformation efficiency, the design of the sgRNA, or the number of transformed sgRNA could be the cause of the lack of induced mutants and for further studies these factors should be revised. Gene editing with the CRISPR/Cas9 system is constantly revised and with updated protocols for sgRNA design and barley transformation it might be possible to enhance the mutagenesis effects.

7.2.1 The effect of overexpression or SRDX-silencing of *HvICE1-1* on plant morphology

A barley orthologue of *ICE1* was identified in a transcriptome analysis of the conditionally sterile *HvMS1* overexpression lines. These lines exhibited sterile anthers at 15˚C but plants grown at >18˚C displayed restored fertility (Fernández-Gómez et al., 2020). The *HvICE1-1* orthologue was identified as differentially expressed with a 1.5 times higher expression in the HvMS1:OE lines grown at 15˚C (José Fernández Gómez, unpublished data). The annotated *ICE1* orthologue *HvICE1-1* was hypothesised to be an interesting target for further analysis of potential correlation between temperature and fertility.

Three putative orthologues of *ICE1,* named *HvICE1-1*, *HvICE1-2* and *HvICE1-3*, were identified in the barley genome. To avoid potential redundancy in the signalling of the *HvICE1* homologs, the function of the putative *ICE1* orthologue, *HvICE1-1,* was studied in transgenic plants with *HvICE1-1* overexpression or SRDX-silencing of the *HvICE1-1* transcript. Induced overexpression or silencing of genes can be used as complementary approaches to mutagenesis of the native gene for the study of gene functions *in planta*.

Through gene expression analysis under control and cold stress the *HvICE1-1* was not sufficient to severely affect the expression of the *HvICE1-2* homolog or the potential regulators, *HvHOS1* and *HvSIZ1*, similar to what was seen in *Arabidopsis* (Dong et al., 2006; Miura et al., 2007). However, the induction of the putative downstream target *HvCBF3* under cold stress was significantly lower in the *HvICE1-1* overexpression and silencing lines, suggesting there is an effect of *HvICE1-1* on this cold response regulator, but the SRDX-silencing of *HvICE1-1* was not sufficient to completely inhibit the *HvCBF3* response. Incomplete silencing of downstream genes through SRDX-mediated silencing has been found for other floral traits. In *Arabidopsis* the expression of the floral patterning gene *LEAFY* coupled with SRDX lead to reduced but not completely silenced expression of downstream genes, which was sufficient to cause sterility, both male and female, similar to the knock-out mutation (Mitsuda et al., 2006). Analysis of a rice orthologue of *APETALA3*, another flower development gene, through SRDX-mediated silencing caused severe sterility in rice, validating the use of the SRDX system in monocots (Mitsuda et al., 2006).

The *HvICE1-1* SRDX-silenced plants showed a minor increased susceptibility to freezing stress with slower recovery but had no effect on yield. In contrast, the *HvICE1-1* overexpression lines displayed 100% survival after freezing stress, but a reduced seed set as a consequence of inhibited growth leading to a reduced number of tillers. The effect of the *ICE1* orthologues on fertility and yield is not clear. *ICE1* was first identified in *Arabidopsis* where the knock-out mutant *ice1* had reduced cold tolerance but there was no effect on fertility or flowering time (Chinnusamy et al., 2003). Another study of a knock-out mutant of *ice1* found that anthers displayed indehiscence and male fertility was affected by the effect of *ICE1* on anther dehydration (Wei et al., 2018). It was also shown that the *ICE1* promoter is highly active in the inflorescence and floral organs (Wei et al., 2018) suggesting *ICE1* has some function in floral biology. The overexpression of the *Arabidopsis ICE1* in rice resulted in an increased yield, higher stress tolerance and higher stomatal density (Verma et al., 2020) whereas the overexpression of the *OsICE1* in *Arabidopsis* led to increased cold tolerance (Deng et al., 2017), suggesting that the function of the *ICE1* orthologues is conserved across species. How the *ICE1* orthologues affect yield and how this relates to cold tolerance is however not known but is of interest for the generation of crops with stable yield under abiotic stresses. Further investigation of the possible effect of the *HvICE1* homologs and the redundancy in the signalling pathway would clarify the function of the genes in barley.

In addition to the effect of *ICE1* on cold response the gene is also involved with the gene network responsible for stomatal formation in *Arabidopsis* (Kanaoka et al., 2008). Previously, the effect of *ICE1* on stomatal conductance or photosynthetic efficiency has not been

investigated, however, photosynthesis is dependent on the gaseous exchange facilitated by the stomata (Dai et al., 2007). Water management through gaseous exchange and photosynthesis capacity are qualities that are valuable for seed set and the effect of *HvICE1-1* in relation to these parameters were investigated in the overexpression and silencing lines. A previous study on the transcriptome of an overexpression mutant of *ICE1*, named *scrm-D*, found that genes predicted to be involved with photosynthesis were not affected by the expression of *ICE1* (Pillitteri et al., 2011) and another study found no connection between stomata and the photosynthetic efficiency in *Arabidopsis* (Schuler et al., 2018). In barley however there appears to be a connection between the cold response (COR) genes and photosynthesis (Dal Bosco et al., 2003) and in maize genes involved with photosynthesis can be induced by cold stress (Nguyen et al., 2009), suggesting that there is a connection between cold signalling and photosynthesis. The influence of *ICE1* on such diverse traits as cold response, yield, stomatal formation, and photosynthesis complicates the analysis of the function on individual processes *in planta* but its role in the different gene networks controlling these traits makes *ICE1* and its orthologues interesting for further investigation.

In this study the *HvICE1-1* overexpression line had a reduced stomatal conductance in control conditions without any difference in stomatal density whereas no difference was detected in the silencing lines. In addition, the silencing of *HvICE1-1* had little effect on the photosynthetic capacity in barley, but the overexpression of *HvICE1-1* appears to increase the photosynthetic efficiency and the electron transport rate under control conditions but led to a stronger reduction in response to cold stress. Together this implies that *HvICE1-1* in barley can influence photosynthetic parameters under normal conditions and under cold stress.

7.2.2 Approaches adopted to identify agriculturally important traits: GWAS and mutant collection screening

Genetic resources for cereals are becoming increasingly available for breeding and research with genotyping platforms with higher density and searchable databases with detailed gene annotations, improved gene predictions for potential orthologues, putative gene functions, and candidate genes. Improved genotyping platforms with higher coverage along with high-throughput phenotyping has the potential to increase the accuracy of genome wide association studies (Saini et al., 2022a) as well as the usefulness of generated mutant populations by enabling fine mapping of loci of interest to more accurately localise the genetic component of valuable traits. The usage of well-maintained mutant populations and genome-wide screening of large populations could enable identification of novel genes or traits useful for future breeding.

7.2.2.1 Mutant populations for male sterility traits

Screening of mutant populations can be valuable for the identification of novel traits (IBGSC, 2012; Druka et al., 2011; Talamè et al., 2008). In this study six selected lines from a collected mutant population consisting of barley mutants backcrossed into Bowman (BW-lines) were investigated. The near isogenic lines are available through NordGen and have previously been used for the investigation of novel loci involved with flowering traits (Druka et al.,

2011; Houston et al., 2012; Ramsay et al., 2011; Zakhrabekova et al., 2012). The selected lines were genotyped for the markers associated with the trait and several plants carrying the mutant genotype were detected. Unfortunately, only one sterile plant was identified, which exhibited both female and male infertility and could not be rescued, preventing any further studies of the selected BW-lines.

In this population the BW-lines categorised as genic male sterile have been described as containing recessive male sterility traits (Franckowiak et al., 2015) and are maintained as fertile heterozygotes resulting in a low proportion of mutant genotypes in the population (Robbie Waugh, personal communication). It is possible that the mutant male sterility trait is only present at a minor level in the population of each BW-line due to repeated selfing of wild types and heterozygotes for the seed stock maintenance. In addition, the lack of mutant phenotypes in the screened plants of the selected BW-lines could be due to low seed availability and the low number of plants screened for each line. For future studies of the male sterile traits in the BW-lines it is recommended to screen large populations to isolate homozygotes mutants or heterozygotes for screening in subsequent generations.

Screening of selected plants with 35k genotyping platform identified regions in the Bowman backgrounds where the genotype of the line carrying the original mutation had been introgressed. This proves that this genotyping platform can detect differences between Bowman and other cultivars and can be a useful tool to genotype other lines to enable fine-mapping of regions of interest. For some of the genotyped lines there was no sterile phenotype despite homozygous non-Bowman genotypes, suggesting that these regions did not contain any loci sufficient for the regulation of male fertility and these regions can therefore be excluded from having an effect on fertility in the line. Screening of other BW-lines with the 35k genotyping platform would enable fine mapping and identification of regions of interest for the study of potentially novel male sterility traits.

7.2.2.2 Genome-wide association studies for anther traits in wheat

The pollen donor in a hybrid breeding program should preferentially have high pollen production and ability to spread the pollen outside of the floret (Boeven et al., 2018). To achieve these qualities anther length has been used as a proxy for pollen production, since longer anthers have been shown to have higher pollen mass (Nguyen et al., 2015), and anther extrusion has been used as a measure of inter-floral pollen shedding capabilities (Beri & Anand, 1971). In contrast, hexaploid bread wheat variates generally have short anthers with low extrusion with few useful pollen donor candidates. The cultivar Piko has been used as the male parent in hybrid breeding since its release in 1994 and is still considered to be one of the best male parents in breeding programs, with high extrusion and pollen production (Boeven et al., 2018; Okada et al., 2021). In this study a bi-parental mapping population of the cultivars Piko and KWS Julius, a cultivar with average anther length and extrusion, was used to identify genetic components underlying anther length. In addition, the Yellowhammer population, a genetically diverse panel of 427 elite cultivars originally composed to study disease resistance, was genotyped and phenotyped for anther length,

anther extrusion and plant height to analyse correlations between the traits and to identify loci related to anther traits through GWAS. Lastly, a population of hexaploid wheat with introgressions from wheat wild relatives was analysed for anther length, anther extrusion and plant height to potentially identify loci related to anther traits that is not present in modern bread wheat.

Genome-wide association study is a powerful tool for genomic research but the outcome of a GWAS is dependent on the genetic diversity in the population as well as the quality of the genotyping platform for the identification of said diversity (Allen et al., 2017; Winfield et al., 2016). The outcome of GWAS can provide a starting point for breeding programs by identifying loci associated to certain traits of interest. GWA studies in wheat have been conducted for agronomic and quality traits, biotic and abiotic resistance, and yield, to identify trait associated markers, identifying thousands of QTLs associated with the various traits (Saini et al., 2022a). The use of GWA studies in wheat have become more frequent however post-GWAS analysis with fine mapping of loci of interest for further studies of causative loci and for validation of candidate loci is not regularly performed (Saini et al., 2022a). In the previous GWA studies conducted on anther length and extrusion (Adhikari et al., 2020; El Hanafi et al., 2021; Muqaddasi et al., 2016; Muqaddasi et al., 2017; Song et al., 2018) there was no further analysis of the QTLs or identification of candidate genes.

Where multiple studies have analysed similar traits, the data can be combined, and analysed through meta-analysis. This could provide better predictions of causative loci and potential candidate genes through a combined analysis of populations with different genetic diversity. Disease resistance is one of the most studied qualities in wheat and to identify QTLs related to disease resistance in wheat, Saini et al. (2022b) combined 16 GWA studies in a meta-analysis. Through this the number of QTLs associated to the traits of interest were reduced from 493 to 85 potential candidate genes (Saini et al. 2022b). Similar approaches for anther traits would be beneficial for an accurate identification of candidate genes in diverse wheat populations.

GWAS is a statistical tool used to predict causative loci and the effect of those loci on a trait of interest, and can detect QTLs with minor effect. However, validation of any identified candidate genes have to be carried out either through other populations or through targeted mutagenesis of the genes in question (Curtin et al., 2017; Ioannidis et al., 2009). The loci and candidate genes identified in the Yellowhammer elite cultivar population were predicted to influence anther length and extrusion and might provide useful information for breeding of the traits in this population but further validation is required to determine the function of the candidate genes.

The available genetic diversity in hexaploid wheat is very limited and there is an increasing need to introduce and use new genetic material from wild relatives (Charmet, 2011; Cox, 1998). Wheat lines generated through introgression of wild wheat relatives into hexaploid elite cultivars (Grewal et al., 2018, 2021a; King et al., 2017, 2019) were analysed to possibly

identify regions containing previously unused genetic diversity that could be useful for breeding of elite bread wheat cultivars. The GWAS conducted on the alien introgression lines consisted of a very small sample set with low marker coverage, resulting in low confidence of the validity of the associated marker, however the high genetic diversity of this population was of interest. The marker identified on chromosome 5A in the *T. urartu* population in relation to anther length was predicted to be associated with a locus related to shorter anthers. A reduction in anther length is not directly useful for breeding purposes however the study of loci that inhibit anther growth could provide valuable knowledge about anther formation. The markers identified for the anther traits in BOP and the Yellowhammer population of elite cultivars could be used to track traits of interest in future breeding programs to aid the selection for higher extrusion and longer anthers.

In addition to the GWAS conducted on the BOP, the lines with introgressions from the wild relatives *Amblyopyrum muticum* and *Triticum urartu* were compared depending on the specific introgressed regions. In the alien introgression population, some lines carried similar introgressions which enabled analysis of the effect of those regions on anther traits and lines with similar introgressions were compared to the remaining population. The lines carrying introgressions from *A. muticum* on chromosome 7D and of *T. urartu* on chromosome 3A had higher extrusion, suggesting that these regions could be worth further investigation to determine if these regions from the wild relatives could contribute with previously underutilised genetic diversity useful for elite cultivars.

7.3 Areas for future work

This work has highlighted areas for future research within anther traits in hexaploid and wild wheat relatives as well as identified three homologous *HvICE1* candidates involved with cold sensing and stomatal formation. As a continuation of these projects, areas of future research have been identified.

- Generation of knock-out mutations of *HvICE1-1* as well as the other *HvICE1* homologs would aid the investigation of the function of the *HvICE1* homologs in barley. Alternatively, overexpression or silencing of all *HvICE1* homologs could provide interesting information of the function of the genes in terms of cold stress or stomatal formation.

- Detailed molecular studies to investigate gene interactions of *HvICE1* homologs. Through gene expression analysis it was not possible to determine any effect of *HvICE1-1* on *HvICE1-2* however it is possible that these proteins as well as HvICE1-3 can interact, similar to the interaction seen for *ICE1* and *ICE2* in stomatal formation in *Arabidopsis*. Yeast-2 hybrid screening of the proteins could help with the investigation of the interactions. This would provide more information about the roles of the homologs in signaling, whether they can regulate each other, and provide more information about signaling pathways in barley.

- To validate the loci associated to anther length and extrusion and the identified candidate genes further studies of the loci through targeted mutagenesis is required. Overexpression, silencing or knock-out of the candidate genes in wheat would be useful for the understanding of anther traits in wheat.

- The regions in the alien introgression lines on chromosome 3A and 7D requires investigation to analyse the effect of the loci. Fine mapping of the regions with more lines would also aid in the determination of the effect of the loci and possibly to identifying causative genes.

7.4 Conclusions

Identification of qualities for good pollen donors as well as strategies for the generation of male sterility are needed to facilitate efficient hybrid breeding. In this study multiple approaches for the study of floral biology have been used to broaden the understanding of male reproduction in cereals. Generation of transgenic plants overexpressing or silencing *HvICE1-1* in barley highlighted the complexity of the cold signalling pathway, the potential redundancies of the *HvICE1* homologs and the mechanisms that are in place to prevent triggering of cold responses and inhibit plant growth. The reduced yield of the *HvICE1-1* overexpression lines suggests that cold sensing and the regulation of *HvICE1-1* is important for the viability of the plant.

In addition, candidate loci and genes involved with anther length and extrusion were identified in hexaploid wheat. This was complemented by analysis of a bi-parental population and wild wheat introgression lines to investigate genetic diversity in anther traits. The identified loci and the candidate genes potentially involved with anther length and anther extrusion can be further analysed through fine mapping to identify novel loci involved with anther traits in wheat.

References

Abiko, M., Akibayashi, K., Sakata, T., Kimura, M., Kihara, M., … Higashitani, A. (2005). High-temperature induction of male sterility during barley (Hordeum vulgare L.) anther development is mediated by transcriptional inhibition. *Sexual Plant Reproduction*, *18*, 91–100. https://doi.org/10.1007/s00497-005-0004-2

Adhikari, A., Basnet, B. R., Crossa, J., Dreisigacker, S., Camarillo, F., … Ibrahim, A. M. H. (2020). Genome-Wide Association Mapping and Genomic Prediction of Anther Extrusion in CIMMYT Hybrid Wheat Breeding Program via Modeling Pedigree, Genomic Relationship, and Interaction With the Environment. *Frontiers in Genetics*, *11*(December), 1–13. https://doi.org/10.3389/fgene.2020.586687

Agarwal, M., Hao, Y., Kapoor, A., Dong, C. H., Fujii, H., … Zhu, J. K. (2006). A R2R3 type MYB transcription factor is involved in the cold regulation of CBF genes and in acquired freezing tolerance. *Journal of Biological Chemistry*, *281*(49), 37636–37645. https://doi.org/10.1074/jbc.M605895200

Alexandrov, V., Kartseva, T., Alqudah, A.M., Kocheva, K., Tasheva, K., Börner, A., Misheva, S. (2021). Genetic diversity, linkage disequilibrium and population structure of Bulgarian bread wheat assessed by genome-wide distributed SNP markers:from old germplasm to semi-dwarf cultivars. *Plants*, 10, 1116. https://doi.org/10.3390/plants10061116

Allen, A. M., Winfield, M. O., Burridge, A. J., Downie, R. C., Benbow, H. R., … Edwards, K. J. (2017). Characterization of a Wheat Breeders' Array suitable for high-throughput SNP genotyping of global accessions of hexaploid bread wheat (Triticum aestivum). *Plant Biotechnology Journal*, *15*(3), 390–401. https://doi.org/10.1111/pbi.12635

Andreuzza, S., Nishal, B., Singh, A., & Siddiqi, I. (2015). The Chromatin Protein DUET/MMD1 Controls Expression of the Meiotic Gene TDM1 during Male Meiosis in Arabidopsis. *PLoS Genetics*. https://doi.org/10.1371/journal.pgen.1005396

Ariizumi, T., Hatakeyama, K., Hinata, K., Sato, S., Kato, T., … Toriyama, K. (2003). A novel male-sterile mutant of Arabidopsis thaliana, faceless pollen-1, produces pollen with a smooth surface and an acetolysis-sensitive exine. *Plant Molecular Biology*, *53*(1–2), 107–116. https://doi.org/10.1023/B:PLAN.0000009269.97773.70

Baker, N. R., Oxborough, K., Lawson, T., & Morison, J. I. L. (2001). High resolution imaging of photosynthetic activities of tissues, cells and chloroplasts in leaves. *Journal of Experimental Botany*, *52*(356), 615–621. https://doi.org/10.1093/jxb/52.356.615

Baker, N. R., & Rosenqvist, E. (2004). Applications of chlorophyll fluorescence can improve crop production strategies: An examination of future possibilities. *Journal of Experimental Botany*, *55*(403), 1607–1621. https://doi.org/10.1093/jxb/erh196

Barnabás, B., Jäger, K., & Fehér, A. (2008). The effect of drought and heat stress on reproductive processes in cereals. *Plant, Cell and Environment*, *31*, 11–38. https://doi.org/10.1111/j.1365-3040.2007.01727.x

Bates, D., Mächler, M., Bolker, B. M., & Walker, S. C. (2015). Fitting linear mixed-effects models using lme4. *Journal of Statistical Software*, *67*(1). https://doi.org/10.18637/jss.v067.i01

Bayer, M. M., Rapazote-Flores, P., Ganal, M., Hedley, P. E., Macaulay, M., … Waugh, R. (2017). Development and evaluation of a barley 50k iSelect SNP array. *Frontiers in*

Plant Science, *8*. https://doi.org/10.3389/fpls.2017.01792

Beck, E. H., Fettig, S., Knake, C., Hartig, K., & Bhattarai, T. (2007). Specific and unspecific responses of plants to cold and drought stress. *Journal of Biosciences*, *32*(3), 501–510. https://doi.org/10.1007/s12038-007-0049-5

Bengtsson, T., Åhman, I., Bengtsson, T., Manninen, O., Veteläinen, M., … Orabi, J. (2017). Genetic diversity, population structure and linkage disequilibrium in Nordic spring barley (Hordeum vulgare L. subsp. vulgare). *Genetic Resources and Crop Evolution*, *64*(8), 2021–2033. https://doi.org/10.1007/s10722-017-0493-5

Benjamini, Y., & Hochberg, Y. (1995). Controlling the False Discovery Rate: A Practical and Powerful Approach to Multiple Testing. *Journal of the Royal Statistical Society: Series B (Methodological)*, *57*(1), 289–300. https://doi.org/10.1111/j.2517-6161.1995.tb02031.x

Beri, S. M., & Anand, S. C. (1971). Factors affecting pollen shedding capacity in wheat. *Euphytica*, *20*(2), 327–332. https://doi.org/10.1007/BF00056096

Bi, X., Esse, W. Van, Mulki, M. A., Kirschner, G., Zhong, J., … Korff, M. Von. (2019). Centroradialis interacts with flowering locus t-like genes to control floret development and grain number. *Plant Physiology*, *180*(2), 1013–1030. https://doi.org/10.1104/pp.18.01454

Boeven, P. H. G., Longin, C. F. H., Leiser, W. L., Kollers, S., Ebmeyer, E., & Würschum, T. (2016). Genetic architecture of male floral traits required for hybrid wheat breeding. *Theoretical and Applied Genetics*, *129*(12), 2343–2357. https://doi.org/10.1007/s00122-016-2771-6

Boeven, P. H. G., Würschum, T., Rudloff, J., Ebmeyer, E., & Longin, C. F. H. (2018). Hybrid seed set in wheat is a complex trait but can be improved indirectly by selection for male floral traits. *Euphytica*, *214*(7). https://doi.org/10.1007/s10681-018-2188-1

Botella, J. R. (2019). Now for the hard ones: is there a limit on CRISPR genome editing in crops? *Journal of Experimental Botany*, *70*(3), 734–737. https://academic.oup.com/jxb/article-abstract/70/3/734/5307184

Bradshaw, J. E. (2016). *Plant breeding: Past, Present and Future*. https://doi.org/10.1007/978-3-319-23285-0

Brendel, V., Kurtz, S., & Walbot, V. (2002). Comparative genomics of Arabidopsis and maize: Prospects and limitations. *Genome Biology*, *3*(3), 1–6. https://doi.org/10.1186/gb-2002-3-3-reviews1005

Buerstmayr, M., & Buerstmayr, H. (2015). Comparative mapping of quantitative trait loci for Fusarium head blight resistance and anther retention in the winter wheat population Capo × Arina. *Theoretical and Applied Genetics*, *128*(8), 1519–1530. https://doi.org/10.1007/s00122-015-2527-8

Buerstmayr, M., & Buerstmayr, H. (2016). The semidwarfing alleles Rht-D1b and Rht-B1b show marked differences in their associations with anther-retention in wheat heads and with fusarium head blight susceptibility. *Phytopathology*, *106*(12), 1544–1552. https://doi.org/10.1094/PHYTO-05-16-0200-R

Bull, H., Casao, M. C., Zwirek, M., Flavell, A. J., Thomas, W. T. B., … Waugh, R. (2017). Barley SIX-ROWED SPIKE3 encodes a putative Jumonji C-type H3K9me2/me3 demethylase that represses lateral spikelet fertility. *Nature Communications*, *8*(1).

https://doi.org/10.1038/s41467-017-00940-7

Cai, K., Chen, X., Han, Z., Wu, X., Zhang, S., … Zeng, F. (2020). Screening of Worldwide Barley Collection for Drought Tolerance: The Assessment of Various Physiological Measures as the Selection Criteria. *Frontiers in Plant Science*, *11*(July), 1–16. https://doi.org/10.3389/fpls.2020.01159

Caldwell, D. G., McCallum, N., Shaw, P., Muehlbauer, G. J., Marshall, D. F., & Waugh, R. (2004). A structured mutant population for forward and reverse genetics in Barley (Hordeum vulgare L.). *Plant Journal*, *40*(1), 143–150. https://doi.org/10.1111/j.1365-313X.2004.02190.x

Carlos, J., Isabel, M., & Dios Alche, J. de. (2011). Systematic and Phylogenetic Analysis of the Ole e 1 Pollen Protein Family Members in Plants. In N.-S. Yang (Ed.), *Systems and Computational Biology - Bioinformatics and Computational Modeling*. InTech. https://doi.org/10.5772/19175

Castel, B., Tomlinson, L., Locci, F., Yang, Y., & Jones, J. D. G. (2019). Optimization of T-DNA architecture for Cas9-mediated mutagenesis in Arabidopsis. *Optimization of T-DNA Architecture for Cas9-Mediated Mutagenesis in Arabidopsis*, *14*(1). https://doi.org/10.1101/419952

Chang, F., Zhang, Z., Jin, Y., & Ma, H. (2014). Cell biological analyses of anther morphogenesis and pollen viability in arabidopsis and rice. In J. L. Riechmann & F. Wellmer (Eds.), *Flower development* (Vol. 1110, pp. 203–216). Humana Press. https://doi.org/10.1007/978-1-4614-9408-9_9

Charmet, G. (2011). Wheat domestication: Lessons for the future. *Comptes Rendus - Biologies*, *334*(3), 212–220. https://doi.org/10.1016/j.crvi.2010.12.013

Chen, L., & Liu, Y.-G. (2014). Male Sterility and Fertility Restoration in Crops. *Annual Review of Plant Biology*, *65*(1), 579–606. https://doi.org/10.1146/annurev-arplant-050213-040119

Chen, R., Zhao, X., Shao, Z., Wei, Z., Wang, Y., … He, G. (2007). Rice UDP-glucose pyrophosphorylase1 is essential for pollen callose deposition and its cosuppression results in a new type of thermosensitive genic male sterility. *Plant Cell*, *19*(3), 847–861. https://doi.org/10.1105/tpc.106.044123

Cheng, S. H., Zhuang, J. Y., Fan, Y. Y., Du, J. H., & Cao, L. Y. (2007). Progress in research and development on hybrid rice: A super-domesticate in China. *Annals of Botany*, *100*(5), 959–966. https://doi.org/10.1093/aob/mcm121

Chinnusamy, V., Ohta, M., Kanrar, S., Lee, B. ha, Hong, X., … Zhu, J. K. (2003). ICE1: A regulator of cold-induced transcriptome and freezing tolerance in arabidopsis. *Genes and Development*, *17*(8), 1043–1054. https://doi.org/10.1101/gad.1077503

Choi, D., Rodriguez, E. M., & Close, T. J. (2002). Barley Cbf3 gene identification, expression pattern, and map location. *Plant Physiology*, *129*, 1781–1787. https://doi.org/10.1104/pp.003046.1

Cigan, A. M., Singh, M., Benn, G., Feigenbutz, L., Kumar, M., … Young, J. (2017). Targeted mutagenesis of a conserved anther-expressed P450 gene confers male sterility in monocots. *Plant Biotechnology Journal*, *15*(3), 379–389. https://doi.org/10.1111/pbi.12633

Close, T. J., Bhat, P. R., Lonardi, S., Wu, Y., Rostoks, N., … Waugh, R. (2009). Development

and implementation of high-throughput SNP genotyping in barley. *BMC Genomics*, *10*(1), 582. https://doi.org/10.1186/1471-2164-10-582

Colas, I., Barakate, A., MacAulay, M., Schreiber, M., Stephens, J., … Ramsay, L. (2019). Desynaptic5 carries a spontaneous semi-dominant mutation affecting Disrupted Meiotic cDNA 1 in barley. *Journal of Experimental Botany*, *70*(10), 2683–2698. https://doi.org/10.1093/jxb/erz080

Colmsee, C., Beier, S., Himmelbach, A., Schmutzer, T., Stein, N., … Mascher, M. (2015). BARLEX - The barley draft genome explorer. *Molecular Plant*, *8*(6), 964–966. https://doi.org/10.1016/j.molp.2015.03.009

Consortium, T. I. B. G. S. (2012). A physical, genetic and functional sequence assembly of the barley genome. *Nature*, *491*(7426), 711–716. https://doi.org/10.1038/nature11543

Conte, M. G., Gaillard, S., Droc, G., & Perin, C. (2008). Phylogenomics of plant genomes: A methodology for genome-wide searches for orthologs in plants. *BMC Genomics*, *9*, 1–16. https://doi.org/10.1186/1471-2164-9-183

Cox, T. S. (1998). Deepening the wheat gene pool. *Journal of Crop Production*, *1*(1), 1–25. https://doi.org/10.1300/J144v01n01_01

Crosatti, C., De Laureto, P. P., Bassi, R., & Cattivelli, L. (1999). The interaction between cold and light controls the expression of the cold-regulated barley gene cor14b and the accumulation of the corresponding protein. *Plant Physiology*, *119*(2), 671–680. https://doi.org/10.1104/pp.119.2.671

Curtin, S. J., Tiffin, P., Guhlin, J., Trujillo, D., Burghart, L., … Young, N. D. (2017). Validating genome-wide association candidates controlling quantitative variation in nodulation. *Plant Physiology*, *173*(2), 921–931. https://doi.org/10.1104/pp.16.01923

Dadshani, S., Mathew, B., Ballvora, A., Mason, A.S., Léon, J. (2021). Detection of breeding signatures in wheat using a linkage disequilibrium-corrected mapping approach. *Scientific Reports*, 11, 5527. https://doi.org/10.1038/s41598-021-85226-1

Dai, F., Zhou, M., & Zhang, G. (2007). The change of chlorophyll fluorescence parameters in winter barley during recovery after freezing shock and as affected by cold acclimation and irradiance. *Plant Physiology and Biochemistry*, *45*(12), 915–921. https://doi.org/10.1016/j.plaphy.2007.09.006

Dal Bosco, C., Busconi, M., Govoni, C., Baldi, P., Michele Stanca, A., … Cattivelli, L. (2003). Cor Gene Expression in Barley Mutants Affected in Chloroplast Development and Photosynthetic Electron Transport. *Plant Physiology*, *131*(2), 793–802. https://doi.org/10.1104/pp.014530

De Vries, A. P. (1974). Some aspects of cross-pollination in wheat (Triticum aestivum L.). 3. Anther length and number of pollen grains per anther. *Euphytica*, *23*(1), 11–19. https://doi.org/10.1007/BF00032735

Deng, C., Ye, H., Fan, M., Pu, T., & Yan, J. (2017). The rice transcription factors OsICE confer enhanced cold tolerance in transgenic Arabidopsis. *Plant Signaling and Behavior*, *12*(5). https://doi.org/10.1080/15592324.2017.1316442

Devos, K. M., Beales, J., Nagamura, Y., & Sasaki, T. (1999). *Arabidopsis-Rice: Will Colinearity Allow Gene Prediction Across the Eudicot-Monocot Divide?* www.genome.org

Ding, Y., Li, H., Zhang, X., Xie, Q., Gong, Z., & Yang, S. (2015). OST1 kinase modulates freezing

tolerance by enhancing ICE1 stability in arabidopsis. *Developmental Cell*, *32*(3), 278–289. https://doi.org/10.1016/j.devcel.2014.12.023

Dixon, LE., Greenwood, JR., Bencivenga, S., Zhang, P., Cockram, J., Mellers, G., Ramm, K., Cavanagh, C., Swain, SM., Boden, SA. (2018). TEOSINTE BRANCED1 Regulates Inflorescence Architecture and Development in Bread Wheat (*Triticum aestivum*). *Plant Cell*, Mar;30(3):563-581. doi: 10.1105/tpc.17.00961. Epub 2018 Feb 14. PMID: 29444813; PMCID: PMC5894836.

Dong, C.-H., Agarwal, M., Zhang, Y., Xie, Q., & Zhu, J.-K. (2006). The negative regulator of plant cold responses, HOS1, is a RING E3 ligase that mediates the ubiquitination and degradation of ICE1. *PNAS*, *103*(21), 8281–8286. www.pnas.orgcgidoi10.1073pnas.0602874103

Druka, A., Franckowiak, J., Lundqvist, U., Bonar, N., Alexander, J., … Waugh, R. (2011). Genetic Dissection of Barley Morphology and Development. *Plant Physiology*, *155*(2), 617–627. https://doi.org/10.1104/pp.110.166249

Dubouzet, J. G., Sakuma, Y., Ito, Y., Kasuga, M., Dubouzet, E. G., … Yamaguchi-Shinozaki, K. (2003). OsDREB genes in rice, Oryza sativa L., encode transcription activators that function in drought-, high-salt- and cold-responsive gene expression. *Plant Journal*, *33*(4), 751–763. https://doi.org/10.1046/j.1365-313X.2003.01661.x

Dulk-Ras, A. den, & Hooykaas, P. J. J. (1995). Electroporation of Agrobacterium tumefaciens. In *Plant Cell Electroporation And Electrofusion Protocols* (pp. 63–72). Humana Press. https://doi.org/10.1385/0-89603-328-7:63

Duran, C., Edwards, D., & Batley, J. (2009). Genetic Maps and the Use of Synteny. *Methods in Molecular Biology, Plant Genomics*, *513*, 41–55. https://doi.org/10.1007/978-1-59745-427-8_3

Eavis, R. M., Batchelor, S. E., Murray, F., & Walker, K. C. (1996). *Hybrid breeding of wheat, barley and rye: developments to date and future prospects*.

El Hanafi, S., Cherkaoui, S., Kehel, Z., Al-Abdallat, A., & Tadesse, W. (2021). Genome-Wide Association and Prediction of Male and Female Floral Hybrid Potential Traits in Elite Spring Bread Wheat Genotypes. *Plants*, *10*(5), 895. https://doi.org/10.3390/plants10050895

Engler, C., Youles, M., Gruetzner, R., Ehnert, T. M., Werner, S., … Marillonnet, S. (2014). A Golden Gate modular cloning toolbox for plants. *ACS Synthetic Biology*, *3*(11), 839–843. https://doi.org/10.1021/sb4001504

Falk, A., Schulman, A. H., Rasmussen, S. K., & Jansson, C. (2001). Genetics Barley Mutagenesis. *Progress in Botany*, *62*. http://www.biocenter.helsinki.fi/bi/genomedynamics/Pdfs/978-3-642-56849-7_3.pdf

Fernández-Gómez, J., Talle, B., Tidy, A., & Wilson, Z. A. (2020). Accurate staging of reproduction development in Cadenza wheat by non-destructive spike analysis. *Journal of Experimental Botany*.

Fernández-Gómez, J., Talle, B., & Wilson, Z. A. (2020). Increased expression of the MALE STERILITY1 transcription factor gene results in temperature-sensitive male sterility in barley. *Journal of Experimental Botany*, *71*(20), 6328–6339. https://doi.org/10.1093/jxb/eraa382

Fernández-González, M., González-Fernández, E., Fernández-González, D., & Rodríguez-Rajo,

F. J. (2020). Secondary Outcomes of the Ole e 1 Proteins Involved in Pollen Tube Development: Impact on Allergies. *Frontiers in Plant Science*, *11*(July), 1–7. https://doi.org/10.3389/fpls.2020.00974

Fernández Gómez, J., & Wilson, Z. A. (2014). A barley PHD finger transcription factor that confers male sterility by affecting tapetal development. *Plant Biotechnology Journal*, *12*(6), 765–777. https://doi.org/10.1111/pbi.12181

Fiebig, A., Mayfield, J. A., Miley, N. L., Chau, S., Fischer, R. L., & Preuss, D. (2000). Alterations in CER6, a gene identical to CUT1, differentially affect long-chain lipid content on the surface of pollen and stems. *Plant Cell*, *12*(10), 2001–2008. https://doi.org/10.1105/tpc.12.10.2001

Franckowiak, J. D., Kleinhofs, A., & Lundqvist, U. (2015). Descriptions of barley genetic stocks for 2015. *Barley Genetics Newsletter*, *43*, 32–36.

Franks, P. J., & Farquhar, G. D. (2007). The mechanical diversity of stomata and its significance in gas-exchange control. *Plant Physiology*, *143*(1), 78–87. https://doi.org/10.1104/pp.106.089367

Fursova, O. V., Pogorelko, G. V., & Tarasov, V. A. (2009). Identification of ICE2, a gene involved in cold acclimation which determines freezing tolerance in Arabidopsis thaliana. *Gene*, *429*(1–2), 98–103. https://doi.org/10.1016/j.gene.2008.10.016

Gale, M. D., Devos, K. M., Hayward, (M, King, I. P., Thomas, H. M., … Morgan, G. (1998). Comparative genetics in the grasses. *Proceedings of the National Academy of Sciences*, *95*, 1971–1974. www.pnas.org.

Gilmour, S. J., Sebolt, A. M., Salazar, M. P., Everard, J. D., & Thomashow, M. F. (2000). Overexpression of the arabidopsis CBF3 transcriptional activator mimics multiple biochemical changes associated with cold acclimation. *Plant Physiology*, *124*(4), 1854–1865. https://doi.org/10.1104/pp.124.4.1854

Gilmour, Sarah J., Zarka, D. G., Stockinger, E. J., Salazar, M. P., Houghton, J. M., & Thomashow, M. F. (1998). Low temperature regulation of the Arabidopsis CBF family of AP2 transcriptional activators as an early step in cold-induced COR gene expression. *Plant Journal*, *16*(4), 433–442. https://doi.org/10.1046/j.1365-313X.1998.00310.x

Gilmour, Sarah J, Fowler, S. G., & Thomashow, M. F. (2004). *Arabidopsis* transcriptional activators *CBF1*, *CBF2*, and *CBF3* have matching functional activities. *Plant Molecular Biology*, *54*, 767–781.

Gioia, T., Galinski, A., Lenz, H., Müller, C., Lentz, J., … Nagel, K. A. (2017). GrowScreen-PaGe, a non-invasive, high-throughput phenotyping system based on germination paper to quantify crop phenotypic diversity and plasticity of root traits under varying nutrient supply. *Functional Plant Biology*, *44*(1), 76–93. https://doi.org/10.1071/FP16128

Goldberg, R. B., Beals, T. P., & Sanders, P. M. (1993). Anther Development : Basic Principles and Practical Applications. *The Plant Cell*, *5*(October), 1217–1229. https://doi.org/10.1105/tpc.5.10.1217

Gómez, J. F., Talle, B., & Wilson, Z. A. (2015). Anther and pollen development: A conserved developmental pathway. *Journal of Integrative Plant Biology*, *57*(11), 876–891. https://doi.org/10.1111/jipb.12425

Gomez, J., & Wilson, Z. A. (2012). Non-destructive staging of barley reproductive development for molecular analysis based upon external morphology. *Journal of*

Experimental Botany, *63*(2), 695–709. https://doi.org/10.1093/jxb/err313

Gray, G. R., Hope, B. J., Qin, X., Taylor, B. G., & Whitehead, C. L. (2003). The characterization of photoinhibition and recovery during cold acclimation in Arabidopsis thaliana using chlorophyll fluorescence imaging. *Physiologia Plantarum*, *119*(3), 365–375. https://doi.org/10.1034/j.1399-3054.2003.00224.x

Grewal, S., Coombes, B., Joynson, R., Hall, A., Fellers, J., … King, J. (2021a). *A novel approach to develop wheat chromosome-specific KASP markers for detecting Amblyopyrum muticum segments in doubled haploid introgression lines*. 1–20.

Grewal, S., Guwela, V., Newell, C., Yang, C., Ashling, S., … King, J. (2021b). Generation of Doubled Haploid Wheat-Triticum urartu Introgression Lines and Their Characterisation Using Chromosome-Specific KASP Markers. *Frontiers in Plant Science*, *12*(May), 1–13. https://doi.org/10.3389/fpls.2021.643636

Grewal, S., Hubbart-Edwards, S., Yang, C., Devi, U., Baker, L., … King, J. (2020). Rapid identification of homozygosity and site of wild relative introgressions in wheat through chromosome-specific KASP genotyping assays. *Plant Biotechnology Journal*, *18*(3), 743–755. https://doi.org/10.1111/pbi.13241

Grewal, S., Hubbart-Edwards, S., Yang, C., Scholefield, D., Ashling, S., … King, J. (2018). Detection of T. Urartu introgressions in wheat and development of a panel of interspecific introgression lines. *Frontiers in Plant Science*, *871*. https://doi.org/10.3389/fpls.2018.01565

Gubler, F., Kalla, R., Roberts, J. K., & Jacobsen, J. V. (1995). Gibberellin-Regulated Expression of a myb Gene in Barley Aleurone Cells: Evidence for Myb Transactivation of a High-pl α-Amylase Gene Promoter. *The Plant Cell*, *7*(November), 1879–1891.

Gupta, P. K., Kulwal, P. L., & Jaiswal, V. (2019). Association mapping in plants in the post-GWAS genomics era. In *Advances in Genetics* (1st ed., Vol. 104). Elsevier Inc. https://doi.org/10.1016/bs.adgen.2018.12.001

Hahn, F., Mantegazza, O., Greiner, A., Hegemann, P., Eisenhut, M., & Weber, A. P. M. (2017). An efficient visual screen for CRISPR/CAS9 activity in arabidopsis thaliana. *Frontiers in Plant Science*, *8*(January), 1–13. https://doi.org/10.3389/fpls.2017.00039

Hannoufa, A., Negruk, V., Eisner, G., & Lemieux, B. (1996). The CER3 gene of Arabidopsis thaliana is expressed in leaves, stems, roots, flowers and apical meristems. *The Plant Journal*, *10*(3), 459–467.

Harrison, E. L., Arce Cubas, L., Gray, J. E., & Hepworth, C. (2020). The influence of stomatal morphology and distribution on photosynthetic gas exchange. *Plant Journal*, *101*(4), 768–779. https://doi.org/10.1111/tpj.14560

Hartley, J. L., Temple, G. T., & Brasch, M. A. (2000). DNA Cloning Using In Vitro Site-Specific Recombination. *Genome Research*, *10*, 1788–1795. https://doi.org/10.1101/gr.143000.that

Harwood, W. A. (2014). A protocol for High-Throughput Agrobacterium-mediated barley transformation. *Cereal Genomics*, *1099*, 251–260. https://doi.org/10.1007/978-1-62703-715-0

Harwood, W. A. (2019). *Barley Methods and Protocols*. http://www.springer.com/series/7651

Hassan, M. M., Zhang, Y., Yuan, G., De, K., Chen, J. G., … Yang, X. (2021). Construct design for CRISPR/Cas-based genome editing in plants. *Trends in Plant Science*, *26*(11), 1133–1152. https://doi.org/10.1016/j.tplants.2021.06.015

Hayama, R., Yokoi, S., Tamaki, S., Yano, M., & Shimamoto, K. (2003). Adaptation of photoperiodic control pathways produces short-day flowering in rice. *Nature*. https://doi.org/10.1038/nature01549

He, X., Singh, P. K., Dreisigacker, S., Singh, S., Lillemo, M., & Duveiller, E. (2016). Dwarfing genes Rht-B1b and Rht-D1b are associated with both type i FHB susceptibility and low anther extrusion in two bread wheat populations. *PLoS ONE*, *11*(9), 1–14. https://doi.org/10.1371/journal.pone.0162499

Hedden, P. (2003). The genes of the Green Revolution. *Trends in Genetics*, *19*(1), 5–9. https://doi.org/10.1016/S0168-9525(02)00009-4

Hellemans, J., Mortier, G., De Paepe, A., Speleman, F., & Vandesompele, J. (2007). qBase relative quantification framework and software for management and automated analysis of real-time quantitative PCR data. *Genome Biology*, *8*(2). https://doi.org/10.1186/gb-2007-8-2-r19

Hepworth, C., Caine, R. S., Harrison, E. L., Sloan, J., & Gray, J. E. (2018). Stomatal development: focusing on the grasses. *Current Opinion in Plant Biology*, *41*(Stage 5), 1–7. https://doi.org/10.1016/j.pbi.2017.07.009

Hiratsu, K., Matsui, K., Koyama, T., & Ohme-Takagi, M. (2003). Dominant repression of target genes by chimeric repressors that include the EAR motif, a repression domain, in Arabidopsis. *Plant Journal*, *34*(5), 733–739. https://doi.org/10.1046/j.1365-313X.2003.01759.x

Hirschmann, F., Krause, F., & Papenbrock, J. (2014). The multi-protein family of sulfotransferases in plants: Composition, occurrence, substrate specificity, and functions. *Frontiers in Plant Science*, *5*(OCT), 1–13. https://doi.org/10.3389/fpls.2014.00556

Holme, I. B., Wendt, T., Gil-Humanes, J., Deleuran, L. C., Colby, ·, … Brinch-Pedersen, H. (2017). Evaluation of the mature grain phytase candidate HvPAPhy_a gene in barley (Hordeum vulgare L.) using CRISPR/Cas9 and TALENs. *Plant Mol. Biol.*, *95*, 111–121. https://doi.org/10.1007/s11103-017-0640-6

Hospital, F. (2001). Size of Donor Chromosome Segments Around Introgressed Loci and Reduction of Linkage Drag in Marker-Assisted Backcross Programs. *Genetics*, *158*, 1363–1379. https://www.ncbi.nlm.nih.gov/pmc/articles/PMC1461714/pdf/11454782.pdf

Houle, D. (1992). Comparing evolvability and variability. *Genetics*, *130*(1), 195–204. http://www.genetics.org.proxy.lib.duke.edu/content/130/1/195.full.pdf+html%5Cnpapers2://publication/uuid/C2A4EA06-AE28-432D-858B-8DE07C5C00A9

Houston, K., Druka, A., Bonar, N., Macaulay, M., Lundqvist, U., … Waugh, R. (2012). Analysis of the barley bract suppression gene Trd1. *Theor Appl Genet*, *125*, 33–45. https://doi.org/10.1007/s00122-012-1814-x

Howe, K. L., Achuthan, P., Allen, J., Allen, J., Alvarez-Jarreta, J., … Flicek, P. (2021). Ensembl 2021. *Nucleic Acids Research*, *49*(D1), D884–D891. https://doi.org/10.1093/nar/gkaa942

Howells, R. M., Craze, M., Bowden, S., & Wallington, E. J. (2018). Efficient generation of stable, heritable gene edits in wheat using CRISPR/Cas9. *BMC Plant Biology*, *18*. https://doi.org/10.1186/s12870-018-1433-z

Hu, Y., Han, X., Yang, M., Zhang, M., Pan, J., & Yu, D. (2019). The transcription factor INDUCER OF CBF EXPRESSION1 interacts with ABSCISIC ACID INSENSITIVE5 and DELLA proteins to fine-tune abscisic acid signaling during seed germination in arabidopsis. *Plant Cell*, *31*(7), 1520–1538. https://doi.org/10.1105/tpc.18.00825

Hu, Y., Jiang, L., Wang, F., & Yu, D. (2013). Jasmonate regulates the INDUCER OF CBF expression-C-repeat binding factor/dre binding factor1 Cascade and freezing tolerance in Arabidopsis. *Plant Cell*, *25*(8), 2907–2924. https://doi.org/10.1105/tpc.113.112631

Huang, M., Liu, X., Zhou, Y., Summers, R. M., & Zhang, Z. (2018). BLINK: A package for the next level of genome-wide association studies with both individuals and markers in the millions. *GigaScience*, *8*(2), 1–12. https://doi.org/10.1093/gigascience/giy154

Huang, X. Q., Börner, A., Röder, M. S., & Ganal, M. W. (2002). Assessing genetic diversity of wheat (Triticum aestivum L.) germplasm using microsatellite markers. *Theoretical and Applied Genetics*, *105*(5), 699–707. https://doi.org/10.1007/s00122-002-0959-4

Hughes, J., Hepworth, C., Dutton, C., Dunn, J. A., Hunt, L., … Gray, J. E. (2017). Reducing stomatal density in barley improves drought tolerance without impacting on yield. *Plant Physiology*, *174*(2), 776–787. https://doi.org/10.1104/pp.16.01844

Ioannidis, J. P. A., Thomas, G., Daly, M. J., Clinical, T., Services, H., … Simches, R. B. (2009). Validating, augmenting and refining genome-wide association signals. *Nat Rev Genet*, *10*(5), 318–329. https://doi.org/10.1038/nrg2544.Validating

Ishitani, M., Xiong, L., Lee, H., Stevenson, B., & Zhu, J. K. (1998). HOS1, a genetic locus involved in cold-responsive gene expression in arabidopsis. *Plant Cell*, *10*(7), 1151–1161. https://doi.org/10.1105/tpc.10.7.1151

Ito, Y., Katsura, K., Maruyama, K., Taji, T., Kobayashi, M., … Yamaguchi-Shinozaki, K. (2006). Functional analysis of rice DREB1/CBF-type transcription factors involved in cold-responsive gene expression in transgenic rice. *Plant and Cell Physiology*, *47*(1), 141–153. https://doi.org/10.1093/pcp/pci230

IWGSC, I. W. G. S. C. (2018). Shifting the limits in wheat research and breeding using a fully annotated reference genome. *Science*, *361*(661). https://doi.org/10.1126/science.aar7191

Izawa, T., Takahashi, Y., & Yano, M. (2003). Comparative biology comes into bloom: genomic and genetic comparison of flowering pathways in rice and Arabidopsis. *Current Opinion in Plant Biology*, *6*, 113–120. https://doi.org/10.1016/S1369-5266(03)00014-1

Jaglo, K. R., Kleff, S., Amundsen, K. L., Zhang, X., Haake, V., … Thomashow, M. F. (2001). Components of the Arabidopsis C-repeat/dehydration-responsive element binding factor cold-response pathway are conserved in Brassica napus and other plant species. *Plant Physiology*, *127*(3), 910–917. https://doi.org/10.1104/pp.010548

Jeknić, Z., Pillman, K. A., Dhillon, T., Skinner, J. S., Veisz, O., … Stockinger, E. J. (2014). Hv-CBF2A overexpression in barley accelerates COR gene transcript accumulation and acquisition of freezing tolerance during cold acclimation. *Plant Molecular Biology*, *84*(1–2), 67–82. https://doi.org/10.1007/s11103-013-0119-z

Jin, Y., Zhai, S., Wang, W., Ding, X., Guo, Z., … Wang, S. (2018). Identification of genes from

the ICE–CBF–COR pathway under cold stress in Aegilops–Triticum composite group and the evolution analysis with those from Triticeae. *Physiology and Molecular Biology of Plants*, *24*(2), 211–229. https://doi.org/10.1007/s12298-017-0495-y

John-Bejai, C. (2017). *Wheat floral biology prospects for improving the efficiency of hybrid seed production and abiotic stress tolerance* (Issue September).

Jost, M., Taketa, S., Mascher, M., Himmelbach, A., Yuo, T., … Stein, N. (2016). A homolog of Blade-On-Petiole 1 and 2 (BOP1/2) controls internode length and homeotic changes of the barley inflorescence. *Plant Physiology*, *171*(June), pp.00124.2016. https://doi.org/10.1104/pp.16.00124

Jung, K.-H., Han, M.-J., Lee, Y.-S., Kim, Y.-W., Hwang, I., … An, G. (2005). Rice Undeveloped Tapetum1 Is a Major Regulator of Early Tapetum Development W. *The Plant Cell*, *17*, 2705–2722. https://doi.org/10.1105/tpc.105.034090

Kanaoka, M. M., Pillitteri, L. J., Fujii, H., Yoshida, Y., Bogenschutz, N. L., … Torii, K. U. (2008). SCREAM/ICE1 and SCREAM2 specify three cell-state transitional steps leading to Arabidopsis stomatal differentiation. *Plant Cell*, *20*(7), 1775–1785. https://doi.org/10.1105/tpc.108.060848

Kapusi, E., Corcuera-Gómez, M., Melnik, S., & Stoger, E. (2017). Heritable Genomic Fragment Deletions and Small Indels in the Putative ENGase Gene Induced by CRISPR/Cas9 in Barley. *Frontiers in Microbiology*, *8*(540). https://doi.org/10.3389/fpls.2017.00540

Kim, Y.-J., & Zhang, D. (2018). Molecular Control of Male Fertility for Crop Hybrid Breeding. *Trends in Plant Science*, *23*(1), 53–65. https://doi.org/10.1016/j.tplants.2017.10.001

Kim, Y. S., Lee, M., Lee, J. H., Lee, H. J., & Park, C. M. (2015). The unified ICE–CBF pathway provides a transcriptional feedback control of freezing tolerance during cold acclimation in Arabidopsis. *Plant Molecular Biology*, *89*(1–2), 187–201. https://doi.org/10.1007/s11103-015-0365-3

King, J., Grewal, S., Yang, C. Y., Hubbart, S., Scholefield, D., … King, I. P. (2017). A step change in the transfer of interspecific variation into wheat from Amblyopyrum muticum. *Plant Biotechnology Journal*, *15*(2), 217–226. https://doi.org/10.1111/pbi.12606

King, J., Newell, C., Grewal, S., Hubbart-Edwards, S., Yang, C. Y., … King, I. P. (2019). Development of stable homozygous wheat/amblyopyrum muticum (Aegilops mutica) introgression lines and their cytogenetic and molecular characterization. *Frontiers in Plant Science*, *10*(January), 1–10. https://doi.org/10.3389/fpls.2019.00034

Koornneef, M., Hanhart, C. J., & Thiel, F. (1989). A genetic and phenotypic description of Eceriferum (cer) mutants in Arabidopsis thaliana. *Journal of Heredity*, *80*(2), 118–122. https://doi.org/10.1093/oxfordjournals.jhered.a110808

Kraft, P., Zeggini, E., & Ioannidis, J. P. A. (2009). Replication in genome-wide association studies. *Statistical Science*, *24*(4), 561–573. https://doi.org/10.1214/09-STS290

Ku, S. J., Cho, K. H., Choi, Y. J., Baek, W. K., Kim, S., … Chung, Y. Y. (2001). Cytological Observation of Two Environmental Genic Male-Sterile Lines of Rice. *Molecules and Cells*, *12*(3), 403–406.

Kubien, D. S., von Caemmerer, S., Furbank, R. T., & Sage, R. . (2003). C4 Photosynthesis at low temperature. A study using transgenic plants with reduced amounts of Rubisco. *Plant Physiology*, *132*, 1577–1585. https://doi.org/10.1016/s0016-0032(64)90585-x

Kumar, N., Galli, M., Ordon, J., Stuttmann, J., Kogel, K.-H., & Imani, J. (2018). Further analysis of barley MORC1 using a highly efficient RNA-guided Cas9 gene-editing system. *Plant Biotechnology Journal*, *16*, 1892–1903. https://doi.org/10.1111/pbi.12924

Kumar, S., Stecher, G., Li, M., Knyasz, C., & Tamura, K. (2018). MEGA X: Molecular Evolutionary Genetics Analysis across computing platforms. *Molecular Biology and Evolution*, *35*, 1547–1549. https://doi.org/https://doi.org/10.1093/molbev/msz312

Langer, S. M., Longin, C. F. H., & Würschum, T. (2014). Phenotypic evaluation of floral and flowering traits with relevance for hybrid breeding in wheat (Triticum aestivum L.). *Plant Breeding*, *133*(4), 433–441. https://doi.org/10.1111/pbr.12192

Lawrenson, T., Shorinola, O., Stacey, N., Li, C., Østergaard, L., … Harwood, W. (2015). Induction of targeted, heritable mutations in barley and Brassica oleracea using RNA-guided Cas9 nuclease. *Genome Biology*, *16*(1), 258. https://doi.org/10.1186/s13059-015-0826-7

Lee, B. H., Henderson, D. A., & Zhu, J. K. (2005). The Arabidopsis cold-responsive transcriptome and its regulation by ICE1. *Plant Cell*, *17*(11), 3155–3175. https://doi.org/10.1105/tpc.105.035568

Lee, H., Xiong, L., Gong, Z., Ishitani, M., Stevenson, B., & Zhu, J. K. (2001). The Arabidopsis HOS1 gene negatively regulates cold signal transduction and encodes a RING finger protein that displays cold-regulated nucleo-cytoplasmic partitioning. *Genes and Development*, *15*(7), 912–924. https://doi.org/10.1101/gad.866801

Li, H., Yuan, Z., Vizcay-Barrena, G., Yang, C., Liang, W., … Zhang, D. (2011). PERSISTENT TAPETAL CELL1 Encodes a PHD-Finger Protein That Is Required for Tapetal Cell Death and Pollen Development in Rice 1. *Plant Physiology*, *156*, 615–630. https://doi.org/10.1104/pp.111.175760

Li, J., Wang, Z., He, G., Ma, L., & Deng, X. W. (2020). CRISPR/Cas9-mediated disruption of TaNP1 genes results in complete male sterility in bread wheat. *Journal of Genetics and Genomics*, *47*(5), 263–272. https://doi.org/10.1016/j.jgg.2020.05.004

Ling, H.-Q., Ma, B., Shi, X., Liu, H., Dong, L., … Liang, C. (2018). Genome sequence of the progenitor of wheat A subgenome Triticum urartu. *Nature*, *557*. https://doi.org/doi.org/10.1038/s41586-018-0108-0

Liu, Q., Kasuga, M., Sakuma, Y., Abe, H., Miura, S., … Shinozaki, K. (1998). Two transcription factors, DREB1 and DREB2, with an EREBP/AP2 DNA binding domain separate two cellular signal transduction pathways in drought- and low-temperature-responsive gene expression, respectively, in Arabidopsis. *Plant Cell*, *10*(8), 1391–1406. https://doi.org/10.1105/tpc.10.8.1391

Liu, T., Ohashi-Ito, K., & Bergmann, D. C. (2009). Orthologs of Arabidopsis thaliana stomatal bHLH genes and regulation of stomatal development in grasses. *Development*, *136*(13), 2265–2276. https://doi.org/10.1242/dev.032938

Lloyd, A. (2003). Vector Construction for Gene Overexpression as a Tool to Elucidate Gene Function. In E. Grotewold (Ed.), *Plant Functional Genomics* (pp. 329–344). Humana Press. https://doi.org/10.1385/1-59259-413-1:329

Lobell, D. B., Schlenker, W., & Costa-Roberts, J. (2011). Climate Trends and Global Crop Production Since 1980. *Science*, *333*(July), 616–621. https://doi.org/10.3726/978-3-653-06341-7/62

Longin, C. F. H., Mühleisen, J., Maurer, H. P., Zhang, H., Gowda, M., & Reif, J. C. (2012). Hybrid breeding in autogamous cereals. *Theor Appl Genet*, *125*, 1087–1096. https://link.springer.com/content/pdf/10.1007%2Fs00122-012-1967-7.pdf

Lourenço, T., Sapeta, H., Figueiredo, D. D., Rodrigues, M., Cordeiro, A., … Oliveira, M. M. (2013). Isolation and characterization of rice (Oryza sativa L.) E3-ubiquitin ligase OsHOS1 gene in the modulation of cold stress response. *Plant Molecular Biology*, *83*(4–5), 351–363. https://doi.org/10.1007/s11103-013-0092-6

Lu, Q., Lillemo, M., Skinnes, H., He, X., Shi, J., … Bjørnstad, Å. (2013). Anther extrusion and plant height are associated with Type I resistance to Fusarium head blight in bread wheat line "Shanghai-3/Catbird." *Theoretical and Applied Genetics*, *126*(2), 317–334. https://doi.org/10.1007/s00122-012-1981-9

Lundqvist, U. (2014). Scandinavian mutation research in barley - a historical review. *Hereditas*, *151*(6), 123–131. https://doi.org/10.1111/hrd2.00077

Ma, L., Yang, Z., & Zhang, S. (2013). DEX1, a plasma membrane-localized protein, functions in microspore development by affecting CalS5 expression in Arabidopsis thaliana. *Developmental Biology August*, *58*(23), 2855–2861. https://doi.org/10.1007/s11434-013-5865-4

Malysheva-Otto, L. V., Ganal, M. W., & Röder, M. S. (2006). Analysis of molecular diversity, population structure and linkage disequilibrium in a worldwide survey of cultivated barley germplasm (Hordeum vulgare L.). *BMC Genetics*, *7*, 1–14. https://doi.org/10.1186/1471-2156-7-6

Marcussen, T., Sandve, S. R., Heier, L., Pfeifer, M., Kugler, K. G., … Mayer, K. F. X. (2014). Ancient hybridizations among the ancestral genomes of bread wheat. *Science*, *345*(6194). http://www.sciencemag.org/content/345/6194/1250092.abstract

Maxwell, K., & Johnson, G. N. (2000). Chlorophyll fluorescence - a practical guide. *Journal of Experimental Botany*, *51*(345), 659–668. https://doi.org/https://doi.org/10.1093/jexbot/51.345.659

Mayer, K. F. X., Martis, M., Hedley, P. E., Šimková, H., Liu, H., … Stein, N. (2011). Unlocking the barley genome by chromosomal and comparative genomics. *Plant Cell*, *23*(4), 1249–1263. https://doi.org/10.1105/tpc.110.082537

McAusland, L., Atkinson, J. A., Lawson, T., & Murchie, E. H. (2019). High throughput procedure utilising chlorophyll fluorescence imaging to phenotype dynamic photosynthesis and photoprotection in leaves under controlled gaseous conditions. *Plant Methods*, *15*(1), 1–15. https://doi.org/10.1186/s13007-019-0485-x

Millar, A. A., Clemens, S., Zachgo, S., Michael Giblin, E., Taylor, D. C., & Kunst, L. (1999). CUT1, an Arabidopsis gene required for cuticular wax biosynthesis and pollen fertility, encodes a very-long-chain fatty acid condensing enzyme. *Plant Cell*, *11*(5), 825–838. https://doi.org/10.1105/tpc.11.5.825

Milner, M. J., Craze, M., Bowden, S., Bates, R., Wallington, E. J., & Keeling, A. (2020). Identification of genes involved in male sterility in wheat (Triticum aestivum L.) which could be used in a genic hybrid breeding system. *Plant Direct*, *4*(3), 1–10. https://doi.org/10.1002/pld3.201

Milohnic, J., & Jost, M. (1970). Pollen production and anther extrusion of wheat (Triticum aestivum L. em. Thell). *Acta Agronomica Hungarica*, *19*(1–2), 17–23.

Mitsuda, N., Hiratsu, K., Todaka, D., Nakashima, K., Yamaguchi-Shinozaki, K., & Ohme-Takagi, M. (2006). Efficient production of male and female sterile plants by expression of a chimeric repressor in Arabidopsis and rice. *Plant Biotechnology Journal*, *4*(3), 325–332. https://doi.org/10.1111/j.1467-7652.2006.00184.x

Mitsuda, N., Matsui, K., Ikeda, M., Nakata, M., Oshima, Y., … Ohme-Takagi, M. (2011). *CRES-T, An Effective Gene Silencing System Utilizing Chimeric Repressors* (pp. 87–105). https://doi.org/10.1007/978-1-61779-154-3_5

Mitsuhara, I., Ugaki, M., Hirochika, H., Ohshima, M., Murakami, T., … Ohashi, Y. (1996). Efficient promoter cassettes or enhanced expression of foreign genes in dicotyledonous and monocotyledonous plants. *Plant and Cell Physiology*, *37*(1), 49–59. https://doi.org/10.1093/oxfordjournals.pcp.a028913

Miura, K., Jing, B. J., Lee, J., Chan, Y. Y., Stirm, V., … Hasegawa, P. M. (2007). SIZ1-mediated sumoylation of ICE1 controls CBF3/DREB1A expression and freezing tolerance in Arabidopsis. *Plant Cell*, *19*(4), 1403–1414. https://doi.org/10.1105/tpc.106.048397

Miura, K., Rus, A., Sharkhuu, A., Yokoi, S., Karthikeyan, A. S., … Hasegawa, P. M. (2005). The Arabidopsis SUMO E3 ligase SIZ1 controls phosphate deficiency responses. *Proceedings of the National Academy of Sciences of the United States of America*, *102*(21), 7760–7765. https://doi.org/10.1073/pnas.0500778102

Monat, C., Padmarasu, S., Lux, T., Wicker, T., Gundlach, H., … Mascher, M. (2019). TRITEX: Chromosome-scale sequence assembly of Triticeae genomes with open-source tools. *Genome Biology*, *20*(1), 1–18. https://doi.org/10.1186/s13059-019-1899-5

Mouradov, A., Cremer, F., & Coupland, G. (2002). *Control of Flowering Time: Interacting Pathways as a Basis for Diversity*. https://doi.org/10.1105/tpc.001362

Mühleisen, J., Maurer, H. P., Stiewe, G., Bury, P., & Reif, J. C. (2013). Hybrid breeding in barley. *Crop Science*, *53*(3), 819–824. https://doi.org/10.2135/cropsci2012.07.0411

Mühleisen, J., Piepho, H. P., Maurer, H. P., Longin, C. F. H., & Reif, J. C. (2014). Yield stability of hybrids versus lines in wheat, barley, and triticale. *Theoretical and Applied Genetics*, *127*(2), 309–316. https://doi.org/10.1007/s00122-013-2219-1

Muqaddasi, Q. H., Lohwasser, U., Nagel, M., Börner, A., Pillen, K., & Röder, M. S. (2016). Genome-wide association mapping of anther extrusion in hexaploid spring wheat. *PLoS ONE*, *11*(5), 1–17. https://doi.org/10.1371/journal.pone.0155494

Muqaddasi, Q. H., Pillen, K., Plieske, J., Ganal, M. W., & Röder, M. S. (2017). Genetic and physical mapping of anther extrusion in elite European winter wheat. *PLoS ONE*, *12*(11), 1–17. https://doi.org/10.1371/journal.pone.0187744

Muqaddasi, Q. H., Reif, J. C., Li, Z., Basnet, B. R., Dreisigacker, S., & Röder, M. S. (2017). Genome-wide association mapping and genome-wide prediction of anther extrusion in CIMMYT spring wheat. *Euphytica*, *213*(3). https://doi.org/10.1007/s10681-017-1863-y

Murchie, E. H., & Lawson, T. (2013). Chlorophyll fluorescence analysis: A guide to good practice and understanding some new applications. *Journal of Experimental Botany*, *64*(13), 3983–3998. https://doi.org/10.1093/jxb/ert208

Narayanan, S., Mohan, A., Gill, K. S., & Vara Prasad, P. V. (2014). Variability of root traits in spring wheat germplasm. *PLoS ONE*, *9*(6). https://doi.org/10.1371/journal.pone.0100317

Nguyen, H. T., Leipner, J., Stamp, P., & Guerra-Peraza, O. (2009). Low temperature stress in maize (Zea mays L.) induces genes involved in photosynthesis and signal transduction as studied by suppression subtractive hybridization. *Plant Physiology and Biochemistry*, *47*(2), 116–122. https://doi.org/10.1016/j.plaphy.2008.10.010

Nguyen, V., Fleury, D., Timmins, A., Laga, H., Hayden, M., … Okada, T. (2015). Addition of rye chromosome 4R to wheat increases anther length and pollen grain number. *Theoretical and Applied Genetics*, *128*(5), 953–964. https://doi.org/10.1007/s00122-015-2482-4

Ni, F., Qi, J., Hao, Q., Lyu, B., Luo, M. C., … Fu, D. (2017). Wheat Ms2 encodes for an orphan protein that confers male sterility in grass species. *Nature Communications*, *8*, 1–12. https://doi.org/10.1038/ncomms15121

Niu, N., Liang, W., Yang, X., Jin, W., Wilson, Z. A., … Zhang, D. (2013). EAT1 promotes tapetal cell death by regulating aspartic proteases during male reproductive development in rice. *Nature Communications*, *4*, 1–11. https://doi.org/10.1038/ncomms2396

Novillo, F., Alonso, J. M., Ecker, J. R., & Salinas, J. (2004). CBF2/DREB1C is a negative regulator of CBF1/DREB1B and CBF3/DREB1A expression and plays a central role in stress tolerance in Arabidopsis. *Proceedings of the National Academy of Sciences of the United States of America*, *101*(11), 3985–3990. https://doi.org/10.1073/pnas.0303029101

Novillo, F., Medina, J., & Salinas, J. (2007). Arabidopsis CBF1 and CBF3 have a different function than CBF2 in cold acclimation and define different gene classes in the CBF regulon. *Proceedings of the National Academy of Sciences of the United States of America*, *104*(52), 21002–21007. https://doi.org/10.1073/pnas.0705639105

Ohashi-Ito, K., & Bergmann, D. C. (2006). Arabidopsis FAMA controls the final proliferation/differentiation switch during stomatal development. *Plant Cell*, *18*(10), 2493–2505. https://doi.org/10.1105/tpc.106.046136

Okada, T., Jayasinghe, J. E. A. R. M., Eckermann, P., Watson-Haigh, N. S., Warner, P., … Whitford, R. (2019). Effects of Rht-B1 and Ppd-D1 loci on pollinator traits in wheat. *Theoretical and Applied Genetics*, *132*(7), 1965–1979. https://doi.org/10.1007/s00122-019-03329-w

Okada, T., Jayasinghe, J. E. A. R. M., Eckermann, P., Watson-Haigh, N. S., Warner, P., … Whitford, R. (2021). Genetic factors associated with favourable pollinator traits in the wheat cultivar Piko. *Functional Plant Biology*, *48*(4), 434–447. https://doi.org/10.1071/FP20181

Pallotta, M. A., Warner, P., Kouidri, A., Tucker, E. J., Baes, M., … Whitford, R. (2019). Wheat ms5 male-sterility is induced by recessive homoeologous A and D genome non-specific lipid transfer proteins. *Plant Journal*, *99*(4), 673–685. https://doi.org/10.1111/tpj.14350

Pareek, A., Khurana, A., Sharma, A. K., & Kumar, R. (2017). An Overview of Signaling Regulons During Cold Stress Tolerance in Plants. *Current Genomics*, *18*(6). https://doi.org/10.2174/1389202918666170228141345

Park, H. C., Kim, H., Koo, S. C., Park, H. J., Cheong, M. S., … Yun, D. J. (2010). Functional characterization of the SIZ/PIAS-type SUMO E3 ligases, OsSIZ1 and OsSIZ2 in rice. *Plant, Cell and Environment*, *33*(11), 1923–1934. https://doi.org/10.1111/j.1365-3040.2010.02195.x

Pavan, S., Delvento, C., Ricciardi, L., Lotti, C., Ciani, E., & D'Agostino, N. (2020). Recommendations for Choosing the Genotyping Method and Best Practices for Quality Control in Crop Genome-Wide Association Studies. *Frontiers in Genetics*, *11*(June). https://doi.org/10.3389/fgene.2020.00447

Paxson-Sowders, D. M., Dodrill, C. H., Owen, H. A., & Makaroff, C. A. (2001). Dex1, a novel plant protein, is required for exine pattern formation during pollen development in Arabidopsis. *Plant Physiology*, *127*(4), 1739–1749. https://doi.org/10.1104/pp.010517

Pearce, S., Saville, R., Vaughan, S. P., Chandler, P. M., Wilhelm, E. P., … Thomas, S. G. (2011). Molecular characterization of Rht-1 dwarfing genes in hexaploid wheat. *Plant Physiology*, *157*(4), 1820–1831. https://doi.org/10.1104/pp.111.183657

Philipp, N., Liu, G., Zhao, Y., He, S., Spiller, M., … Li, Z. (2016). Genomic Prediction of Barley Hybrid Performance. *The Plant Genome*, *9*(2), 1–8. https://doi.org/10.3835/plantgenome2016.02.0016

Pillitteri, L. J., Peterson, K. M., Horst, R. J., & Torii, K. U. (2011). Molecular profiling of stomatal meristemoids reveals new component of asymmetric cell division and commonalities among stem cell populations in Arabidopsis. *Plant Cell*, *23*(9), 3260–3275. https://doi.org/10.1105/tpc.111.088583

Pinthus, M. J., & Levy, A. A. (1983a). The relationship between the Rht 1 and Rht 2 dwarfing genes and grain weight in Triticum aestivum L. spring wheat. *Theor Appl Genet*, *66*, 153–157. https://doi.org/10.1007/BF00265191

Pinthus, M. J., & Levy, A. A. (1983b). The relationship between the Rht1 and Rht2 dwarfing genes and grain weight in Triticum aestivum L. spring wheat. *Theor Appl Genet*, *66*(2). https://doi.org/10.1007/BF00265191

Poirier, B. C., Feldman, M. J., & Lange, B. M. (2018). bHLH093/NFL and bHLH061 are required for apical meristem function in Arabidopsis thaliana. *Plant Signaling and Behavior*, *13*(7). https://doi.org/10.1080/15592324.2018.1486146

Price, A. L., Patterson, N. J., Plenge, R. M., Weinblatt, M. E., Shadick, N. A., & Reich, D. (2006). Principal components analysis corrects for stratification in genome-wide association studies. *Nature Genetics*, *38*(8), 904–909. https://doi.org/10.1038/ng1847

Putarjunan, A., Ruble, J., Srivastava, A., Zhao, C., Rychel, A. L., … Torii, K. U. (2019). Bipartite anchoring of SCREAM enforces stomatal initiation by coupling MAP kinases to SPEECHLESS. *Nature Plants*, *5*(7), 742–754. https://doi.org/10.1038/s41477-019-0440-x

Qi, J., Ni, F., Wang, X., Sun, M., Cui, Y., … Fu, D. (2019). The anther-specific CYP704B is potentially responsible for MSG26 male sterility in barley. *Theoretical and Applied Genetics*, *132*(8), 2413–2423. https://doi.org/10.1007/s00122-019-03363-8

Qi, Y., Liu, Q., Zhang, L., Mao, B., Yan, D., … He, Z. (2014). Fine mapping and candidate gene analysis of the novel thermo-sensitive genic male sterility tms9-1 gene in rice. *Theoretical and Applied Genetics*, *127*(5), 1173–1182. https://doi.org/10.1007/s00122-014-2289-8

Rafalski, A. (2002). Applications of single nucleotide polymorphisms in crop genetics. *Current Opinion in Plant Biology*, *5*(2), 94–100. https://doi.org/10.1016/S1369-5266(02)00240-6

Raissig, M. T., Abrash, E., Bettadapur, A., Vogel, J. P., & Bergmann, D. C. (2016). Grasses use an alternatively wired bHLH transcription factor network to establish stomatal identity.

Proceedings of the National Academy of Sciences of the United States of America, *113*(29), 8326–8331. https://doi.org/10.1073/pnas.1606728113

Ramsay, L., Comadran, J., Druka, A., Marshall, D. F., Thomas, W. T. B., … Waugh, R. (2011). INTERMEDIUM-C, a modifier of lateral spikelet fertility in barley, is an ortholog of the maize domestication gene TEOSINTE BRANCHED 1. *Nature Genetics*, *43*(2), 169–172. https://doi.org/10.1038/ng.745

Ray, D. K., West, P. C., Clark, M., Gerber, J. S., Prishepov, A. V, & Chatterjee, S. (2019). Climate change has likely already affected global food production. *PLoS ONE*, *14*(5). https://doi.org/https://doi.org/10.1371/journal.pone.0217148

Reddy, T. V., Kaur, J., Agashe, B., Sundaresan, V., & Siddiqi, I. (2003). The DUET gene is necessary for chromosome organization and progression during male meiosis in Arabidopsis and encodes a PHD finger protein. *Development*, *130*, 5975–5987. https://doi.org/10.1242/dev.00827

Rensink, W. A., & Buell, C. R. (2004). Arabidopsis to Rice. Applying Knowledge from a Weed to Enhance Our Understanding of a Crop Species 1. *Plant Physiology*, *135*, 622–629. https://doi.org/10.1104/pp.104.040170

Riechmann, A. J. L., Heard, J., Martin, G., Reuber, L., Jiang, C., … Yu, G. (2000). Arabidopsis Transcription Factors : Genome-Wide Comparative Analysis among Eukaryotes. *Science*, *290*(5499), 2105–2110.

Rigden, D. J., Woodhead, D. D., Wong, P. W. H., & Galperin, M. Y. (2011). New structural and functional contexts of the Dx[DN]xDG linear motif: insights into evolution of calcium-binding proteins. *PLoS ONE*, *6*(6). https://doi.org/10.1371/journal.pone.0021507

Rodríguez, A., Rodríguez, M., Córdoba, J. J., & Andrade, M. J. (2015). Design of Primers and Probes for Quantitative Real-Time PCR Methods. In C. Basu (Ed.), *PCR Primer Design* (pp. 31–56). Springer New York. https://doi.org/10.1007/978-1-4939-2365-6_3

Saini, Dinesh K., Chopra, Y., Singh, J., Sandhu, K. S., Kumar, A., … Srivastava, P. (2022a). Comprehensive evaluation of mapping complex traits in wheat using genome-wide association studies. In *Molecular Breeding* (Vol. 42, Issue 1). Springer Netherlands. https://doi.org/10.1007/s11032-021-01272-7

Saini, Dinesh Kumar, Chahal, A., Pal, N., Srivastava, P., & Gupta, P. K. (2022b). Meta-analysis reveals consensus genomic regions associated with multiple disease resistance in wheat (Triticum aestivum L.). *Molecular Breeding*, *42*(3). https://doi.org/10.1007/s11032-022-01282-z

Sakata, T., Takahashi, H., Nishiyama, I., & Higashitani, A. (2000). Effects of High Temperature on the Development of Pollen Mother Cells and Microspores in Barley Hordeum vu/gwe L. *Journal of Plant Research*, *113*, 395–402. https://link.springer.com/content/pdf/10.1007%2FPL00013947.pdf

Salse, J., Piégu, B., Cooke, R., & Delseny, M. (2002). Synteny between Arabidopsis thaliana and rice at the genome level: a tool to identify conservation in the ongoing rice genome sequencing project. In *Nucleic Acids Research* (Vol. 30, Issue 11). http://www.bioperl.org

Samarina, L. S., Bobrovskikh, A. V., Doroshkov, A. V., Malyukova, L. S., Matskiv, A. O., … Orlov, Y. L. (2020). Comparative Expression Analysis of Stress-Inducible Candidate Genes in Response to Cold and Drought in Tea Plant [Camellia sinensis (L.) Kuntze].

Frontiers in Genetics, *11*(December), 1–17. https://doi.org/10.3389/fgene.2020.611283

Sander, J. D., & Joung, J. K. (2014). CRISPR-Cas systems for genome editing, regulation and targeting. *Nat Biotechnol*, *32*(4), 347–355. https://doi.org/10.1038/nbt.2842

Schneider, C. A., Rasband, W. S., & Eliceiri, K. W. (2012). NIH Image to ImageJ: 25 years of image analysis. *Nature Methods*, *9*(7), 671–675. https://doi.org/10.1038/nmeth.2089

Schuler, M. L., Sedelnikova, O. V., Walker, B. J., Westhoff, P., & Langdalea, J. A. (2018). SHORTROOT-mediated increase in stomatal density has no impact on photosynthetic efficiency. *Plant Physiology*, *176*(1), 757–772. https://doi.org/10.1104/pp.17.01005

Scott, M. F., Ladejobi, O., Amer, S., Bentley, A. R., Biernaskie, J., … Mott, R. (2020). Multi-parent populations in crops: a toolbox integrating genomics and genetic mapping with breeding. *Heredity*, *125*(6), 396–416. https://doi.org/10.1038/s41437-020-0336-6

Sharma, K. D., & Nayyar, H. (2016). Regulatory Networks in Pollen Development under Cold Stress. *Fronteirs in Plant Science*, *7*(402). https://doi.org/10.3389/fpls.2016.00402

Shkryl, Y., Yugay, Y., Avramenko, T., Grigorchuk, V., Gorpenchenko, T., … Bulgakov, V. (2021). Crispr/cas9-mediated knockout of hos1 reveals its role in the regulation of secondary metabolism in arabidopsis thaliana. *Plants*, *10*(1), 1–18. https://doi.org/10.3390/plants10010104

Simmons, A. R., & Bergmann, D. C. (2016). Transcriptional control of cell fate in the stomatal lineage. *Current Opinion in Plant Biology*, *29*, 1–8. https://doi.org/10.1016/j.pbi.2015.09.008

Singh, B. D., & Singh, A. K. (2015). *Marker-Assisted Plant Breeding: Principles and Practices*. Springer India. https://doi.org/0.1007/978-81-322-2316-0

Singh, M., Albertsen, M. C., & Cigan, A. M. (2021). Male fertility genes in bread wheat (Triticum aestivum l.) and their utilization for hybrid seed production. *International Journal of Molecular Sciences*, *22*(15). https://doi.org/10.3390/ijms22158157

Singh, M., Kumar, M., Albertsen, M. C., Young, J. K., & Cigan, A. M. (2018a). Concurrent modifications in the three homeologs of Ms45 gene with CRISPR-Cas9 lead to rapid generation of male sterile bread wheat (Triticum aestivum L.). *Plant Molecular Biology*, *97*(4–5), 371–383. https://doi.org/10.1007/s11103-018-0749-2

Singh, M., Kumar, M., Albertsen, M. C., Young, J. K., & Cigan, A. M. (2018b). Concurrent modifications in the three homeologs of Ms45 gene with CRISPR-Cas9 lead to rapid generation of male sterile bread wheat (Triticum aestivum L.). *Plant Molecular Biology*, *97*(4–5), 371–383. https://doi.org/10.1007/s11103-018-0749-2

Skinner, J. S., Szucs, P., Von Zitzewitz, J., Marquez-Cedillo, L., Filichkin, T., … Hayes, P. M. (2006). Mapping of barley homologs to genes that regulate low temperature tolerance in Arabidopsis. *Theoretical and Applied Genetics*, *112*(5), 832–842. https://doi.org/10.1007/s00122-005-0185-y

Skinnes, H., Semagn, K., Tarkegne, Y., Marøy, A. G., & Bjørnstad, Å. (2010). The inheritance of anther extrusion in hexaploid wheat and its relationship to Fusarium head blight resistance and deoxynivalenol content. *Plant Breeding*, *129*(2), 149–155. https://doi.org/10.1111/j.1439-0523.2009.01731.x

Smedley, M. A., & Harwood, W. A. (2015). Gateway-Compatible Plant Transformation Vectors. In K. Wang (Ed.), *Agrobacterium Protocols: Volume 1, Methods in Molecular*

Biology (Vol. 1, pp. 3–16). Springer Science + Business Media. https://doi.org/10.1007/978-1-4939-1695-5_1

Smith, A. R., & Zhao, D. (2016). Sterility Caused by Floral Organ Degeneration and Abiotic Stresses in Arabidopsis and Cereal Grains. *Frontiers in Plant Science*, *7*(October), 1–15. https://doi.org/10.3389/fpls.2016.01503

Song, X., Feng, J., Cui, Z., Zhang, C., & Sun, D. (2018). Genome-wide association study for anther length in some elite bread wheat germplasm. *Czech Journal of Genetics and Plant Breeding*, *54*(3), 109–114. https://doi.org/10.17221/70/2017-CJGPB

Spannagl, M., Mayer, K., Durner, J., Haberer, G., & Fröhlich, A. (2010). Exploring the genomes: From Arabidopsis to crops. *Journal of Plant Physiology*, *168*, 3–8. https://doi.org/10.1016/j.jplph.2010.07.008

Sparkes, I. A., Runions, J., Kearns, A., & Hawes, C. (2006). Rapid, transient expression of fluorescent fusion proteins in tobacco plants and generation of stably transformed plants. *Nature Protocols*, *1*(4), 2019–2025. https://doi.org/10.1038/nprot.2006.286

Stockinger, E. J., Gilmour, S. J., & Thomashow, M. F. (1997). Arabidopsis thaliana CBF1 encodes an AP2 domain-containing transcriptional activator that binds to the C-repeat/DRE, a cis-acting DNA regulatory element that stimulates transcription in response to low temperature and water deficit. *Proceedings of the National Academy of Sciences of the United States of America*, *94*(3), 1035–1040. https://doi.org/10.1073/pnas.94.3.1035

Sun, C., Dong, Z., Zhao, L., Ren, Y., Zhang, N., & Chen, F. (2020). The Wheat 660K SNP array demonstrates great potential for marker-assisted selection in polyploid wheat. *Plant Biotechnology Journal*, *18*(6), 1354–1360. https://doi.org/10.1111/pbi.13361

Talamè, V., Bovina, R., Sanguineti, M. C., Tuberosa, R., Lundqvist, U., & Salvi, S. (2008). TILLMore, a resource for the discovery of chemically induced mutants in barley. *Plant Biotechnology Journal*, *6*(5), 477–485. https://doi.org/10.1111/j.1467-7652.2008.00341.x

Tang, Z., Zhang, L., Yang, D., Zhao, C., & Zheng, Y. (2011). Cold stress contributes to aberrant cytokinesis during male meiosis I in a wheat thermosensitive genic male sterile line. *Plant, Cell and Environment*, *34*(3), 389–405. https://doi.org/10.1111/j.1365-3040.2010.02250.x

Thiel, T., Graner, A., Waugh, R., Grosse, I., Close, T. J., & Stein, N. (2009). Evidence and evolutionary analysis of ancient whole-genome duplication in barley predating the divergence from rice. *BMC Evolutionary Biology*, *9*(209). https://doi.org/10.1186/1471-2148-9-209

Tondelli, A., Francia, E., Barabaschi, D., Aprile, A., Skinner, J. S., … Pecchioni, N. (2006). Mapping regulatory genes as candidates for cold and drought stress tolerance in barley. *Theoretical and Applied Genetics*, *112*(3), 445–454. https://doi.org/10.1007/s00122-005-0144-7

Tucker, E. J., Baumann, U., Kouidri, A., Suchecki, R., Baes, M., … Whitford, R. (2017). Molecular identification of the wheat male fertility gene Ms1 and its prospects for hybrid breeding. *Nature Communications*, *8*(1). https://doi.org/10.1038/s41467-017-00945-2

United Nations, Department of Economic and Social Affairs, Population Division, . (2017).

World Population Prospects The 2017 Revision, Key Findings and Advance Tables. ESA/P/WP/248.
https://population.un.org/wpp/Publications/Files/WPP2017_KeyFindings.pdf

Vandesompele, J., De Preter, K., Pattyn, F., Poppe, B., Van Roy, N., … Speleman, F. (2002). Accurate normalization of real-time quantitative RT-PCR data by geometric averaging of multiple internal control genes. *Genome Biology*, *3*(7). https://doi.org/10.1186/gb-2002-3-7-research0034

Veltri, D., Wight, M. M., & Crouch, J. A. (2016). SimpleSynteny: a web-based tool for visualization of microsynteny across multiple species. *Nucleic Acids Research*, *44*, 41–45. https://doi.org/10.1093/nar/gkw330

Verma, R. K., Kumar, V. V. S., Yadav, S. K., Kumar, T. S., Rao, M. V., & Chinnusamy, V. (2020). Overexpression of Arabidopsis ICE1 enhances yield and multiple abiotic stress tolerance in indica rice. *Plant Signaling and Behavior*, *15*(11), 1–13. https://doi.org/10.1080/15592324.2020.1814547

Waddington, S. R., Cartwright, P. M., & Wall, P. C. (1983). A Quantitative Scale of Spike Initial and Pistil Development in Barley and Wheat. *Annals of Botany Company*, *51*, 119–130. https://academic.oup.com/aob/article-abstract/51/1/119/174757

Walker, N. S., Stiffler, N., & Barkan, A. (2007). POGs/PlantRBP: A resource for comparative genomics in plants. *Nucleic Acids Research*, *35*(SUPPL. 1), 852–856. https://doi.org/10.1093/nar/gkl795

Wambugu, P. W., Ndjiondjop, M.-N., & Henry, R. (2018). Role of genomics in promoting the utilization of plant genetic resources in genebanks. *Briefings in Functional Genomics2*, *17*(3), 198–206. https://doi.org/10.1093/bfgp/ely014

Wang, J., & Zhang, Z. (2020). GAPIT Version 3: Boosting Power and Accuracy for Genomic Association and Prediction. *BioRxiv*. https://doi.org/10.1101/2020.11.29.403170

Wang, Jun, Niu, B., Huang, J., Wang, H., Yang, X., … Wang, Y. (2016). The PHD Finger Protein MMD1/DUET Ensures the Progression of Male Meiotic Chromosome Condensation and Directly Regulates the Expression of the Condensin Gene CAP-D3 OPEN. *The Plant Cell*, *28*, 1894–1909. https://doi.org/10.1105/tpc.16.00040

Wang, S. B., Feng, J. Y., Ren, W. L., Huang, B., Zhou, L., … Zhang, Y. M. (2016). Improving power and accuracy of genome-wide association studies via a multi-locus mixed linear model methodology. *Scientific Reports*, *6*(December 2015), 1–10. https://doi.org/10.1038/srep19444

Wei, D., Liu, M., Chen, H., Zheng, Y., Liu, Y., … Lin, J. (2018). INDUCER OF CBF EXPRESSION 1 is a male fertility regulator impacting anther dehydration in Arabidopsis. *PLoS Genetics*, *14*(10). https://doi.org/10.1371/journal.pgen.1007695

Whitford, R., Fleury, D., Reif, J. C., Garcia, M., Okada, T., … Langridge, P. (2013). Hybrid breeding in wheat: Technologies to improve hybrid wheat seed production. *Journal of Experimental Botany*, *64*(18), 5411–5428. https://doi.org/10.1093/jxb/ert333

Wickham, H. (2016). *ggplot2: Elegant graphics for data analysis* (ISPN 978-3-319-24277-4). Springer-Verlag. https://ggplot2.tidyverse.org

Wilson, Z. A., Morroll, S. M., Dawson, J., Swarup, R., & Tighe, P. J. (2001). The Arabidopsis MALE STERILITY1 (MS1) gene is a transcriptional regulator of male gametogenesis, with homology to the PHD-finger family of transcription factors. *Plant Journal*, *28*(1), 27–39.

https://doi.org/10.1046/j.1365-313X.2001.01125.x

Winfield, M. O., Allen, A. M., Burridge, A. J., Barker, G. L. A., Benbow, H. R., … Edwards, K. J. (2016). High-density SNP genotyping array for hexaploid wheat and its secondary and tertiary gene pool. *Plant Biotechnology Journal*, *14*(5), 1195–1206. https://doi.org/10.1111/pbi.12485

Wolfe, R. I., & Franckowiak, J. D. (1991). Multiple dominant and recessive gentic marker stocks in spring barley. *Barley Genetics Newsletter*, *20*.

Wu, Z., Chen, L., Yu, Q., Zhou, W., Gou, X., … Hou, S. (2019). Multiple transcriptional factors control stomata development in rice. *New Phytologist*, *223*(1), 220–232. https://doi.org/10.1111/nph.15766

Würschum, T., Langer, S. M., Longin, C. F. H., Tucker, M. R., & Leiser, W. L. (2017). A modern Green Revolution gene for reduced height in wheat. *Plant Journal*, *92*(5), 892–903. https://doi.org/10.1111/tpj.13726

Xia, C., Gong, Y., Chong, K., & Xu, Y. (2020). Phosphatase OsPP2C27 directly dephosphorylates OsMAPK3 and OsbHLH002 to negatively regulate cold tolerance in rice. *Plant Cell and Environment*, *44*(2), 491–505. https://doi.org/10.1111/pce.13938

Xu, C., Liu, Z., Zhang, L., Zhao, C., Yuan, S., & Zhang, F. (2013). Organization of actin cytoskeleton during meiosis I in a wheat thermo-sensitive genic male sterile line. *Protoplasma*, *250*(1), 415–422. https://doi.org/10.1007/s00709-012-0386-6

Yadav, S., Ross, E. M., Aitken, K. S., Hickey, L. T., Powell, O., … Hayes, B. J. (2021). A linkage disequilibrium-based approach to position unmapped SNPs in crop species. *BMC Genomics*, *22*(1), 1–9. https://doi.org/10.1186/s12864-021-08116-w

Yang, X., Makaroff, C. A., & Ma, H. (2003). The Arabidopsis MALE MEIOCYTE DEATH1 Gene Encodes a PHD-Finger Protein That Is Required for Male Meiosis. *The Plant Cell*, *15*, 1281–1295. https://doi.org/10.1105/tpc.010447

Yang, Z., Sun, L., Zhang, P., Zhang, Y., Yu, P., … Cheng, S. (2019). TDR INTERACTING PROTEIN 3, encoding a PHD-finger transcription factor, regulates Ubisch bodies and pollen wall formation in rice. *Plant Journal*, *99*(5), 844–861. https://doi.org/10.1111/tpj.14365

Yu, J., Meng, Z., Liang, W., Behera, S., Kudla, J., … Zhang, D. (2016). A Rice Ca2+ Binding Protein Is Required for Tapetum Function and Pollen Formation. *Plant Physiology*, *172*(3), 1772–1786. https://doi.org/10.1104/pp.16.01261

Zadoks, J. C., CHANGt, T. T., Konzak, C. F., & Fryer, J. D. (1974). A decimal code for the growth stages of cereals. In *Weed Research* (Vol. 14).

Zakhrabekova, S., Gough, S. P., Braumann, I., Müller, A. H., Lundqvist, J., … Hansson, M. (2012). Induced mutations in circadian clock regulator Mat-a facilitated short-season adaptation and range extension in cultivated barley. *PNAS*, *109*(11). https://doi.org/10.1073/pnas.1113009109

Zang, Y. X., Kim, H. U., Kim, J. A., Lim, M. H., Jin, M., … Park, B. S. (2009). Genome-wide identification of glucosinolate synthesis genes in Brassica rapa. *FEBS Journal*, *276*(13), 3559–3574. https://doi.org/10.1111/j.1742-4658.2009.07076.x

Zanke, C. D., Ling, J., Plieske, J., Kollers, S., Ebmeyer, E., … Röder, M. S. (2014). Whole genome association mapping of plant height in winter wheat (Triticum aestivum L). *PLoS ONE*, *9*(11). https://doi.org/10.1371/journal.pone.0113287

Zhai, Q., Zhang, X., Wu, F., Feng, H., Deng, L., … Li, C. (2015). Transcriptional mechanism of jasmonate receptor COI1-mediated delay of flowering time in arabidopsis. *Plant Cell*, *27*(10), 2814–2828. https://doi.org/10.1105/tpc.15.00619

Zhang, F., Wen, Y., & Guo, X. (2014). CRISPR/Cas9 for genome editing: progress, implications and challenges. *Human Molecular Genetics*, *23*(1), 40–46. https://doi.org/10.1093/hmg/ddu125

Zhang, H., Xu, C., He, Y., Zong, J., Yang, X., … Zhang, D. (2013). Mutation in CSA creates a new photoperiod-sensitive genic male sterile line applicable for hybrid rice seed production. *Proceedings of the National Academy of Sciences of the United States of America*, *110*(1), 76–81. https://doi.org/10.1073/pnas.1213041110

Zhang, H., Zhang, J., Lang, Z., Botella, J. R., & Zhu, J. K. (2017). Genome Editing—Principles and Applications for Functional Genomics Research and Crop Improvement. *Critical Reviews in Plant Sciences*, *36*(4), 291–309. https://doi.org/10.1080/07352689.2017.1402989

Zhang, J. Z., Creelman, R. A., & Zhu, J.-K. (2004). Perspectives on Translational Biology From Laboratory to Field. Using Information from Arabidopsis to Engineer Salt, Cold, and Drought Tolerance in Crops 1. *Plant Physiology*, *135*, 615–621. https://doi.org/10.1104/pp.104.040295

Zhang, W., Sun, Y., Timofejeva, L., Chen, C., Grossniklaus, U., & Ma, H. (2006). Regulation of Arabidopsis tapetum development and function by DYSFUNCTIONAL TAPETUM1 (DYT1) encoding a putative bHLH transcription factor. *Development*, *133*(16), 3085–3095. https://doi.org/10.1242/dev.02463

Zhang, Z., Li, J., Li, F., Liu, H., Yang, W., … Xu, Y. (2017). OsMAPK3 Phosphorylates OsbHLH002/OsICE1 and Inhibits Its Ubiquitination to Activate OsTPP1 and Enhances Rice Chilling Tolerance. *Developmental Cell*, *43*(6), 731-743.e5. https://doi.org/10.1016/j.devcel.2017.11.016

Zhao, C., Liu, B., Piao, S., Wang, X., Lobell, D. B., … Asseng, S. (2017). Temperature increase reduces global yields of major crops in four independent estimates. *PNAS*, *114*(35), 9326–9331. https://doi.org/10.1073/pnas.1701762114

Zhou, H., Muehlbauer, G., & Steffenson, B. (2012). Population structure and linkage disequilibrium in elite barley breeding germplasm from the United States. *Journal of Zhejiang University: Science B*, *13*(6), 438–451. https://doi.org/10.1631/jzus.B1200003

Zhou, X., & Stephens, M. (2013). Genome-wide Efficient mixed model analysis for association studies. *Nat Genet*, *44*(7), 821–824. https://doi.org/10.1016/0030-4220(61)90035-4

Appendix 1

***Table S3.1**. Vectors used for cloning. Amp = ampicillin, Kan =kanamycin, Rif = rifampicin, Spec = spectinomycin*

Vectors	**Usage**	**Inserts**	**Antibiotic resistance**
pCR/8/GW	Entry vector	NA	Spec
pBract214	Destination vector, ZmUbi promoter	NA	Kan
pENTR/D	Entry vector	NA	Amp
pUBC YFP	Destination vector with YFP		Spec
pICH86966	CRISPR	sgRNA template vector	
p47751	CRISPR	sgRNA 1	
p47761	CRISPR	sgRNA 2	
p47772	CRISPR	sgRNA 3	
p90003	CRISPR	Promoter sequence TaU6	
pICSL11059	CRISPR	Hygromycin resistance gene	
pICSL11056	CRISPR	Cas9 gene	
pAGM8031	CRISPR	Destination vector	
pICSL50914	CRISPR	3’ linker for 3 sgRNAs (p47751, p47761 and p47772)	
pICH50892	CRISPR	3’ linker for 1 sgRNA (p47751)	

Table S3.2. *Primers used for the generation of constructs for the CRISPR targets, transient expression, overexpression and SRDX constructs as well as the primers used for genotyping and for the cloning of the gene sequences for the transgenes.*

Application	**Primer number**	**Sequence**	**Annea-ling temp (˚C)**	**size (bp)**
Amplification of CRISPR targets				
Common reverse primer	6464	TGTGGTCTCAAGCGTAATGCCAACTTTGTAC	59	
HvDEX1-CR-F1	7153	TGTGGTCTCACTTGTACCAAGTGTCCAAAACACGGTTTTAGAGCTAGAAATAGCAAG	59	
HvDEX1-CR-F2	7154	TGTGGTCTCACTTGCACACGGGAAATAGTGTGTTTTAGAGCTAGAAATAGCAAG	59	
HvDEX1-CR-F3	7155	TGTGGTCTCACTTGCGAAACAAGCTGCTTCTGGTTTTAGAGCTAGAAATAGCAAG	59	
HvDEX1-CR-F4	7156	TGTGGTCTCACTTGAAGTGCTTGAAGGTTCCGAGTTTTAGAGCTAGAAATAGCAAG	59	
HvDEX1-CR-F5	7157	TGTGGTCTCACTTGACAAGCTAGAGGTACCTCGTGTTTTAGAGCTAGAAATAGCAAG	59	
HvDEX1-CR-F6	7158	TGTGGTCTCACTTGAAACTCATGGTAGTGATGCGTTTTAGAGCTAGAAATAGCAAG	59	
HvHvICE1-CR-T1	8186	TGTGGTCTCACTTGAGGACTGGTACTTCGGCGCGTTTTAGAGCTAGAAATAGCAAG	59	
HvHvICE1-CR-T2	8187	TGTGGTCTCACTTGAAGCATCGGGGTCCAGCTCGTTTTAGAGCTAGAAATAGCAAG	59	
HvHvICE1-CR-T3	8188	TGTGGTCTCACTTGACCTCGGCAGCTCCGGCGCGTTTTAGAGCTAGAAATAGCAAG	59	
HvHvICE1-CR-T4	8189	TGTGGTCTCACTTGGCGACGGCCATGAACAACAGTTTTAGAGCTAGAAATAGCAAG	59	
HvHvICE1-CR-T5	8190	TGTGGTCTCACTTGCACAGATGACAGAGTTTGGGTTTTAGAGCTAGAAATAGCAAG	59	
HvHvICE1-CR-T6	8191	TGTGGTCTCACTTGGTTTCGACTTGTTCGACACGTTTTAGAGCTAGAAATAGCAAG	59	
HvMMD1-CR-F1	7159	TGTGGTCTCACTTGTCGGCCTCGAAGCCCGCGTTTTAGAGCTAGAAATAGCAAG	59	
HvMMD1-CR-F2	7160	TGTGGTCTCACTTGCCACCACTGGGTGTCAAAAGTTTTAGAGCTAGAAATAGCAAG	59	
HvMMD1-CR-F3	7161	TGTGGTCTCACTTGCCGACATGTCCGTCGCGGTTTTAGAGCTAGAAATAGCAAG	59	
HvMMD1-CR-F4	7162	TGTGGTCTCACTTGCGGACGCAGACTGGGACGTTTTAGAGCTAGAAATAGCAAG	59	
HvMMD1-CR-F5	7163	TGTGGTCTCACTTGCTGGGGATACTGCCTTGCCGTTTTAGAGCTAGAAATAGCAAG	59	
HvMMD1-CR-F6	7164	TGTGGTCTCACTTGAAGCCGTGTACGATGAAGGTTTTAGAGCTAGAAATAGCAAG	59	

Amplification of genes for transient expression				
HvDEX1YFP	7947	CTGCTGATGTGCATGGTAATG	60	1814
	8129	AAGTCGTGCTGCTTCATGTG		
HvDEX1 CDS	8534	ATGCGTCCCCTCCTCGC	60	2280
	8535	GAATCTGGACCCTTGTGGCCT		
HvICE1 YFP	8196	CCAACCGTTGAGGTTAGGCT	60	686
	8129	AAGTCGTGCTGCTTCATGTG		
HvICE1 CDS	8192	ATGCTATCGCGGTTCAATAAC	60	1786
	8193	CATCGTGGGATGGAACCC		
HvMMD1 YFP	7740	CATGTGCGCTTCAACGTACT	60	1853
	8129	AAGTCGTGCTGCTTCATGTG		
HvMMD1 CDS	7740	CATGTGCGCTTCAACGTACT	60	1642
	2380	CTTGGCTAGCGTTAGTGCCTC		
Genotyping of overexpression lines				
HvDEX1	824	TTTAGCCCTGCCTTCATACG	60	2280
	7738	ATGGATATCTGGGATCGCCTC		
HvICE1	824	TTTAGCCCTGCCTTCATACG	60	1786
	8193	CATCGTGGGATGGAACCC		
HvMMD1	824	TTTAGCCCTGCCTTCATACG	60	1642
	4605	TCACTTGGCTAGCGTTAGTG		
Genotyping of SRDX lines				
HvICE1-1	8192	ATGCTATCGCGGTTCAATAAC	59	1609
	8086	AGCGAAACCCAAACGGAGTTC		
HvMMD1	7740	CATGTGCGCTTCAACGTACT	59	1465
	8086	AGCGAAACCCAAACGGAGTTC		
Amplification of CDS for overexpression				
HvDEX1	7736	CCACTAATCGATGTTGTTCCGC	60	2066
	7738	ATGGATATCTGGGATCGCCTC		
HvICE1-1	8192	ATGCTATCGCGGTTCAATAAC	60	1572
	8217	CTACATCGTGGGATGGAA		
HvMMD1	7740	CATGTGCGCTTCAACGTACT	60	1428
	4605	TCACTTGGCTAGCGTTAGTG		
Amplification of CDS with SRDX				
HvICE1-1	8192	ATGCTATCGCGGTTCAATAAC	59	1609
	8194	CTAAGCGAAACCCAAACGGAGTTCTAGA TCCAGATCCAGCATCGTGGGATGGAACCC		
HvMMD1	7740	CATGTGCGCTTCAACGTACT	59	1465
	8195	TCAAGCGAAACCCAAACGGAGTTCTAGAT C CAGATCCAGCTTGGCTAGCGTTAGTGCCT		

Amplification of CDS for cloning into pUBC vector				
HvDEX1	8606	CACCATGCGTCCCCTCCTCGC	60	2063
	8535	GAATCTGGACCCTTGTGGCCT		
HvICE1-1	8192	ATGCTATCGCGGTTCAATAAC	60	1569
	8193	CATCGTGGGATGGAACCC		
HvMMD1	8608	CACCATGGATATCTGGGATCGCCTC	60	1425
	2380	CTTGGCTAGCGTTAGTGCCTC		
Colony PCR of entry vectors				
pCR/8/GW and pENTR D	6591	TGTAAAACGACGGCCAG	60	
	4977	CAGGAAACAGCTATGAC		
Genotyping of transgenic lines for Cas9				
Cas9 screening	7260	CATCCCTGGGAACGTATCAC	59	717
	7261	GTTCCTGATCCACGTACATG		
Screening for CRISPR mutations – primers for sequencing				
HvDEX1 T1	8534	ATGCGTCCCCTCCTCG	NA	NA
HvDEX1 T2	7658	ATGGCCTGCGTTTCACCAGTC	NA	NA
HvDEX1 T3	7736	TGATGATGGACAAGCTAGAGGT	NA	NA
HvDEX1 T4	8401	GCTGCCTTAGCGCCTTCTAT	NA	NA
HvDEX1 T5	7735	AGGATGGCACACGGGAAATA	NA	NA
HvDEX1 T6	7869	ACATGCTCAGAGAAGGTTGCT	NA	NA
HvICE1-1 T1+T2+T3	8192	ATGCTATCGCGGTTCAATAAC	NA	NA
HvICE1-1 T4	8221	CGGTCATAACCGCACCAAAC	NA	NA
HvICE1-1 T5+T6	8218	GGAGAAAGGGGCGGTCAA	NA	NA
HvMMD1-1 T1	2379	ATGCCGTCCATCCGCGCGCT	NA	NA
HvMMD1-1 T2+T4	8397	GTGGTGGTTTGCGCATTGAT	NA	NA
HvMMD1-1 T3+T5+T6	8399	GAGAGCTTTCTTTGCAGGGCT	NA	NA

Barley transformation media components from Harwood (2019)

Table S3.3 *The Phytagel was prepared at two times the required concentration and autoclaved. The solution was heated to 60°C before use.*

Component	Stock concentration	Final concentration
Phytagel	7 g/L	3.5 g/L

Table S3.4 *MG/L media for growth of* Agrobacterium *used for co-cultivation of immature barley embryos. MG/L was prepared by dissolving media components in water and adjusting to pH 7.2. The medium was autoclaved, and stored at 4°C.*

Component	Final concentration
Tryptone	5 g/l
Mannitol	5 g/l
Yeast extract	2.5 g/l
L-Glutamic acid	1 g/l
KH_2PO_4	250 mg/l
NaCl	100 mg/l
$MgSO_4.7H_2O$	100 mg/l
Biotin	10 µl (0.1 mg/l Stock)

Table S3.5 *Stock concentration of callus induction media was prepared at of two times the required concentration, adjusted to pH 5.8 and filter sterilised into an autoclaved bottle.*

Component	Stock concentration	Final concentration
Murashige & Skoog Plant salt base (Duchefa M0221)	8.6 g/l	4.3 g/l
Maltose	60 g/l	30 g/l
Casein Hydrolysate	2 g/l	1 g/l

Table S3.6 *Callus induction media for transformation. The callus induction (CI) media specified in Table S3.5 was heated to 60˚C before the following growth enhancers and selection agents were added. An equal volume of heated 2x Phytagel was added, and the solution was poured into ø10 cm Petri dishes.*

Component	Stock concentration	Final concentration
Myo-inositol	35 g/l	350 mg/l
Proline	69 g/l	690 mg/l
Thiamine HCl	10 g/l	1 mg/l
Dicamba (Sigma-Aldrich D5417)	2.5 g/l	2.5 mg/l
$CuSo_4.5H_2O$	1.25 g/l	1.25 mg/l
Hygromycin (Roche)	50 mg/ml	50 mg/l
Timentin (Duchefa)	160 mg/ml	160 mg/l

Table S3.7. *Stock concentration of transition and regeneration media was prepared at of two times the required concentration, adjusted to pH 5.8 and filter sterilised into an autoclaved bottle.*

Component	Stock concentration	Final concentration
Murashige and Skoog modified Plant salt base (without NH_4NO_3) (Duchefa M0238)	5.4 g/l	2.7 g/l
Maltose	40 g/l	20 g/l
NH_4NO_3	330 mg/l	165 mg/l
Glutamine	1.5 g/l	750 mg/l

Table S3.8. *Transition media for transformation. The transition media specified in Table S3.7 was heated to 60˚C before the following growth enhancers and selection agents were added. An equal volume of heated 2x Phytagel was added and the solution was poured into 15 cm square Petri dishes.*

Component	Stock concentration	Final concentration
Myo-inositol	35 g/l	100 mg/l
Thiamine HCl	10 g/l	0.4 mg/l
2,4-dichlorophenoxy acetic acid (2,4-D) (Duchefa)	2.5 mg/l	2.5 mg/l
6-benzylaminopurine (BAP) (Duchefa)	1 mg/l	0.1 mg/l
$CuSo_4.5H_2O$	1.25 g/l	1.25 mg/l
Hygromycin (Roche)	50 mg/ml	50 mg/l
Timentin (Duchefa)	160 mg/ml	160 mg/l

Table S3.9 *Regeneration media for transformation. The media specified in Table S3.7 was heated to 60˚C before the following growth enhancers and selection agents were added. An equal volume of heated 2x Phytagel was added and the solution was poured into 15 cm square Petri dishes.*

Component	Stock concentration	Final concentration
Myo-inositol	35 g/l	100 mg/l
Thiamine HCl	10 g/l	0.4 mg/l
Hygromycin	50 mg/ml	50 mg/l
Timentin	160 mg/ml	160 mg/l

Table S3.10 *Callus Induction without growth regulators. The media specified in Table S3.5 was heated to 60˚C before the following components were added. An equal volume of heated 2x Phytagel was added and the solution was poured into cultivation tubes.*

Component	**Stock concentration**	**Final concentration**
Myo-inositol	35 g/l	35 mg/l
Proline	65 g/l	650 mg/l
Thiamine HCl	10 g/l	1 mg/l
Hygromycin (Roche)	50 mg/ml	50 mg/l
Timentin (Duchefa)	160 mg/ml	160 mg/l

Table S3.3. *Micro-synteny in region surrounding the potential candidate* HvMMD1-2*.*

Barley	**Rice**	**% Gene identity**
HORVU7Hr1G061720	NA	NA
HORVU7Hr1G061730	NA	NA
HORVU7Hr1G061740	NA	NA
HORVU7Hr1G061750	NA	NA
HORVU7Hr1G061760	NA	NA
HORVU7Hr1G061770	*Os08g0282400*	53.6
HORVU7Hr1G061780	NA	NA
HORVU7Hr1G061790 (HvMMD1-2)	*Os03g0716200*	72.8
HORVU7Hr1G061800	*Os08t0481200*	63.2
HORVU7Hr1G061810	NA	NA
HORVU7Hr1G061820	NA	NA
HORVU7Hr1G061830	NA	NA
HORVU7Hr1G061840	NA	NA
HORVU7Hr1G061850	*Os02g0131700*	NA
HORVU7Hr1G061860	NA	NA

```
OsICE2          ----------------MDEAEAAAAAAKMDE-----------------------------
HvICE1-2        ----------------MENPAAVVGAEKEDE-----------------------------
AtICE2          MNSDGVWLDGSGESPEVNNGEAASWVRNPDEDWFNNPPPPQHTNQNDFRFNGGFPLNPSE
                               :::  *.  . : **

OsICE2          ----LAGGGGGGGGDWSYLAADALAAASFTAFPFHHHHHHHHRDVLSASTPSSLLLNMDA
HvICE1-2        ----LVGGGGG---DWGYLTSEAMATAGFPAFGFPCGTRGGVTPAPNSAS------LLMS
AtICE2          NLLLLLQQSIDSSSSSSPLLHPFTLDAASQQQQQQQQQQEQSFLATKACIVSLLNVPTIN
                    *   . .   . . *       *.          :     . .:.

OsICE2          ATAAAMFDFQAAFPSSS-----VPPPPPTTTAALPPFHDFASSNPFDDAPPPFLAPPGQK
HvICE1-2        MEHAALFDYNAAFPSSSSSAVPAPPAYHDFGSGGNPFSVDAPPFLLEAPPPLTAGAGGQK
AtICE2          NNTFDDFGFDSGFLGQQFHGNHQSPNSMNFTGLNHSVPDFLPAPENSSGSCGLSPLFSNR
                      *.:::.* ...      .*      .   ..    ..   .  .       .::

OsICE2          LGFLGPPGGAFGGG-------------------MGWDDDDEIEQS-VDASSMGVSASLEN
HvICE1-2        GGFLAPPLSAFGDG-------------------MGWDDEDELDQQSMDASSLGVSASLEN
AtICE2          AKVLKPLQVMASSGSQPTLFQKRAAMRQSSSSKMCNSESSSEMRKSSYEREIDDTSTGII
                  .* *     ..*                   *  .:...  :.     .:. :::

OsICE2          AAPVAAGGGGGGGGGGGRGKKKGMPAKNLMAERRRRKKLNDRLYMLRSVVPKISKMDRAS
HvICE1-2        AAVGAPGGGGGGGNG--KGKKKGMPAKNLMAERRRRKKLNDRLYMLRSVVPKISKMDRAS
AtICE2          DISGLNYESDDHNTNNNKGKKKGMPAKNLMAERRRRKKLNDRLYMLRSVVPKISKMDRAS
                        ... . .  :****************************************

OsICE2          ILGDAIEYLKELLQRINDLHNELESAPSSSLTGPSSAS--FHPSTPTLQTFPGRVKEELC
HvICE1-2        ILGDAIDYLKELLQRISDLHSELESAPSSAALGGPSTANTFLPSTPTLQPFPGRIKEERC
AtICE2          ILGDAIDYLKELLQRINDLHTELESTPPSSSS--------LHPLTPTPQTLSYRVKEELC
                ******:*********.***.****:*.*:          : * *** *.:. *:*** *

OsICE2          PTS-FPSPSGQQATVEVRMREGHAVNIHMFCARRPGILMSTLRALDSLGLGIEQAVISCF
HvICE1-2        PPAPFPSPSGQQATVEVRMREGQAVNIHMFCARRPGILLSTMRALDSLGLDIEQAVISCF
AtICE2          PSSSLPSPKGQQPRVEVRLREGKAVNIHMFCGRRPGLLLSTMRALDNLGLDVQQAVISCF
                *.: :***.***. ****:***:********.****:*:**:****.***.::*******

OsICE2          NGFAMDVFRAEQCRDGPGLGPEEIKTVLLHSAGLQNAM
HvICE1-2        DGFAMDVFRAEQCREGPGLLPEEIKAVLLHCAGLQNAM
AtICE2          NGFALDVFRAEQCQEDHDVLPEQIKAVLLDTAGYAGLV
                :***:********::. .: **:**:***. **  . :
```

Figure S3.1*. Alignment of protein sequences of AtICE2, OsICE2 and the putative barley orthologue HvICE1-2.*

Table S5.1. *Primer sequences for allele specific PCR and sequencing of SNP. Marked in red are nucleotides that differ between the alleles to achieve the allele specific binding. Marked in blue are nucleotides that were added to control for melting temperature differences between the allele specific primers. Annealing temperatures 59˚C for all primer pairs.*

Primer number	Primer name	Sequence
7692	BW554snp1R1	CAGAACGGGGACTTGATGGG
7695	BW579snp1F1	TCGATGTCAATGCGGGGAAC
7696	BW579snp1R1	CAGCAGCCTGTGAAGGAGTA
7697	BW579snp2F1	ACCGGGAGCTACATTGGC
7698	BW579snp2R1	TCCGATCGTGTTCATCACCG
7700	BW588snp1R1	CCAGCAGCAGAAAAGAGAGGA
7703	BW591snp1F1	GACCAGTCGCTCGTGATGAT
7704	BW591snp1R1	GCTGGTTTGATAAAGAAAGGGCA
7711	BW545snp1F1	AAATGGAACCAACGGTGCTG
7712	BW545snp1R1	CATGGCCTTGTAGCACCTGA
7713	BW545snp2F1	GACCGGCTACGCCATCATC
7714	BW545snp2R1	AACCCTCTTGTTCTATCAAATTGC
7715	BW546snp1F1	CGCGATTTCGACGTTTAGGG
7717	BW546snp2F1	CAACACCGTCGACGCCC
7718	BW546snp2R1	GCGATCTCGGAGGTGAGC
7724	BW546snp1R2	CGTCGTCTACTCTCGAACCG
7725	BW554snp1F2	TGATCCAGTACACTTGTGGGT
7726	BW554snp2F2	GGGAGTACTACGTATCTCGATTGG
7727	BW554snp2R2	CACTCATTTTGTTCCGTATCTAGTC
7728	BW588snp1F2	GCCCGTGCTGAACTATGAGA
7729	BW588snp2F2	CCTCCTCCTGTGGACGAAGAT
7730	BW588snp2R2	CCATTTCCATTTTGGGTGTGGA
7731	BW591snp2F2	TTCGTTGGTTTCTCCCTGTGT
7732	BW591snp2R2	CTGGATCTGAGTTCGGGACTT
7997	545snp1A	CAGCTGAGCAGAAGCGCAA
7998	545snp1G	CCAGCTGAGCAGAAGAACAG
7999	545snp2C	ACAAGCAGCTCTGGACGC
8000	545snp2G	ACAAGCAGCTCTGCTCGG
8001	546snp1A	ACTGGGGAGGTCGAGGCA
8002	546snp1G	ACTGGGGAGGTCGTAGCG
8003	546snp2G	GCAAGGTCCACACCCTACAG
8004	546snp2A	AAGGTCCACACCCAGCAA
8005	554snp1A	ATGAACATGGGGGCGCATA
8006	554snp1G	ATGAACATGGGGGCCTATG
8007	554snp2A	GGGAGAAACGATGTCGCA
8008	554snp2C	GGGAGAAACGATGATGCC
8009	579snp1A	CGGCTTCTGCTGTGCCA

8010	579snp1G	CGGCTTCTGCTGAACCG
8011	579snp2A	AAGATTGAGCGATTACGAAGAGA
8012	579snp2C	AGATTGAGCGATTACGACAAGC
8013	588snp1T	GAGGGCCATTATCAATGGGT
8014	588snp1C	GAGGGCCATTATCAAGAGGC
8015	588snp2T	CAAGAACCCTAGCTTGGTAGCTCT
8016	588snp2C	CAAGAACCCTAGCTTGGTACTTCC
8017	591snp1T	TGGGTTGAATTCTTGAAACGAAT
8018	591snp1C	TTGGGTTGAATTCTTGAAAGAAAC
8019	591snp2T	GCTACTCTAGTCGATACATCTGGCT
8020	591snp2A	GCTACTCTAGTCGATACATCGAGCA
8028	554snp2R1	GGTCCTGGGAGGGTTCAT
8029	579snp2R1	GCCAAGCAGAAGGCCGG

Table S6.1. *Number of markers per chromosomes in all populations after quality control and marker density in elite cultivars. Markers not assigned to a chromosome were categorised as unknown (UN).*

Chromosome	**Yellowhammer**		**Piko x Julius**		**BOP *A. muticum***	**BOP *T. urartu***
	No. markers	***Markers /Mbp***	***No. markers***	***Markers /Mbp***	***No. markers***	***No. markers***
1A	934	1.169	47	0.059	13	12
1B	1362	1.515	136	0.151	16	3
1D	1062	1.284	20	0.024	14	4
2A	952	1.112	218	0.255	22	19
2B	1212	1.466	142	0.172	19	3
2D	1035	1.468	36	0.051	11	4
3A	812	0.999	75	0.092	9	12
3B	1006	1.185	132	0.155	10	6
3D	743	0.801	8	0.009	11	3
4A	508	0.512	52	0.052	13	13
4B	555	0.677	135	0.165	23	1
4D	271	0.311	10	0.011	20	2
5A	912	0.998	146	0.160	12	16
5B	1079	1.214	190	0.214	12	2
5D	758	1.255	26	0.043	10	5
6A	752	1.034	63	0.087	10	20
6B	988	1.283	24	0.031	9	3
6D	562	0.867	48	0.074	20	4
7A	940	1.257	199	0.266	15	15
7B	798	1.121	190	0.267	22	3
7D	665	0.915	42	0.058	24	4
UN	147	-	32	-	-	-
Total	**18053**		**1971**		**315**	**154**